Novel Support Materials for Jetting based Additive Manufacturing Processes

By

Muhammad Fahad

Doctoral thesis submitted in partial fulfilment of the requirements of Doctor of Philosophy of Loughborough University

February 2011

Additive Manufacturing Research Group

Wolfson School of Mechanical and Manufacturing Engineering

Loughborough University

Abstract

Inkjet printing (jetting) technology, due to its high speed of operation and accuracy, is utilised in Additive Manufacturing (AM) of three dimensional parts. Commercially available AM processes that use jetting technology include three dimensional printing (3DP by Z-Corporation), Polyjet (by Objet), Multi – Jet Modelling (MJM by 3D Systems) and three dimensional printing by Solidscape. Apart from 3D Printing by Z-corporation, all the other jetting based processes require a support material to successfully build a part. The support material provides a base to facilitate the removal of the part from the build platform and it helps manufacturing of cavities, holes and overhanging features. These support materials present challenges in terms of their removability and reusability. This research is therefore, aimed towards finding a support material composition that can be used with jetting based AM processes. The support material should be easily removable either by melting or by dissolution and also, if possible, it should be reusable.

AM processes often process materials with poor mechanical properties and therefore, the parts produced by these processes have limited functionality. In an attempt to obtain complex shaped, functional parts made of nylon (i.e. Polyamide 6), a new jetting based AM process is under research at Loughborough University. The process uses two different mixtures of caprolactam (i.e. the monomer used to produce polyamide). These mixtures are to be jetted using inkjet heads and subsequently polymerised into polyamide 6. Therefore, another aim of this research was to consider the support material's suitability for jetting of caprolactam.

Two different polymers were researched which included Pluronic F-127 and methylcellulose (MC). Both these polymers are known for gel formation upon heating in aqueous solutions. Due to the inhibition of polymerisation of polyamide 6 by the presence of water, non-aqueous solvents such as ethylene glycol, propylene glycol and butylene glycol were studied. Since both F-127 and MC in the glycols mentioned above had not been studied before, all the compositions prepared and investigated in this report were novel. F-127 did not show gel formation in propylene and butylene glycol but formed a gel in ethylene glycol at a concentration of 25% (w/w) F-127. MC, on the other hand, showed gel formation upon cooling in all the three glycols at concentrations as low as 5% for ethylene glycol and 1% for both

propylene and butylene glycol. These compositions were characterised using experimental techniques such as Fourier Transform Infrared (FTIR) spectroscopy, hot stage microscopy, differential scanning calorimetry (DSC) and X-ray diffraction (XRD). A mechanism of gelation for both F-127 and MC in glycols is presented based on the results of these characterisation techniques.

Viscosity and surface tension measurements along with the texture analysis of selected compositions were also performed to evaluate their suitability for jetting. All these compositions, due to their water solubility and/or low melting temperatures (i.e. near 50^0C) present the advantage of ease of removal. Removal by melting at low temperatures can also provide reusability of these support materials and thus advantages such as reduction in build cost and environmental effect can be achieved.

Keywords: Support Material, Additive Manufacturing, Jetting, Pluronic F-127, Methylcellulose, Thermal Gel Formation, Non-Aqueous Solvents.

Acknowledgment

In the name of God the most Gracious most Merciful

I would like to thank my supervisors, Professor Phill Dickens and Professor Marianne Gilbert for their invaluable guidance and encouragement throughout my research.

Thanks to the technical staff in the Department of Materials, Loughborough University including Dr David Ross, Dr Keith Yendall, Dr Carol Raymond (visiting scientist), Andrew Lau and Ray Owens for their help in getting familiarised with different experimental techniques used in this research. Also, many thanks to Mitaben Lad and Antonio Sullo for their help during hot stage FTIR and texture analysis experiments at the School of Biosciences, Nottingham University (Sutton Bonington Campus).

I would also like to acknowledge NED University of Engineering and Technology for providing a scholarship for this research.

Finally, I thank my family especially abbo and ammi for their constant support during this research.

Table of Contents

Publications

[1] Muhammad Fahad, Marianne Gilbert, Phill Dickens, “Thermal Gelation of Pluronic F-127 in Ethylene Glycol as a Non-Aqueous Solvent”, First review submitted to Plastics, Rubber and Composites: Macromolecular Engineering.

[2] Muhammad Fahad, Phill Dickens, Marianne Gilbert. “Novel polymeric support materials for jetting based additive manufacturing processes” Submitted to the Rapid Prototyping Journal.

[3] Muhammad Fahad, Marianne Gilbert, Phill Dickens, “A novel polymeric support material composition for jetting based additive manufacturing (AM) processes” Proceedings of 2nd International Conference on High Performance Plastics 2011.

[4] Muhammad Fahad, Marianne Gilbert, Phill Dickens, “Research into a novel support material for jetting based RM process”, Proceedings of 21st Solid Freeform Fabrication Symposium, 9 – 11th August 2010, University of Texas at Austin, Texas (USA).

Presentations

[1] 2nd International Conference on High performance Plastics, 23-24th February 2011, Marriott Hotel, Cologne (Germany)

[2] SAMPE/BCS Annual Students' Seminar, 23rd November 2010, IOM^3 Headquarter, London (UK).

[3] 21st Annual International Solid Freeform Fabrication Symposium – An Additive Manufacturing Conference, 9 – 11th August 2010, University of Texas at Austin, Texas (USA).

[4] Department of Materials Research Day 2010, 8th June 2010, Loughborough University, Loughborough (UK).

[5] Wolfson School of Mechanical and Manufacturing Engineering Research Student Conference, 9 – 11th June 2009, Loughborough University, Loughborough (UK).

List of Figures

List of Tables

1 Introduction

1.1 Scope of Research

Additive manufacturing (AM) encompasses a set of technologies/processes capable of producing complex 3 dimensional shapes directly from computer aided design (CAD) data, typically in a layer by layer manner. A variety of processes are commercially available that come under the umbrella of AM. These include processes such as stereolithography (SL), selective laser sintering (SLS), fused deposition modelling (FDM), three dimensional printing (3DP), polyjet and multijet modelling (MJM). All the AM processes can be categorized in different ways. A common method is to classify the commercially available AM processes based on the state of raw material used [1]. According to this classification, AM processes have been categorised into the following three categories [1]:

1. Liquid based (e.g. SL and PolyJet)
2. Powder based (e.g. SLS and 3DP)
3. Solid based (e.g. FDM and MJM)

Another classification of AM processes is based on the technology used to build the part [2] such as lasers (SL, SLS), extrusion (FDM) and jetting (PolyJet, MJM, 3DP). Processes such as SL, SLS and FDM are well established and have mainly been the focus of research, but jetting based processes have gained attention in the past few years and have been researched and used extensively due to their accuracy, resolution, relatively low cost and high processing speed [2,3]. Similar to other processes, the materials used by jetting based processes are limited and the main drawback of these processes is the material properties of the parts [1]. As with other AM processes, jetting based processes such as PolyJet and MJM require support materials. The support material not only ensures the fabrication of overhanging features, cavities and holes, it also facilitates the removal of the part from the build platform after completion. Removal of support material can be a tedious job especially from parts having features with fine details. Typical removal methods include manual breaking, dissolution in a solvent such as water or melting by raising the temperature. A common problem with these support materials is that their removal results in “witness marks” on the surfaces to which

they are attached [2]. Also, none of the commercially available support materials for jetting based processes can be reused. Therefore, a support material which can support the layers of build material when they are being deposited and is soft enough to be removed easily without leaving any marks on the part surfaces is important for jetting based AM processes. Also, if the support material is reusable, not only it will reduce the cost of the build, the environmental effect will also be reduced. Therefore, this report presents the research carried out to find novel compositions which can be used as support materials for jetting based AM processes. The objectives for this research were as follows:

- Determine/prepare polymeric compositions which can form soft solids/gels and can be easily soluble in a solvent and/or easily melt-able (i.e. at low temperatures).
- Investigate the behaviour of compositions at different temperatures to determine a suitable working temperature limit.
- Explain the phenomenon that lead to formation and melting of gels to get a better understanding of gels. This will help in enhancing the compositions according to the specific requirements of the jetting processes.
- Determine the jettability of possible compositions by measuring viscosity and surface tension at a temperature suitable for commercially available print heads.

A parallel research project involving a novel process of jetting of caprolactam is also being carried out at Loughborough University [4,5]. This process involves jetting of caprolactam and subsequent polymerisation into polyamide 6 to build three dimensional parts. The polymerisation of caprolactam into polyamide 6 takes place at temperatures ≥ 150^0C [5]. Therefore, another objective was to investigate the suitability of the support material for jetting of caprolactam. The challenge with respect to jetting of caprolactam was to find a material which can support layers of caprolactam/polyamide 6 at higher temperatures (i.e. 150^0C or above) without affecting the polymerisation process.

1.2 Organisation of Thesis

This thesis is organized into 7 chapters. Chapter 1 presents an introduction to the project and outlines the objectives of the research. A detailed literature review related to the research carried out in this report is presented in Chapter 2. The details of different materials and the experimental techniques used in this project are presented in Chapter 3. In Chapter 4, heating/cooling results related to different compositions of Pluronic F-127 in solvents such as water, formamide, octanol and a variety of glycols are presented. Techniques such as Fourier Transform Infrared (FTIR) spectroscopy, hot stage microscopy and differential scanning calorimetry (DSC) for F-127 in ethylene glycol are discussed. Chapter 5 discusses binary compositions of cellulose ethers (methylcellulose and hydroxypropyl methylcellulose) in water and in ethylene glycol. Methylcellulose (MC) was further studied in propylene glycol and butylene glycol and a detailed discussion of results is presented. Results related to ternary compositions comprising of MC, glycol (propylene or butylene) and low concentrations of water (between 2 – 20%, w/w) are presented in chapter 6. The jettability of selected compositions using viscosity and surface tension measurements is also discussed in this chapter. Finally, chapter 7 presents conclusions and provides recommendations for future work.

2 Literature Review

2.1 Introduction to Inkjet Printing

Phenomena that apply to inkjet printing have been observed for the last 200 years but the industrial applications were developed in the late 1970's [6]. The earliest work carried out relating to inkjet technology is attributed to Plateau (1856) who studied the relationship of jet diameter to drop size and frequency and Lord Raleigh (1878) who investigated the instability of jets and described the mechanism of breaking up of a liquid stream into droplets [7]. Since then, continuous development of the technology in terms of reduced cost, increased speed and resolution along with colour printing capabilities have led to a wide variety of inkjet printing systems for home, office and industrial applications by manufacturers such as Canon, HP, Xerox, 3M, Imation, Tektronix, Dataproducts and Spectra [7]. The technology can be broadly classified into two categories as follows (Figure 2-1):

1. Continuous Inkjet Printing (CIJ)
2. Drop-on-Demand Inkjet Printing (DOD)

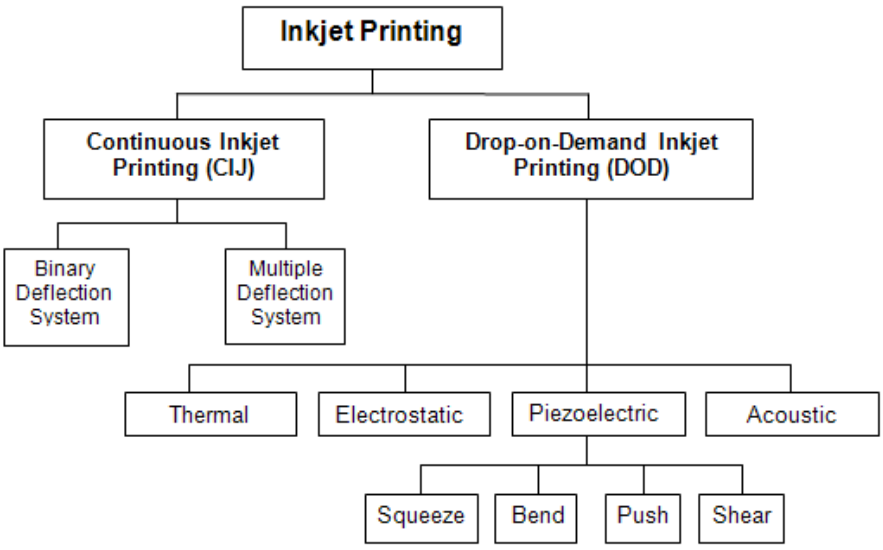

Figure 2-1. Inkjet printing classification (inspired by [7]**)**

2.1.1 Continuous Inkjet Printing

Continuous inkjet printing (Figure 2-2.a) involves sending a steady stream of droplets onto the substrate surface at a controlled rate. The stream of drops is

produced and controlled by the vibration of a piezoelectric crystal inside the head which is capable of producing hundreds of thousands of drops per second [6]. A waveform signal generation system is used to stimulate and vibrate the piezoelement at a specific frequency and this vibration of the piezoelement creates a pressure wave in the chamber where the ink is held. This pressure wave forces the ink out through a nozzle, creating a stream of droplets. This stream is then allowed to strike a substrate surface to achieve the desired print. When the droplets are not needed to strike the substrate during printing, they are deflected towards a gutter by the application of two electrostatically charged deflection plates (Figure 2-2.a). The ink collected in the gutter can then be recycled to print on the substrate. The stream of droplets can be deflected onto the substrate by either the binary-deflection system or multiple-deflection system.

In the binary deflection system (Figure 2-2.b), the droplets are either charged or uncharged with only the charged droplets allowed to reach the substrate and the uncharged droplets are collected for recirculation [7]. In the multiple-deflection system (Figure 2-2.c), the droplets are charged and deflected towards the substrate at different levels allowing a single nozzle to print a small strip [7].

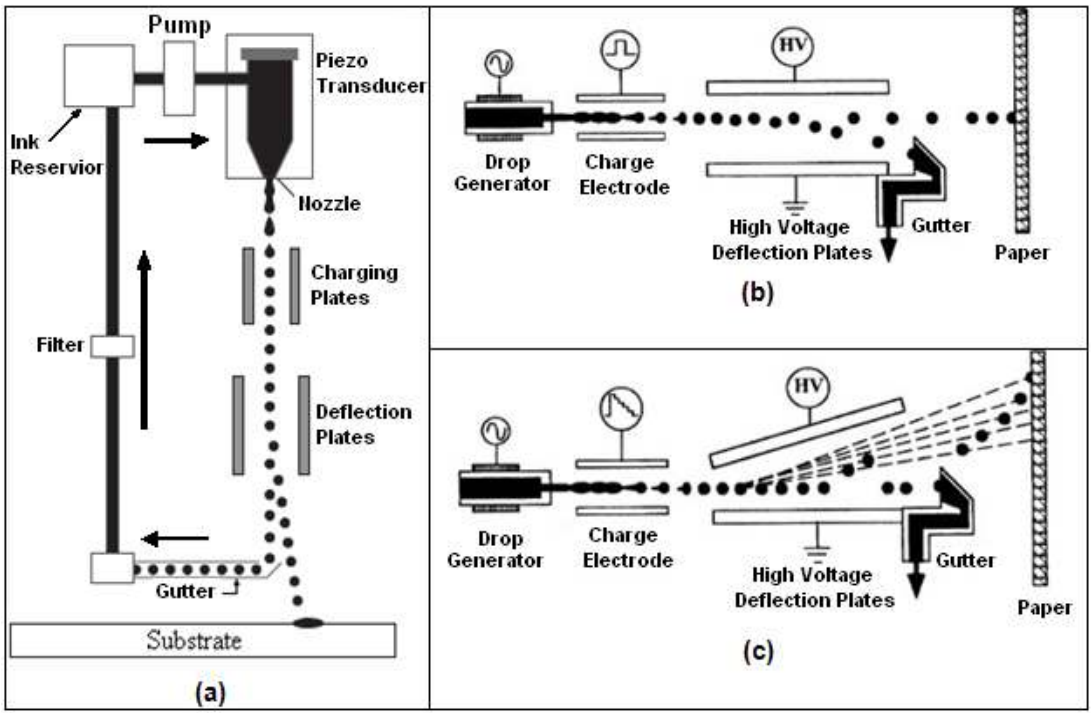

Figure 2-2.(a) Operation of Continuous Inkjet Printing (b) Binary Deflection (c) Multiple Deflection [7-9]

2.1.2 Drop-on-Demand Inkjet Printing

Drop-on-demand (DoD) inkjet printing, shown in Figure 2-3 operates by sending an input signal to force the drop of ink through the nozzle only when it is needed (i.e. demand). Since the drops are only generated when they are needed, there is no need for the additional units for deflection, collection and recirculation making the system simple compared with the continuous inkjet system. The liquid ink resists flow from the nozzle by the meniscus surface tension as it is supplied to the head at a very low pressure [9]. A voltage signal is used to force the drop of ink to overcome the surface tension and viscous forces of the ink within the nozzle.

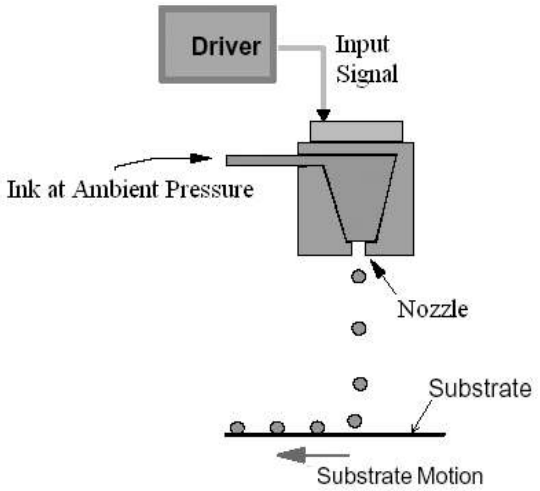

Figure 2-3. Operation of Drop on Demand Inkjet Printing [8]

DoD can be categorized on the basis of the actuation system into four types [7,10]:

1. Electrostatic
2. Acoustic
3. Thermal
4. Piezoelectric

2.1.2.1 Electrostatic Inkjet Printing

In Electrostatic inkjet printing, an electric field is applied between the inkjet head comprising of stylus electrodes and an opposite electrode which is behind the substrate. The application of an electric field causes the ink to fly towards the substrate from the head and thus print [11].

2.1.2.2 Acoustic Inkjet Printing

Acoustic inkjet printing involves the formation of ink droplets by the use of acoustic waves. The drops of ink are produced and subsequently printed on a substrate by applying focused acoustic energy on the surface of the ink through a polyamide membrane [12]. A laser source is typically used for the purpose of producing acoustic energy which is then focused using lenses [13].

2.1.2.3 Thermal Inkjet Printing

Thermal inkjet printing is considered the most successful printing method currently available [7]. It is based on using heat energy to produce droplets. An electric voltage is applied to a heating resistor (usually a resistive layer) in contact with the water based ink. The applied voltage causes the resistor to heat up which in turn heats and vaporizes the water to form a bubble in the ink forcing a droplet of ink to flow out of the nozzle.

2.1.2.4 Piezoelectric Inkjet Printing

Piezoelectric inkjet printing is also a very commonly used system. It is based on the mechanical displacement of the ink within the ink chamber to produce the droplets [14]. A polarized piezoceramic element is used which changes shape or volume by the application of an electric field. A voltage signal is applied to produce the electric field which causes the deformation or displacement of the piezoceramic element. This deformation causes a compression of ink in the chamber leading to the flow of a droplet from the nozzle. The change in the shape or volume of the element is dependent upon the direction of applied electric field.

Depending upon how the piezoceramic is deformed, the piezoelectric inkjet head can be categorized into the following four types [7]:

1. **Squeeze Mode** : Compression of piezoceramic element by the application of voltage causes drop ejection (Figure 2-4.a)
2. **Bend Mode** : Bulging of piezoceramic element by the application of voltage causes drop ejection (Figure 2-4.b)
3. **Push Mode** : Expansion of piezoceramic element by the application of voltage causes drop ejection (Figure 2-4.c)
4. **Shear Mode** : The voltage signal is applied orthogonally to the piezoceramic wall free to reciprocate in a direction transverse to the ink chamber (Figure 2-4.d)

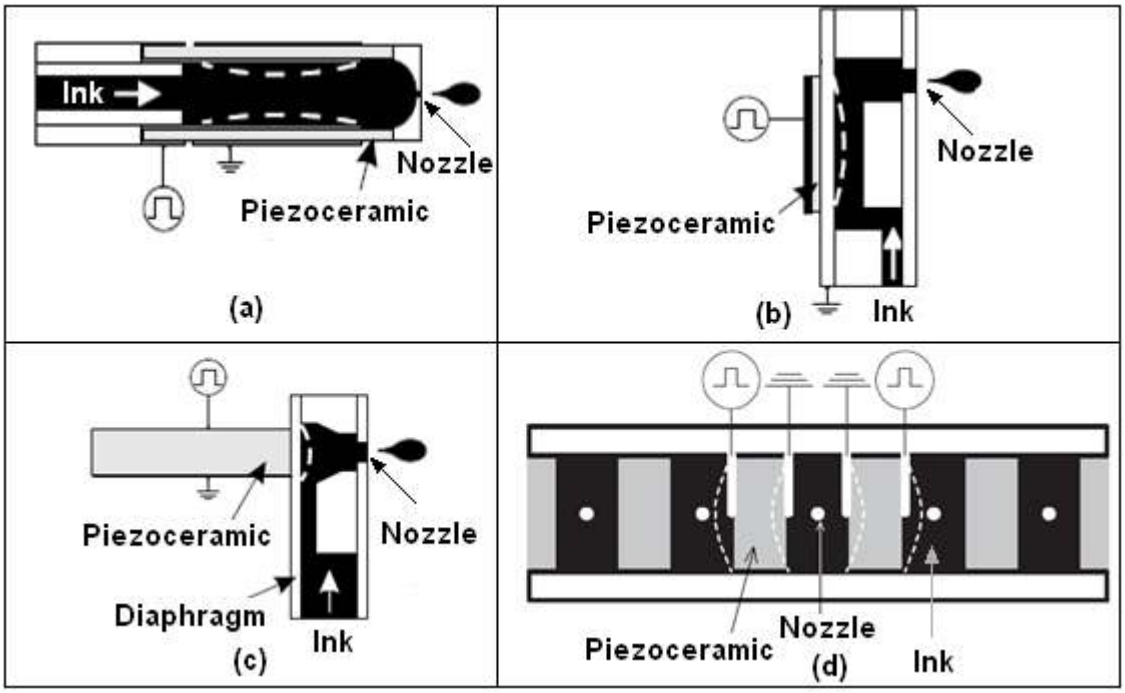

Figure 2-4. Types of Piezoelectric Inkjet Heads: (a) Squeeze Mode (b) Bend Mode (c) Push Mode (d) Shear Mode [15,16]

2.2 Jetting Materials

A wide variety of materials have been printed using inkjet technology. These materials include polymers (both thermoset and thermoplastic), organic solvents, ceramic suspensions, nanoparticle based materials, sol-gel materials, molten metals and biological materials (DNA and protein arrays). Properties of the jetted material such as surface tension and viscosity along with the molecular weight and concentration of the polymer (in the case of polymer suspensions or solutions) are important parameters in deciding the final quality of print and these must be matched to the performance of a specified printer (i.e. printhead) [17].

The behaviour of a fluid where it shows a linear relationship between the applied shear stress and the rate of deformation (i.e. constant viscosity at all shear stress values) is called Newtonian behaviour. Whereas, if the fluid shows a non-linear behaviour between the applied shear stress and the deformation rate (i.e. change of viscosity with increased stress), then this behaviour is known as Non-Newtonian behaviour (Figure 2-5). Ideally, but not strictly, Newtonian behaviour is required whereas viscoelastic behaviour creates significant performance problems during jetting [18].

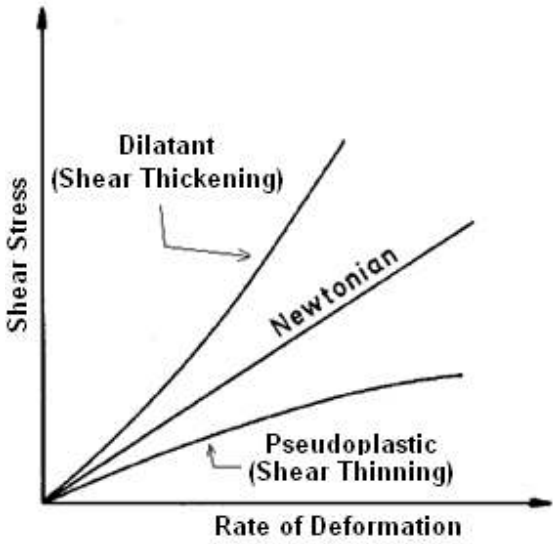

Figure 2-5. Newtonian and Non-Newtonian Behaviour of Fluids [19]

If the viscosity is decreased by increasing the stress, the behaviour is termed as pseudoplastic (shear thinning) whereas, if the viscosity is increased by increasing the stress, the behaviour is termed as dilatant (shear thickening) [19]. If shear stress on a fluid element is represented by τ and the resulting rate of deformation by (du/dy) then:

For Newtonian Fluid: $\tau = \mu\,(du/dy)$

For Non-Newtonian Fluid: $\tau = k(du/dy)^n = \eta(du/dy)$

$\eta = k(du/dy)^{-1}$

Where μ represents the kinematic (or dynamic) viscosity, k is the consistency index, n is the flow behaviour index and η represents the apparent viscosity. Note that n = 1 and $\eta = \mu$ for Newtonian fluids whereas n < 1 for pseudoplastic fluids and n > 1 for dilatant fluids [19].

During inkjet printing, polymer solutions and suspensions behave as dilatant fluids [20,21]. In inkjet printing, polymer solutions and suspensions also show viscoelastic behaviour which is characterized by a partial return to the original shape after the stress is released. The increase in viscosity of a fluid due to applied stress is also termed as strain hardening [22,23]. The increase in the viscosity of polymer solutions and suspensions is attributed to the clustering of particles in the solution. Increased concentration reduces the interparticle distances (i.e. increased clustering) which results in strain hardening of the solution [23]. For jetting, typical viscosity values range between 0.5 – 40 mPa.s whereas the surface tension values range between 20-70 mN/m [18]. Polymer

solutions with molecular weights ranging from $0.5x10^6$ to $6x10^6$ Da and concentration ranging from 0-200 ppm (of the order of few percent by volume) have been jetted [21,22,24]. For suspensions, it is generally considered best to use a particle size of less than 5% of the nozzle diameter [18,25].

2.3 Applications

Inkjet printing finds its applications in a wide range of areas including office/home, industrial, electronics, textile, bio-medical and additive manufacturing [7]. A brief discussion of these applications is presented next and due to its relevance to this report, inkjet printing applications in additive manufacturing will be discussed in detail in a later section (i.e. section 2.4).

2.3.1 Office/Home

This application area of inkjet printers is considered as “one of the largest users of desktop printers” and “the most rapidly growing market” for inkjet printers [6]. Fax machines, office documents, letters, posters, overhead presentations, presentation handouts are a few examples of inkjet applications in home and office printing.

2.3.2 Industrial

Inkjet printing was used in industrial application before the home and office applications. Industrial applications mainly include package printing, bar code printing, short run colour graphics on paper, plastic and board [26]. Printing on glass, especially for automotive applications, is another major industrial application [27]. Decoration of ceramic tiles using inkjet printing [28] and fabrication of refractive microlenses on glass substrates using inkjet printing have also been reported [29,30].

2.3.3 Electronics

Electronic applications of inkjet printng are very recent and include printing (manufacturing) of printed circuit boards (PCB), polymer light emitting diodes (PLED), colour filters for liquid crystal display (LCD) and organic thin film transistors (OTFT) [21,31-33]. Due to the ability of patterning high-purity electrically functional materials without the need of a mask, inkjet technology is considered to play an important role in printed electronics manufacturing [34].

Pixel printing for organic light emitting diodes (OLED) is one of the most extensive applications of inkjet technology [32]. Electrically conductive patterns of carbon nanotubes (CNTs) have also been successfully printed on paper and plastic surfaces [35,36]. Membrane electrode assemblies (MEAs) for polymer electrolyte membrane fuel cells (PEMFCs) have also been fabricated using an office/home type inkjet printer [37,38].

2.3.4 Textile

Applications related to printing of carpets using inkjet technologies were one of the earliest applications of the technology and date back to the early 1970's [39,40]. Due to the elimination of set up cost associated with conventional textile printing, inkjet technology is considered suitable for cost-effective short run production with the other potential advantage being the ability to print repeated patterns [41]. Standard inkjet heads are employed in textile applications leading to advantages such as lower parts/maintenance costs and easier handling with improved property inks for a variety of textile substrates (fabrics) [39]. Inkjet printing was applied on cotton and satisfactory results were found [42]. Various projects in Europe, USA and Japan are targeted towards development of a full size textile printer to replace existing conventional systems [40]. However, a variety of companies including Stork, Canon, Toxot, DuPont and Seiren have commercial inkjet printers for textile printing which can be used for sampling and short run/customized production [7,39,40].

2.3.5 Medical/Bio-Medical

Inkjet printing of proteins and DNA has been of interest for the last two decades and commercial inkjet printers have been used to print high density DNA micro-arrays without molecular degradation [43,44]. Microscale patterning of different biological materials including proteins, monofunctional acrylate esters, sinapinic acid, DNA and multiwalled carbon nanotube/DNA hybrid composite was successfully demonstrated [45] and biologically active proteins were used to print cellular patterns of varying complexity using inkjet printing [46]. Three dimensional tissue engineered scaffolds (cylindrical nerve conduits) have also been printed using inkjet technology [47] and three dimensional tubular and shell structures of human cells have been printed using a specialized inkjet printer [48].

Another relatively new and expanding application area of inkjet technology is in drug development [49,50]. Inkjet technology is considered advantageous in drug development applications due to its ability to print small drops (in picoliters) without any physical contact and with high dispensing speed [51]. Three dimensional printing (based on inkjet printing) of oral dosage forms (tablets) with complex release profiles has been successfully performed [52].

2.4 Additive (Rapid) Manufacturing

Additive manufacturing (AM) is based on building accurate profiles in an additive, layer by layer manner to achieve a desired three dimensional shape without the need of any machining [53,54] and is defined as follows [1]:
“The use of computer aided design (CAD) based automated additive manufacturing process to construct parts that are used directly as finished products or components.”

A variety of commercial inkjet printing based additive manufacturing systems are available from 3D Systems, Z Corporation, Solidscape and Objet Geometries [7,8,55]. These systems can be categorised in two main configurations: a build up method and a bonding method [56].

In the build up method, the raw material in the form of liquid (a solution or suspended micro/nano particles) is directly printed using the inkjet head. Whereas, in the bonding method, the inkjet head deposits binder material on a powder bed to selectively bind the powder and build a part.

Ceramic printing using inkjet printing has found increased attention over the past few years [49] and both continuous and drop-on-demand inkjet printing technologies have been successfully used to print ceramic three dimensional structures [57-62]. Polymers [63-67], along with waxes [68-70], metals [25,71-73] and water based [74,75] three dimensional structures have been successfully printed using inkjet technology.

As the focus of this report is related to inkjet based Additive Manufacturing (AM) processes, the following sections present an introduction to commercially available inkjet technology based Additive Manufacturing processes.

2.4.1 Three Dimensional Printing (3DP)

Developed at Massachusetts Institute of Technology (MIT) and licensed to Z Corporation, this process uses an inkjet printhead to deposit a liquid binder that solidifies layers of powdered material. Two types of materials are used including starch based and plaster based materials [1].

2.4.1.1 Process Description

The process starts by filling the feed box with powder. The binder is held in a cartridge in the machine. To start the build, the build piston moves down by one layer thickness (i.e. along the z-axis) and the feed piston rises to present the amount of powder suitable to completely fill one layer thickness in the build chamber. This powder is then moved to the build chamber using a scraper which sweeps the powder from the feed chamber to the build chamber. Excess powder is swept down to an overflow chute and this powder can then be reused in subsequent builds. After the layer of powder is deposited, an inkjet head assembly (Figure 2-6), mounted on a carriage, traverses over the build chamber along the x and y axes to deposit a liquid binder on top of the layer of the powder using a raster-like mechanism. For monochrome printing, only one print head is used whereas for full colour printing multiple heads (i.e. up to 5) are used. This binder material joins the desired particles in each layer. After a layer is bonded successfully, the piston supporting the powder bed lowers so that the next layer of powder can be spread and selectively joined. The process continues to deposit the successive layers until the desired geometry is completed. Typical layer thickness ranges between 0.080-0.250 mm. The process is very fast compared with other AM processes and can produce coloured parts using a 24-bit colour palette. Since the powder material surrounds the part, the parts are produced without any support structures. Built parts are usually fragile and infiltration can be used to improve the strength [1,76,77].

Other advantages include cheap build materials and reusability of powder (i.e. the powder that is not printed during build). Disadvantages of the process include poor surface finish, more limited materials and weaker parts compared with other processes [76-82].

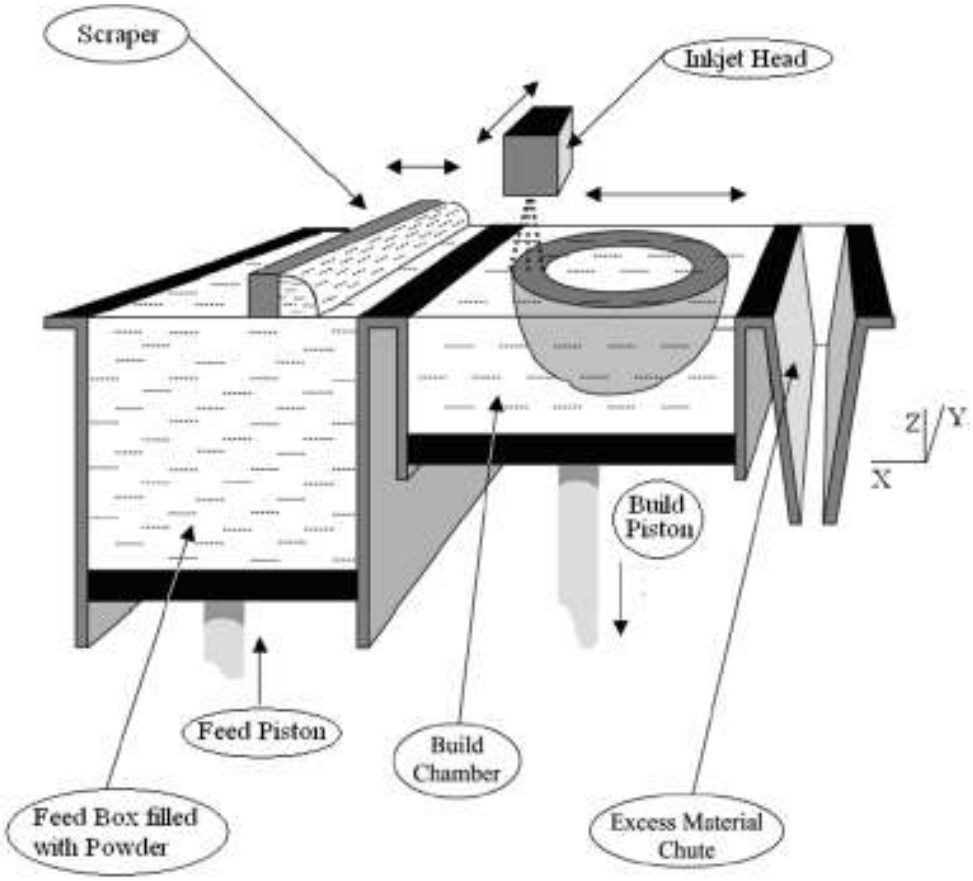

Figure 2-6. Schematic illustration of 3DP process (inspired by [79]**)**

2.4.2 Multi-Jet Modelling (MJM^{TM})

MJM^{TM} was introduced by 3D Systems and is considered a "concept modeller" process [79,80]. It is based on the principle of thermal phase change inkjet printing in which a solid, wax based ink is melted and subsequently ejected from a set of nozzles to form the desired object as the wax is solidified. It utilizes a print head comprising a large number of jets (nozzles) to deposit successive layers of the molten wax to build a three dimensional part.

2.4.2.1 Process Description

A wax billet is loaded inside the machine, into a reservoir. The wax is kept molten in the reservoir and is fed using a siphoning technique to the inkjet head. To start a build, the inkjet head traverses along the x-axis to deposit droplets of molten wax which are solidified after being jetted. If the width of the part is greater than the width of the inkjet head, the platform moves along the y-axis and the inkjet head again traverses along the x-axis so that the cross section can be completed. After each layer, the platform moves downwards relative to the inkjet head (i.e. in the z-axis) so that the next layer can be printed (Figure 2-7). Typical layer

thickness ranges between 0.04 – 0.10 mm. Support structures are required not only to support overhangs and cavities, but also to facilitate the removal of the part form the platform. Therefore, the first few layers built are used as support structures, which are very thin strands of the same wax material used to build the part. These supports can be easily removed by breaking away when the part is completely built [76,77,79-81,83].

Apart from the advantage of the high speed building of parts, the process provides an added advantage of being office friendly due to its simple operation and cleanliness as no post curing of the part is required. Disadvantages of the process include limited materials (i.e. only waxes can be printed), weak mechanical properties of the parts and poor surface finish on the down facing surfaces due to support structures [76,77,79-81,83,84].

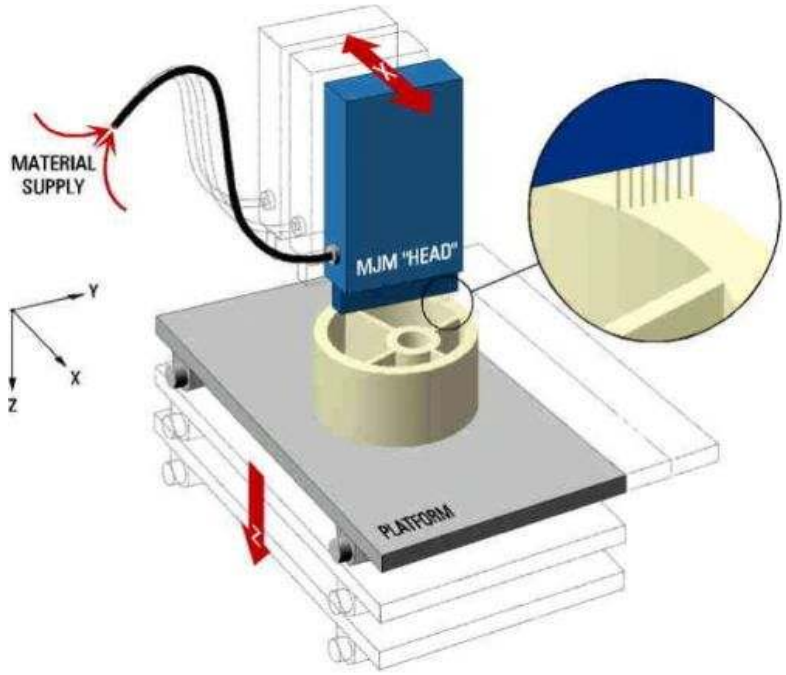

Figure 2-7. Schematic illustration of Multi-Jet Modelling [85]

2.4.3 PolyJet™

Patented by Objet Geometries Inc., PolyJet™ is also based on inkjet printing but, it uses acrylic-based photopolymer materials rather than the hot melt ink used in MJM [83]. It utilizes a large number of nozzles (typically more than 1500) to jet an acrylate-based photopolymer build material and a photo-curable support material. Ultra Violet (UV) light is used to cure the materials to produce three dimensional parts.

2.4.3.1 Process Description

The cartridges (one each for build and support material) are loaded into the machine to start the process. A print head assembly comprising eight inkjet heads traverses the x-axis to deposit layers of both support and build materials. Two Ultra Violet (UV) lamps, located on the printhead assembly, are used to cure the layer of material immediately after it has been deposited. The build material is cured to a solid state where as the support material is cured to a gel-like state. The support structure comprises solid layers compared to the thin strands in MJM. To print wide parts, the print head can also move along the y-axis to deposit a layer of material. After the layer is completed, the platform is lowered along the z-axis to print the next layer (Figure 2-8). Layer thicknesses as low as 0.016 mm (16 micron) are achievable using the process. After the build is completed, the gel-like support material is easily removed with a water jet [1,67,76,83,86,87].

Along with advantages such as the high speed of the process, fine surface finish, high accuracy and resolution, the process also provides a significant advantage in that all the photopolymer resin is cured so that the user is not exposed to uncured resin after the build is completed. Material properties achieved are better than those achievable using the MJM materials but are still considered as the main weakness of the process [1,67,83,86,87].

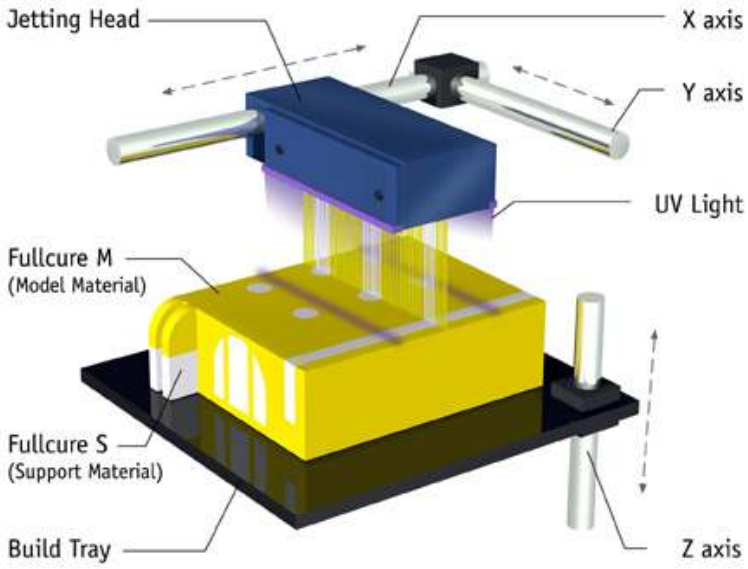

Figure 2-8. Schematic illustration of PolyJet process [88]

2.4.4 Solidscape 3D Printing

Solidscape 3D printing (formerly known as ModelMaker) is a process similar to MJM as it utilizes a wax-like thermoplastic material for building parts along with a water soluble wax as a support material. Two piezoelectric inkjet heads are used, one each to deposit support and build material [25,76,77].

2.4.4.1 Process Description

The starting material is in the form of granules and both the support and build materials are stored in molten form in the machine in separate, heated tanks. The material is supplied to the respective inkjet head through heated lines. Printheads can move simultaneously along the x and y directions (Figure 2-9). The process starts by printing support layers to facilitate ease of removal. After a layer of material is successfully deposited and solidified, a cutter (similar to a milling cutter) trims the material from the surface of the built layer to flatten it. The build platform is then lowered and the subsequent layer of material is deposited. A vacuum based particle collecting system, attached with the cutter head assembly collects the removed material as it is machined. This ensures that there is no unwanted material present on the surface. After the build is finished, the support material is removed by dissolving it in a hot solvent bath, typically at 55^0C. Typical layer thickness ranges between 0.013 – 0.076 mm [25,76,77,89,90].

Due to its simple and clean operation, the process is considered office-friendly and its high precision/accuracy combined with the minimal post processing operation enables it to be used for tooling and casting applications. Similar to other jetting based processes, the process has the disadvantage of limited materials as only waxes (one for support and one for part) can be used [76,77,90].

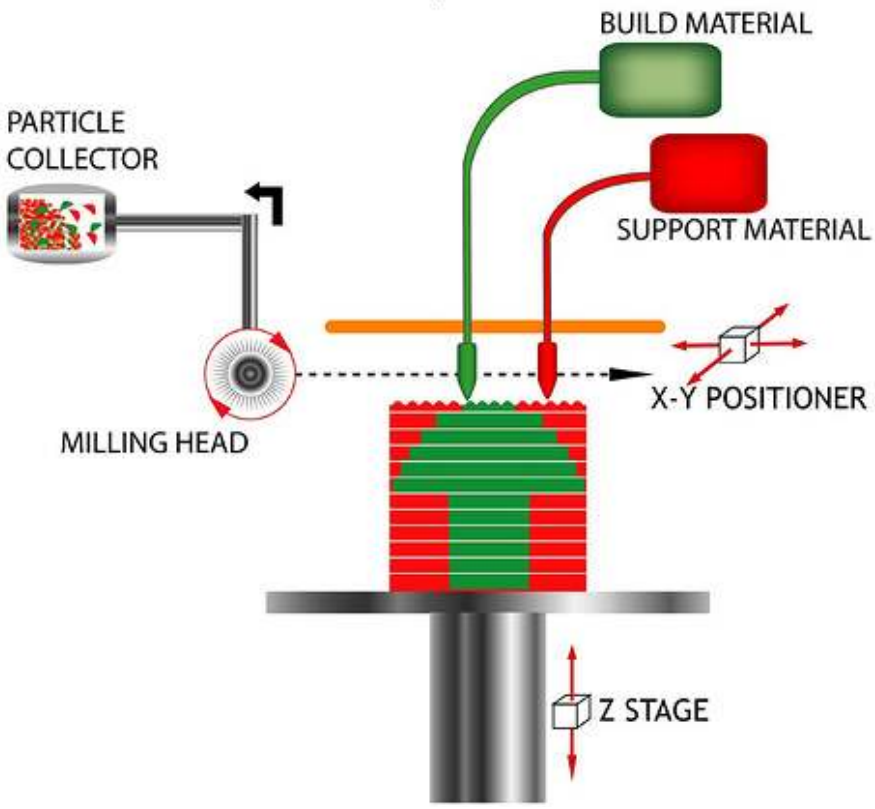

Figure 2-9. Schematic of Solidscape 3D Printing Process [91]

2.5 Introduction to Support Materials

The initial state (i.e. during deposition) of material used to build a part by Additive Manufacturing processes is different for different processes, for example liquids for Stereolithography (SL), Multi-Jet Modelling (MJM) and PolyJet, powders for Selective Laser Sintering (SLS) and Three-Dimensional Printing (3DP) and solids for Fused Deposition Modelling (FDM). For the processes such as SLS and 3DP, the excess unused powder surrounding the part acts as support material whereas for the processes such as Polyjet, Multi-Jet Modelling and FDM, where the part is actually built in open space, other materials, called support materials are used to avoid shifting and/or sagging of features such as overhangs, horizontal flanges, holes and cavities. Thus many RM processes actually make use of the following two types of materials [78,92]:

1. **Build Material:** This is the actual part material and the bulk of the geometry to be produced is made-up of this material.
2. **Support Material:** This is the material used to build structures that act as scaffolding upon which the overhanging part features are supported.

Support materials are required for the following reasons [78,93]:

- They comprise the first structures built to form a base in order to facilitate the removal of the part from the build platform.
- They provide support to overhanging structures which are not directly supported by the build material.
- They resist the tendency of a model to deform by providing a support to resist the forces applied to a partially completed model during build.

2.5.1 Support Materials for Jetting

Inkjet based additive processes such as Multi-Jet Modelling, PolyJet and Solidscape 3D Printing processes have been described previously. These processes also make use of support materials during part building and these support materials are jetted in the same way as the build material. The support material should be such that it can be easily removed from the desired geometry without affecting the surface finish or features of the build geometry [78]. Different support removal methods have been discussed which include [94]:

1. **Application of Force:** The support material establishes a weak bond at the interface of the build material and is thus easily removed by applying force (usually by hand).
2. **Melting:** The support material has a lower melting point than the build material and after the part is completely built, it is heated to melt away the support material.
3. **Dissolving:** The support material is selected such that it is soluble in a solvent and the build material is insoluble in the same solvent. Thus by dipping the completed part in the solvent, the support material is removed.

Other methods such as powered washing [92], use of mechanical vibration or energy (i.e., from a microwave) to weaken and thus remove the support structure [95,96] have also been discussed.

A variety of support materials have been jetted using inkjet based processes with the aim of ease of removal. They include wax, water swellable gels and readily meltable/soluble materials [92,97]. Phase change waxes are the most commonly used inkjet based support materials. These compositions are mixtures of waxes and polymers, which are jettable liquids at elevated temperatures (i.e jetting temperature which is usually higher than 70^0C) and they become solid at ambient

temperatures. These waxes include paraffin, microcrystalline waxes, polyethylene waxes, ester waxes and fatty amide waxes. Although, waxes are the most commonly used support materials and they can be easily removed either by melting or by dissolving in a solvent such as water, a major problem associated with them is that they are weak and brittle. Due to their brittleness, these waxes are prone to cracking after they are jetted and solidified and thus can cause accuracy issues for the part being built [98-100].

Xu et al. have discussed fatty alcohol (i.e Hexadecanol, Octadecanol) based phase change support material compositions in their patents related to 3D Systems [98-100]. These compositions were successfully jetted using a piezoelectric inkjet print head and have a melting point of 60 – 65^{0}C and viscosity ranging between 11.3–11.8 mPa.s at 80^{0}C (i.e. jetting temperature). They can be easily removed by heating the completed part either by placing it in a heated oven or heated vat of liquid material (i.e. water or oil) or by directing a heated jet of liquid material at the support material.

Neilsen et al. [97] have discussed the jetting of water soluble support materials. These compositions comprised water and fusible water containing (FWC) substances such as brine, sodium sulphate decahydrate and sodium acetate trihydrate. These materials are considered environment friendly and non-hazardous and they can be easily removed by dissolving the support in water. However, these materials need a thermally-controlled fabrication chamber as the temperature of the inkjet head dispensing the support material is to be maintained at a temperature higher than the freeze temperature of the composition so that the material is liquid while being dispensed and the build chamber should be maintained at a temperature lower than the freeze temperature of the composition so that it is solidified after being dispensed form the inkjet head. The freeze temperature of these materials depends upon the FWC substance and thus can vary from 30 – 100^{0}C. Use of water or brine has also been discussed as a support material but, it requires complicated thermal control of the entire system as the build chamber has to be maintained at temperatures lower than the freezing temperature of water/brine solution which is around 0^{0}C and also, any heat from the exothermic polymerization of the build material using ultraviolet radiations can re-melt the support structure.

Napadensky in his patents (assigned to Objet Geometries) described methacrylate based support material compositions [101-103]. These compositions were targeted for use in inkjet based three dimensional printing of objects. They consisted of water miscible components which can be dissolved in water, alkaline water or a water detergent solution. Also, for ease of removal, these compositions may contain acidic substances that liberate bubbles when dissolved in water containing bubble releasing substances (BRS). These bubble releasing substances react with the acidic substance in the support composition, releasing bubbles of carbon dioxide and thus facilitate the swelling and removal of the support in a water based solution. Examples of BRS include carbonates or bicarbonates such as sodium bicarbonate. These support materials show low viscosities of about 8-15 mPa.s at jetting temperatures higher than 60^0C, so are suitable for jetting at higher temperatures. After jetting, these become gel-like solids with weak mechanical properties at ambient temperature.

Support material compositions exhibiting Reverse Thermal Gelation (RTG) have been discussed by Levy in his patents (assigned to Objet Geometries) [104,105]. Reverse Thermal Gelation is a phenomenon in which the solution (usually aqueous solution) of material is liquid (i.e. low viscosity) at low temperature such as room temperature and becomes solid (i.e. high viscosity) at higher temperatures such as 30-40^0C. When the temperature is reduced to the low value, the material reverts to a liquid state, meaning that the behaviour is reversible. These gels show toughness and dimensional stability appropriate for supporting material layers as the part is built and are soluble in water leading to ease of removal after the part is completed.

The polymers exhibiting RTG phenomena in their solutions are termed temperature sensitive polymers [106] and are mainly block copolymers, that is, they consist of chains of sequences of two or more polymers attached at their ends [107]. Examples of these materials are pluronics, cellulose ethers and poly n-isopropylacrylamide (PNIPAM) [104,105].

Reverse Thermal Gelation behaviour of the support material compositions discussed by Levy is considered an interesting possibility for the current project and therefore, it was decided to investigate selected polymers which exhibit RTG behaviour. Pluronics and cellulose ethers (methylcellulose and hydroxypropyl

methylcellulose) were selected due to their wide spread applications as gel forming (i.e. RTG) polymers [108,109]. The following sections describe these polymers in more detail.

2.6 Pluronic®

Pluronic (BASF) is a trade name of a family of more than 30 block copolymers. These are triblock copolymers and have a structure consisting of polyethylene oxide-polypropylene oxide-polyethylene oxide (PEO_a-PPO_b-PEO_a) where a and b represent the degree of polymerization of each block (i.e. number average chain length). The chemical structure of Pluronics is shown in Figure 2-10.

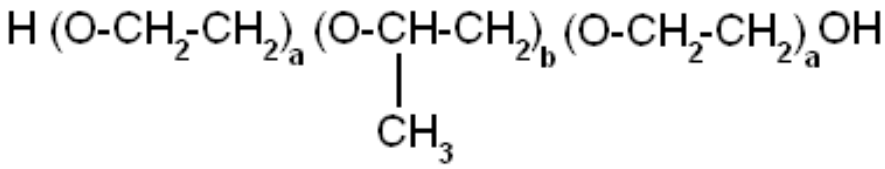

Figure 2-10. Chemical structure of pluronics [110]

Pluronics are considered an important class of surfactants and have been used in a variety of industrial applications such as detergents, foaming, lubrication emulsification, controlled drug release and gelling [106,111]. Concentrated aqueous solutions of Pluronics have shown reverse thermal gelation (RTG) characteristics and the gelation mechanism of these polymer solutions has been extensively studied [112]. These polymers are considered “the most widely used reverse thermal gelation polymers” [108] and F-127 is the most commonly used Pluronic polymer [113].

They are available in the form of liquids, pastes and solids with molecular weight ranging between 2,000-14,000 and PEO/PPO weight ratio ranging between 1:9 to 8:2 (see Table 2-1) [111,112,114]. Pluronics are identified by using a letter-number combination. Letters designate the physical state of the pluronic such as “L” for liquids, “P” for pastes and “F” for flakes (i.e. solid form). The letter is followed by a two or three digit number. The first number (or first two numbers in the case of three digits) multiplied by 300 gives the approximate molecular weight of the PPO (hydrophobe) and the last digit multiplied by 10, gives the percentage of PEO in the molecule. Thus, for example, F 127 is available in the form of flakes (M_W ~ 12600), has a PPO molecular weight of approximately 3600 and PEO content of 70 % of the total molecular weight.

Pluronic	Molecular Weight	PEO (wt. %)	Melting Point (^{o}C)	Viscosity* (mPa.s)
L31	1100	10	-32	175
L35	1900	50	7	375
F38	4700	80	48	260
L43	1850	30	-1	310
L44	2200	40	16	440
L61	2000	10	-29	325
L62	2500	20	-4	450
L63	2650	30	10	490
L64	2900	40	16	850
P65	3400	50	27	180
F68	8400	80	52	1000
L72	2750	20	-7	510
P75	4200	50	34	280
F77	6600	70	48	480
L81	2750	10	-37	475
P84	4200	40	34	280
P85	4600	50	34	310
F87	7700	70	49	700
F88	11400	80	54	2300
L92	3650	20	7	700
F98	13000	80	58	2700
L101	3800	10	-23	800
P103	4950	30	30	285
P104	5900	40	32	390
P105	6500	50	35	750
F108	14600	80	57	2800
L121	4400	10	5	1200
L122	5000	20	20	1750
P123	5750	30	31	350
F127	12600	70	56	3100

* Liquids at 25^{0}C, pastes at 60^{0}C and solids at 77^{0}C

= Liquid = Paste Solid

Table 2-1. Commercially available Pluronics [115-118]

2.6.1 Micellization and Gel Formation

At low temperatures (usually lower than 15^{0}C), both PEO and PPO blocks are soluble in water and are present in the form of polymer chains called unimers (Figure 2-11). PEO is more polar than PPO [119-123]. Since water is a polar solvent, the PEO – solvent (water) interactions, in the form of hydrogen bonding, are strong (attractive) and PEO – PPO interactions are weak (repulsive) at low temperatures. Therefore, strong water structuring due to hydrogen bonding is present around PEO chains in aqueous solutions at low temperatures. PPO, due

to the presence of methyl (CH_3) group, presents relatively higher steric hindrance to water molecules as compared to PEO and results in weak water structuring around PPO chains at low temperatures [123]. Upon increasing the temperature, due to its weak interactions with water, PPO becomes less soluble in water (i.e. hydrophobic) whereas the PEO remains soluble [124]. At or above a certain concentration, called the critical micelle concentration (CMC), the increased dehydration (i.e. hydrophobicity) of the PPO chains results in the aggregation of individual chains (i.e. unimers) into spherical micelles upon increasing the temperature above a certain value called critical micelle temperature (CMT). The conversion of unimers into micelles is accompanied with a gradual increase in the viscosity of the solution (Figure 2-11). The core of the micelle comprises of PPO molecules whereas the PEO molecules form the corona of the micelle [111,112,119,122-124]. Also, the hydrogen bond structure (due to water molecules) around PEO becomes weak and PEO – water interactions become less favourable whereas PEO – PPO interactions become more favourable. Thus, upon further increasing the temperature to a value called gel temperature (T_{gel}), due to increased polymer – polymer attractions, the micelles come into contact and micelle entanglement takes place with sharp rise in the viscosity of the solution. This entanglement is caused due to the linking of PEO chains between adjacent micelles. Due to this entanglement, the micelles cannot move freely and thus form a gel phase (Figure 2-11) [112,124-129]. The gel phase represents a physically cross linked network with a measureable yield stress or elastic modulus [126]. The entanglement of micelles resulting in the formation of a lyotropic crystalline phase is considered the driving force for the gel formation in Pluronic solutions [112,115,125,126]. These crystalline phases can include cubic, hexagonal and lamellar structures (Figure 2-12) [130-133]. Upon cooling, the gel phase converts into solution phase with a gradual expansion of micelles into unimers.

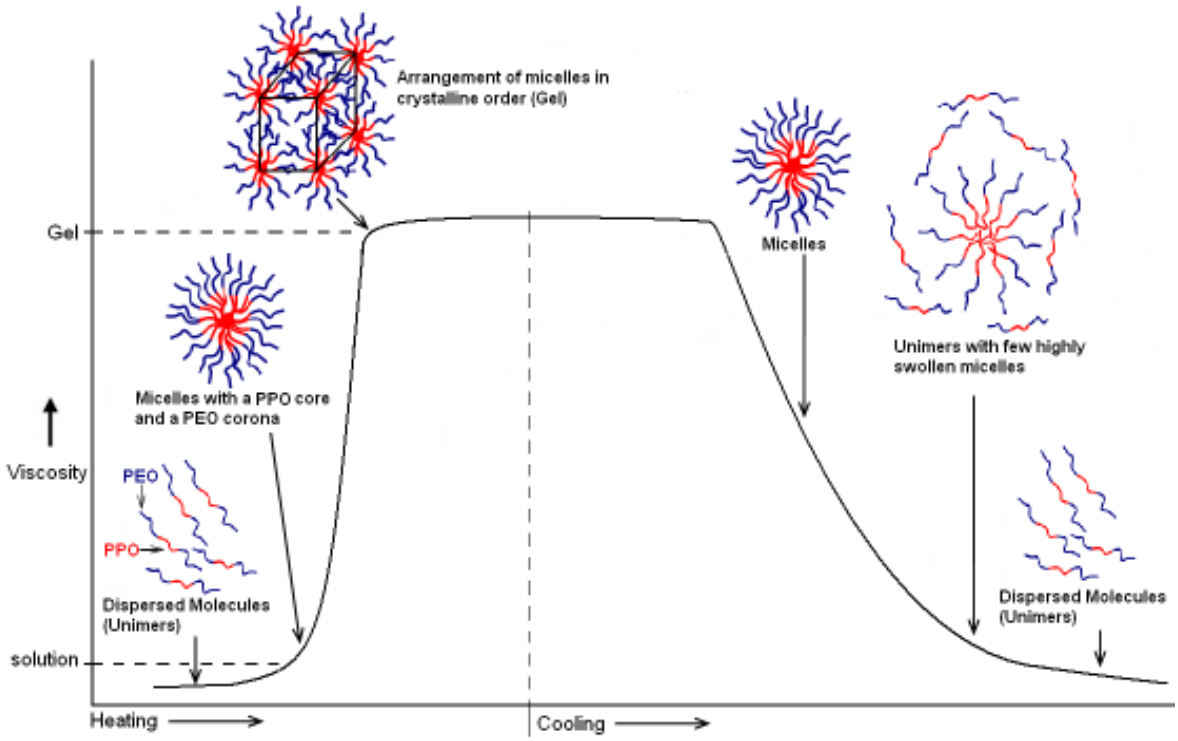

Figure 2-11. Formation of micelles and unimers upon respectively increasing and decreasing the temperature of aqueous solution of Pluronics

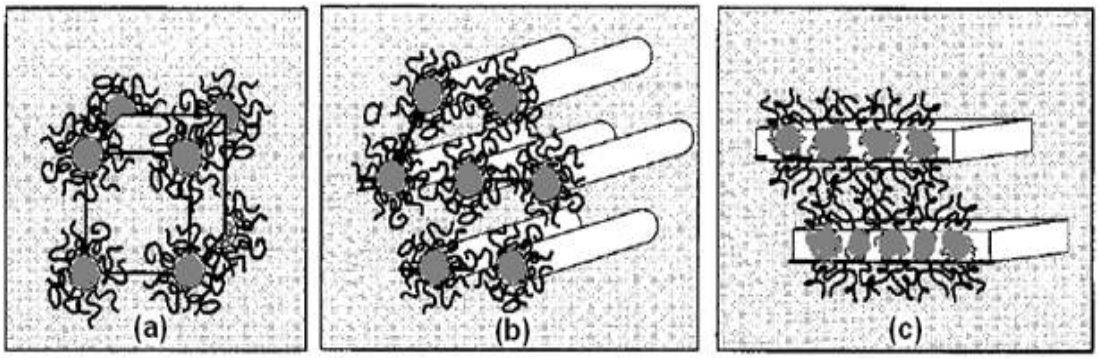

Figure 2-12. Crystalline phases formed by Pluronics in aqueous solutions (a) Cubic (b) Hexagonal (c) Lamellar [132]

2.6.2 Molecular Weight

Pluronics with molecular weights ranging from 1700 to 13000 have been studied and it has been suggested that increasing molecular weight (for constant PEO/PPO ratio) results in reduced CMC/CMT and T_{gel} [115,123,124,134]. Also, lower molecular weight Pluronics (M_w ~ 2500) do not form a gel at any concentration whereas Pluronics with higher molecular weight form a gel at low concentration and/or temperature [134]. This behaviour can be understood on the basis of micelle/gel formation explanation presented in the previous section as for low molecular weight Pluronics the miceller interactions even at high concentration or temperature are not sufficient to cause the formation of gel whereas increased

molecular weight results in longer polymers chains and thus strong micellar interactions take place at high concentration/temperature to cause the formation of gel.

2.6.3 PEO/PPO Chain Length

The effect of varying the relative molecular weight (i.e. chain length) of PEO and PPO blocks upon CMC and CMT has been evaluated and the following conclusions were drawn [122]:

- For constant PEO chain length, a decrease in PPO molecular weight (chain length) leads to increased CMC at a given temperature or an increase in the CMT at a given concentration.
- For constant length of PPO chain, a decrease in the PEO chain length results in reduced CMC at a given temperature or reduced CMT at a given concentration.

These effects are observed because increasing the PPO fraction results in an increased hydrophobic character and also, the fraction of non – polar states present in the solution increase with increasing the PPO chain length resulting in increased dehydration and polymer – polymer interaction at lower temperature and/or concentration (i.e. reduced CMT/CMC) and consequently, the gel temperature is also reduced [115,121-123,128,135].

2.6.4 Concentration

The effect of varying concentration of Pluronic in water has been studied and both the CMT and T_{gel} are found to decrease with increasing concentration [115,123,125,127,134,136-139]. This is attributed to reduction of intermicellar distance upon increasing concentration which in turn reduces the degree of micellar swelling necessary for micellar entanglement and thus T_{gel} is reduced and the gel strength is also increased [127,134]. Typically, for concentrations lower than 15%, no gel formation is observed [127,134].

2.6.5 Solvents

Self assembly and the microstructure of Pluronics is highly dependent upon the solvent quality [140]. Water has been the most commonly used solvent for the pluronic solutions but different cosolvents including a variety of alcohols/glycols, glycerol, acids and formamide have been used for modifying the solution and

aggregation properties of Pluronic solutions for specific applications [129-133,141-148]. In aqueous solutions, addition of short chain alcohols (C_1 – C_3) such as methanol, ethanol and 1–propanol increase the CMT values whereas longer chain alcohols (C_4 – C_6) such as 1–butanol, 1–pentanol, and 1–hexanol decrease the CMT values for a given concentration of Pluronic [129,141,148,149]. It is suggested that this is because the short chain alcohols are good solvents for both PPO and PEO blocks reducing the dehydration of the PPO block (hydrophobic effect) and thus resulting in increased CMT value. On the other hand, increasing chain length decreases the solubility significantly resulting in an increased hydrophobic effect and thus reduced CMT value [141]. The effect of C_{14} diol (known as Surfynol® 104) on the micelles of a Pluronic solution (P85) was studied and a reduction in CMT was observed because the diol associates with the PPO block of the Pluronic and expels the water out of the core to increase the dehydration and thus the CMT is reduced [142]. Effect of glycerol, propylene glycol and ethanol have been studied and isothermal (at 25^0C) ternary phase diagrams comprising of water, Pluronic (F127) and the respective co-solvent have been developed [132,133,143]. Glycerol has been found to decrease the CMT and sol-gel temperature of the Pluronic solutions whereas the addition of propylene glycol was found to have the opposite effect to that of glycerol [132,133,140,150]. This was attributed to the PPO having a similar structure to propylene glycol which enables better solvency for PPO in water in the presence of propylene glycol [132,133]. On the other hand, glycerol, due to its strong affinity for water, decreases the PEO hydration and thus CMT and T_{gel} are reduced [140]. Addition of hydrochloric acid to the aqueous solutions of Pluronic (P123) was also found to increase the CMT values [113]. This increase in CMT is attributed to strengthening of the hydrogen bond between the Pluronic and water molecules due to the protons (H^+) supplied by the acid. The increase in hydrogen bonding results in reduced dehydration of the Pluronic and thus the CMT value is increased by adding the acid [113]. Formamide has been used as a cosolvent (i.e. with water) as well as a solvent (without water) to form Pluronic solutions and is considered “the most studied non-aqueous polar solvent” [145]. It was reported that formamide is a better solvent than water and thus a water-formamide mixture as well as formamide alone, when used as solvent, resulted in increased CMC/CMT and T_{gel} values for Pluronic solutions [38,145-147].

2.7 Cellulose

Cellulose is considered the most abundant naturally occurring organic compound available worldwide [151-154]. It is a polysaccharide composed of linear chains of anhydrogluco-pyranose units (AGU) linked together at 1 and 4 positions of carbon atoms through beta (β) configuration glucosidic bonds (i.e. β(1→4) linked D-glucose). It has a formula of $(C_6 H_{10} O_5)_n$ where n is the chain length or degree of polymerisation. The structure of cellulose is shown in the Figure 2-13. There are three hydroxyl groups in each glucose unit of cellulose on second, third and sixth carbon atom.

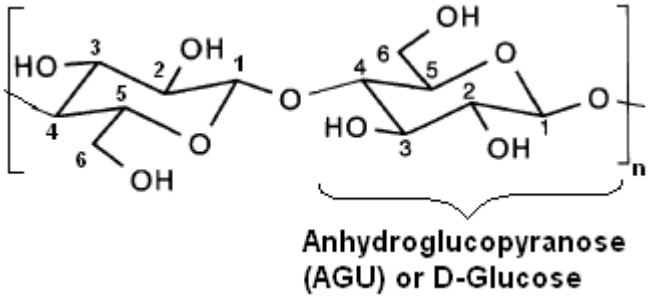

Figure 2-13. Structure of Cellulose [151]

2.7.1 Cellulose Derivatives

Cellulose itself is insoluble in water. If the hydroxyl groups in cellulose are substituted with other functional groups such as ethyl, methyl and/or hydroxypropyl, it results in a cellulose derivative which is soluble in water or other organic solvents. The extent of substitution is usually characterised by the number of hydroxyl groups modified per anhydroglucopyranose unit (AGU) and is referred to as the degree of substitution (DS). For cellulose ethers with branched substitutions (such as hydroxypropyl methylcellulose) because the addition of alkylene oxides results in the presence of new hydroxyl groups, the number of moles of alkylating reagent added per mole of AGU, termed as molar substitution (MS) is also used to define the structure [151,154]. The value of degree of substitution ranges between 0 – 3. The solubility of a cellulose derivative in water or in any other organic solvent depends upon the type of substituent, the molecular weight of derivative and the degree of substitution (DS) of the derivative. Cellulose derivatives are categorised as either esters or ethers and further classifications are organic and inorganic esters, water soluble ethers and ethers soluble in organic solvents (Figure 2-14) [153].

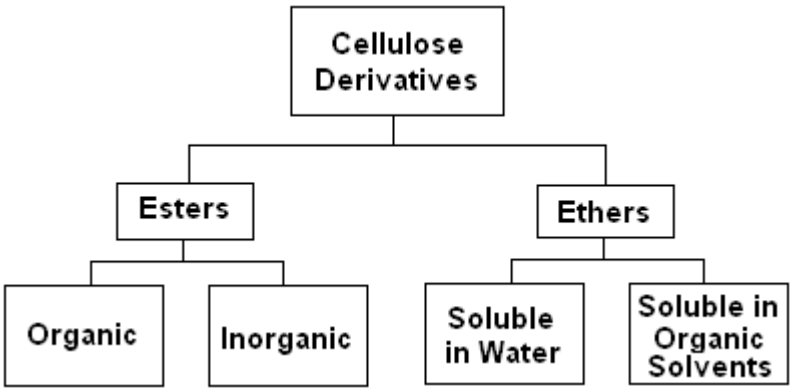

Figure 2-14. Categories of cellulose derivatives [153]

A complete discussion of cellulose esters is beyond the scope of this report, other reports can be viewed [155] for further details about cellulose esters. However, a brief introduction of cellulose ethers will be presented in the next section.

2.7.2 Cellulose Ethers

Cellulose ethers are usually achieved by alkylation of cellulose. These derivatives are obtained by converting the cellulose into an alkali form by treating it with an alkali, usually sodium hydroxide (NaOH). This alkali cellulose is then reacted with a suitable alkylation reagent to achieve the desired cellulose ether. Examples of alkylation reagents include methyl chloride for methylcellulose, methyl chloride and propylene oxide for hydroxypropyl methylcellulose and ethyl chloride for ethylcellulose [155-157]. In order to suspend/disperse the cellulose during the etherification, an inert diluent is also sometimes used. The inert diluents also serve other purposes such as to provide heat transfer, to moderate the reaction kinetics and to improve the substituent distribution uniformity along the glucose chain [156-158]. A variety of alcohols (ethanol, isopropyl alcohol, ter-butyl alcohol), acetone and water are the commonly employed inert diluents [156,158,159]. The degree of substitution (DS) along with degree of polymerisation, molecular weight and the type of substituent are important in determining the properties of cellulose ether. Also, the distribution of substituents along the glucose chain and the polymer unit is an important characteristic which governs the rheological characteristics of the resulting cellulose ether [153,157]. It is worth mentioning here that the degree of substitution, as defined earlier, only describes the average number of hydroxyl groups substituted by the substituent and it does not specify the actual distribution of the substituent either within a polymer chain or among the polymer chains. Therefore, cellulose ethers with the same alkyl group and the same value of DS

can show different rheological characteristics due to the different distribution of alkyl groups within the cellulose ether [157]. The distribution pattern of the substituent is not controlled during the commercial scale manufacturing of cellulose ethers, however, it has been shown that by selecting appropriate reaction conditions during laboratory production of cellulose ethers that a selective substitutional structure and thus desired characteristics can be achieved [160-165].

Availability of a variety of substituent groups, degree of substitution, molecular weight and structure of cellulose ethers results in a variety of useful properties. These properties include water retention, water absorbance, solubility in different solvents (i.e. water and other organic solvents), film formation, lubrication, surface activity, controllable rheology and gel formation [153,157,166]. Modulation of flow behaviour (i.e. rheology) is considered the most important property of cellulose ethers [157]. Because of their highly varied and useful properties, cellulose ethers have found applications in a wide range of industries including oil recovery, textiles, paper, paints, construction/building materials, ceramics, detergents and adhesives. Also, the fact that the cellulose ethers are physiologically harmless, allows their use in industries such as pharmaceutical, food, cosmetics and personal care products [153,157,166].

Table 2-2 summarizes some of the commonly used cellulose ethers along with their physical properties and uses.

Cellulose Ether	Typical Properties	Common Uses
Sodium Carboxy-methylcellulose (CMC)	• Soluble in hot and cold water, insoluble in organic solvents • Molecular weight (M_w) ranges between $9x10^4$ and $7x10^5$ • Depending on M_w, solutions can be pseudoplastic or thixotropic	• **Thickener** in dessert toppings, pet food, toothpaste and pharmaceutics • **Binder** in ceramics and paper products • **Film former** in textiles and adhesives
Ethylcellulose (EC)	• Soluble in organic solvents • Forms mechanically tough and stable films in organic solvents • Elongation, tensile strength and flexibility of film is a direct function of molecular weight	• **Film former** in printing inks, lacquers and varnishes • **Additive to increase toughness** in hot melts, lacquers and varnishes
Hydroxyethylcellulose (HEC)	• Soluble in hot and cold water, insoluble in hydrocarbon solvents • Molecular weight (M_w) ranges between $9x10^4$ and $1.4x10^5$ • Depending on M_w, solutions can be Newtonian or pseudoplastic	• **Water-binder** in ceramic glazes and paper coatings • **Thickener** in polymer emulsions, latex paints, cements and shampoos
Ethylhydroxy Ethylcellulose (EHEC)	• Ethyl modification of HEC • Soluble in water and aqueous solutions are soluble in alcohols, glycols and ketones • Aqueous solutions can be Newtonian or pseudoplastic	• **Thickener and stabilizer** in plasters, detergents, water-borne paints, cosmetics and pharmaceutical applications
Methylcellulose (MC)	• Soluble in water and for DS>2.4, in a variety of organic solvents • Aqueous solutions gel at approximately 55 ^{0}C (independent of M_w) • Solutions are pseudoplastic (liquid state) and thixotropic (gel state)	• **Thickener** in latex paints, food and cosmetics • **Binder** in tablet formulations and slip cast ceramics • **Controlled release** in tablets due to gelation
Hydroxypropyl Methylcellulose (HPMC)	• Soluble in water and for DS>2.4, in a variety of organic solvents • Aqueous solutions gel at approximately 55 ^{0}C (independent of M_w) • Solutions are pseudoplastic (liquid state) and thixotropic (gel state)	• **Stabilizer and thickener** bakery and other food items and personal care items • **Binder and emulsifier and controlled release** in tablet formulations

Table 2-2. Commercially available cellulose ethers, typical properties and uses [157]

2.8 Methylcellulose (MC) and Hydroxypropyl Methylcellulose (HPMC)

Substitution of hydroxyl groups (OH) of cellulose by methyl groups (CH_3) using methyl chloride, results in the simplest derivative of cellulose which is called methyl cellulose (MC) [167]. Addition of propylene oxide with methyl chloride during this substitution results in hydroxypropyl methylcellulose (HPMC) [155,157]. Heymann [168], in 1935 was the first to investigate the reverse thermal gelation behaviour of both MC and HPMC in water. Since then, many authors have investigated aqueous solutions of MC and HPMC for their reverse thermal gelation tendencies and these cellulose ethers (in their aqueous solutions) are therefore considered some of the largest members of reverse thermal gel forming polymers [109,157,168-183]. Aqueous solutions of both MC and HPMC form a gel upon heating and revert back to a solution phase upon cooling. It is generally agreed that similar to Pluronics, hydrophobic interactions between different molecular chains resulting in increased polymer – polymer interaction, are the main reason behind the formation of reverse thermal gels by MC and HPMC. At low temperatures, depending upon their degree of substitution, both MC and HPMC are soluble in water and this solubility is caused by hydration of both methoxy and hydroxyl groups at low temperatures. As the temperature is increased, the hydrogen bonds between water molecules and methoxy groups are broken causing an increase in hydrophobicity of chains containing of methoxy groups. Depending upon the concentration of the polymer in the solution, above a certain temperature called the Lower Critical Solution Temperature or LCST, this increased hydrophobicity results in increased molecular association (i.e. polymer – polymer) interaction and thus the solution phase separates and converts into a three dimensional, physically cross linked gel phase. Since the gel formation does not involve making or breaking of any covalent bonds, it is considered completely reversible and as the formed gel is cooled back, it returns to a solution phase [177,179,184-186]. It is important to note that only methyl celluloses for which the distribution of substituents in the anhydroglucopyranose units and along the chains is not uniform (i.e. a heterogeneous substitutional structure) form gel whereas those with uniform (inter and intra chain) substitutional structure do not form gel in water [170,177,179,184,186]. Molecular weight, degree of substitution

(both DS and MS), concentration and heating rate are the main parameters which control the gelation characteristics such as gelation temperature, cloud point temperature and gel strength [157,167,185]. The effect of varying different parameters on the characteristics of aqueous solutions/gels of MC and HPMC is discussed below and table 2-3 summarises the effect of increasing these parameters.

Parameter	Solution/Gel Characteristics			
	Precipitation Temperature (IPT)	Cloud Point Temperature (T_{cp})	Gelation Temperature (T_{gel})	Gel Strength
Molecular Weight	Independent	Decrease	Decrease	Increase
Concentration	Decrease	Decrease	Decrease	Increase
DS	Independent	Decrease	Decrease	Increase
MS	Independent	Increase	Increase	Decrease

Table 2-3. Effect of Increasing Different Parameters on the Characteristics of Aqueous Solutions/Gels of MC and HPMC

2.8.1 Molecular Weight

MC and HPMC with average molecular weights ranging from 20,000 to 400,000 have been studied [109,173,176,187,188] and it was found that increasing the molecular weight results in a slight decrease in the clouding temperature (T_{cp}) and gel temperature (T_{gel}) whereas the mechanical strength of the gels is increased by increasing the molecular weight of the cellulose ethers. The lack of dependence of T_{cp}, T_{gel} on molecular weight is mainly attributed to the high degree of polydispersity (i.e. presence of different molecular weight fractions in the sample) of those celluloses as the polydispersity index ranges between 3 – 10 [109,188]. Also, the wide molecular weight distribution results in clouding occurring over a range of temperature, with the onset of clouding identified as incipient precipitation temperature (IPT) and cloud point temperature (T_{cp}) as the temperature when the solution is completely turbid. Due to the polydispersity, the IPT values of MC and HPMC solutions were found to be independent of the average molecular weight [109,188]. The increase in gel strength was attributed mainly to the presence of

longer polymer chains enabling strong polymer – polymer (i.e. hydrophobic) interactions with increased temperature [109,176,187,188].

2.8.2 Concentration

Typically, the concentration values studied for aqueous solutions of both MC and HPMC range between 0.1 – 2.5% [109,167,171,173,174,176,178,183,187,189-191], however high concentrations such as 20% have also been studied [192]. The effect of concentration on IPT, T_{cp}, T_{gel} and gel strength is more profound compared with the effect of molecular weight as only slightly increasing the concentration (e.g. 0.5%) of MC and HPMC in water results in decreased values of IPT, T_{cp} and T_{gel} and increased values of gel strength [109,167,171,173,174,176,178,187,189,190]. This behaviour of aqueous solutions of MC and HPMC is observed because there is increased intermolecular hydrogen bonding between water and the polymer chains as almost all the MC (or HPMC) molecules are hydrogen bonded with water (at low concentrations). Upon increasing the concentration, the intramolecular hydrogen bonds (within MC or HPMC chains) are increased compared with the intermolecular bonds between MC (or HPMC) and water molecules and thus the hydrophobic effect takes place at lower temperature resulting in lowering of IPT, clouding temperature and gelling temperature [109,167,171,189]. These increased polymer interactions are also responsible for increased gel strength at high concentrations.

2.8.3 Substitution

As defined earlier, degree of substitution (DS) of MC and HPMC along with the molar substitution (MS) of HPMC are also important in determining the gel formation characteristics. It is considered that the methoxyl substitution, due to its hydrophobic nature, is mainly responsible for the gel formation ability of both MC and HPMC whereas the hydroxypropyl substitution only effects the gel formation characteristics but is not the main cause behind the gel formation [109]. The MC and HPMC are only soluble in water in the DS range of 1.4 – 2.0 [109,178,180,183,188,193,194]. Below this range, due to low substitution of the hydroxyl groups by the hydrophobic methoxyl groups, there are sufficient intramolecular and intermolecular hydrogen bonds present within the cellulose chain which do not allow water to form hydrogen bonding with the cellulose chain

and thus the cellulose is insoluble in water. Similarly, for higher substitution of hydroxyl groups with methoxyl group, the cellulose chain is strongly hydrophobic and thus the resulting MC or HPMC is rendered water insoluble. Changing the values of DS and MS did not change the IPT greatly due to the polydispersed nature of substitution but increased DS resulted in lowering of T_{CP}, T_{gel} and formation of strong gels [109,173]. This is due to the increased hydrophobic characteristic of the cellulose chain caused by the increased substitution of hydroxyl groups by the methoxy groups, resulting in increased polymer – polymer interactions. On the other hand, the effect of adding hydroxypropyl groups (i.e. increasing MS) is the reverse to that of adding methoxy groups as increased MS results in increased T_{CP} and T_{gel} and reduced gel strength [109,173,174]. This effect of hydroxypropyl substitution is a result of relatively less hydrophobic nature of hydroxypropyl groups compared with the methyl group (i.e. due to additional hydroxyl groups in hydroxypropyl). This behaviour of hydroxypropyl substitution was also attributed to the molecular level (i.e. steric) arrangement of the structure of cellulose chains [109].

The pattern of substitution (i.e. homogeneous or heterogeneous) of the substituents also affects the characteristics of MC and HPMC aqueous solutions [184,194,195]. Clouding in heterogeneously substituted celluloses starts earlier (i.e. reduced T_{cp}) and it takes place over a wider range of temperature compared with methylceluloses with the same degree of substitution but homogenous distribution of substituents [184,196]. Also, as mentioned earlier, MC and HPMC with a homogenous substitutional pattern do not form a gel upon heating. This difference in behaviour is considered to be due to the presence of highly substituted regions in heterogeneously substituted celluloses [184,194,196]. Due to homogenous substitution of hydroxyl groups with methoxyl groups, the variation of size (i.e. chain length) with substituted and non-substituted regions is small. Therefore, upon heating, homogenously substituted celluloses phase separate in aqueous solutions as short chained, individual structures and thus very little hydrophobic effect takes place with no strong, long chain polymer interactions. Heterogeneously substituted celluloses contain chains with relatively higher substitution (i.e. more hydrophobic) and relatively lower substitution (i.e. less hydrophobic). The presence of highly hydrophobic regions allows early phase

separation (i.e. reduced T_{cp}) when heating aqueous solutions and also, as the phase separation starts, molecular chains with relatively lower substitution remain dissolved whereas only the chains with highly substituted regions start to cloud, and thus the clouding takes place over a wider temperature interval [184,196]. The presence of these varying substitutional regions is also the reason behind gel formation as the polymer interactions are not in the form of short chain, discrete structures as in the homogenously substituted MC and HPMC. Due to the presence of regions of varying substitution (i.e. varying hydrophobicity), the hydrophobic interactions are enhanced and strong, long chained polymer – polymer interaction takes place upon heating resulting in the formation of gel structure with highly substituted regions acting as “cross-linking loci” [184,195].

Apart from the effect of the above mentioned factors (i.e. molecular weight, concentration and structure) which are intrinsic to MC and HPMC, factors extrinsic to MC and HPMC such as the effect of additives have also been studied. These additives include salts and surfactants [109,168,189,197], alcohols and glycols [109,168,185,198,199], glycerol [167] and polymers [167,200]. Adding ionic compounds such as sodium chloride (NaCl), potassium chloride (KCl), potassium sulphate (K_2SO_4), ammonium chloride (NH_4Cl) and sodium carbonate (Na_2CO_3) was found to decrease the cloud point and the gelation temperature of MC and HPMC solutions [109,168,189]. This decrease in T_{cp} and T_{gel} is due to the fact that water forms hydrogen bonds with the ions of these compounds and thus the intermolecular hydrogen bonding between water and MC (or HPMC) is reduced which allows the hydrophobic interactions to take place at lower temperatures [109,189]. For the same reason, addition of ionic compounds was also found to increase the gel strength [109]. Some compounds such as urea and sodium dodecyl Sulphate ($C_{12}SO_4Na$, SDS) were found to have an effect opposite to the above mentioned salts and surfactants on gelation characteristics (i.e. increased T_{cp} and T_{gel}) [109,197]. This is due to the association of these molecules to MC molecules in the aqueous solutions. The dissociation temperatures of these molecules are higher which in turn increases the temperature at which the hydrophobic interactions of cellulose chains take place [109]. Addition of alcohols such as ethanol and propanol, and glycols such as ethylene glycol, diethylene glycol, tetraethylene glycol and propylene glycol have been found to increase the

gelation temperature, due to their solvent characteristics for methyl substituents which enhance the intermolecular hydrogen bonding of MC with water and the respective co-solvent [167,185,198,199]. Glycerol, on the other hand, had an inverse effect upon gelation temperature. Adding glycerol resulted in reduction in T_{gel} and this was attributed to affinity of glycerol to water molecules resulting in increased hydrophobic effect in methylcellulose [167]. It must be mentioned here that the different alcohols and glycols were studied as additives with aqueous methylcellulose solutions and no literature was found for solutions of methylcellulose or hydroxypropyl methylcellulose in a non-aqueous solvent (i.e. without the presence of water). Like glycerol, addition of polymers such as polyethylene glycol (PEG), polyvinyl alcohol (PVA) and polyvinyl pyrrolidone (PVP) was also observed to reduce the gel temperature [167,200]. However, the reduction in T_{gel} depended only slightly on the amount of these polymers and the competition for the solubility in water between these polymers and the molecules of MC, resulting in reduced solubility of MC molecules was considered the main reason for this effect [167,200].

Commercially available MC and HPMC are heterogeneous in nature and their degree of substitution is an important factor in determining their solubility in a variety of solvents. Usually, methyl celluloses are categorised as alkali soluble with a DS value between 0.25 – 1 and water soluble with a DS value between 1.4 – 2 whereas above a DS value of 2.4, they are soluble in a wide variety of solvents [157,201].

As mentioned earlier, the pattern of substitution is not controlled during commercial scale production, therefore commercially available MC and HPMC are supplied in different viscosity grades (i.e. viscosity in 2% aqueous solution is usually specified). Both MC and HPMC are available in a large variety of viscosity grades from various manufacturers under different trade names such as Benecel by Aqualon and Methocel by Dow Chemical Company.

2.9 Summary

The literature review showed that the interesting behaviour (i.e. reverse thermal gelation) of polymers such as Pluronics and MC requires investigations to produce possible support material for the jetting of caprolactam. However, it was noticed

during the literature review that both Pluronics and MC were mainly investigated in their aqueous solutions and at temperatures lower than 100^0C. Whereas, for jetting of caprolactam, water inhibits the polymerisation of caprolactam into nylon and the polymerisation takes place at higher temperatures (i.e. near 150^0C). Therefore, investigations of novel combinations of a pluronic as well as MC in non-aqueous solvents at temperatures around 150^0C were identified as the foundations for this research.

3 Experimental

3.1 Introduction

This chapter presents an introduction to the different materials (polymers and solvents) used in the research along with the sample preparation methods. In order to characterize and understand the behaviour of the samples prepared by mixing/dissolving selected polymers and solvents, different experiments such as sample heating, Fourier transform infrared (FTIR) spectroscopy, differential scanning calorimetry (DSC), hot stage microscopy, X–ray diffraction (XRD), viscosity measurements and surface tension measurements were performed on these samples and details of these experimental techniques as applied to the samples during this project are described in this chapter. As the expected build chamber temperature when jetting the mixtures of caprolactam was 150^0C, all the experiments involving heating the samples such as sample heating, hot stage microscopy and differential scanning calorimetry were performed up to a maximum temperature of 150^0C.

3.2 Materials

Polymers used in this project included Pluronic F-127, methylcellulose (MC) and hydroxypropyl methylcellulose (HPMC). These polymers were mainly selected due to their well known reverse thermal gel formation tendencies in aqueous solutions as described in the previous chapter.

3.2.1 Pluronic F-127

Pluronic F-127 (M_w = 12,600, PEO content = 70% of total molecular weight) was purchased from BASF and was used as received. Figure 3-1 represents the chemical structure of Pluronic F-127.

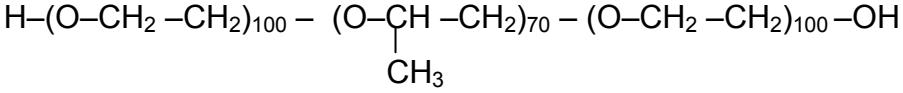

Figure 3-1. Chemical structure of Pluronic F-127

3.2.2 Methylcellulose and Hydroxypropyl Methylcellulose

Methylcellulose (M_n = 13,000, viscosity of 2% aqueous solution = 12-18 mPa.s) and hydroxypropyl methylcellulose (M_n = 86,000, viscosity of 2% aqueous solution = 4000 mPa.s), manufactured by Acros Organics, were purchased from Fisher Scientific (authorized distributors for Acros Organics products in UK). The degree of substitution (DS) value of methylcellulose as supplied by the manufacturer was 1.8 whereas the values of degree of substitution and/or molar substitution for hydroxypropyl methylcellulose were not supplied by the manufacturer. The chemical structure of MC (and HPMC) is shown in Figure 3-2.

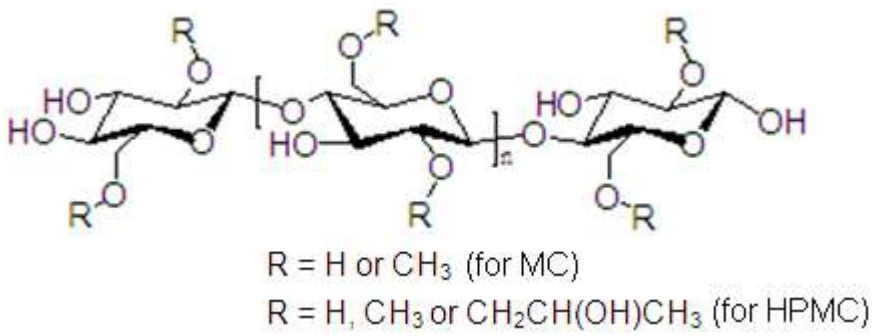

Figure 3-2. Chemical structure of MC and HPMC

3.2.3 Solvents

A variety of non–aqueous solvents were used in this project and all these were purchased from Fisher Scientific and used as received. Table 3-1 presents a list of solvents used in this research.

Solvent	Chemical Formula	Molecular Weight	Boiling Point (^{0}C)	Viscosity (mPa.s at 20^{0}C)
Formamide	CH_3NO	45.04	210	n/a
Ethanediol (Ethylene Glycol, EG)	$C_2H_6O_2$	62.06	197	21
1,2 Propanediol (Propylene Glycol, PG)	$C_3H_8O_2$	76.09	187	45
1,3 Butanediol (Butylene Glycol, BG)	$C_4H_{10}O_2$	90.12	203	25.83[1]
Octanol	$C_8H_{18}O$	130.23	195	9

Table 3-1. Solvents used in this research (data supplied by manufacturers in material safety data sheets)

[1] At 50^{0}C

3.3 Sample Preparation

Samples of different compositions were prepared by mixing a weighed amount of polymer in solvent and a variety of combinations were studied. Total weight of each composition was held constant at 50 g. Table 3-2 presents the details of different compositions prepared. Mixing was performed at room temperature (i.e. 20^0C) using a magnetic stirrer. In order to prepare a composition, a carefully weighed amount of the solvent was added into a wide mouth glass bottle (capacity 125 ml). The bottle was then placed on the magnetic stirrer and the magnet was placed inside the bottle to start the stirring. A carefully weighed amount of the respective polymer was then added gradually into the solvent being stirred. All the samples were allowed a minimum of 24 hours mixing time. After mixing, these samples were kept in a refrigerator (temperature 2–4^0C) for approximately 24 hours for stabilisation of the composition.

Polymer	Solvent	Compositions (w/w)
F-127	Water	15, 20, 25 and 30%
	Formamide	15, 20, 25, 30 and 35%
	Ethylene Glycol	25% (in each solvent)
	Propylene Glycol	
	Butylene Glycol	
	Octanol	
	Ethylene Glycol	10, 15, 20 and 25%
HPMC	Water	2, 3, 4 and 5%
	Ethylene Glycol	5, 10, 15 and 20%
MC	Water	2, 3, 4, 5, 6, 8 and 10%
	Ethylene Glycol	1, 2, 5, 10, 15 and 20%
	Propylene Glycol	1, 2, 5, 10, 15 and 20%
	Butylene Glycol	1, 2, 5, 10, 15 and 20%

Table 3-2. Binary compositions prepared and analysed during current research

Ternary compositions, comprising of methylcellulose, water and either propylene glycol or butylene glycol were also prepared to analyze the effect of adding water as a solvent. Due to the wide range of possible compositions involving three components, experimental design software (Design Expert 7 for Windows) was used to obtain an experimental design for both propylene glycol and butylene glycol based compositions. The following constraints on each component were used in designing the mixture experiments for ternary compositions:

$$2\% \leq MC \geq 10\%$$

$$2\% \leq Water \geq 20\%$$

$$70\% \leq Glycol \geq 96\%$$

The binary compositions of MC in glycols showed that a soft gel forms for a concentration as low as 2% whereas for a concentration of 10%, a strong, solid like structure is obtained. Therefore, the limits for MC concentration were based on the results achieved from the binary compositions of MC and glycols. Also, as the addition of water lowers the boiling point of the glycols, it was decided to use a maximum limit of 20% of water to minimize lowering of the boiling point of the binary solvent (i.e. water and glycol). Finally, upper and lower limits for the remaining component (i.e. glycol) were respectively calculated based on the minimum and the maximum of both MC and water so that the total of each composition remained the same. Table 3-3 lists the different ternary compositions prepared. Mixture compositions generated by the software were prepared by first mixing, using a magnetic stirrer, the two solvents (i.e. water and glycol) in wide mouth glass bottles for approximately 1 hour and then adding the weighed amount of MC while the solvent was constantly stirred. As for the binary compositions, a minimum of 24 hours was allowed for the mixing of all the ternary compositions and they were kept in the refrigerator for 24 hours after the mixing was stopped.

Sample Number	MC (%)	Water (%)	Glycol (%)
1	2	2	96
2	6	2	92
3	10	2	88
4	6	6	88
5	2	11	87
6	6	11	83
7	10	11	79
8	2	20	78
9	6	20	74
10	10	20	70

Table 3-3. Ternary compositions prepared and analysed during current research

3.4 Thermal Gravimetric Analysis

Thermal gravimetric analysis (TGA) is a commonly employed technique to measure the change in weight of a sample with respect to the change in temperature. As all the compositions were to be heated to a high temperature (i.e. 150^0C), it was important to measure the fraction of weight lost by each solvent at high temperatures. All the solvents used during this project were subjected to TGA to measure the weight loss caused by heating. TGA was performed by a TA Instruments Q5000 IR using Platinum pans. Purge gas (i.e. Nitrogen) was supplied to the heating chamber at a rate of 25cm^3/min. The approximate starting weight of each sample was 50 mg. The samples (i.e. solvents) were heated from 25^0C up to 200^0C at a rate of 5^0C/min and weight fraction at each degree rise of temperature was recorded.

3.5 Sample Heating

In order to observe the change in the state of samples, they were heated from 25 to 150^0C (25 to 90^0C for water based samples). Approximately 3 gof each sample was placed in a glass sample tube (inner diameter 16 mm) and heating was performed using an oil bath. Samples were heated using an average heating rate of approximately 5^0C/min and were allowed to cool under natural cooling. Qualitative observations of each sample were made by tilting the sample tube and poking the sample with a steel rod. Up to 50^0C observations were made after every 5^0C whereas after 50^0C, observations were made after every 10^0C rise in

the temperature. Different states were identified based on the relative thickness/strength of samples such as liquid, viscous liquid, soft gel, strong gel and solid. Observations were also made during the cooling of samples.

3.6 Infrared (IR) Spectroscopic Analysis

It is well known that all the atoms present in a molecule are in continuous vibration with respect to each other (above absolute zero). Atoms, based on their relative arrangements within a molecule can vibrate in different ways such as stretching, wagging, scissoring, twisting and rocking. A good example is methylene or CH_2 group in which there are three atoms, a central carbon atom with two hydrogen atoms. All the bonds in methylene are single bonds and therefore its atoms can show all the above mentioned modes of vibration (Figure 3-3). Each molecule thus has specific vibrational frequencies associated with it corresponding to its chemical structure and movement of atoms within it. The molecule absorbs the infrared (IR) radiation focussed on it when the frequency of the IR radiation is equal to the frequency of a specific vibration present in the molecule due to the relative vibration of atoms. IR spectroscopy is thus based on this principle that each different chemical structure (molecule or compound) absorbs different frequencies (or wavelengths) of IR radiations based upon its chemical structure and the arrangement of atoms within the molecule. Plotting the transmitted radiation intensity (on a vertical axis) against the frequency (on a horizontal axis) shows what is termed the FTIR spectrum of the molecule or the compound. Since, each molecule has its own distinctive energy levels, no two compounds (unless very similar) can have the same IR spectra. Therefore, the IR absorption spectrum is considered the most unique physical property of a molecule and it is also referred to as the *'fingerprint'* of a molecule [202-205]. Due to its simple, easy and quick operation and relatively low cost equipment, Infrared spectroscopy is a very commonly employed technique for polymer characterization. Each different functional group (such as methyl (CH_3), hydroxyl (OH), carbon to carbon double bond etc) or molecules in a polymer have a specific spectrum of radiations absorbing at specific frequencies. Recording the spectrum of a molecule and comparing it with the spectra of different functional groups enables the determination of functional group(s) present and thus the chemical structure of the molecule can be determined.

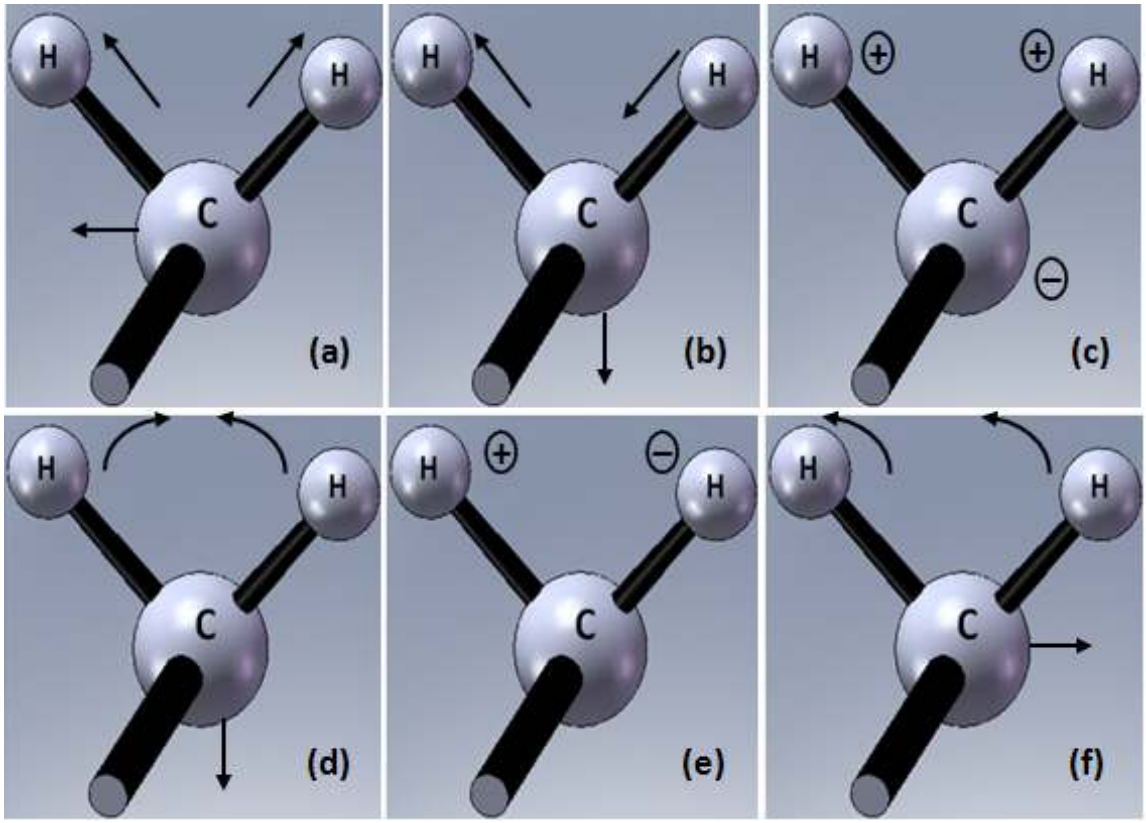

Figure 3-3. Vibrational Modes[2] of Methylene (CH_2) (a) Symmetrical Stretching (b) Antisymmetrical Stretching (c) Wagging (d) Scissoring (e) Twisting (f) Rocking [202,205]

Infrared radiation is passed through the sample and depending upon the functional groups present and the molecular arrangement of the sample composition, the sample absorbs radiation at specific wavelengths (or frequencies) corresponding to its molecular structure. A spectrum for the sample is thus obtained by measuring the intensity of absorbed radiation at each particular wavelength. Typically, a mathematical function transformation technique known as Fourier Transform is used to continuously and simultaneously record the transmitted radiation wavelengths and corresponding intensities. Therefore, the technique is commonly referred to as Fourier Transform Infrared (FTIR) spectroscopy.

Different sample preparation techniques are used in FTIR spectrometers depending upon the type of material to be examined (i.e. liquid, powder or solid). For liquids, the sample is prepared in the form of a very thin film (approximately 2 μm) by pressing the sample between two crystalline discs. Commonly used

[2] Arrows show the relative motion of atoms within the plane of page and "+" and "–" signs indicate motion perpendicular to the plane of page, towards and away from the reader respectively.

materials for discs include pure salts such as sodium chloride (NaCl), calcium fluoride (CaF_2) and barium fluoride (BaF_2) which are IR transparent. For solids, the same method can be used by melting the solid and pressing it between the two crystals. In the case of powders and solids, a cast film technique is also employed whereby the material (i.e. solid or powdered) is dissolved in a suitable solvent. A drop of this solution is deposited and subsequently dried in order to evaporate the solvent and obtain a thin film of the sample. Another method commonly used for solids and powdered materials involves the crushing of the material with a salt such as potassium bromide (KBr) to produce a fine powdered mixture. This mixture is then pressed in a die to produce a pellet with the sample material suspended in the KBr and this pellet is used as the sample to be analysed by FTIR spectrometer. This method is typically employed when it is difficult to produce a thin film by melting the solid and/or when the material is not soluble in any appropriate solvent [205].

To obtain IR spectra of solids, a technique known as Total Attenuated Reflectance (ATR) is also used. This technique is based on the reflection caused by a difference in the refractive index of two materials. When a radiation beam enters into a low refractive index (rarer) medium from a high refractive index (denser) medium, some fraction of radiation is reflected back. The amount of reflected radiation is a function of angle of incidence of the beam and therefore, increases as the angle of incidence increases. If the beam enters the medium at an incident angle greater than a critical angle, all the radiation is reflected back. Also, before reflecting back, the radiation penetrates a few micrometers (μm) into the less dense medium and this penetration is termed an evanescent wave. The intensities of the reflected radiations related to those frequencies which the material absorbs due to its chemical structure, are reduced and the IR spectrum of the sample is thus achieved. The sample (i.e. material to be analysed) is pressed against a crystal of high refractive index and low IR absorbance in order to obtain an IR spectrum using ATR. Typical crystals used in ATR include diamond, zinc selenide (ZnSe), silicon and germanium [202,205].

In order to understand the changes caused by heating the samples, it was decided to perform Fourier Transform Infrared (FTIR) of samples before and after heating. For Pluronic F-127 and F-127 in ethylene glycol, a Shimadzu FTIR-8400S

spectrometer was used to analyse all the samples with a standard deuterated L-alanine doped triglycine sulphate (DLaTGS) detector. Spectral resolution was 4 cm^{-1} and infrared (IR) spectra were recorded by scanning 64 times for each measurement. IR spectra for all the F-127 in ethylene glycol samples were obtained by sandwiching the sample between two round (25 mm diameter x 4 mm thick) sodium chloride (NaCl) crystal windows whereas the IR spectra for Pluronic F-127 was obtained by using the Attenuated Total Reflectance (ATR) technique with a diamond crystal. For MC, due to its powdered state, the KBr pellet method was used to obtain the IR spectra. Due to the high concentration of MC, 20% MC in any of the three glycols could not be sandwiched between NaCl crystals, therefore, IR spectra of these samples were obtained using the ATR technique. Hot stage FTIR-ATR was performed on 20% MC in ethylene, propylene and butylene glycol using a Bruker Tensor 27 spectrometer with a spectral resolution of 4 cm^{-1} (scanned 64 times). Each sample was placed on the ATR cell (Golden Gate, Graceby-Specac). FTIR spectra were obtained at different temperatures during cooling and heating and an equilibrium time of 2 minutes at each temperature was used.

3.7 Hot Stage Microscopy

Optical microscopy is an experimental technique which is frequently used to observe physical phenomena that are difficult to observe with the naked eye. Observing the samples using an optical microscope while they are being heated using a hot stage provides useful information about changes in the physical state of the samples with respect to temperature. Therefore, hot stage microscopy of selected samples was performed using a Leica DM/LM microscope. An objective lens of 10x magnification with a total magnification of 100 times was used to observe the samples. The microscope was setup for transmitted light and crossed polarisers were used to observe the samples for any change in the crystalline state during heating and cooling. A Mettler Toledo FP90 central processor was used to control the temperature during microscopic examination of the samples and they were mounted on the microscope slide using a Mettler Toledo FP82HT hot stage. Samples for microscopic examination were prepared carefully by dropping a small volume of the material on a glass slide (76mm x 26mm, 0.8mm to 1.0mm thick) and placing a cover slip on top of the sample. All the samples

were heated from 25 to 150^{0}C using a heating rate of 5^{0}C/min and were kept at 150^{0}C for 1 min. The maximum temperature for Pluronic in ethylene glycol samples was restricted to 100^{0}C. The reason for heating up to 100^{0}C was that if the sample was heated to 150^{0}C, it flowed out of the field of view making it difficult to observe during the cooling process. Samples were cooled at natural cooling rate. The images were captured using a JVC colour video camera at 1 frame per second. A video file was recorded for each sample and images at the desired temperature were obtained from the recorded files using a video file playback, editing and image capturing software (Studio Player version 3.0).

3.8 Differential Scanning Calorimetry

Differential Scanning Calorimetry (DSC) is a thermal analysis technique which is based on measuring and comparing the heat absorbed (or released) by a sample and a reference with respect to the temperature [206]. The sample is typically contained in a small metallic container (pan), as shown in Figure 3-4 whereas a similar empty container is used as the reference. Typical sample size is between 10–20 mg. Both the sample and the reference pans are heated/cooled at a controlled rate inside a closed chamber and the difference in the heat flow between the two pans is recorded. During any phase change process such as melting or crystallisation, the heat flow to or from the sample pan is different than the reference pan. Thus, by recording the differential heat flow between the two pans, when the sample absorbs heat (i.e. during melting), an endothermic peak is obtained whereas if the heat is rejected by the sample (i.e. typically during crystallisation), an exothermic peak is obtained. Flow of an inert gas (commonly nitrogen) is also maintained inside the heating chamber to ensure a dry atmosphere and to avoid possible oxidation that can be caused by the presence of air. The technique is commonly employed to find the melting temperature and/or crystallisation temperature of polymers. DSC of selected samples was performed in order to observe endothermic and exothermic changes and to observe the melting temperature during heating and crystallisation/solidification temperature upon cooling of different samples. The equipment used for the DSC was a DSC Q200 from TA Instruments. Three different samples of each selected composition were tested and the approximate weight of each sample tested was 15 ±3 mg. All the samples were prepared in hermetically sealed aluminium pans with lids (see

Figure 3-5) and placed in the heating chamber. Nitrogen gas (N_2) was supplied to the heating chamber at a rate of 50 cm^3/min. All the samples were heated from 15 to 150^{0}C and cooled back to 10^{0}C using heating/cooling rates of 5^{0}C per minute. Isothermal conditions (thermal equilibrium) were maintained at the maximum temperature for one minute for all samples.

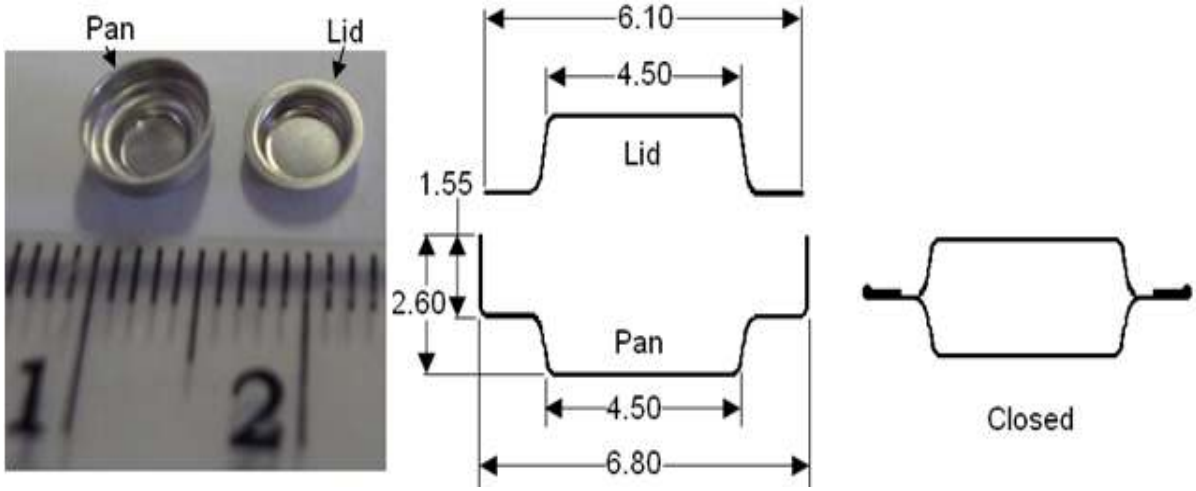

Figure 3-4. Hermetically sealed aluminium DSC pan and lid

3.9 X-Ray Diffraction

X-ray diffraction (XRD) is a commonly employed analytical technique for crystallographic analysis and can be used for characterization of polymers [207]. X-rays of known energy and wavelength are allowed to strike the surface of the sample at a specified range of incident angles. By recording the diffraction pattern created after the X-rays strike the sample, information about the presence of amorphous or crystalline phases present in the sample is provided. In order to determine changes in the ordering of the molecular arrangement (i.e. crystalline or amorphous) caused by heating and cooling of the samples, X-ray diffraction (XRD) of the highest concentration samples was performed. XRD was performed using a Bruker D8. All the samples were analysed between 2θ = 1^o to 30^o at a scan speed of 0.02^o/second using CuKα radiation (wavelength = 1.5418 Å, 40kV and 40 mA). A sample holder, shown in Figure 3-5, was used to hold the samples during XRD measurements. The sample holder was formed by sticking a metallic plate (dimensions shown in Figure 3-5(b)) on a glass slide having dimensions 23 x 56 mm.

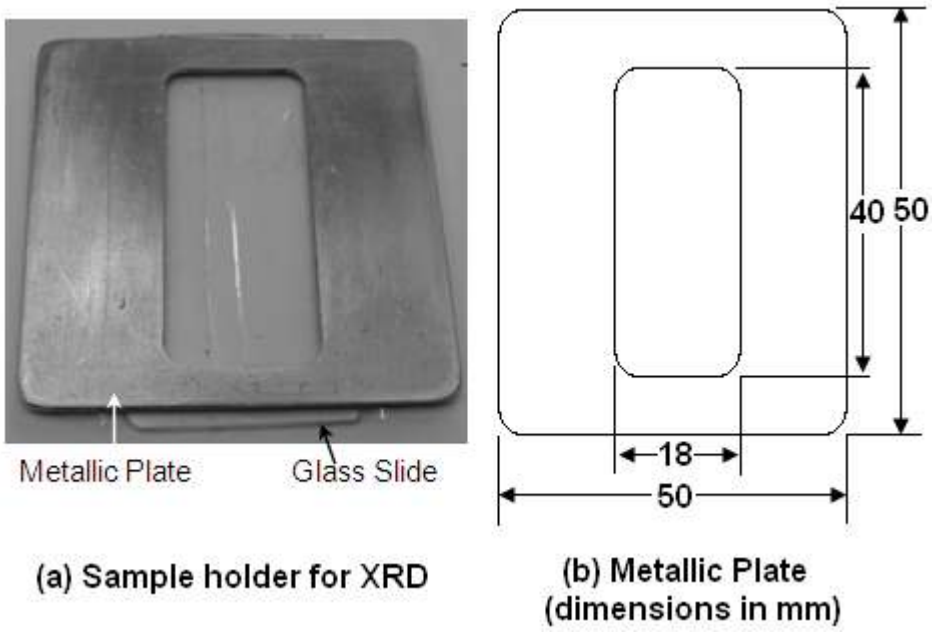

Figure 3-5. Sample holder used for XRD measurements

3.10 Viscosity Measurements

The viscosity of a liquid is considered a key parameter in determining its jettability as well as the quality (i.e. resolution) of the printed pattern [17,21,208]. The viscosity of a liquid is a strong function of temperature and in order to be jetted using a piezoelectric inkjet head, the viscosity value must be within 0.5-40 mPa.s [18]. In order to quantify the observations made during heating and cooling of the samples and to analyse the behaviour of gels at high temperatures and shear rates to evaluate their suitability for jetting, viscosities of selected samples were measured. Viscosity measurements were performed using an Anton Paar Physica MCR 101 bench-top rheometer. Parallel plates (diameter 25 mm) with a gap of 1 mm were used to measure the viscosity (Figure 3-6). Although, using a cone and plate typically gives better shear profile, a parallel plate arrangement was used because of the gelation of compositions upon cooling. Viscosities of selected samples were measured at constant temperatures of 50, 60, 70, 80 and 90^0C. At each temperature, the shear rate varied linearly from 100 to 1500 s^{-1} in 5 minutes and 15 measuring points were used between this interval to record the viscosity.

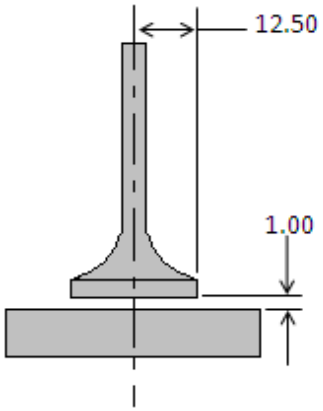

Figure 3-6. Parallel plate arrangement used for viscosity measurements (dimensions in mm)

3.11 Surface Tension Measurements

The surface tension of a liquid is also an important characteristic which affects the jettability of the liquid at a given temperature. The spherical shape of the droplet ejecting from the nozzle is mainly due to the surface tension [21]. Surface tension is a weak function of temperature and the required range for inkjet printing is 20-70 mN/m [18]. The contact lamella method was used to measure the surface tension values of samples. In the contact lamella method, the liquid for which the surface tension is to be measured is held in a specially shaped container shown in Figure 3-7. A cylindrical shaped test body (Figure 3-8) is brought into contact with the liquid. Typically, less than half of the spherical head of the test body is immersed inside the liquid. Due to its wetting characteristics, the liquid forms a curvature around the test body and thus a lamella is formed. By measuring the lamella contour at equilibrium (i.e. between surface tension and weight of liquid) the surface tension of the liquid is calculated. Surface tension measurements of selected samples were carried out at 80^0C using Dataphysics OCA 20 contact angle equipment. The sample was heated to 80^0C and was poured into the sample container. The amount of sample used was such that it filled the cavity of the container and completely wet the top surface of the container. The container was then held inside a thermal chamber (TEC 400) and the temperature was held at 80^0C with a temperature controller (TC 400). Before measurement, the sample was stabilised for approximately 30 minutes to ensure thermal equilibrium. The test body was brought into contact with the surface of the sample so that a lamella contour was formed (Figure 3-8). The shape of the formed lamella contour was

detected using a CCD camera (included with the OCA 20) and the SCA 20 software. The software (SCA 20) utilized the lamella contour information obtained by the camera and the Young – Laplace equation to calculate the surface tension value of the sample.

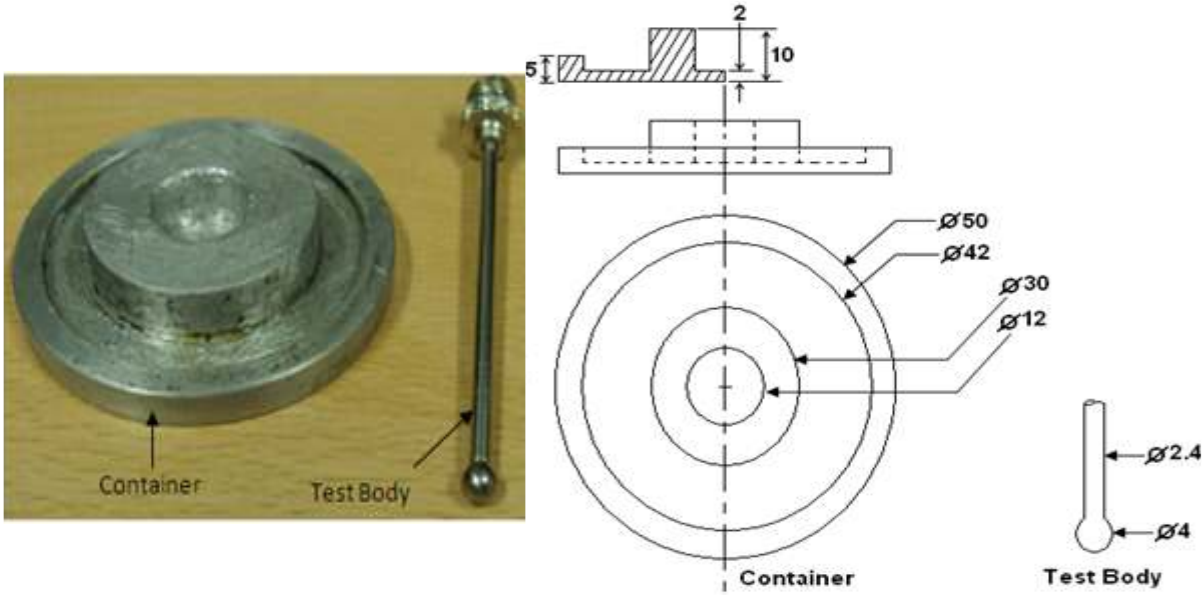

Figure 3-7. Sample container and test body used for surface tension measurements

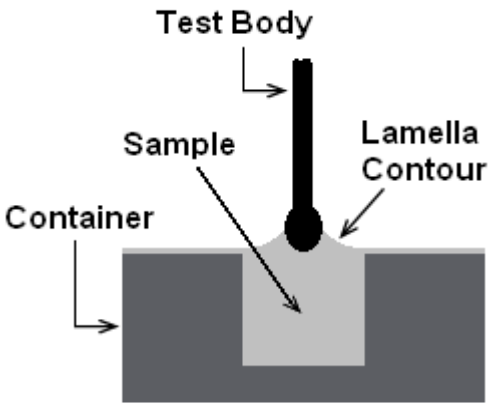

Figure 3-8. Measurement of surface tension by lamella method

3.12 Texture Analysis

Texture analysis is a technique commonly employed in the food industry for measuring the sensory effects perceived by mouth and/or fingers such as the mechanical properties and surface structure of food items [209]. Commonly measured properties using texture analysis include hardness, toughness, tackiness, flowability, and compressibility. The technique mainly involves use of compressive force and probes of different shapes to evaluate different properties.

Both food gels and non-food gels (i.e. used in cosmetics, pharmaceutics and hair products) can be physically characterised using texture analysis. In order to investigate the behaviour of selected (i.e. suitable for jetting) gels under the action of a compressive force, texture analysis was performed and force – displacement graphs were obtained. The texture analysis was performed using a TA.XT plus texture analyser (Stable Micro Systems). A 15 mm diameter cylindrical probe (Perspex) was used. Pre test speed was 10 mm/second and the trigger force was 2.5 g. Test speed was 1 mm/second and the penetration distance, over which the compressive force was measured, was 5 mm. Data was acquired at a rate of 200 points per second. The sample was placed on the platform of the texture analyser so that both the sample (i.e. gel) and the cylindrical probe were nearly concentric. Five samples of each concentration were tested to confirm the repeatability of the results.

4 Pluronic F-127 Based Compositions

4.1 Introduction

This chapter presents experiments performed on compositions prepared by dissolving (mixing) Pluronic F-127 in different solvents. Initially, water based solutions were studied for their gel formation tendencies and later on, in order to observe gel formation at temperatures higher than the boiling point of water (i.e. up to 150^0C) other solvents such as formamide and a variety of glycols were also investigated. Apart from heating of samples to observe gel formation, FTIR, DSC and hot stage microscopy of selected samples of Pluronic in ethylene glycol were also performed to understand and characterize the behaviour with ethylene glycol as a solvent.

4.2 Thermo Gravimetric Analysis (TGA)

In order to find the loss of weight at high temperatures and to determine the volatility of each solvent, TGA of all the solvents was performed and the results are presented in Figure 4-1. The volatility at higher temperatures (e.g. at 150^0C) of these alcohols is evident from the TGA results. Considerable weight was lost by all four alcohols (see table 4-1). Ethylene glycol was the least volatile of these alcohols as more solvent remained at 150^0C compared to the other three alcohols.

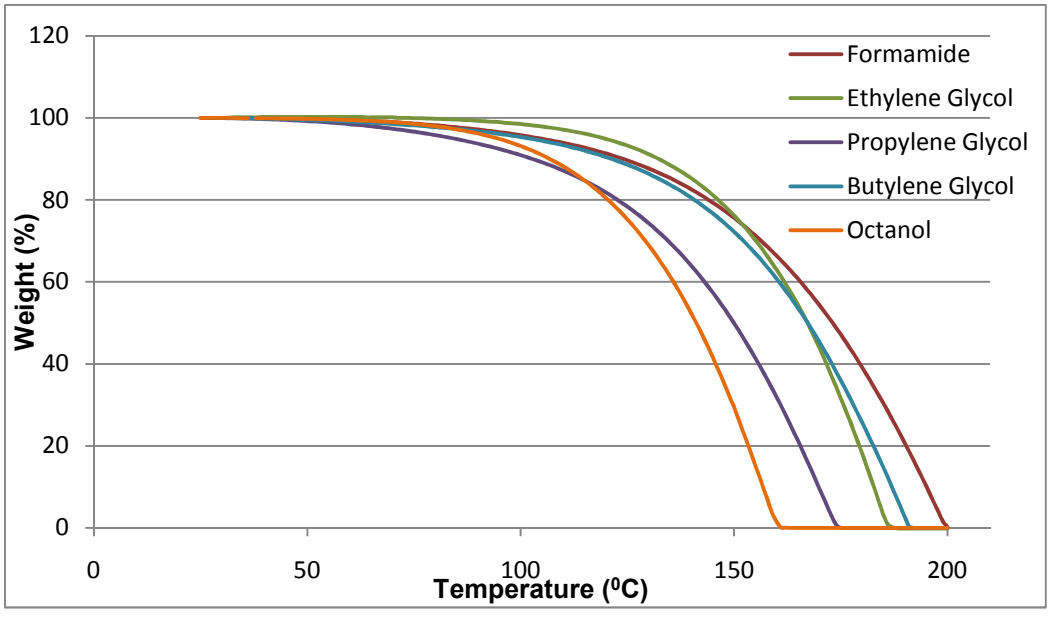

Figure 4-1. TGA results of the solvents used in the project

Temperature (^{0}C)	Weight %				
	Formamide	Ethylene Glycol	Propylene Glycol	Butylene Glycol	Octanol
150	75.62	76.18	49.89	72.22	29.43

Table 4-1. Weight percentage of each solvent remaining at 150^{0}C

4.3 Sample Heating

4.3.1 Water based Samples

Four different samples were prepared with concentrations of 15, 20, 25 and 30% (w/w) of Pluronic in water. The heating results of these samples are summarized in Figure 4-2 whereas a temperature – concentration graph is presented in Figure 4-3.

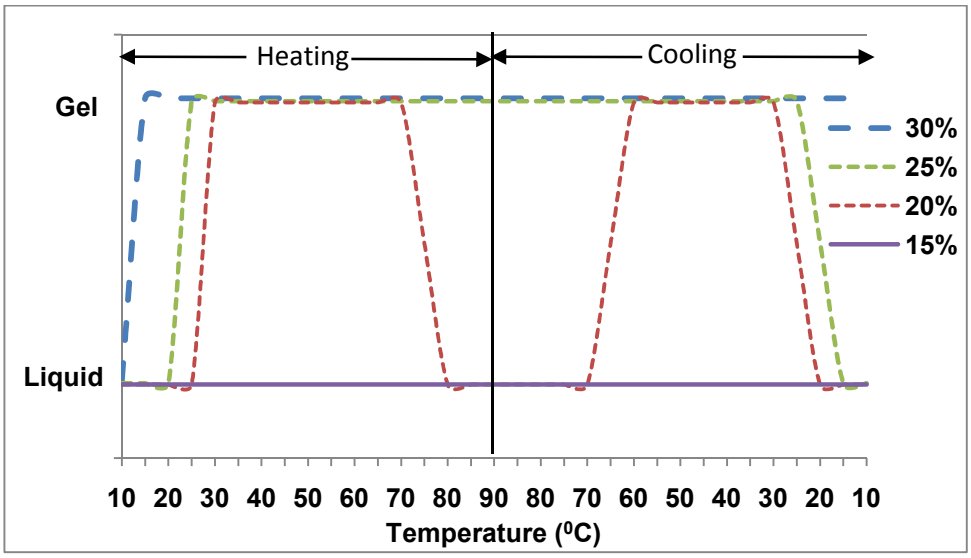

Figure 4-2. Behaviour of Pluronic – Water samples

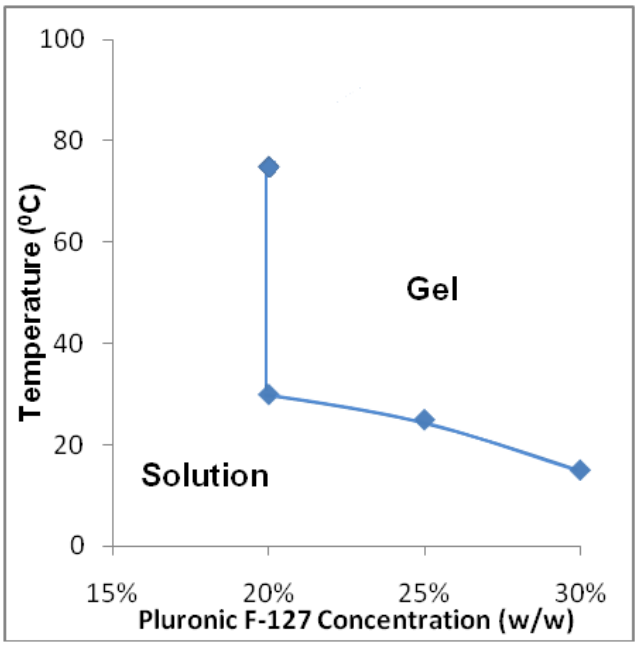

Figure 4-3. Temperature – concentration graph for Pluronic – Water samples

During solution preparation, all these samples showed agglomerate formation but after mixing, when they were kept in the refrigerator (i.e. between 2 – 4^{0}C) for 24 hours, the agglomerates dissolved and were clear liquids (Figure 4-4.a). The sample with the highest Pluronic concentration (i.e. 30%) formed a gel at 15^{0}C whereas 20 and 25% samples turned from solution to a gel state at 25^{0}C and 20^{0}C respectively. The lowest concentration sample studied (i.e. 15%) did not show any gel formation at any temperature. Also, the gel formed by the 20% sample melted between 70 - 80^{0}C and turned into a clear liquid at 80^{0}C. At 90^{0}C, both 30 and 25% were still in a gel state whereas the 20 and 15% samples were liquids (Figure 4-4.b). Upon cooling, the 20% sample again converted into a gel state between 70 – 60^{0}C but no change in the state of other three samples was observed. As the samples were cooled down to 25^{0}C, the 20% sample started to become liquid (Figure 4-4.c). Similarly, the 25% sample turned into liquid at 15^{0}C. The 30% sample did not melt and remained as a gel at 10^{0}C.

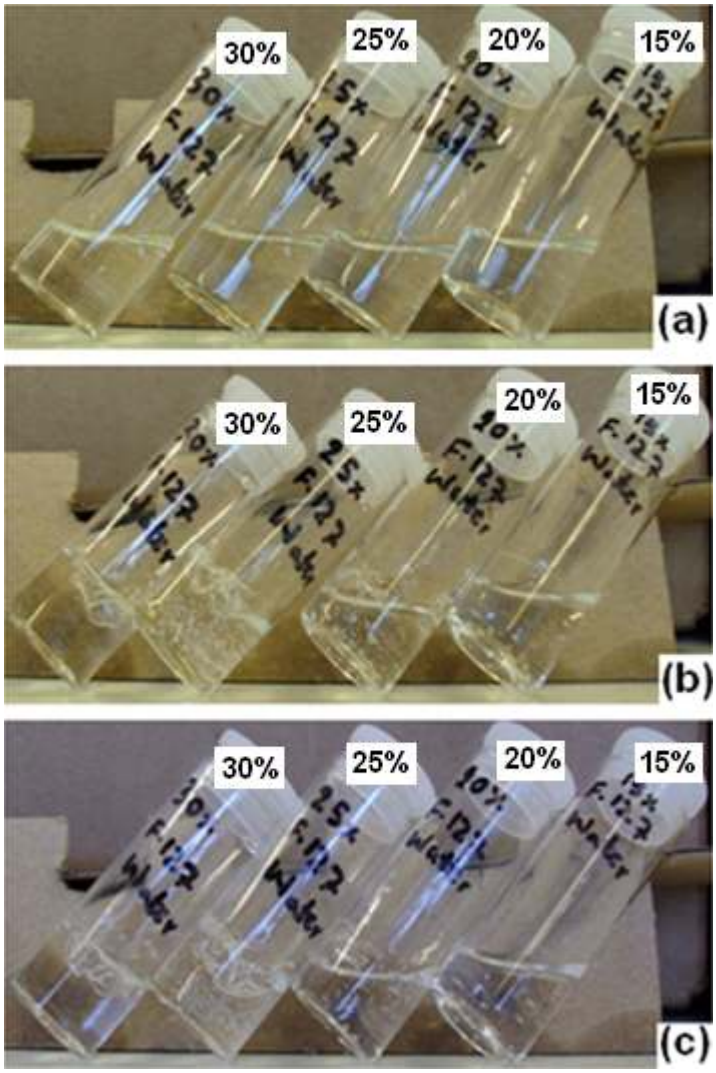

Figure 4-4. Pluronic – Water samples at different temperatures (a) 4^0C, all samples are liquid (b) 90^0C, 15 and 20% are liquid whereas 25 and 30% are gel (c) after cooling at 25^0C, 15 and 20% are liquid whereas 25 and 30% are gel

4.3.2 Non-Aqueous Solvents

Water has a boiling point of 100^0C at atmospheric pressure, whereas for the jetting of caprolactam, the build chamber is expected to be at a higher temperature (i.e. around 150^0C), so it was necessary to use a solvent with a higher boiling point (approximately 175^0C or higher) to make sure that upon heating, the solvent was not boiled out of the solution. The literature revealed that non-aqueous solvents used to dissolve pluronic materials are mainly from the family of alcohols such as methanol, ethanol, propylene glycol, glycerol [130-133,140,141,147,210]. The literature also revealed that all these alcohols/non–aqueous solvents were mainly used in conjunction with water as the solvent. However, Alexandridis demonstrated gelation in formamide as a

solvent without adding water [140,145-147]. Therefore, it was decided to use formamide as the solvent for gel formation. As no information was found in the literature which studied Pluronic in an alcohol without using water, it was decided to use 1–octanol, ethylene glycol, propylene glycol (1,2–propanediol) and butylene glycol (1,3–butanediol) due to their higher boiling points, as solvents to observe gel formation.

4.3.2.1 Formamide

Five different Pluronic in Formamide solutions were prepared with concentrations ranging from 15–35% (w/w) in increments of 5%. The observations during heating of the samples are summarized in Figure 4-5. Based on the observations, a temperature – concentration graph was plotted as shown in Figure 4-6.

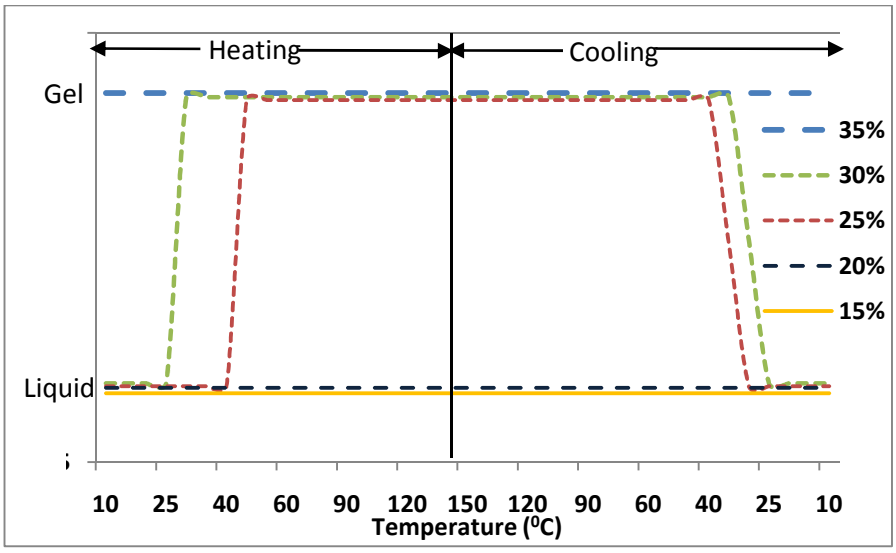

Figure 4-5. Behaviour of Pluronic – Formamide samples

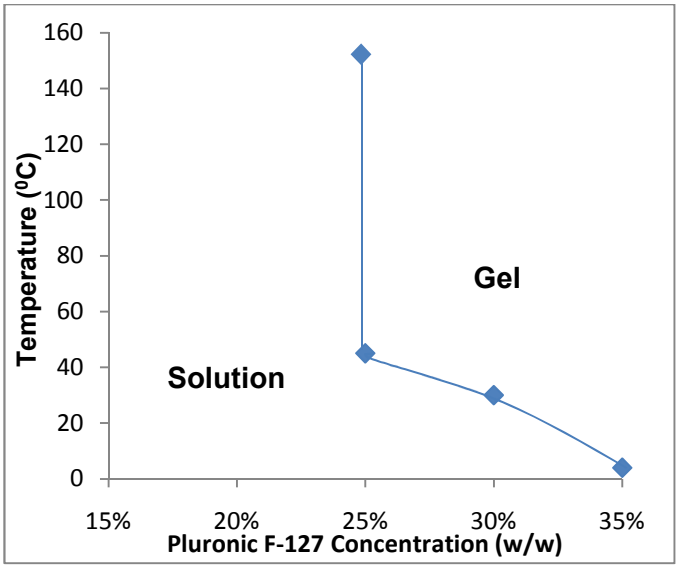

Figure 4-6. Temperature – concentration graph for Pluronic – Formamide samples

Except for the 35% sample which was a gel at temperatures as low as 4^0C, all the other samples (i.e. 15–30%) were liquid at 25^0C (Figure 4-7.a). Both the 15% and 20% solutions remained as liquid solutions up to 150^0C whereas the three higher concentrations showed gel formation at different temperatures. The highest concentration (35%) solution was a gel at all temperatures up to 150^0C whereas the 30% solution formed a gel at approximately 30^0C and the 25% solution formed a gel between 40–45^0C. These gels persisted upon reaching 150^0C (Figure 4-7.b). As the samples were allowed to cool down, the 25% sample converted from gel to solution (liquid) between 35 – 30^0C and at 25^0C, only the 30 and 35% samples were gel (Figure 4-7.c). The 30% sample showed the gel – solution transition between 25–20^0C.

Since the 35% sample was a gel, therefore, during the transfer of this gel from the bottle in which the mixing was performed, into the sample tube resulted in breaking of the gel structure. Due to this breaking, the gel which was clear looked turbid in Figure 4-7 and since it did not melt during the heating cooling, the appearance remained same during heating and after cooling.

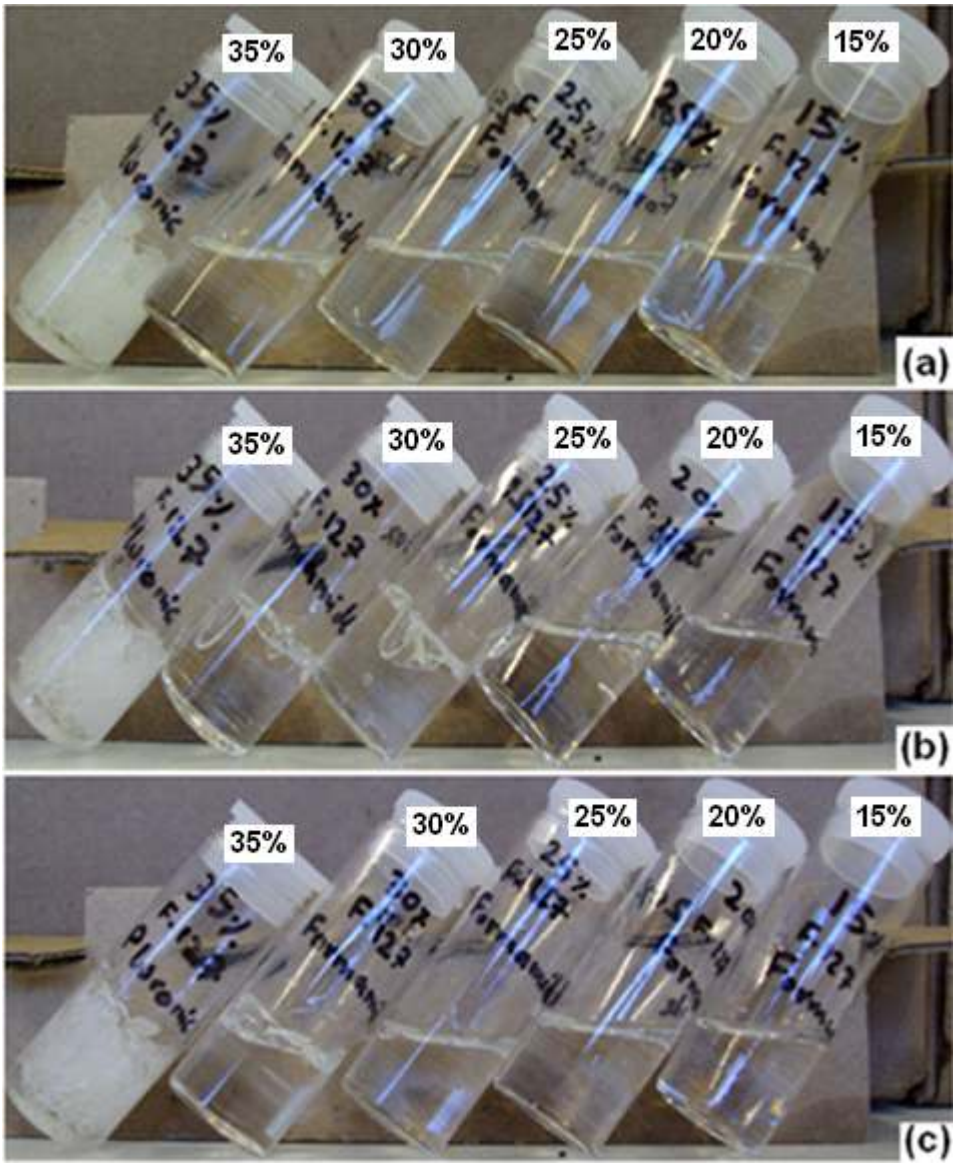

Figure 4-7. Pluronic – Formamide samples at different temperatures (a) 25^{0}C (b) 150^{0}C (c) 25^{0}C (after cooling)

4.3.2.2 Alcohols

To analyze the behaviour of Pluronic in alcohols, 25% (w/w) samples in each solvent (i.e. ethylene glycol, propylene glycol, butylene glycol and octanol) were prepared. The behaviour of the alcohol based samples during heating and cooling and reheating (i.e. second heating cycle) are summarized in Figure 4-8. The samples after the first heating cycle did not return to their original state and formed a solid, therefore, to determine the behaviour of the solidified samples upon heating, a second heating cycle was performed.

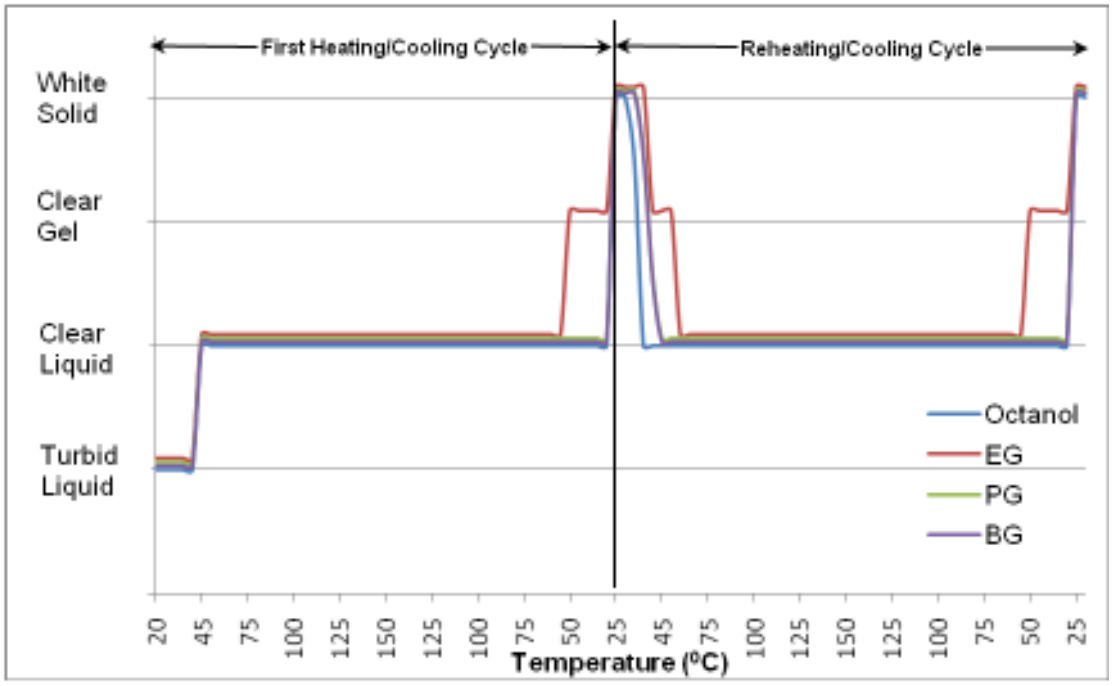

Figure 4-8. Behaviour of 25% Pluronic in octanol, ethylene glycol (EG), propylene glycol (PG) and butylene glycol (BG)

All four alcohol based samples showed similar behaviour upon mixing, as F-127 remained insoluble and formed turbid liquids (Figure 4-9.a). Upon heating, all the samples started turning clear around 35^0C. Between 35–45^0C, all the samples turned completely clear liquids indicating dissolution of Pluronic in all the alcohols within this temperature range. Increasing the temperature up to 150^0C did not change the state of the samples and all the samples remained clear liquids at 150^0C (Figure 4-9.b). The samples were allowed to cool down to the initial temperature. During cooling, it was observed that between 50–60^0C, the ethylene glycol solution turned into a soft gel whereas the other three samples were clear liquid solutions (Figure 4-9.c). Upon further cooling, all the samples became white soft solids near 25^0C (Figure 4-9.d).

The samples were allowed approximately 24 hours at room temperature (i.e. 20^0C) before a reheating experiment was started. At the start of reheating (i.e. at 25^0C) all the samples were soft white solids, as at the end of the first heating cycle. Upon increasing the temperature, the octanol sample started melting and turning clear at 30^0C whereas no significant change was observed in the other three samples. At 35^0C, the propylene glycol and butylene glycol samples also started melting into clear liquids whereas the ethylene glycol sample started turning clear but did not melt (did not show any meniscus

movement) and remained as a gel. At 45^0C, all the samples were completely clear with ethylene glycol being a clear gel and the other three being clear liquids. Increasing the temperature resulted in melting of the gel formed by the ethylene glycol sample between 60–70^0C. At 150^0C, all the samples were in the liquid state similar to that observed during the cooling in the first cycle. Cooling the samples resulted in the formation of a gel state for the ethylene glycol sample near 60^0C whereas the other three samples were clear liquids. Further cooling resulted in the appearance of turbidity in the octanol sample at 30^0C. Turbidity started to appear in the butylene glycol and propylene glycol samples in the range of 25 – 30^0C. Upon reaching 25^0C, the three samples were white soft solids whereas the ethylene glycol sample was a clear gel (Figure 4-9.e). The appearance of turbidity at this temperature was observed in the ethylene glycol sample and it turned into a white solid state in approximately 5-10 minutes.

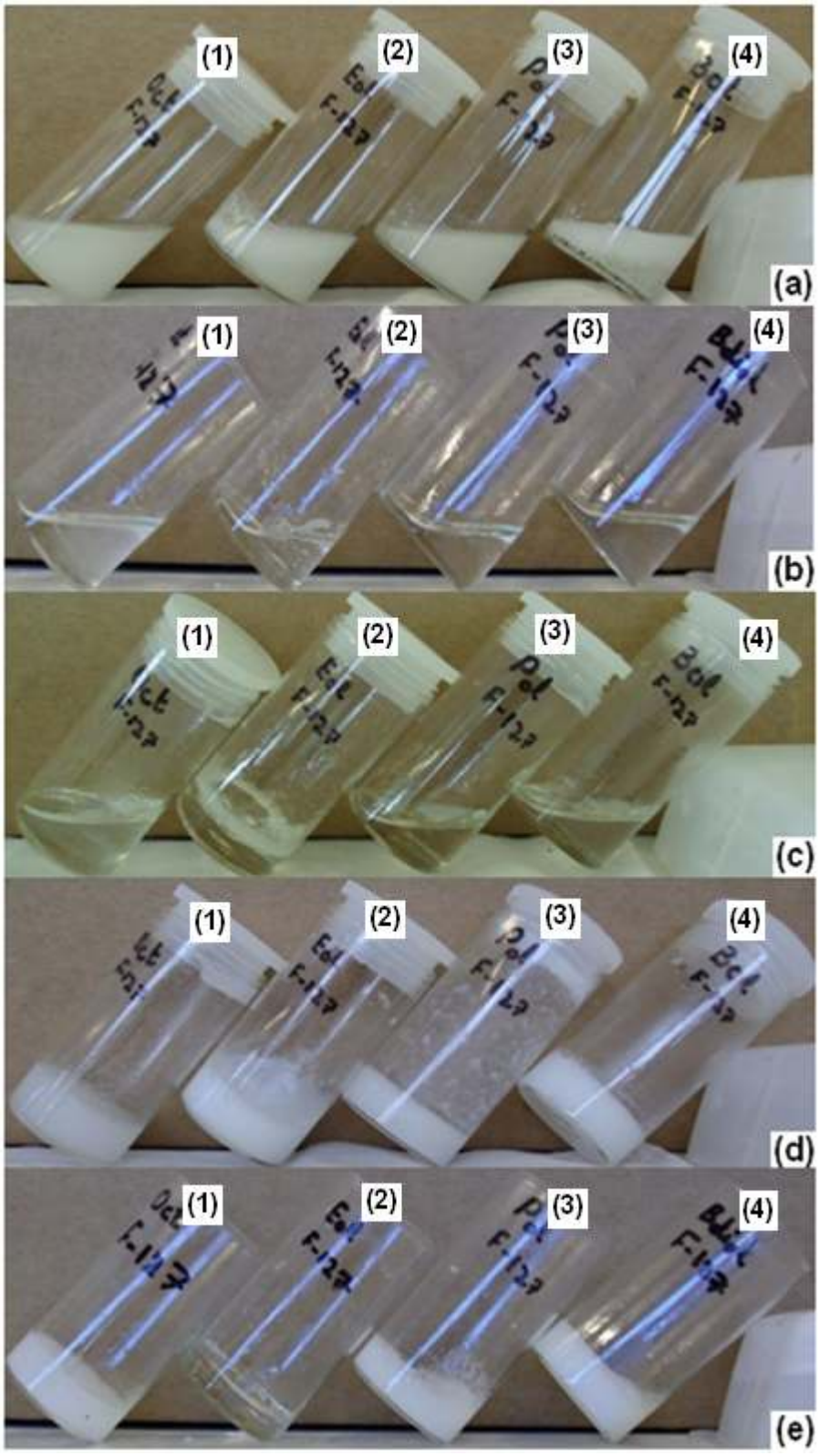

Figure 4-9. Pluronic F-127 in (1) octanol (2) ethylene glycol (3) propylene glycol (4) butylene glycol at different temperatures (a) 20^{0}C (b) 150^{0}C (c) during cooling at 50^{0}C (d) cooled down to 20^{0}C (e) after reheating at 25^{0}C

4.3.2.3 Ethylene Glycol Based Samples

Since the ethylene glycol based sample showed gel formation, it was decided to further investigate the behaviour of Pluronic F-127 in ethylene glycol. Pluronic in ethylene glycol samples were prepared at four different concentrations (10-25%, increment of 5%). Figure 4-10 presents a summary of observations made during heating and cooling of these samples during two cycles.

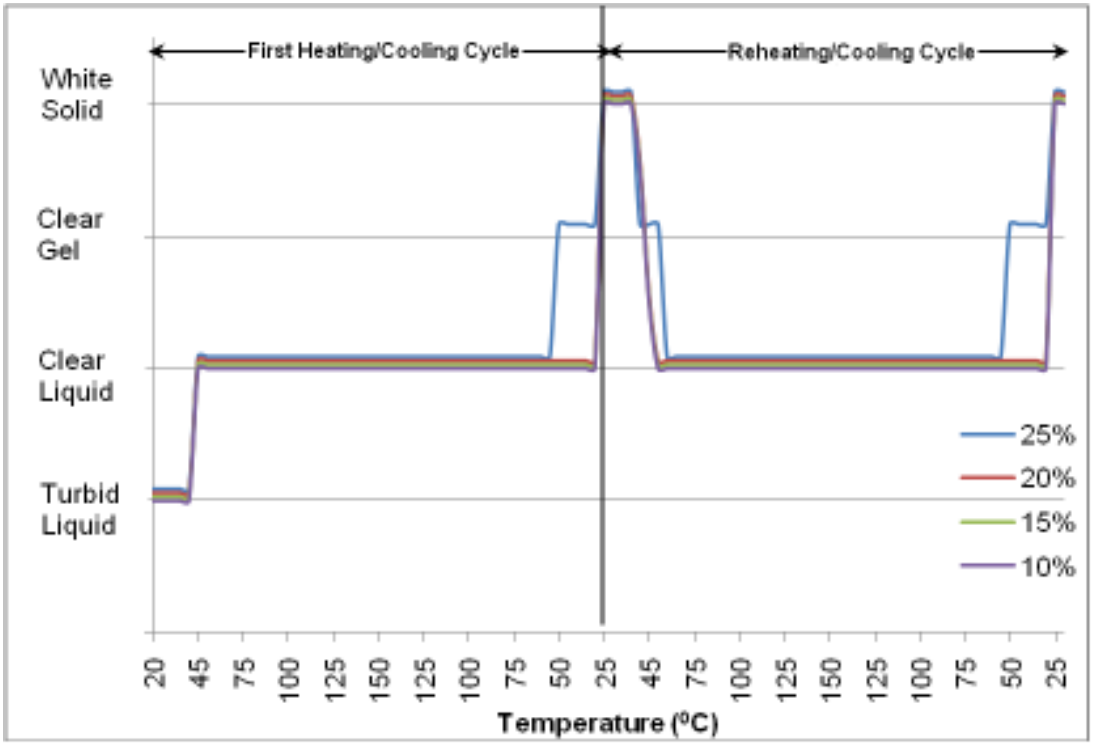

Figure 4-10. Observed behaviour of Pluronic – ethylene glycol samples during heating and reheating cycles

All four samples were turbid solutions at room temperature (Figure 4-11.a) which reflected the insolubility of Pluronic in ethylene glycol. As the temperature increased, the solutions started turning clear around 35^0C and all four samples were completely clear solutions at 50^0C. All four samples remained clear liquids up to 150^0C (Figure 4-11.b). After reaching 150^0C, the solutions were allowed to cool to room temperature. As the solutions cooled, the 25 % solution was a clear, soft gel near 50^0C whereas the other three samples were liquid at this temperature (Figure 4-11.c). Further cooling to near 25^0C resulted in appearance of turbidity in all samples. Also, all samples turned into white, soft (wax like) solid between 20-25^0C (Figure 4-11.d). The

samples were allowed approximately 24 hours at room temperature (i.e. 20^{0}C) before a reheating experiment was started.

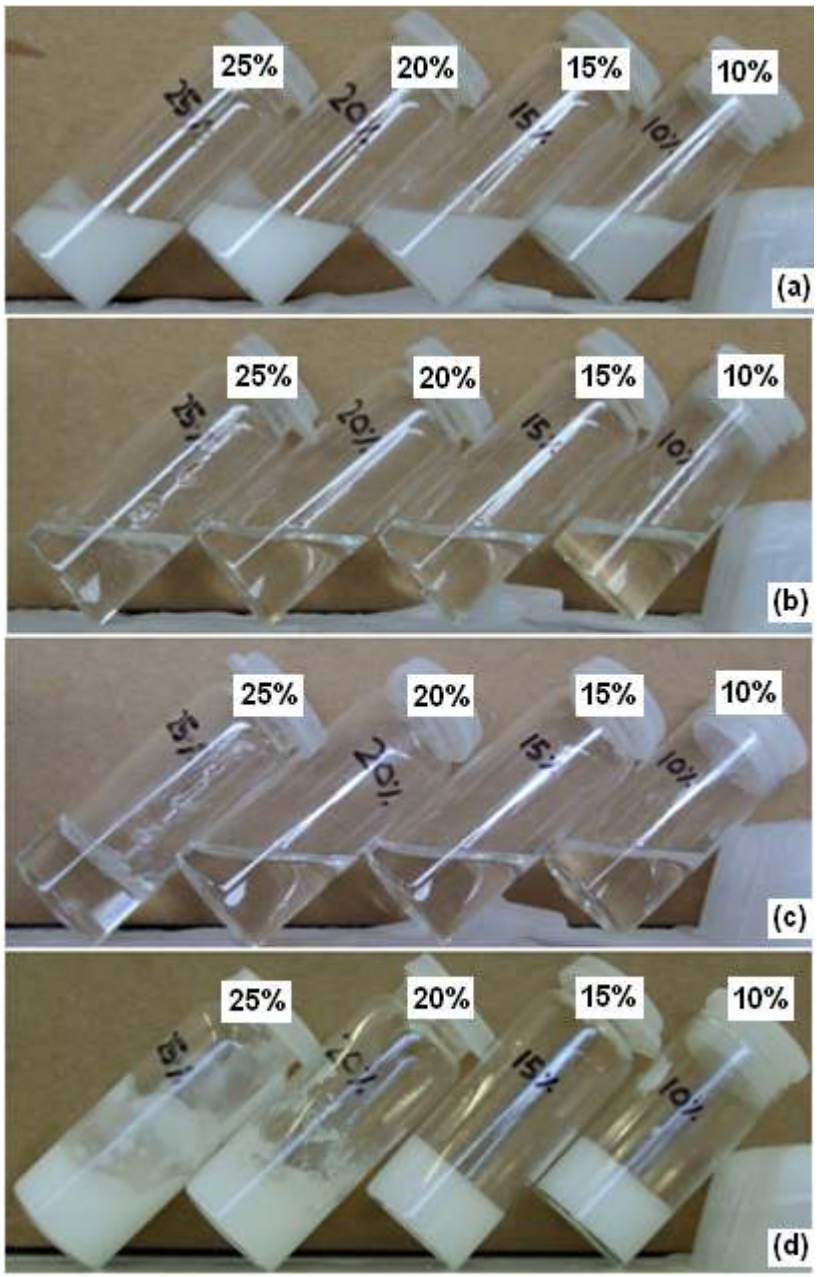

Figure 4-11. Pluronic in ethylene glycol samples at (a) 20^{0}C (b) 150^{0}C (c) 50^{0}C, during cooling (d) cooled to 20^{0}C

At the start of reheating, all four samples were soft white solids. Upon increasing the temperature to 35^{0}C, all samples started to become clear. Also, the three low concentrations (i.e. 10, 15 and 20%) started turning liquid whereas the 25% sample was a gel at 35^{0}C. At 50^{0}C, the 25% sample was a clear gel whereas the other three samples where clear liquids. Between 50 – 60^{0}C, the 25% sample melted into a clear liquid. All samples remained clear

liquids up to 150^{0}C. Upon cooling, a similar trend was observed as in the case of cooling after the first heating cycle. The viscosity of the 25% sample increased and it turned into a clear gel near 60^{0}C. All other samples remained liquid at this temperature. Further cooling resulted in appearance of turbidity in the samples near 25^{0}C which led to appearance of the same white soft solid structure as appeared at the end of the first heating cycle.

4.3.3 Fourier Transform Infrared (FTIR) Spectroscopy

All four ethylene glycol based samples were subjected to FTIR analysis and spectra were measured for each sample before and after heating. Figure 4-12 shows the IR spectra (transmittance) for the Pluronic F-127 and ethylene glycol. FTIR spectra of the F-127 in ethylene glycol samples before heating (liquids) and the same samples after heating (solids) are shown in the Figures 4-13 and 4-14 respectively. Table 4-2 summarises the FTIR frequencies obtained for ethylene glycol, Pluronic F-127 and the four Pluronic in ethylene glycol solutions in the liquid state (i.e. before heating) and in the solid state (i.e. after heating) along with the functional groups assigned to these frequencies.

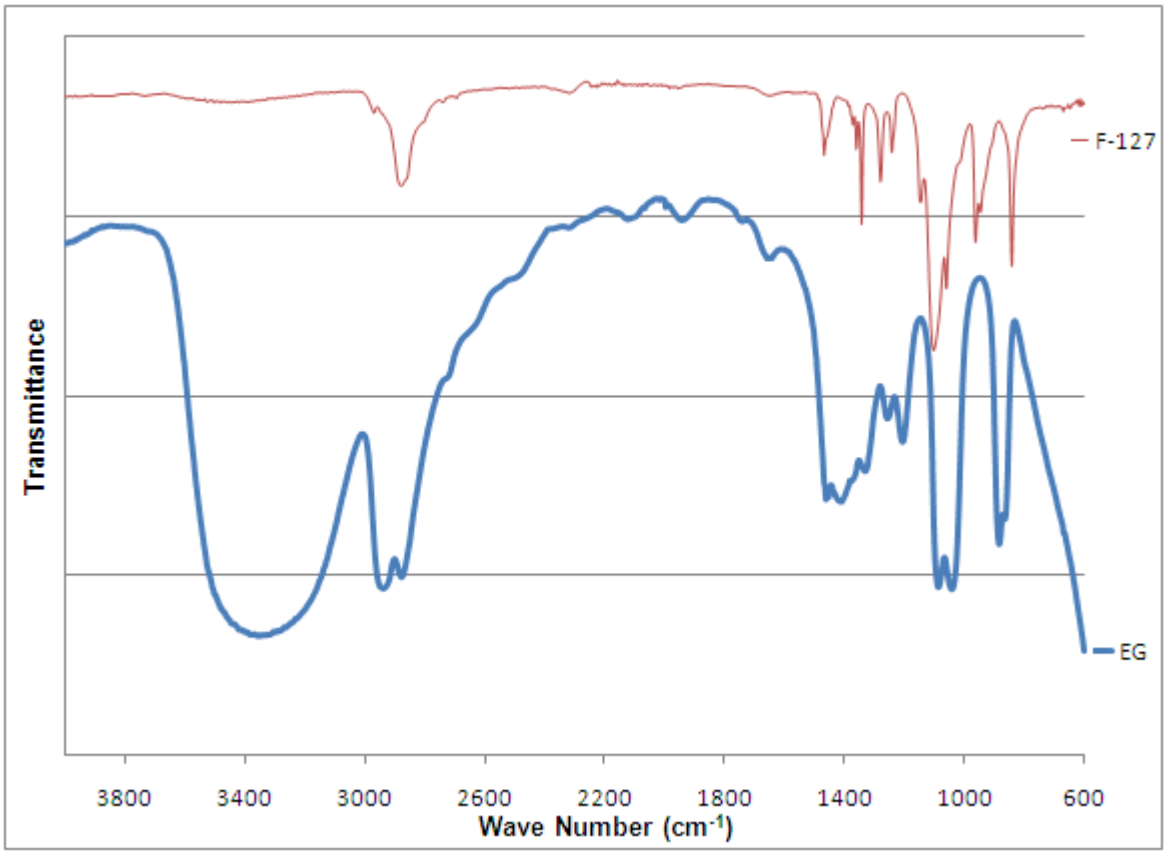

Figure 4-12. FTIR spectra of Pluronic F-127 and Ethylene glycol

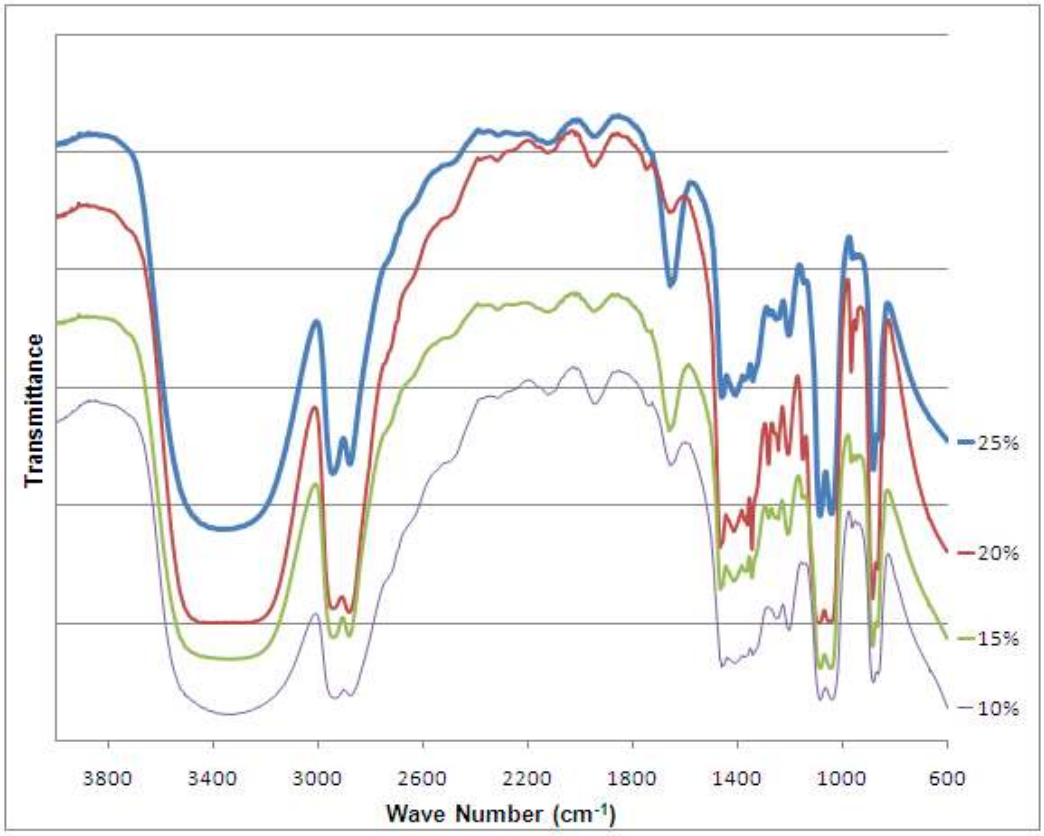

Figure 4-13. FTIR spectra of Pluronic in ethylene glycol (liquids)

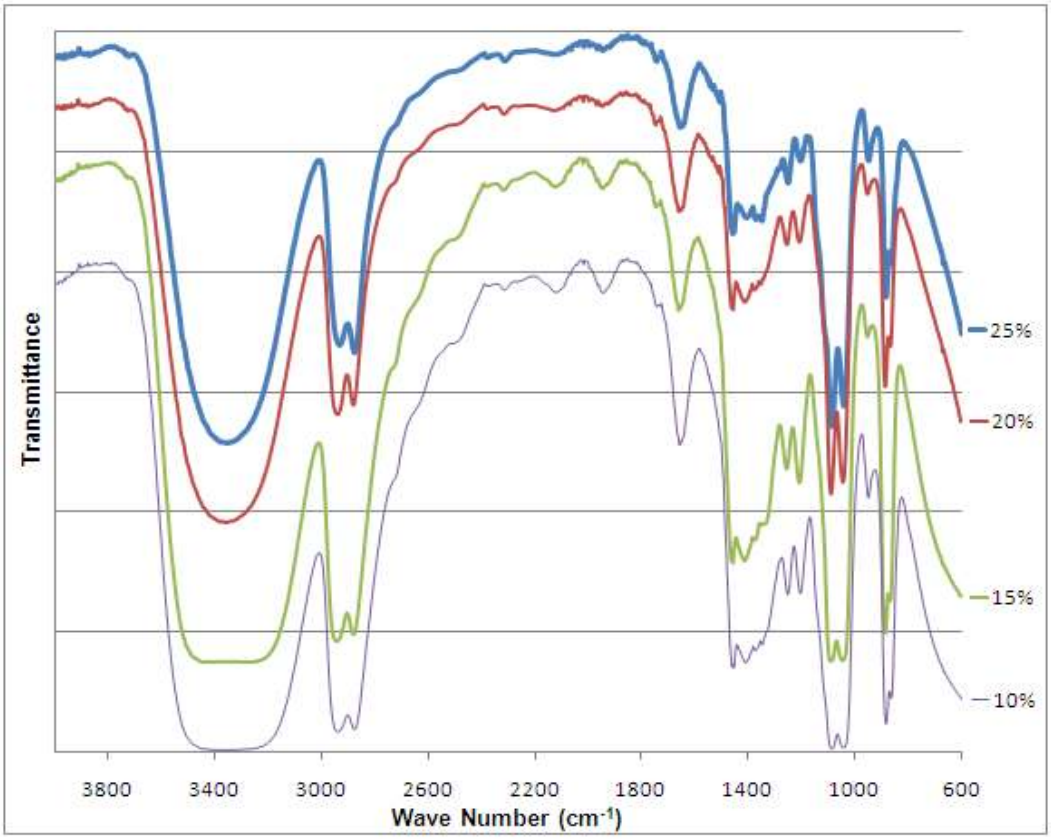

Figure 4-14. FTIR spectra of Pluronic in ethylene glycol (solids)

Ethylene Glycol	Pluronic F-127	Pluronic – Ethylene Glycol solutions								Functional Group Assignment[3]	Peak Related to[4]
		Liquid				Solid (after heating)					
		10%	15%	20%	25%	10%	15%	20%	25%		
	840									CH_2 rocking	PEO,PPO
864		864	864	864	864	864	864	864	862	CH_2 rocking	EG
883		883	883	883	883	883	883	883	883	CH_2 rocking	EG
	947	943	945	947	949	949	950	949	949	CH_2 rocking	PEO , PPO
	960	964	962	964	962					CH_2 rocking, C-O-C stretching	PEO
1041		1039	1041	1043	1043	1041	1043	1041	1041	CH_2 rocking, C-O-C stretching	EG
	1058									CH_2 rocking, C-O-C stretching	PEO
1085		1085	1082	1089	1085	1085	1085	1085	1087	C-O-C stretching	EG
	1101									C-O-C stretching	PEO, PPO
	1145	1149	1147	1149	1147					C-O-C stretching, C-C stretching	PEO
1205		1205	1205	1205	1205	1205	1205	1205	1203	CH_2 twisting	EG
	1242	1244	1242	1242	1244					CH_2 twisting	PEO, PPO
1255		1253	1253	1253	1253	1251	1251	1251	1251	CH_2 twisting	EG
	1278	1278	1278	1278	1278				1280	CH_2 twisting	PEO, PPO
1330	1342	1342	1342	1342	1342	1346	1340	1340	1348	CH_2 wagging	EG, PEO, PPO
	1359	1359	1359	1359	1359					CH_2 wagging, C-C stretch	PEO
	1373	1371	1371	1371	1371	1371	1371	1373	1373	CH_3 symmetric deformation	PPO
1411		1410	1410	1410	1410	1410	1410	1410	1406	CH_2 wagging, C-C stretching	EG
1452		1454	1454	1456	1454	1454	1454	1454	1454	CH_2 scissor, CH_3 asymmetric deformation	EG,
	1465	1464	1462	1464	1464					CH_3 asymmetric deformation	PPO
1658		1658	1658	1658	1658	1658	1658	1658	1658	OH bending	EG
2877	2879	2877	2879	2879	2879	2877	2877	2877	2877	Symmetric C-H stretch of CH_2	EG, PEO, PPO
2939		2937	2937	2939	2945	2939	2941	2937	2933	Antisymmetric C-H stretch of CH_2	EG
	2970									Antisymmetric C-H stretch of CH_3	PPO
3346		3346	3346	3346	3346	3346	3346	3346	3346	OH stretching	EG

Table 4-2. Peaks obtained for different samples used in the FTIR spectroscopy

[3] Assignments are based on references [213-219]

[4] PPO = polyethylene oxide, PEO = polyethylene oxide, EG = ethylene glycol

4.3.4 Hot Stage Microscopy

Hot stage microscopy of Pluronic F-127, and 25% F-127 in ethyelene glycol samples before and after heating was performed to observe the change in the crystalline behaviour of samples upon heating. Figure 4-15a and b depict the micrographs of Pluronic F-127 at 25 and 55^0C showing the presence of crystalline structure at these temperatures while Figures 4-15c represents completion of melting of Pluronic F-127 at 58^0C. Figure 4-15d represent the start of crystallization near 38^0C and Figures 4-15e and f represent crystallized Pluronic F-127 at 36^0C and 25^0C respectively. Similarly, Figures 4-16a and b represent the micrographs obtained at 25 and 40^0C respectively, showing the presence of crystalline structure due to the presence of undissolved F-127 particles. The onset of dissolution of F-127 in ethylene glycol near 43^0C is visible in the micrograph shown in Figure 4-16c whereas Figure 4-16d depicts complete dissolution of F-127 in ethylene glycol. The behaviour of the 25% F-127 in ethylene glycol sample upon cooling is presented in Figures 4-17a to d. The onset of crystallinity near 28^0C is shown in Figure 4-17b whereas growth of the crystalline structure at 25 and 24^0C is shown in Figures 4-17c and d respectively.

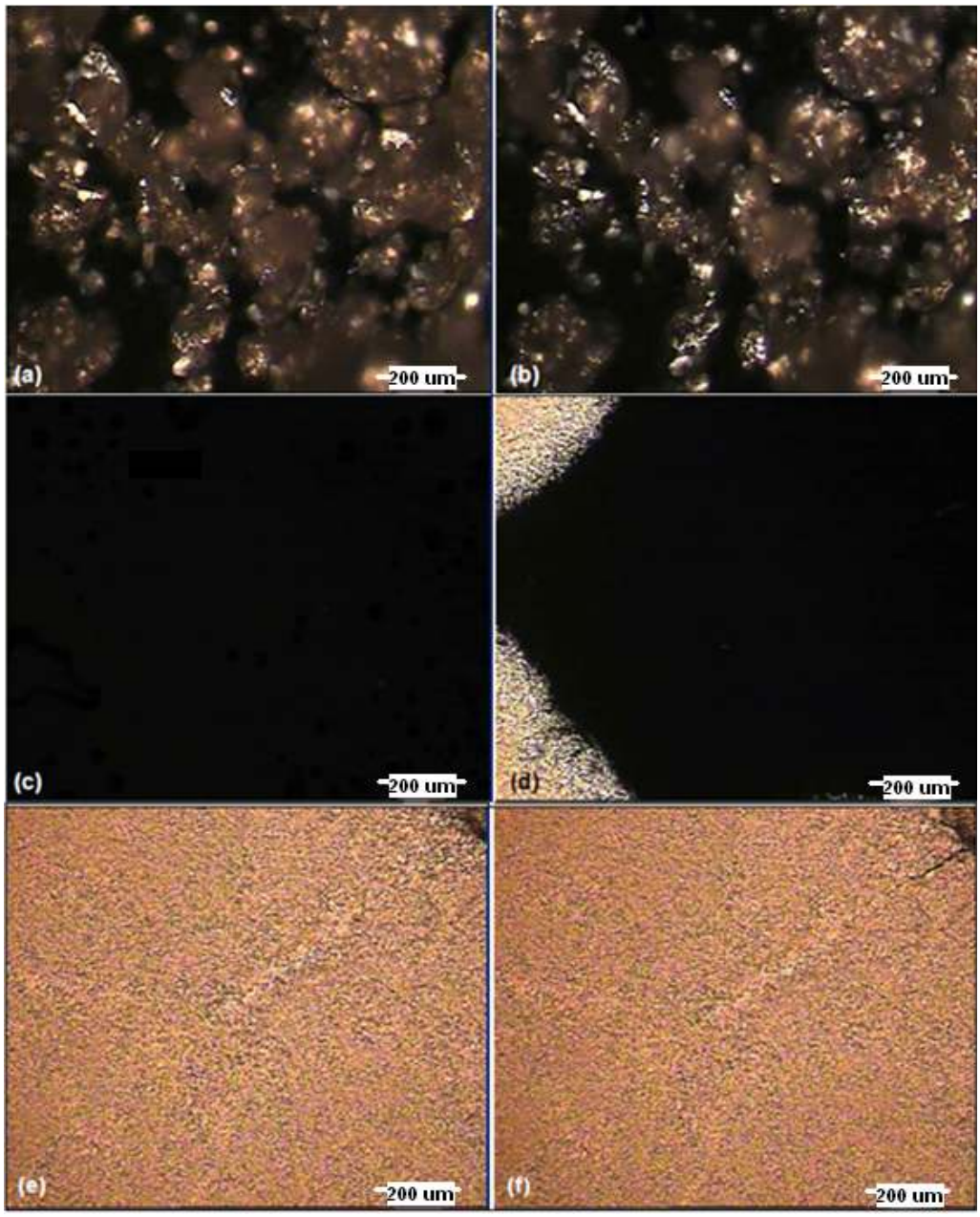

Figure 4-15. Micrographs of Pluronic F-127 at (a) 25^{0}C (b) 55^{0}C (c) 58^{0}C (d) 38^{0}C, during cooling (e) 36^{0}C, during cooling (f) 25^{0}C, cooled down

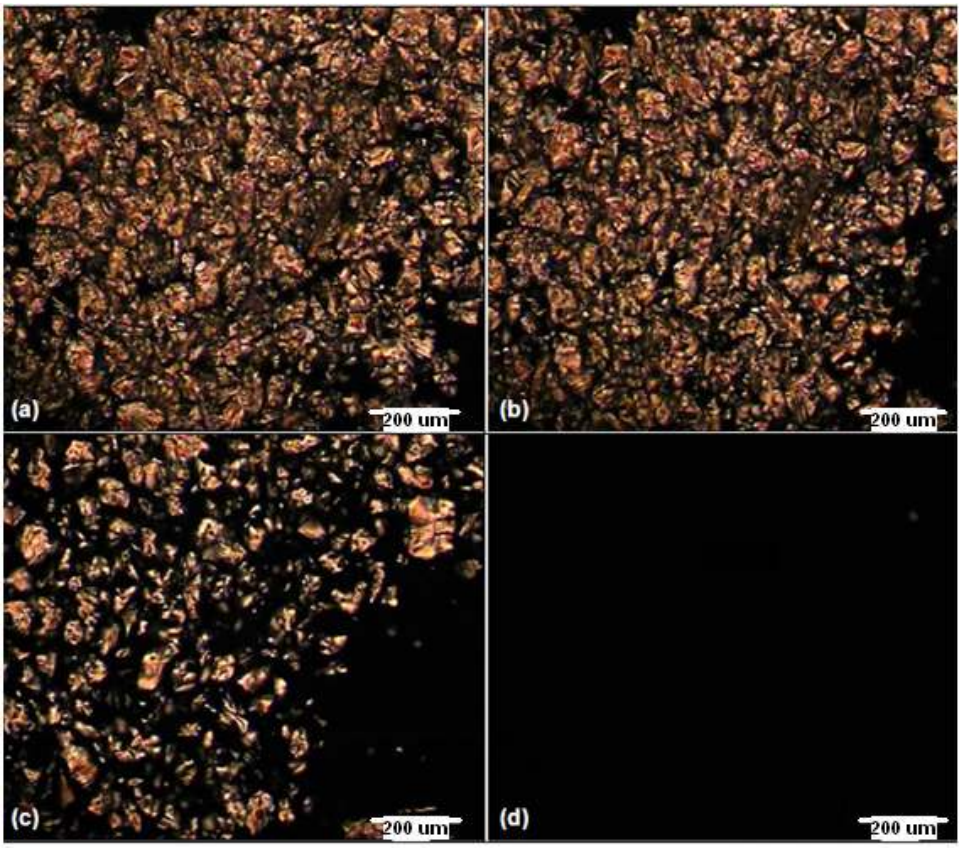

Figure 4-16. 25% F-127 in ethylene glycol during heating at (a) 25^{0}C (b) 40^{0}C (c) 43^{0}C (d) 46^{0}C

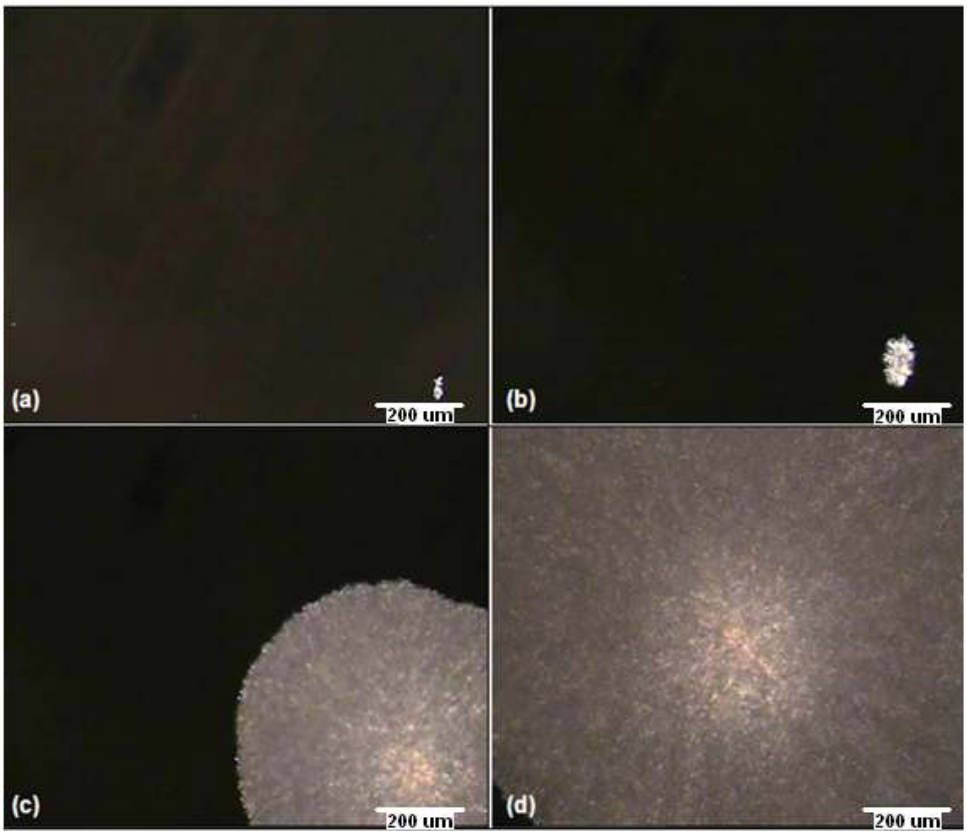

Figure 4-17. 25% F-127 in ethylene glycol during cooling at (a) 30^{0}C (b) 28^{0}C (c) 25^{0}C (d) 24^{0}C

4.4 Differential Scanning Calorimetry

Differential scanning calorimetry of Pluronic F-127, 25% F-127 in ethylene glycol (liquid) sample and 25% F-127 in ethylene glycol after heating (i.e. solid) sample were performed and the resulting endothermic and exothermic curves are presented in Figure 4-18. The change in enthalpy during melting (heating) and crystallisation (cooling), calculated from the DSC curves for these samples along with the corrected values for 25% F-127 are presented in the Table 4-3. Upon heating, Pluronic F-127 showed a melting peak at 58.8^0C whereas during cooling, the recrystallisation occurred at 35.1^0C. The melting peak for 25% F-127 in ethylene glycol occurred at 42.7^0C, representing the dissolution temperature of F-127 in ethylene glycol and the same sample then showed an exothermic peak at 16.2^0C representing crystallisation of F-127 in ethylene glycol upon cooling. Endothermic and exothermic peaks for the 25% F-127 in ethylene glycol (solid) were obtained at 39.2^0C and 9.8^0C respectively. These crystallisation peaks obtained by the DSC are below room temperature which is because the sample cooling in DSC was performed at a controlled rate (i.e. 5^0C/min) to ensure comparable heating and cooling curves. In contrast, the heating and cooling of samples in glass tubes and during hot stage microscopy, the cooling was performed under natural cooling rate and thus the crystallisation temperatures achieved during DSC are lower than room temperature.

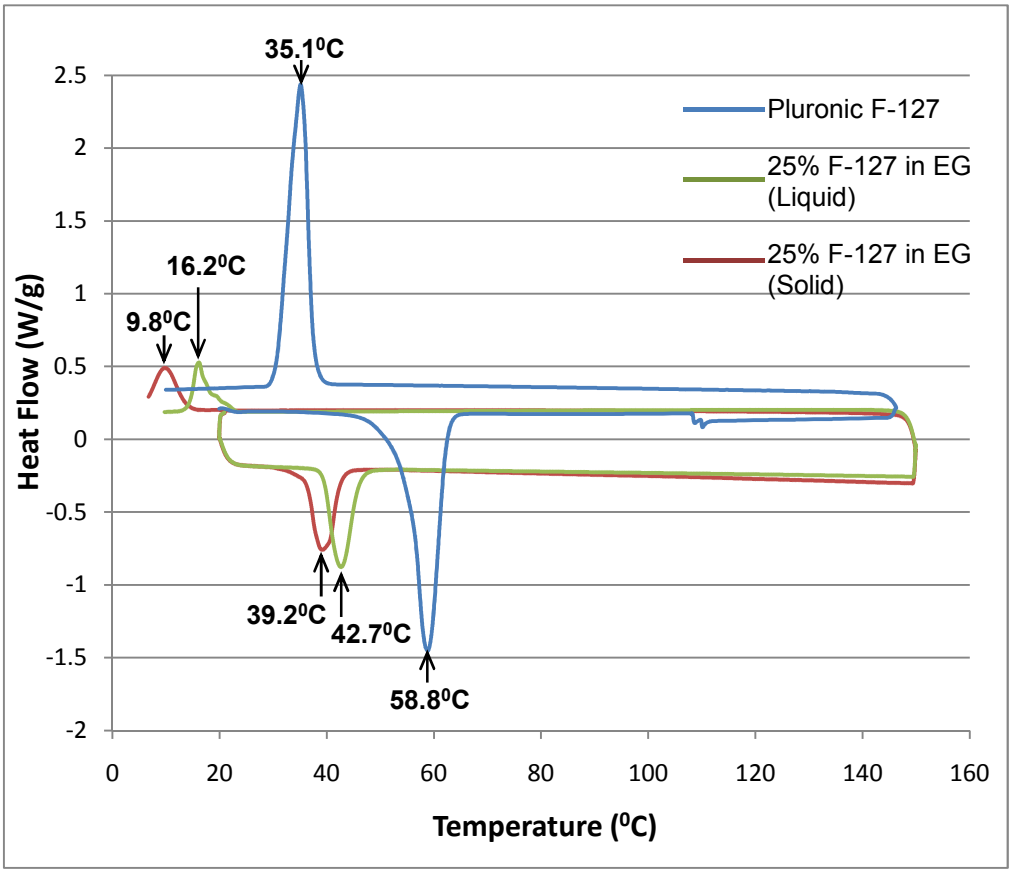

Figure 4-18. DSC curves for Pluronic F-127, 25% F-127 in ethylene glycol (Liquid) and 25% F-127 in ethylene glycol (solid)

Sample	Heating (J/g)	Cooling (J/g)
F-127	114	109
Value corrected for 25% F-127	28.5	27
25% F-127 in Ethylene Glycol (Liquid)	26.1	14
25% F-127 in Ethylene Glycol (Solid)	21.83	18

Table 4-3. Enthalpy values for F-127 and F-127 in ethylene glycol (liquid and solid)

4.5 Viscosity Measurements

The viscosity of ethylene glycol and 25% F-127 in ethylene glycol were measured at constant temperatures (i.e. 50 to 90^{0}C, increment 10^{0}C) and the shear rate was varied between 100-1500 s^{-1}. These viscosity curves (log–log) are shown in the

Figure 4-19 and the values at the highest shear rate (i.e. 1500 s^{-1}) are listed in the Table 4-4.

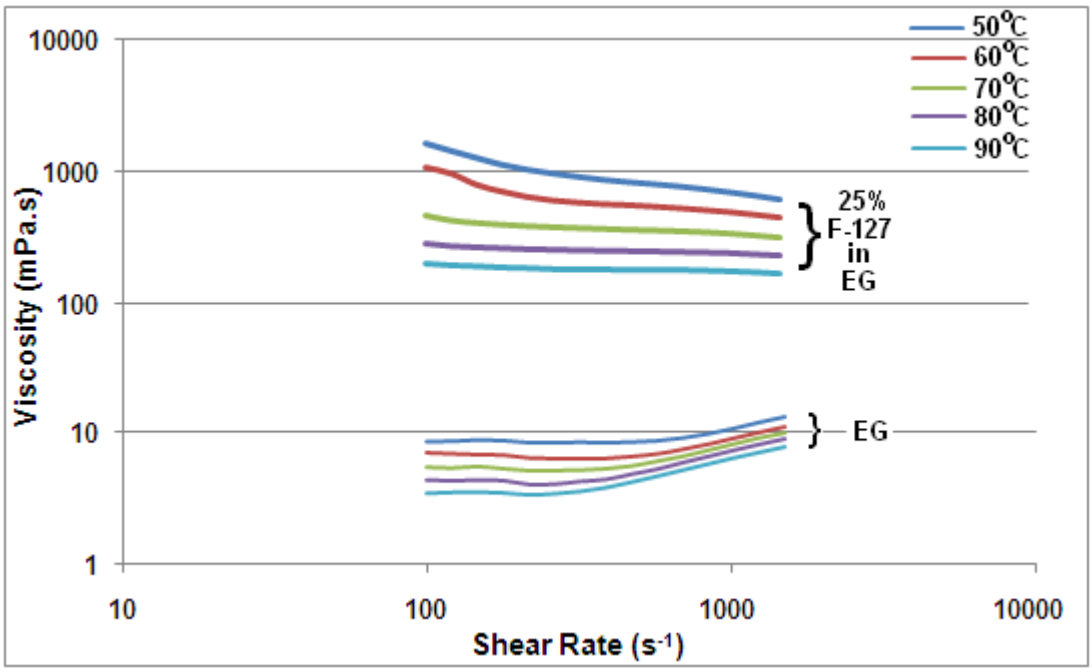

Figure 4-19. Viscosity of ethylene glycol (EG) and 25% F-127 in ethylene glycol at different temperatures and shear rates

T (^{0}C)	Viscosity at 1500 s^{-1} (mPa.s)	
	EG	25% F-127 in EG
70	9.8	325
80	8.8	230
90	7.9	170

Table 4-4. Viscosity values for ethylene glycol and 25% F-127 in ethylene glycol

4.6 Discussion

4.6.1 Water Based Samples

The observed behaviour of F-127-water samples conforms to the results obtained by Schmolka [134], Mortensen [124], Mortensen and Brown [135], Pandit and McGowan [128], Cabana et al [125], Guzmán [127], Wanka et al [115] and Malmsten and Landman [137]. As discussed in the literature review (i.e. chapter 2), this gel formation was attributed to the conversion of unimers into micelles upon heating and subsequent entanglement of the formed micelles into lyotropic liquid crystalline structures upon further heating. As the gel is allowed to cool, the

micellar entanglements become weak and the gel melts into a solution state. For lower concentration samples (i.e. 15% or less), the number of micelles present is not enough to cause the formation of a gel, therefore, the gel formation of aqueous solutions of Pluronic F-127 was only observed for higher concentrations (i.e. 20% and higher).

4.6.2 Non-Aqueous Solvents

4.6.2.1 Formamide

The formamide based F-127 solutions had a gel formation similar to the aqueous F-127 solutions. However, it is clearly seen that the 20% F-127 in formamide did not produce gel formation at any temperature up to 150^0C whereas 20% aqueous F-127 formed a gel near 25^0C. Similarly, the 25% F-127 – formamide sample formed a gel near 45^0C as opposed to 20^0C for the same concentration in water. These results, therefore, confirm the findings of Alexandridis [140,145-147] who concluded that for Pluronics, formamide shows enhanced solvency than water and relatively smaller sized micelles are formed in formamide than in water. The results obtained for F-127 – formamide (Figures 4-5 and 4-6) clearly showed that formamide based solutions required a higher temperature and/or concentration to form a gel. In the literature there was no reference to gel formation at higher temperatures (i.e. higher than 100^0C) for F-127 – formamide solutions. These results show that the gel formed by F-127 in formamide can persist up to 150^0C. The F-127 – formamide samples produced a gel state at high temperatures (i.e. 150^0C). However, the possible decomposition of formamide into harmful products [211] such as carbon monoxide, carbon dioxide, nitrous oxides and hydrogen cyanide led to its exclusion as a solvent for the current study.

4.6.2.2 Alcohols

Although the effects of alcohols on aqueous solutions of Pluronics have been studied before [129,132,133,141-144,148,212], none have used an alcohol as a solvent alone (i.e. without water). As seen in Figures 4-8 and 4-9, F-127 remained undissolved in all the glycols and octanol. However, upon heating, the solubility of F-127 increased and was dissolved, forming a clear solution in all four solvents. Upon cooling, a gel phase was formed with the ethylene glycol sample and an explanation of this gel phase will be presented in the following section. All four

samples, upon cooling, turned into white wax like solids. The formation of this solid can be due to the re-solidification of the PEO and PPO chains upon cooling. As the chains are cooled down and the solidification starts, the solvent is entrapped between the chains of PEO and PPO and thus a soft, wax like solid structure forms. No gel formation was produced by octanol, propylene glycol and butylene glycol based samples. The ethylene glycol based sample formed a gel state during cooling, so ethylene glycol was selected for further study and the next section presents a discussion of the results obtained.

4.6.3 Ethylene Glycol Based Samples

Table 4-2 summarises the FTIR frequencies obtained for ethylene glycol, Pluronic F-127 and the four F-127 in ethylene glycol samples in the liquid state (i.e. before heating) and in the solid state (i.e. after heating) along with the functional groups assigned to these frequencies. The assignments were based on references [213-219]. It is well known that Pluronic is comprised of blocks of polyethylene oxide (PEO) and polypropylene oxide (PPO) with a PPO chain centred between two PEO chains where the PEO is present in both amorphous and crystalline form and the PPO is preset in the amorphous form [213-217]. Therefore, in Table 4-2, the FTIR frequencies for all the samples have also been related to the structural components of the composition (i.e. ethylene glycol, PPO, PEO). The bands at 840, 947, 960, 1058, 1101, 1145, 1242, 1278, 1342, 1359, 1465, and 2879 cm^{-1} are the characteristic peaks related to the PEO structure in the Pluronic F-127. Similarly, the bands due to PPO include 840, 947, 1101, 1242, 1278, 1342, 1373, 2879 and 2970 cm^{-1}. Ethylene glycol gives rise to bands at 864, 883, 1041, 1085, 1205, 1255, 1330, 1411, 1452, 1658, 2939 and 3346 cm^{-1}. It is worth noting here that some of these bands, such as 840, 947, 1101, 1242, 1278, 1342 and 2879 cm^{-1}, can be associated with both the PPO and PEO parts of Pluronic since both contain similar groups (e.g. CH_2, C – O). Compared to the bands related to the PPO, a large number of bands in the Pluronic F-127 spectra are related to the PEO which is due to the relatively high proportion of PEO chains in the F-127 molecule (i.e. 70% PEO, 30% PPO). From FTIR results (Figures 4-12 to 4-14 and Table 4-2) it is clear that some of the peaks (840, 1058, and 1101 cm^{-1}) associated with PEO disappear in the liquid samples whereas the remaining bands associated with PEO (960, 1145, 1242, 1278, 1359, 1465 cm^{-1}) also

disappear in the solid samples (i.e. after heating). Bands associated with PPO (i.e. 840, 1101 and 1270 cm^{-1}) disappear in all the samples whereas PPO bands at 960, 1145, 1242, 1278 cm^{-1} disappear in the solid samples. All the bands associated with ethylene glycol appear in all the samples. The behaviour of solutions upon heating can thus be explained on the basis of these results along with the micrographs and DSC of Pluronic F-127 and 25% Pluronic in ethylene glycol solution as follows.

Loss of Turbidity near 50^0C

When the Pluronic F-127 is mixed in the ethylene glycol, both PEO and PPO present in the Pluronic F-127 are insoluble as indicated by the presence of crystals in the 25% solution at 25 and 40^0C (Figures 4-16a and b), resulting in turbid liquids at this temperature. A straight forward reason for the disappearance of turbidity could be the melting of Pluronic F-127 near 50^0C. The melting temperature of F-127 (as quoted in the data sheet supplied by manufacturer) is $53\text{-}57^0C$. This melting point is also confirmed by both the microscopic image of F-127 at 58^0C (Figure 4-15c) and the DSC of F-127 (Figure 4-18). Therefore, melting of F-127 can be considered a reason for increased solubility and thus, appearance of clear solutions near 50^0C. However, as suggested by the disappearance of bands at 840, 1058 and 1101 cm^{-1}, it can be said that some of the crystalline PEO has dissolved in ethylene glycol. The reason for the disappearance of peaks associated with PPO (i.e. 840, 1101 and 1270 cm^{-1}) can be due to the masking of these peaks under the relatively broader peaks associated with ethylene glycol at 864 and 1085 and 2939 cm^{-1} so PPO is insoluble and PEO is partially soluble at room temperature in ethylene glycol resulting in turbid liquids. The remaining PEO bands at 960, 1145, 1242, 1278, 1359 and 1465 cm^{-1} which appeared in the liquid samples, disappeared in the solid samples indicating increased solubility of PEO as a result of heating to a higher temperature. Some of these bands (i.e. 960, 1145, 1242, 1278 cm^{-1}) are also associated with PPO so PPO solubility has increased with increasing temperature. The micrographs of 25% F-127 in ethylene glycol at 43 and 46^0C (Figure 4-16c and d) clearly suggest the complete dissolution above 40^0C. This increased solubility of both PEO and PPO can be considered the main reason

behind the disappearance of turbidity and appearance of clear solutions near 50^0C.

Gel Formation by 25% Sample on Cooling near 50^0C

As the samples were cooled, the highest concentration solution (i.e. 25%) converted from a viscous liquid into a soft gel structure near 50^0C. As suggested by the FTIR spectra (Figures 4-12 to 4-14, Table 4-2), the bands associated with crystalline PEO at 960, 1145, 1242, 1278, 1359 and 1465 cm^{-1} disappeared in all the samples after they were heated and cooled back to a solid state. The disappearance of these bands can be caused by a change in the crystalline structure and/or the conformational structure of the PEO [214]. Also, the micrographs at 30 and 28^0C (Figures 4-17a and b) and DSC curves of both liquid and solid 25% F-127 in ethylene glycol samples (Figure 4-18) clearly showed the absence of any crystallisation between 30–50^0C. The absence of FTIR bands associated with crystalline PEO at 960, 1145, 1242, 1278, 1359, 1465 cm^{-1} can thus be due to a change in the conformational structure of crystalline PEO, as a change in the conformation of PEO from trans – gauche – trans (tgt) in the crystalline state to gauche – gauche – trans (ggt) upon melting into the amorphous state has been observed previously [214,220]. From the FTIR results it is clear that the band near 1242 cm^{-1} disappeared in the solid samples and the intensity of the band near 1251 cm^{-1} is higher than that of the liquid samples (Figure 4-13 and 4-14). The bands near 1240 and 1280 cm^{-1} were assigned to trans conformation and the band near 1250 cm^{-1} was assigned to gauche conformation [220,221] therefore, the disappearance of bands near 1240 and 1280 cm^{-1} and increased intensity of 1250 cm^{-1} band also presents an evidence of increased gauche conformation.

Conformation of a polymer is defined as the relative geometric arrangement of the chemical groups along the polymer chain [202,222,223]. Rotation of the atoms or functional groups about a carbon to carbon (i.e. C – C) bond results in a change in the shape of the polymer chain and thus the conformation is said be changed. Commonly observed conformational structures include '*trans*' and '*gauche*' conformations which are caused due to the rotation of carbon atoms along the chain. To understand the difference between the two conformational structures,

consider a polymer chain with 6 carbon atoms attached through single bonds (Figure 4-20). The conformational state (i.e. trans or gauche) for any carbon – carbon bond, say x, along the chain is defined by the rotational angle between the two planes created by the C – C bond (x) and its adjacent C – C bonds respectively (i.e. bonds x-1 and x+1). If the angle between the two planes is zero, the conformation is termed as trans (Figure 4-20a) whereas if the angle between the two planes is 120^{O}, the conformation is termed as gauche (Figure 4-20b). Figure 4-21 shows the two conformations as viewed along the C – C bond. A polymer chain can show more than one conformation (for example, the structure in Figure 4-20b is gauche–trans– gauche) depending upon the thermal history of the polymer and a regular conformational structure (such as all trans, all gauche or any repeating combination of both) is usually observed in the crystalline state [222,223].

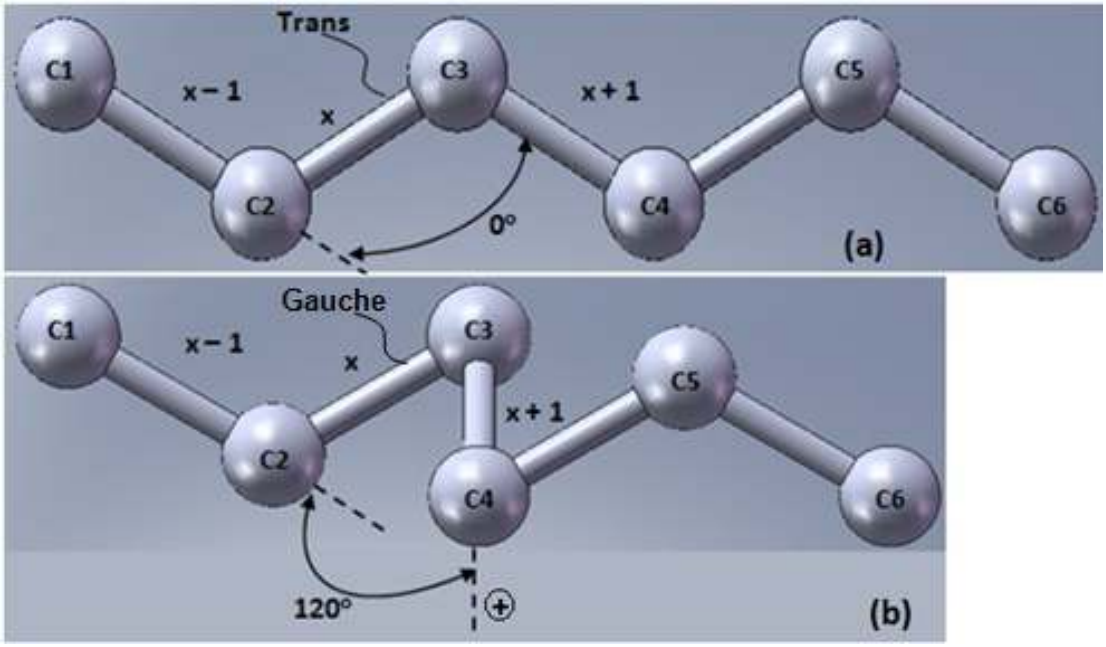

Figure 4-20. Conformational Structures in a Polymer Chain (a) Trans Conformation at Bonds between C2–C3, C3–C4 and C4–C5 (b) Gauche Conformation at Bonds between C2–C3 and C4–C5, plus (+) sign indicates that the bond is perpendicular to the plane of paper

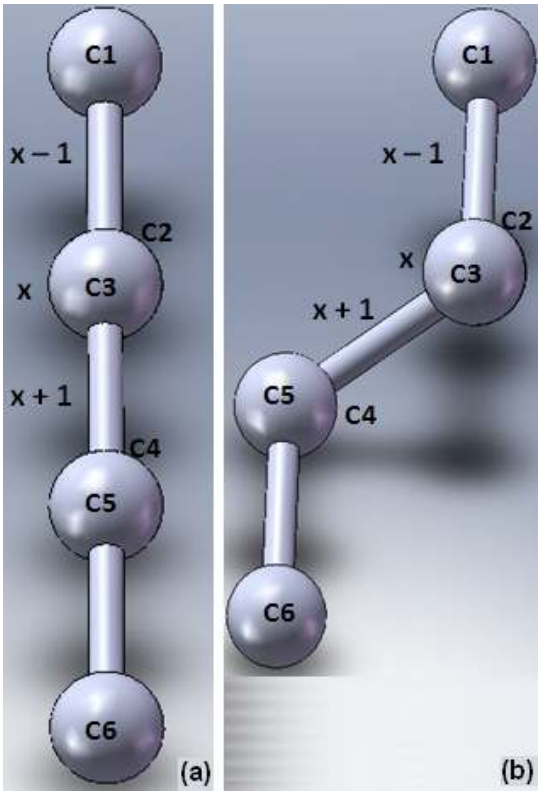

Figure 4-21. Polymer Chain Conformation as Viewed Along x (i.e. C2 – C3) Bond

(a) Trans Conformation (b) Gauche Conformation

As the conformation changes in a polymer dissolved in a solvent, this can also result in formation of a gel phase [224]. The gel formation shown by 25% F-127 in ethylene glycol could thus be caused by this conformational change. Both PEO and ethylene glycol have strong hydrogen bonding tendencies, therefore the strong hydrogen bonding between the PEO chains and ethylene glycol as compared to hydrogen bonding between the less polar PPO and ethylene glycol resulting in increased polymer to polymer interaction (entanglements) can also be a cause of this gel formation [225]. Ether oxygen present within the PEO is the hydrogen bonding site available in these systems and it has been suggested previously that hydrogen bonding is represented by changes in the C–O–C stretching and CH_2 rocking vibrations [221,226,227]. The intensity of the band at 1658 cm^{-1} decreased in the solid samples. This band has been assigned to OH bending vibration and it has been reported that an increase in hydrogen bonded OH bonded as opposed to free OH bending results in increased intensity of this band [228]. Thus, the disappearance of bands near 840, 960, 1958, 1101 and 1145 cm^{-1} along with the reduced intensity of 1658 cm^{-1} band clearly present evidence of hydrogen bonding in the solid samples. Also, the observation of the

same solution-to-gel and gel-to-solution transformation temperature (i.e. near 50^0C) along with the evidence of lack of crystallinity demonstrated by micrographs and DSC results (Figures 4-17a,b and 4-16) and the conformational change represented by the disappearance of PEO peaks suggest that this gel phase could be an amorphous gel [224,229]. The gel phase formed by F-127 in ethylene glycol is therefore different from the gels formed by F-127 in water in the way that the Pluronic in water gels are considered crystalline in nature whereas the gel formed by F-127 in ethylene glycol can be amorphous as suggested by the results obtained in this research.

Since the lower concentrations (i.e. 10 – 20%) did not form a gel at any temperature, it can be said that the polymer – polymer interactions (entanglements) resulting in gel formation were only observed at a concentration of 25%.

Formation of Soft Wax like Solids

Further cooling results in appearance of turbidity in all the samples near 25^0C which can be a result of re-solidification of Pluronic F-127 as indicated by the DSC results (Figure 4-18). This is also confirmed by microscopic images (Figures 4-17a and b) as at temperatures below 28^0C, only a very small amount of crystallised structure can be seen indicating the absence of crystalline PEO. However, as the solution is cooled to 25^0C, very slow crystal formation was observed (Figures 4-17c and d). Recrystallisation was observed near room temperature during the microscopy and heating/cooling experiments since cooling during both these experiments was performed more slowly whereas during DSC, a faster cooling rate was used (i.e. 5^0C/min). The FTIR spectra of samples after they were cooled back (i.e. solid) clearly showed that most of the peaks associated with crystalline PEO have disappeared. Since the conformational structure of PEO has changed, the appearance of a white, wax like solid state upon cooling back to near 25^0C can be considered as the re-crystallisation of the PEO with a changed conformational (i.e. less perfect) structure. Enthalpy values during heating and cooling and F-127 and 25% F-127 in ethylene glycol before and after heating obtained from the DSC curves are presented in Table 4-3. The change in enthalpy for F-127 during heating (114 J/g) and cooling (109 J/g) is nearly the same. On the other hand, the

change in enthalpy for 25% F-127 in ethylene glycol during cooling (13.9 J/g) is significantly reduced as compared to that during heating (26.1 J/g). Comparing the enthalpy values of 25% F-127 in ethylene glycol to corrected values for 25% of F-127 also highlights that the change in enthalpy for 25% F-127 in ethylene glycol during heating is nearly the same as the corrected value for 25% of F-127 whereas the change in enthalpy during cooling is significantly lower than the corrected value during cooling. This reduced value of enthalpy during cooling of 25% F-127 in ethylene glycol suggests that the ethylene glycol becomes entrapped between the solidified PEO and PPO structures with some of the PEO dissolved in ethylene glycol and/or present in the form of gel and thus a white wax like solid structure appears. When these solids are subjected to compression (i.e. pressure applied by hands), the ethylene glycol entrapped between solidified PPO and PEO is released out. The presence of all the bands associated with ethylene glycol in both liquid and solid samples also confirmed the presence of ethylene glycol in the resulting solid structure.

The viscosity results (i.e. Figure 4-19 and Table 4-4) show that ethylene glycol has a very low viscosity at high temperatures (i.e. 70 – 90^0C). But, due to the high concentration of Pluronic, the viscosity of 25% F-127 in ethylene glycol was very high (i.e. 230 mPa.s at 80^0C and 1500 s^{-1}, Table 4-4). Therefore, even though the 25% F-127 in ethylene glycol was a liquid at temperatures higher than 50^0C, the high viscosity would make the composition difficult to jet at temperatures near 80^0C. However, a jetting head with a higher operating temperature (i.e. higher than 100^0C) could possibly allow the jetting of this composition.

5 Methylcellulose Based Compositions

5.1 Introduction

Since Pluronic F-127 based compositions did not show a gel formation at temperatures near 150^0C, it was decided to investigate methylcellulose (MC) based compositions. This chapter presents the experimental results achieved for methylcellulose (MC) and hydroxypropyl methylcellulose (HPMC) based compositions. The structure of these polymers is shown in Figure 3-2 (Chapter 3). Initially, aqueous MC and HPMC solutions were examined to observe reverse thermal gel formation. Novel compositions utilizing ethylene glycol as a solvent for both MC and HPMC were prepared and analysed to observe gel formation upon heating/cooling. HPMC, due to its high molecular weight, did not provide the required results and was therefore only studied with ethylene glycol as a solvent whereas MC was further investigated with propylene glycol and butylene glycol. To explain the changes upon heating and cooling, FTIR, hot stage microscopy, DSC and XRD were performed on selected MC samples and the results are presented followed by a discussion of the results.

5.2 Sample Heating

5.2.1 Water Based Samples

Seven different solutions of MC with concentrations of 2, 3, 4, 5, 6, 8, and 10% (w/w) and 4 solutions of HPMC of concentrations including 2, 3, 4 and 5% (w/w) were prepared. The reason for not using concentrations higher than 5% for HPMC was that the solutions above 5% were highly viscous and showed almost no flow behaviour. Figure 5-1 shows the observed behaviour of aqueous MC solutions in water upon heating up to 90^0C and a temperature – concentration graph is shown in Figure 5-2. The behaviour of aqueous HPMC solutions upon heating, and a temperature – concentration graph are shown in the Figures 5-3 and 5-4 respectively.

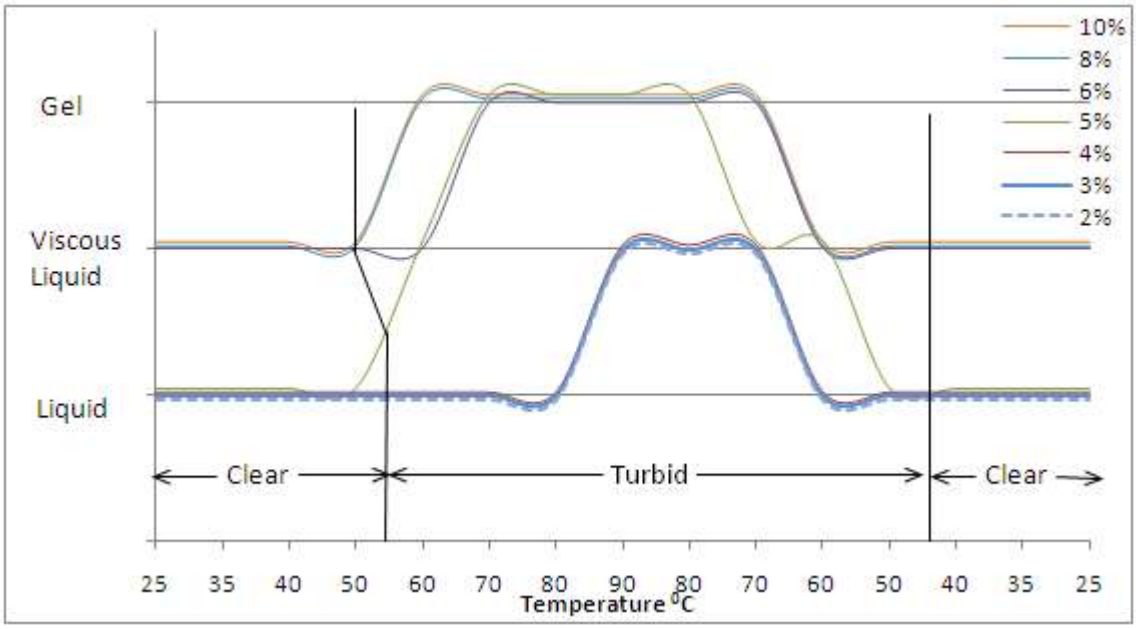

Figure 5-1. Behaviour of MC – Water solutions during heating and cooling

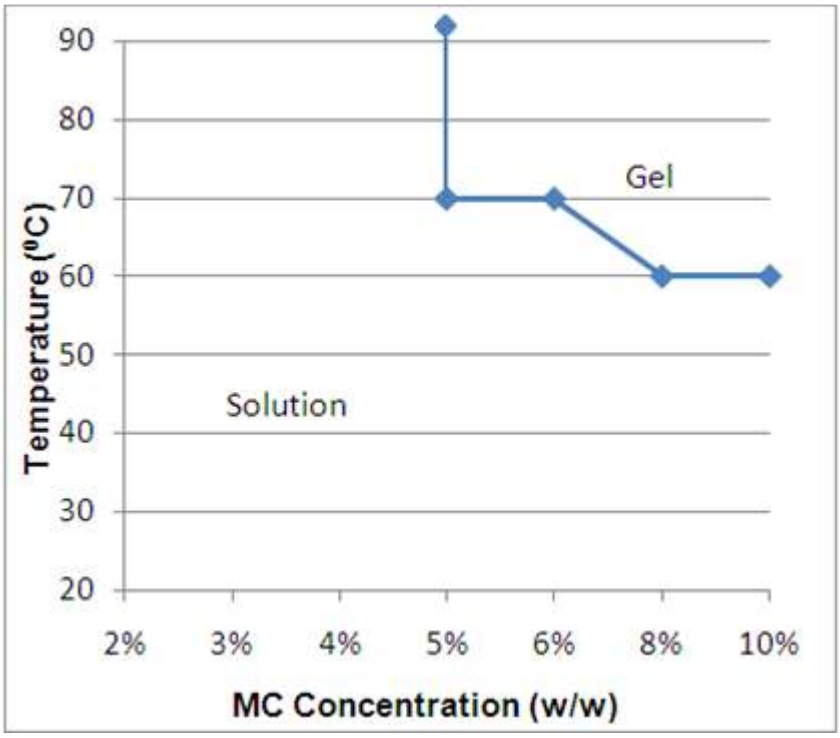

Figure 5-2. Temperature – concentration graph for MC–Water samples

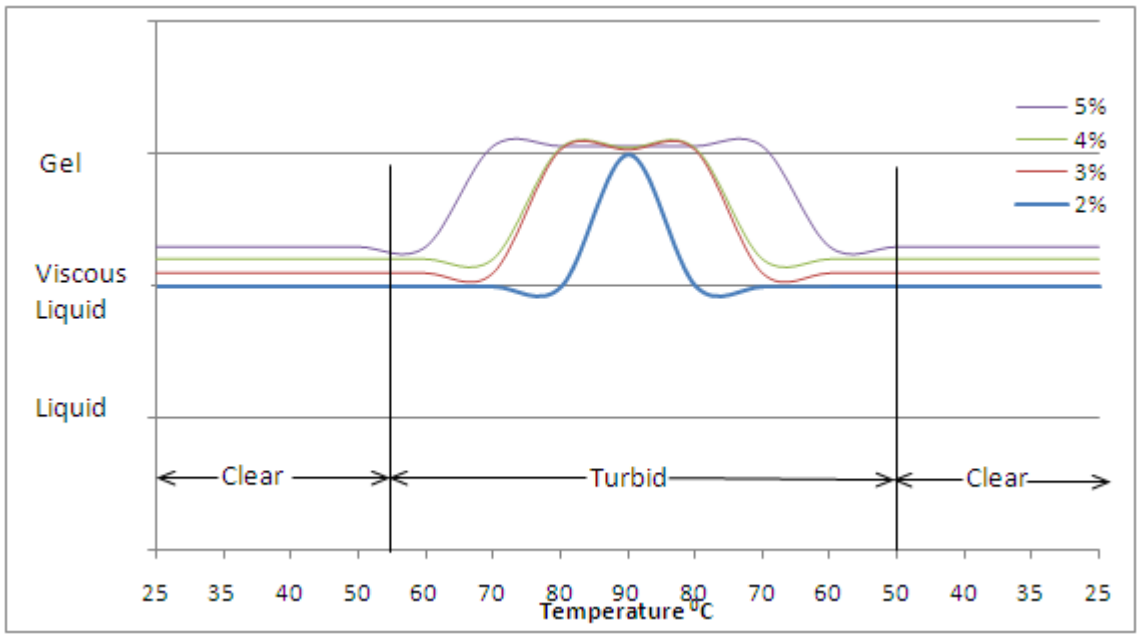

Figure 5-3. Behaviour of HPMC – Water solutions during heating and cooling

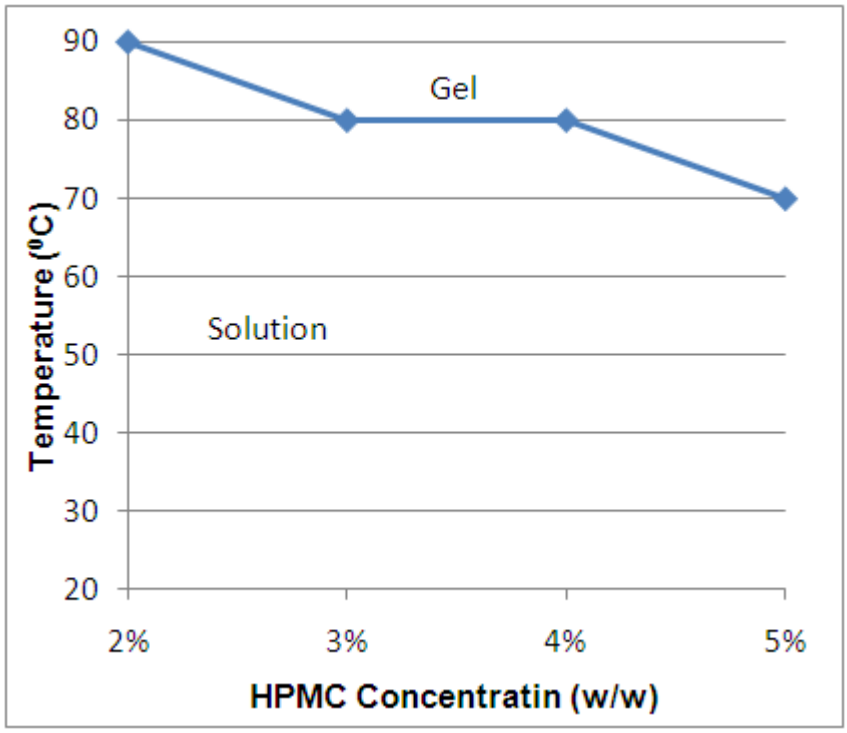

Figure 5-4. Temperature – concentration graph for HPMC–Water samples

5.2.1.1 MC – Water Samples

Methylcellulose in water formed clear solutions at room temperature (i.e. 20^{0}C) and 25^{0}C (Figure 5-5a). Upon heating these solutions started turning turbid. For the higher concentrations (i.e. 6 – 10%), turbidity started near 50^{0}C and for 2-5% samples, it started between 50–60^{0}C. At 60^{0}C, the three higher concentrations

(i.e. 6 – 10%) were completely turbid and 2-5% samples were partially turbid. Also, both 8 and 10% samples showed gel formation near 60^0C. At 70^0C, all samples were completely turbid and gel formation in 5 and 6% samples was observed. At 80^0C, 5-10% samples were turbid gels whereas 2-4% samples were viscous liquids (turbid). Further increasing the temperature to 90^0C did not result in any change in the state with 2-4% samples remaining as turbid viscous liquids and 5 – 10% samples as turbid gels (Figure 5-5b). Cooling led to a gradual decrease in viscosity for all the samples. A gel to solution transition was observed for the 5% sample near 80^0C and 6-10% samples showed gel melting near 70^0C. Further cooling resulted in a gradual decrease in the viscosity of all the samples. At 50^0C, the turbidity started to disappear and all the samples turned into clear solutions near 45^0C. At 25^0C, all the samples were clear liquids (Figure 5-5c).

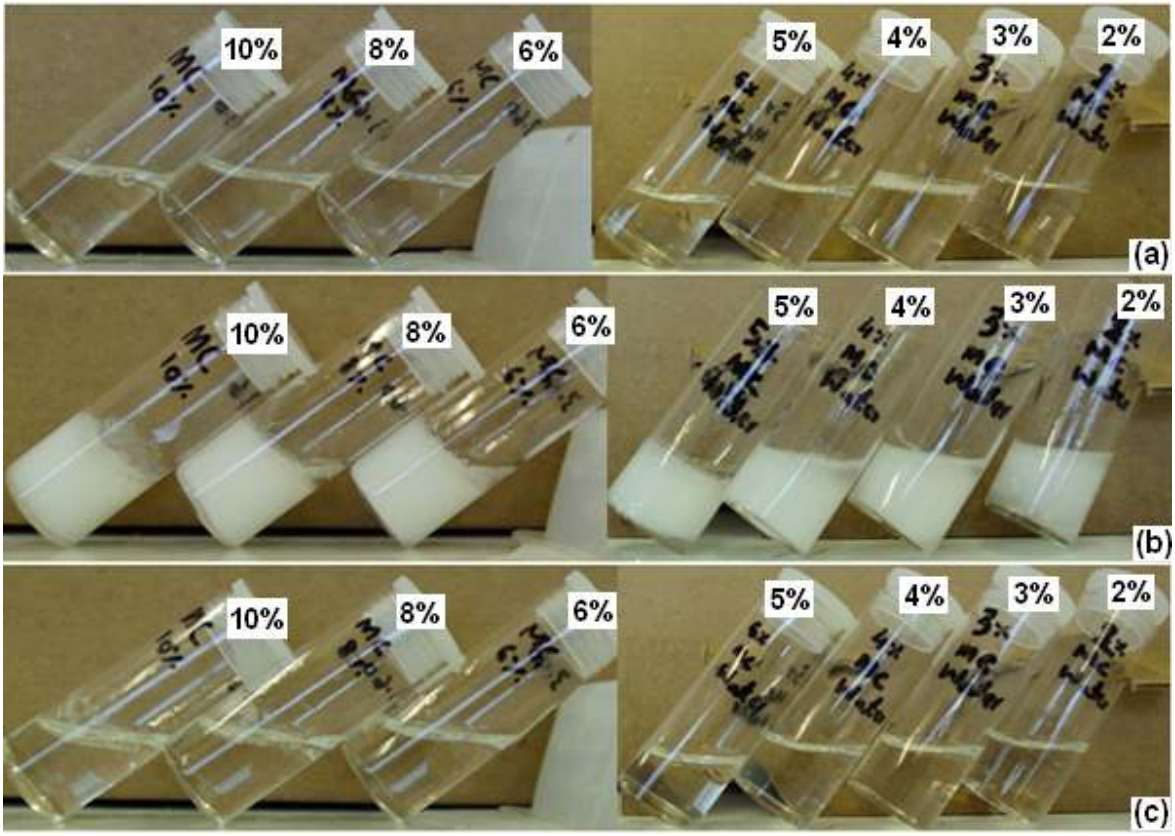

Figure 5-5. MC – water samples at (a) 25^0C (b) 90^0C (c) 25^0C, after cooling

5.2.1.2 HPMC – Water Samples

The four aqueous HPMC solutions were clear liquids at 25^0C (Figure 5-6a). These solutions were more viscous compared to the same concentration of MC. Upon heating, no change was observed until 50^0C. At 50^0C, the onset of turbidity took

place in all the samples and at 60^0C, the samples were completely turbid viscous liquids. At 70^0C, the 5% sample turned into a soft gel. The 3 and 4% samples showed gel formation near 80^0C. Near 90^0C, the 2% sample also turned into a gel. However, between 80 – 90^0C, water separation was observed and the white gel was surrounded by water (Figure 5-6b). Upon cooling, all four samples showed a reversible behaviour and the gels melted near 70^0C. The turbidity started disappearing near 50^0C and at 45^0C, all the samples were completely clear liquids No further change was observed and all four samples remained clear liquids at 25^0C (Figure 5-6c).

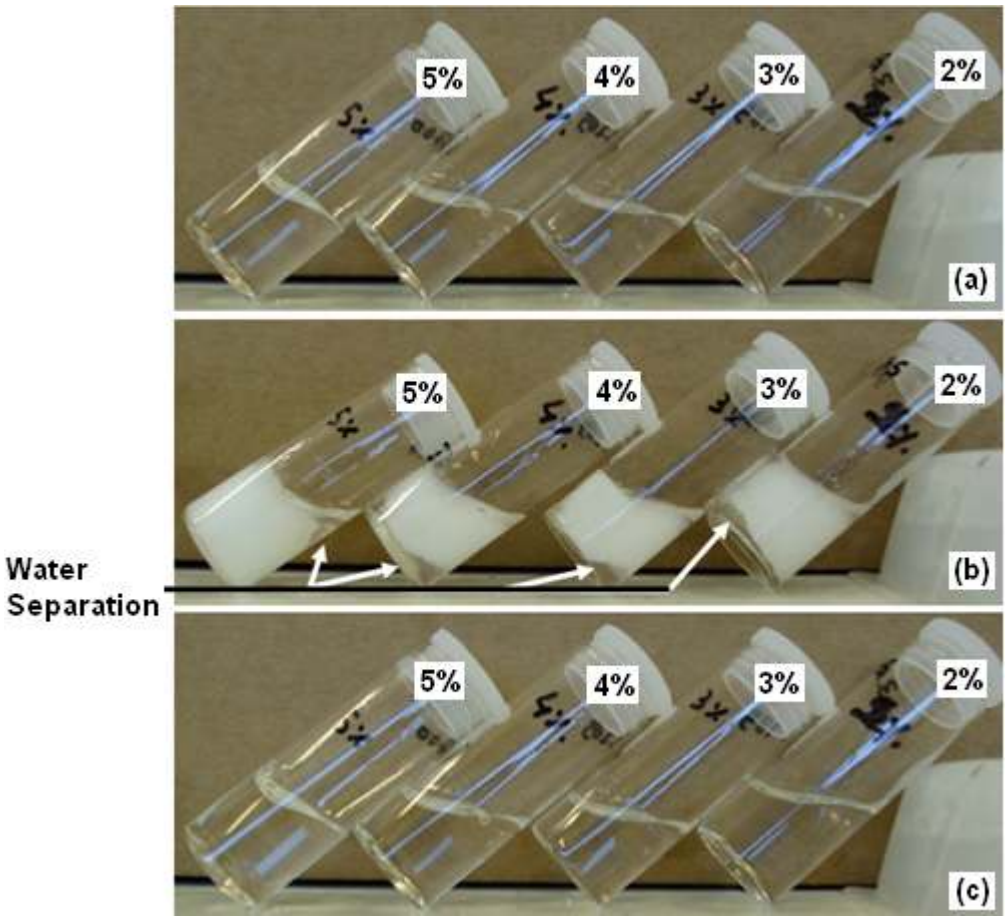

Figure 5-6. HPMC – water samples at (a) 25^0C (b) 90^0C, water separation is visible (c) 25^0C, after cooling

5.2.2 Ethylene Glycol Based Samples

Qualitative observations of MC and HPMC samples in ethylene glycol are represented in Figures 5-7 and 5-8 respectively. For these samples, apart from liquid, viscous liquid and soft gel, strong gel and solid states were also observed. The term soft gel here represents the gels which are similar to those observed

with water based solutions but because the gels formed by MC and HPMC showed an increase in strength with chnge in temperature, strong gel and solid states were also observed.

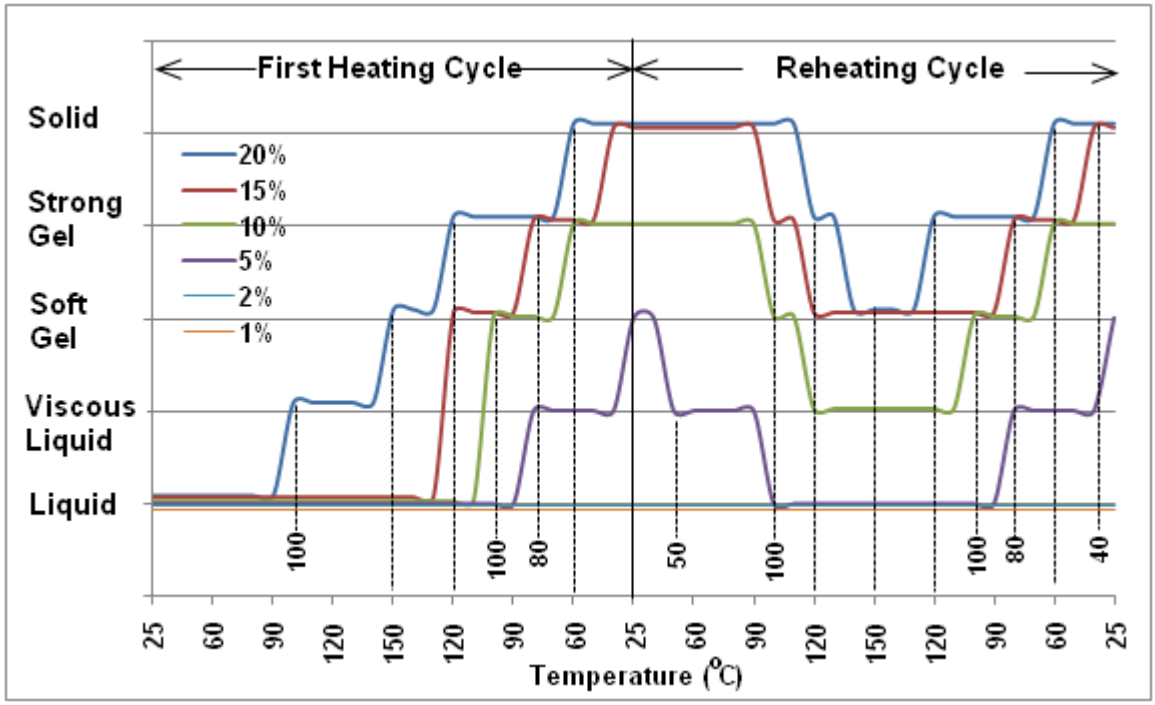

Figure 5-7. Behaviour of MC in ethylene glycol during heating and reheating cycles

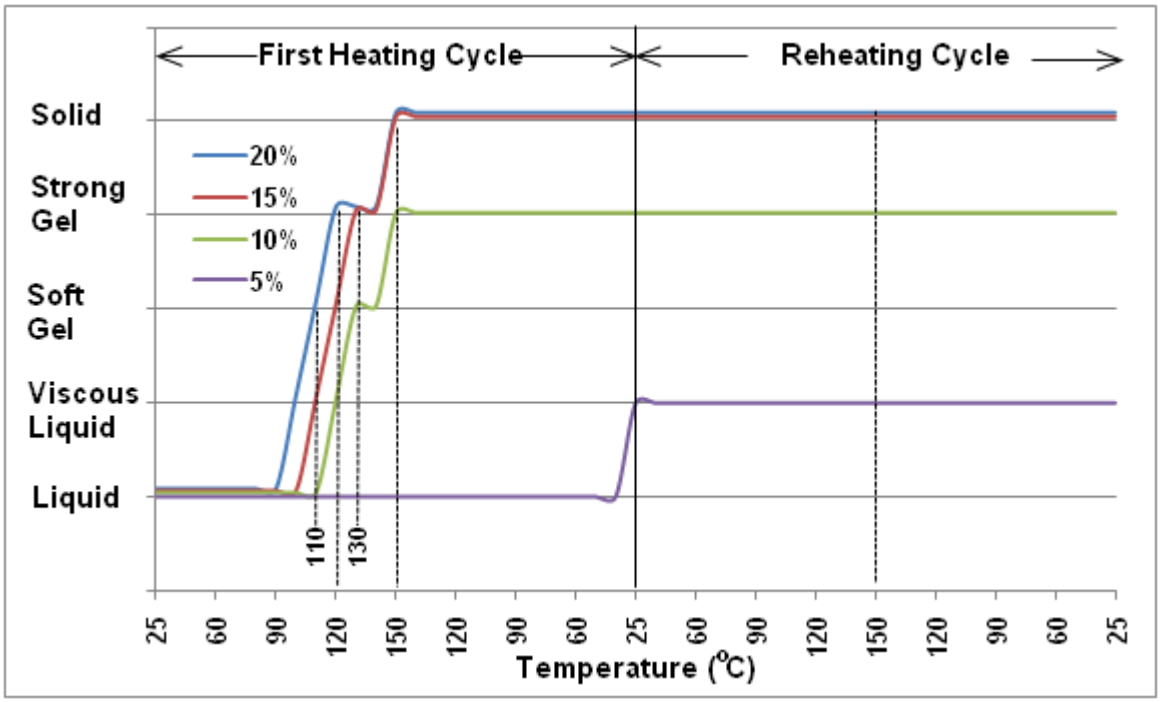

Figure 5-8. Behaviour of HPMC in ethylene glycol during heating and reheating cycles

5.2.2.1 MC – Ethylene Glycol Samples

Methyl cellulose did not dissolve in ethylene glycol at any concentration studied during these experiments (5 – 20%) therefore all MC samples were white turbid liquids at 25^0C (Figure 5-9a). Upon heating these samples, no change was observed until 90^0C. Between 90 – 100^0C, the 20% sample showed an increase in viscosity. Further heating resulted in appearance of brownish golden colour in all the samples near 130^0C.Between 140 – 150^0C, the 20% solution formed a soft gel. The three lower concentration samples (i.e. 5 – 15%) were liquids at 150^0C (Figure 5-9b).

After reaching 150^0C, the solutions were allowed to cool under natural cooling. Upon cooling, the 20% sample turned into a strong gel at 120^0C whereas the 15% sample formed a soft gel. Similarly at 100^0C, the 10% sample formed a gel. At 80^0C the 5% sample turned into a viscous liquid and the 15% sample changed to a strong gel. The 20% sample became solid and the 10% sample formed a strong gel at 60^0C whereas the 15% sample changed to a solid at 40^0C. Upon reaching 25^0C, the 20 and 15% samples were solids whereas the 10% sample was a strong gel and the 5% sample formed a soft gel (Figure 5-9c). Since, the 5% sample showed a soft gel upon cooling, 1 and 2% samples were also prepared and heated/cooled between 25-150^0C but these two concentrations did not form a gel at any stage during heating and cooling (Figure 5-9a to c)

After allowing approximately 24 hours at room temperature (i.e. 20^0C), the samples were reheated. The gel formed by the 5% sample melted near 50^0C and converted to a viscous liquid. Near 100^0C, the 15% sample softened from solid into a strong gel state and the 10% sample, which was a strong gel, converted to a soft gel. Also, the 5% sample changed into a liquid (low viscosity) state. At 120^0C, the 20% sample turned from solid into a strong gel, the 15% sample converted into a soft gel and the 10% sample melted from a gel into a viscous liquid. The 20% sample softened from a strong gel to a soft gel. At the end of second heating cycle (i.e. at 150^0C) 1,2 and 5% sample were clear liquids, the 10% sample was a viscous liquid and the 15% and 20% samples were soft gels. Upon cooling, at 120^0C, the 20% sample turned into a strong gel state and the 10% sample formed a soft gel at 100^0C. At 80^0C, both 5 and 15% samples changed to a viscous liquid and a strong gel respectively. At 60^0C, the 10%

sample formed a strong gel and the 20 and 15% samples became solid at 60^0C and 40^0C respectively. Cooling to 25^0C resulted in formation of a soft gel by the 5% sample and the two low concentrations (i.e. 1 and 2%) remained liquid. The 10% sample was a strong gel whereas the 15 and 20% samples were solid.

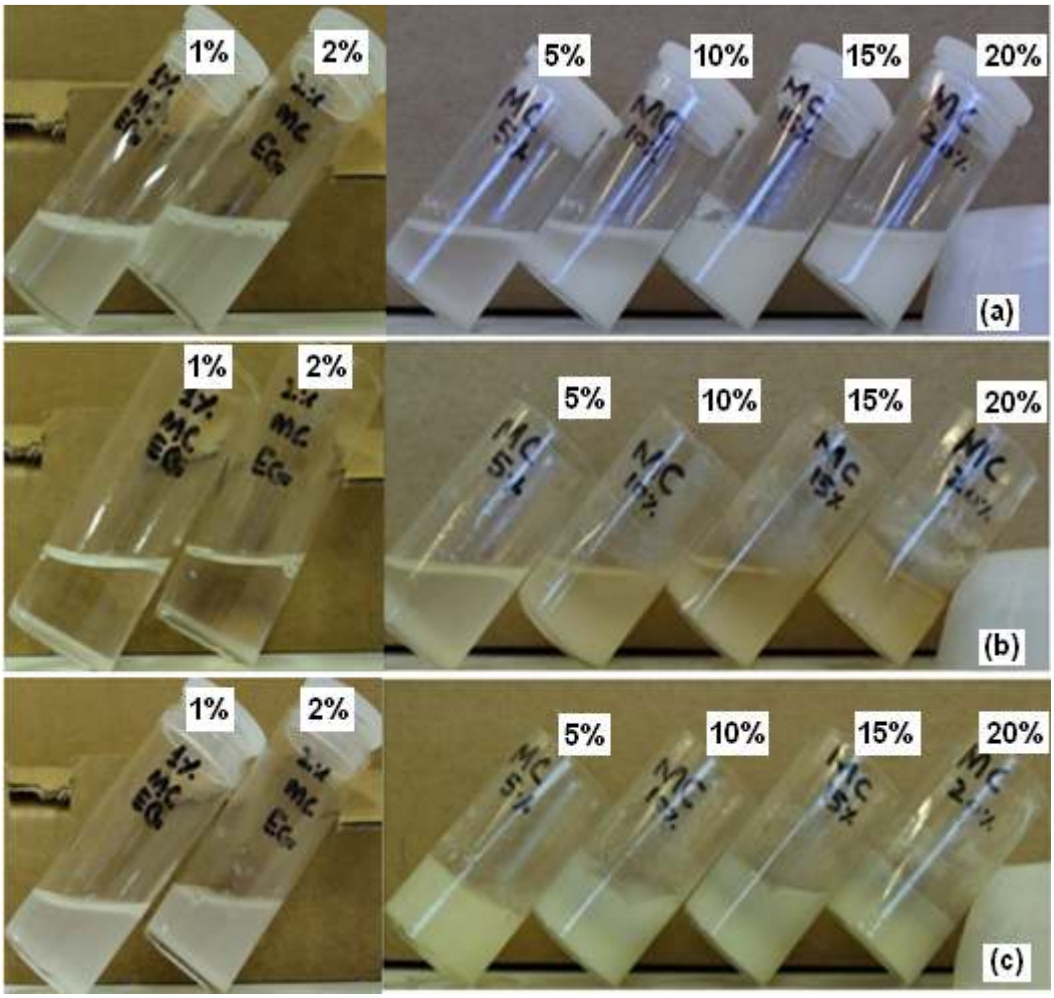

Figure 5-9. MC – ethylene glycol samples at (a) 25^0C (b) 150^0C (c) 25^0C, after cooling

5.2.2.2 HPMC – Ethylene Glycol Samples

HPMC in ethylene glycol was examined at concentrations from 5 – 20% (5% increments). Because the 5% sample did not form a gel upon heating/cooling, concentrations lower than 5% were not studied. Similar to the MC samples, all the HPMC- ethylene glycol samples were turbid liquids (Figure 5-10a). Upon heating, the 20% sample changed to a viscous liquid at 100^0C and it formed a soft gel near 110^0C. Also, the 15% sample turned to a viscous liquid at 110^0C. At 120^0C the 20% sample was a strong gel whereas the 15% and 10% samples formed soft gel and viscous liquid respectively. The 15% sample formed a strong gel and 10%

sample formed a soft gel at 130^{0}C. Finally, at 150^{0}C, 20 and 15% samples converted into solid and the 10% sample changed to a strong gel state. The 5% sample was liquid at this temperature with a soft gel near the bottom of the tube (Figure 5-10b). As the samples were cooled, the 5% sample turned into a part gelled viscous liquid near 25^{0}C and the other three samples remained unchanged (Figure 5-10c). During the reheating cycle, no change was observed in the state of the four samples at any temperature.

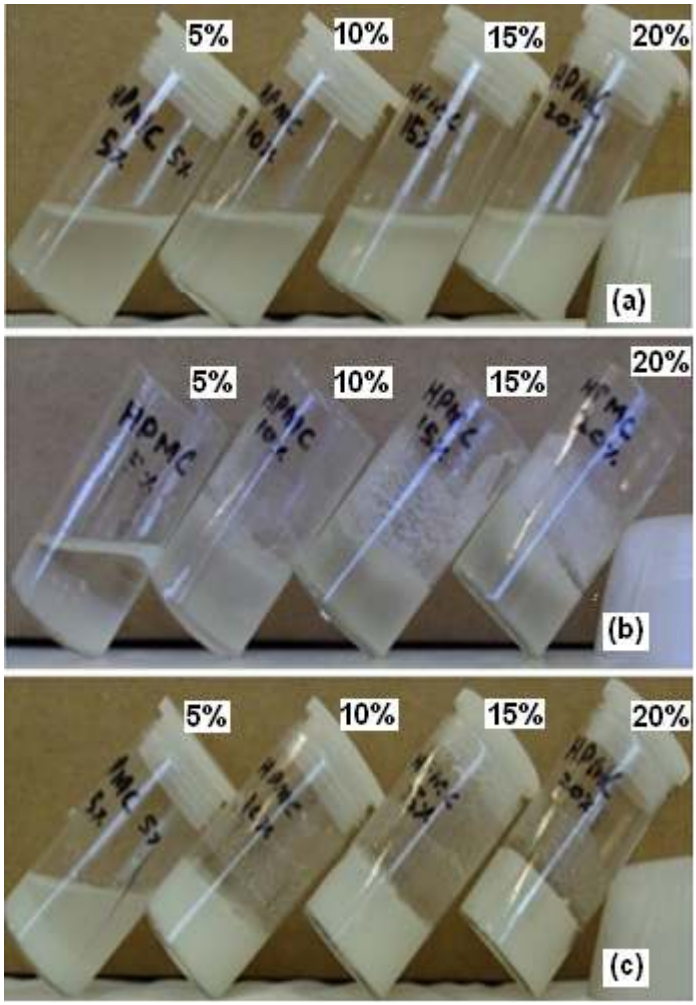

Figure 5-10. HPMC – ethylene glycol samples at (a) 25^{0}C (b) 150^{0}C (c) 25^{0}C, after cooling

5.2.3 Propylene Glycol Based Samples

HPMC in ethylene glycol formed a permanent gel/solid structure and the samples did not change during reheating/cooling, whereas MC in ethylene glycol samples showed a gel/solid which formed during cooling and melted/reformed during subsequent heating (i.e. reheating) and cooling respectively. Therefore, it was decided to continue further experiments with MC in different solvents. Six different

compositions including 1, 2 and 5 – 20% (increments of 5%, w/w) of MC in propylene glycol were prepared and investigated for thermal gelation. Figure 5-11 shows the behaviour of MC in propylene glycol samples during heating and reheating cycles.

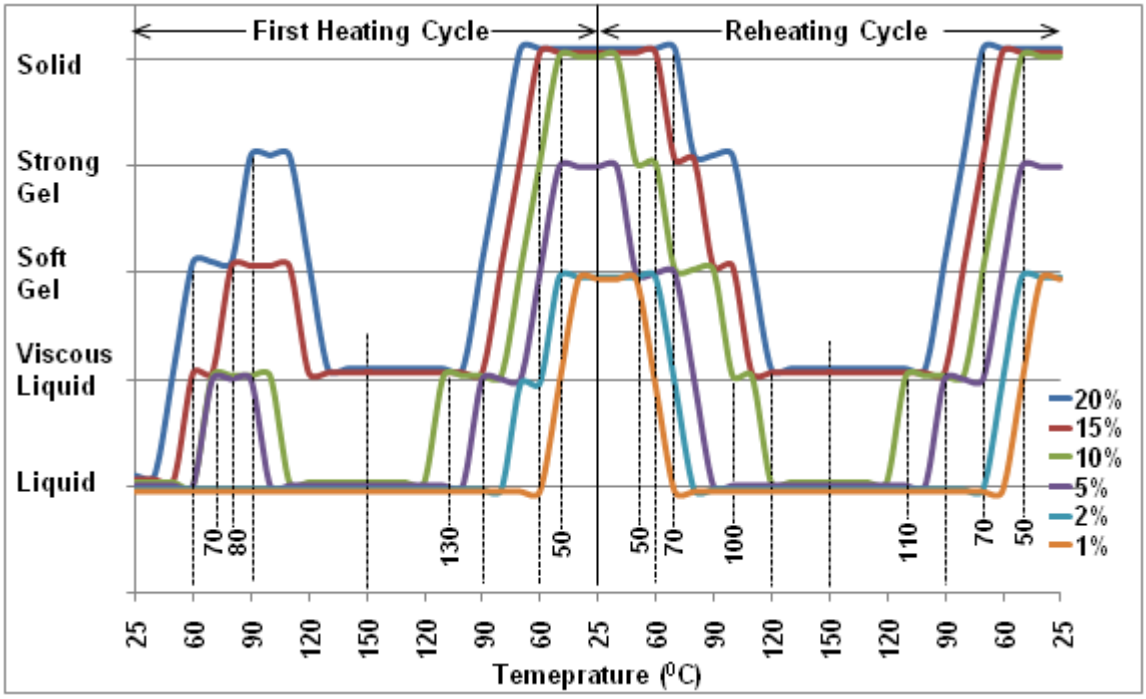

Figure 5-11. Behaviour of MC in propylene glycol during heating and reheating cycles

Figure 5-12a shows the six MC in propylene glycol samples before the start of heating. Upon heating, the 20 and 15% samples changed to viscous liquids at 50^{0}C and 60^{0}C respectively. At 60^{0}C, the 20% sample formed a soft gel and at 70^{0}C, the 5 and 10% samples converted to viscous liquids. The 15% sample formed a soft gel at 80^{0}C. At 90^{0}C, the 20% sample formed a strong gel. All the samples started turning clear near 90^{0}C and were completely clear at 100^{0}C. The three lower concentration samples (i.e. 1, 2 and 5%) were clear liquids whereas the 10, 15 and 20% samples were clear viscous liquid, soft gel and strong gel at 100^{0}C. At 110^{0}C, the 10% sample changed to a relatively low viscosity liquid. The 15% and 20% samples formed viscous liquid and soft gel respectively at 120^{0}C and the soft gel formed by 20% subsequently melted into a viscous liquid at 130^{0}C. At 150^{0}C, the four lower concentrations (i.e. 1, 2, 5 and 10%) were liquids and the 15 and 20% samples were viscous liquids (Figure 5-12b).

Cooling resulted in a gradual increase in the viscosity/strength of the samples as the 20,15 and 10% samples formed soft gels at 90, 80 and 70^{0}C respectively. The

gel formed by 20% sample converted to a strong gel at 80^0C and into a solid at 70^0C. The 15% sample changed to a strong gel and a solid respectively at 70 and 60^0C and the same changes occurred for 10% sample at 60 and 50^0C respectively. The 5, 2 and 1% sample formed soft gels at 60, 50 and 40^0C respectively and the 5% sample turned into a strong gel at 50^0C. At 25^0C, the three higher concentrations (i.e. 10-20%) were solids, 5% was a strong gel and the 2 and 1% samples were soft gels (Figure 5-12c).

The samples gradually converted to lower viscosity states upon reheating and at 150^0C, all the samples were liquids similar to the first heating cycle. Cooling of the samples resulted in changes similar to those during cooling after the first heating cycle. When the samples cooled to 25^0C, the three higher concentrations (i.e. 10 – 20%) were solids, the 5% sample was a strong gel and the 2 and 1% samples were soft gels.

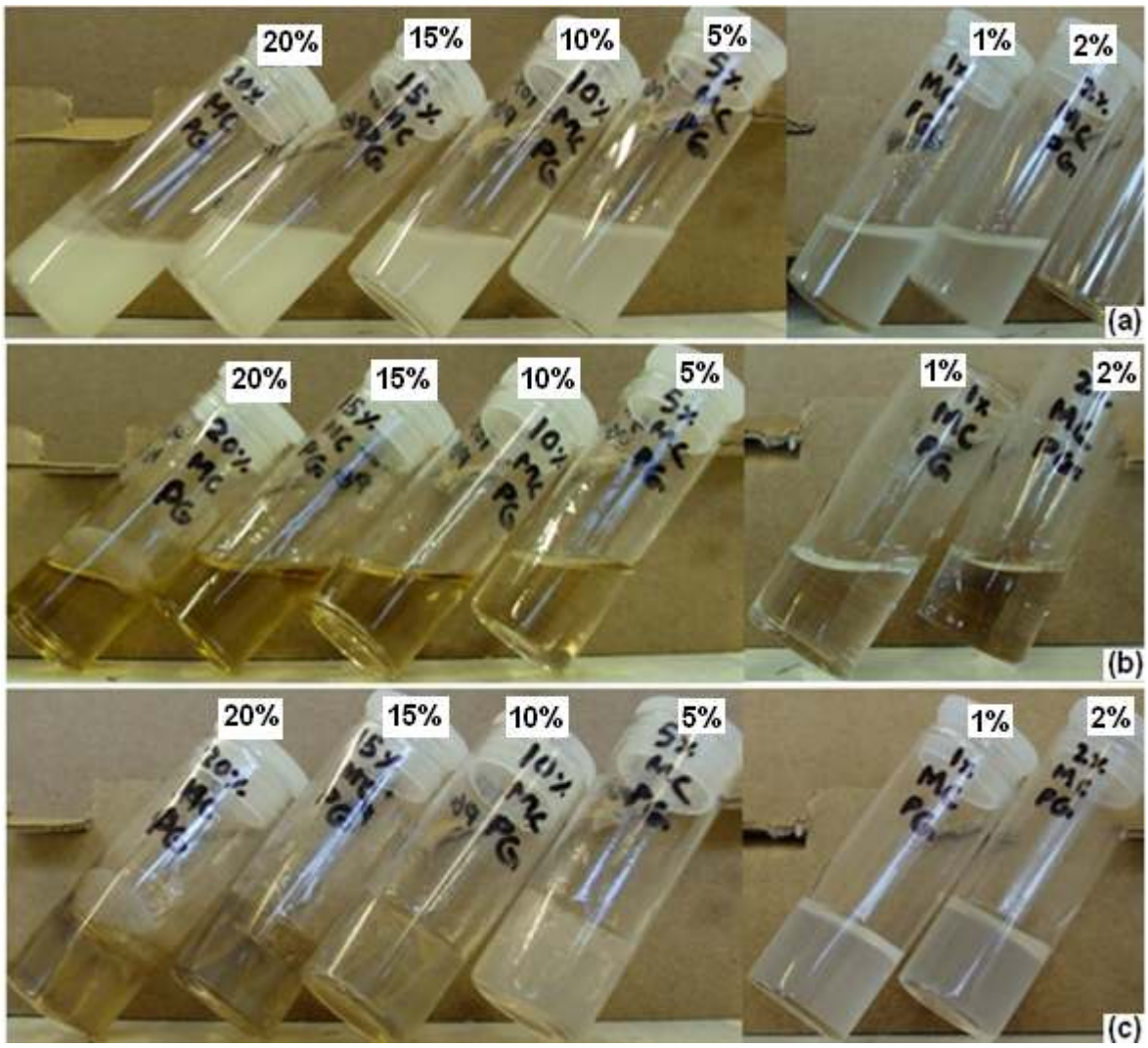

Figure 5-12. MC – propylene glycol samples at (a) 25^0C (b) 150^0C (c) 25^0C, after cooling

5.2.4 Butylene Glycol Based Samples

MC in butylene glycol at six different concentrations of 1, 2 and 5 – 20% (w/w) in 5% increments were prepared and investigated for gelation upon heating/cooling. Behaviour of these samples during two heating cycles is shown in Figure 5-13.

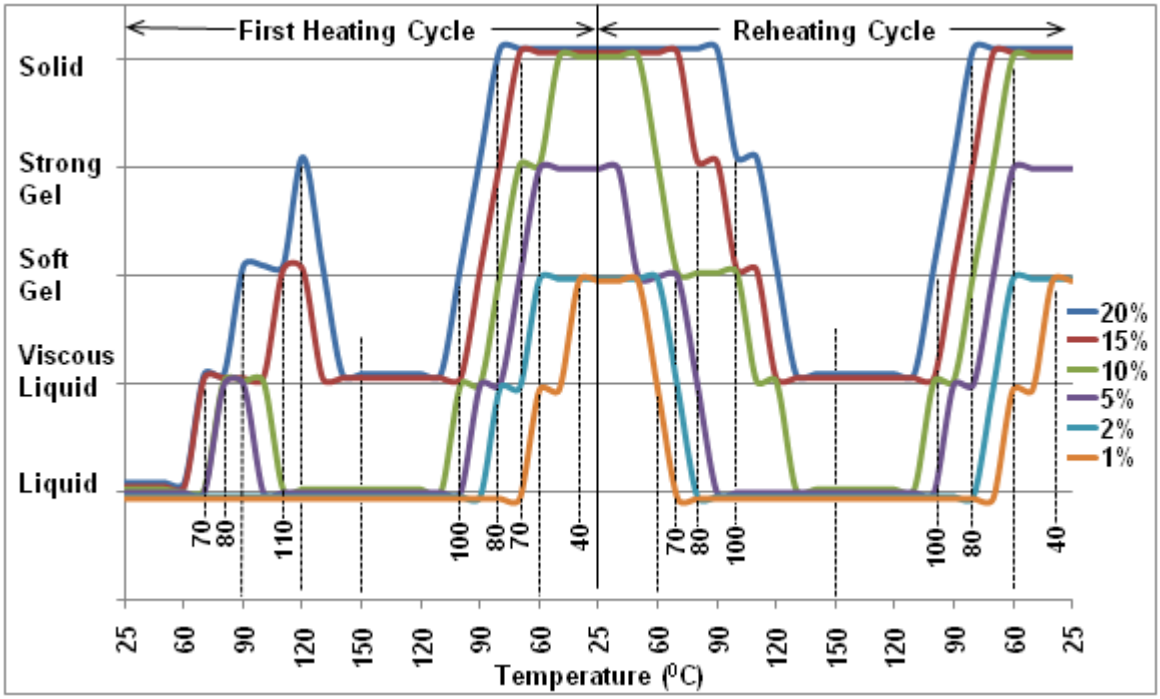

Figure 5-13. Behaviour of MC in butylene glycol during heating and reheating cycles

These samples showed a similar behaviour to MC in propylene glycol (Figure 5-14a). At 70^{0}C, the 20 and the 15% samples and at 80^{0}C, the 10 and 5% samples converted to viscous liquids. A soft gel was formed by the 20% sample at 90^{0}C and by the 15% sample at 110^{0}C. Between 100 – 110^{0}C, all the samples started turning clear and at 110^{0}C, the four lower concentrations (i.e. 1, 2, 5 and 10%) were clear liquids and the 15 and 20% samples were clear soft gels. At 120^{0}C, the 20% sample formed a strong gel. Further heating resulted in melting of the gels formed by 15 and 20% samples at 130 and 140^{0}C respectively and at 150^{0}C, these two samples were viscous liquids whereas the lower concentrations were less viscous (Figure 5-14b). During cooling, all these samples showed a gradual increase in viscosity and the 20% sample formed a soft gel and a strong gel at 100 and 90^{0}C respectively. The 15% sample formed a soft gel at 90^{0}C and a strong gel at 80^{0}C. At, 80^{0}C, the 20% sample converted to a solid and the 10% sample formed a soft gel. At 70^{0}C, the 15 and 10% samples changed into solid and strong gel respectively and the 5% sample formed a gel. The soft gel formed

by the 5 % sample turned into a strong gel at 60^0C and the 10% sample converted to a solid at 50^0C. Both the 2 and the 1% samples formed soft gels near 60 and 40^0C respectively. At 25^0C, the three higher concentrations (10-20%) were solids, the 5% sample was a strong gel and the two low concentrations (1 and 2%) were soft gels (Figure 5-14c).

Reheating the samples resulted in gradual melting and all samples were liquids at 150^0C. The 20 and 15% samples had a higher viscosity than the other four samples. Subsequent cooling of the samples resulted in behaviour similar to that during cooling in the first heating cycle and the samples turned into gels at different temperatures as shown in Figure 5-13.

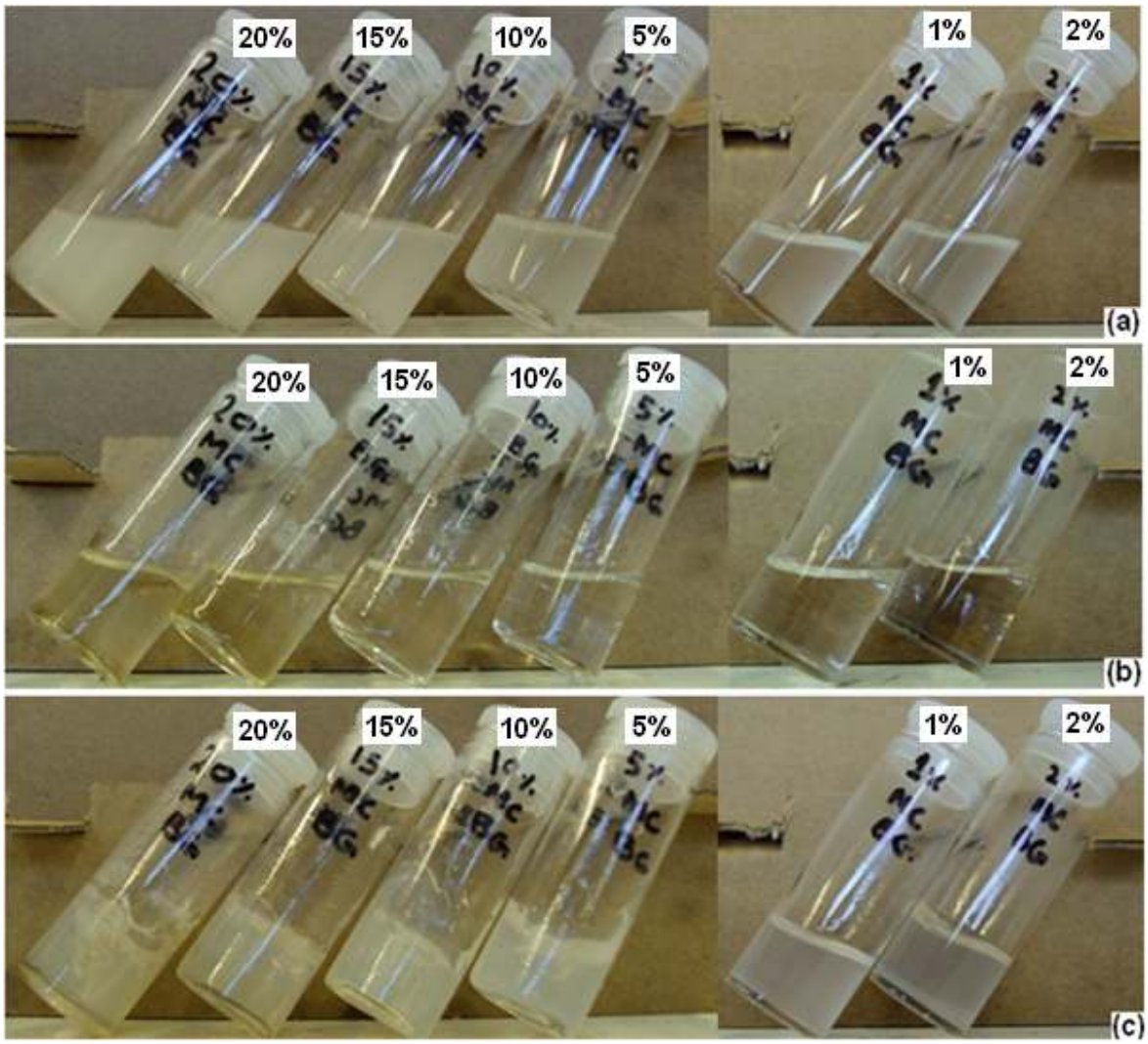

Figure 5-14. MC – butylene glycol samples at (a) 25^0C (b) 150^0C (c) 25^0C, after cooling

5.3 Fourier Transform Infrared (FTIR) Spectroscopy

In order to understand the changes of MC in the three glycols upon heating, ATR-FTIR spectroscopy was performed on the highest concentration samples (i.e. 20%) during heating and cooling. The IR spectra of all the glycols by the ATR technique and for MC by the potassium bromide (KBr) pellet method were also obtained at room temperature and are shown in Figure 5-15. IR Spectra for 20% MC in ethylene, propylene and butylene glycol are presented in Figures 5-16, 5-18 and 5-20 respectively. During heating and cooling, changes were observed in the spectra of all these samples within the range 800-1500 cm^{-1} and for the OH stretching band near 3300 cm^{-1}. Therefore, Figures 5-17, 5-19 and 5-21 show the spectra in the range 800-1500 cm^{-1} for MC in ethylene, propylene and butylene glycol respectively and the variation of peak position for the OH stretching band (i.e. near 3300 cm^{-1}) for each sample is presented in the Figure 5-22. An explanation of these results will be presented in the discussion (i.e. section 5.7).

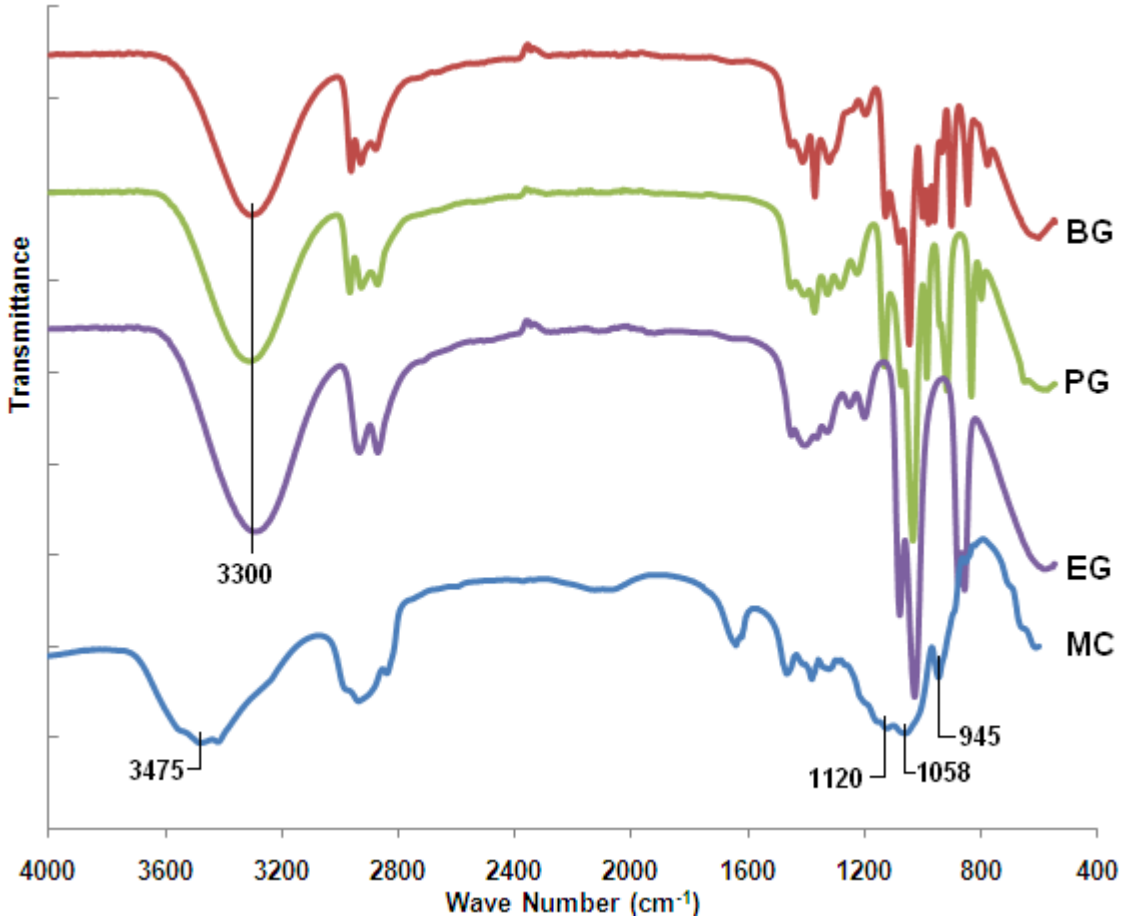

Figure 5-15. FTIR spectra of MC, ethylene (EG), propylene (PG) and butylene glycol (BG)

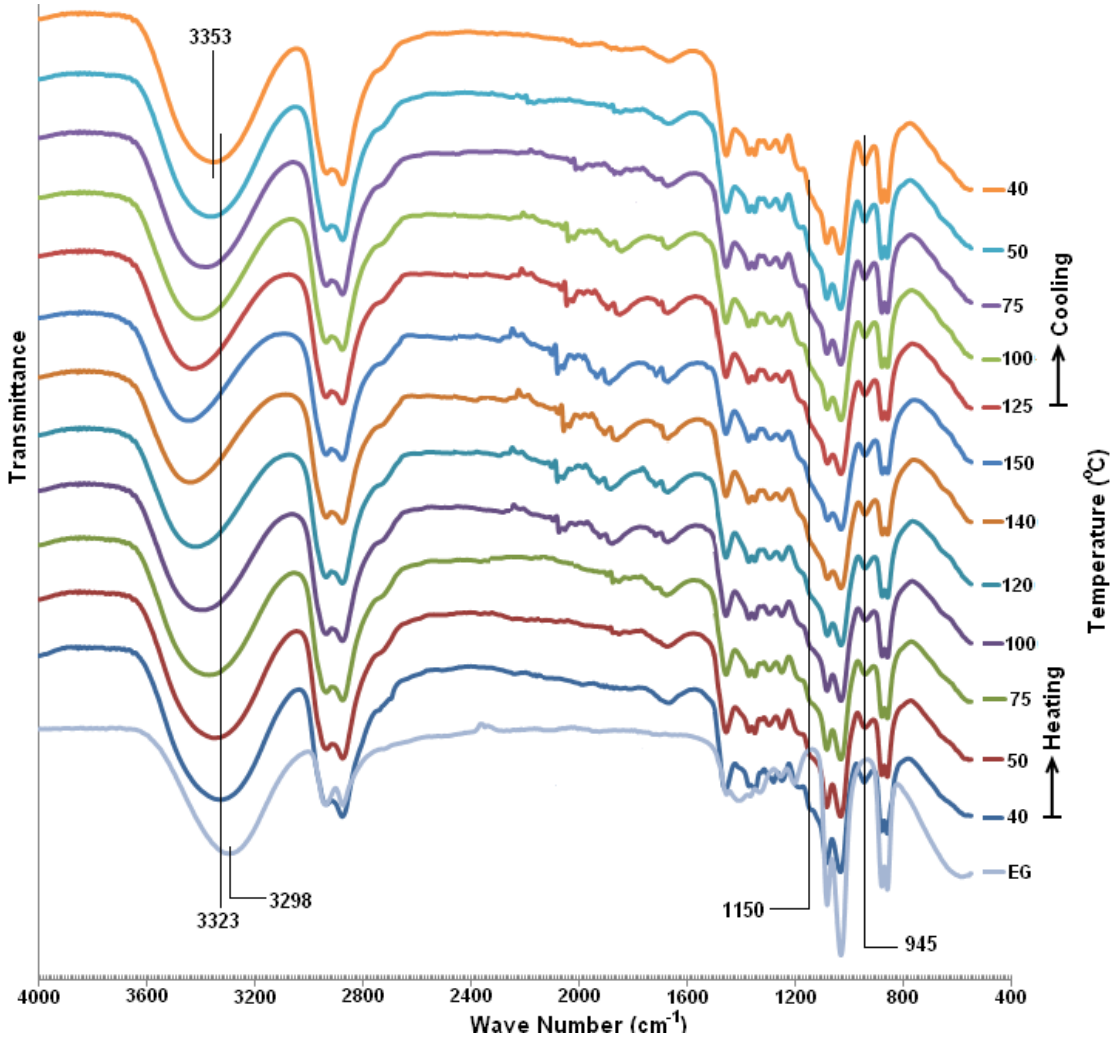

Figure 5-16. FTIR spectra of 20% MC in ethylene glycol at different temperatures

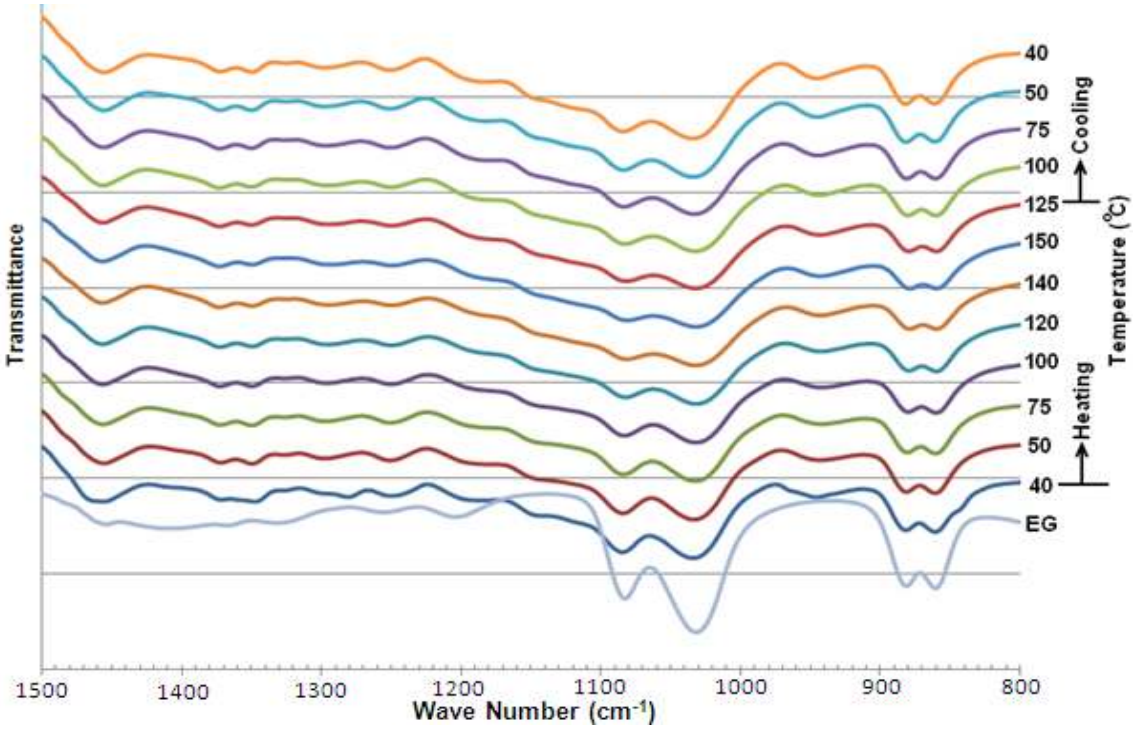

Figure 5-17. FTIR spectra of 20% MC in ethylene glycol between 800 – 1500 cm^{-1}

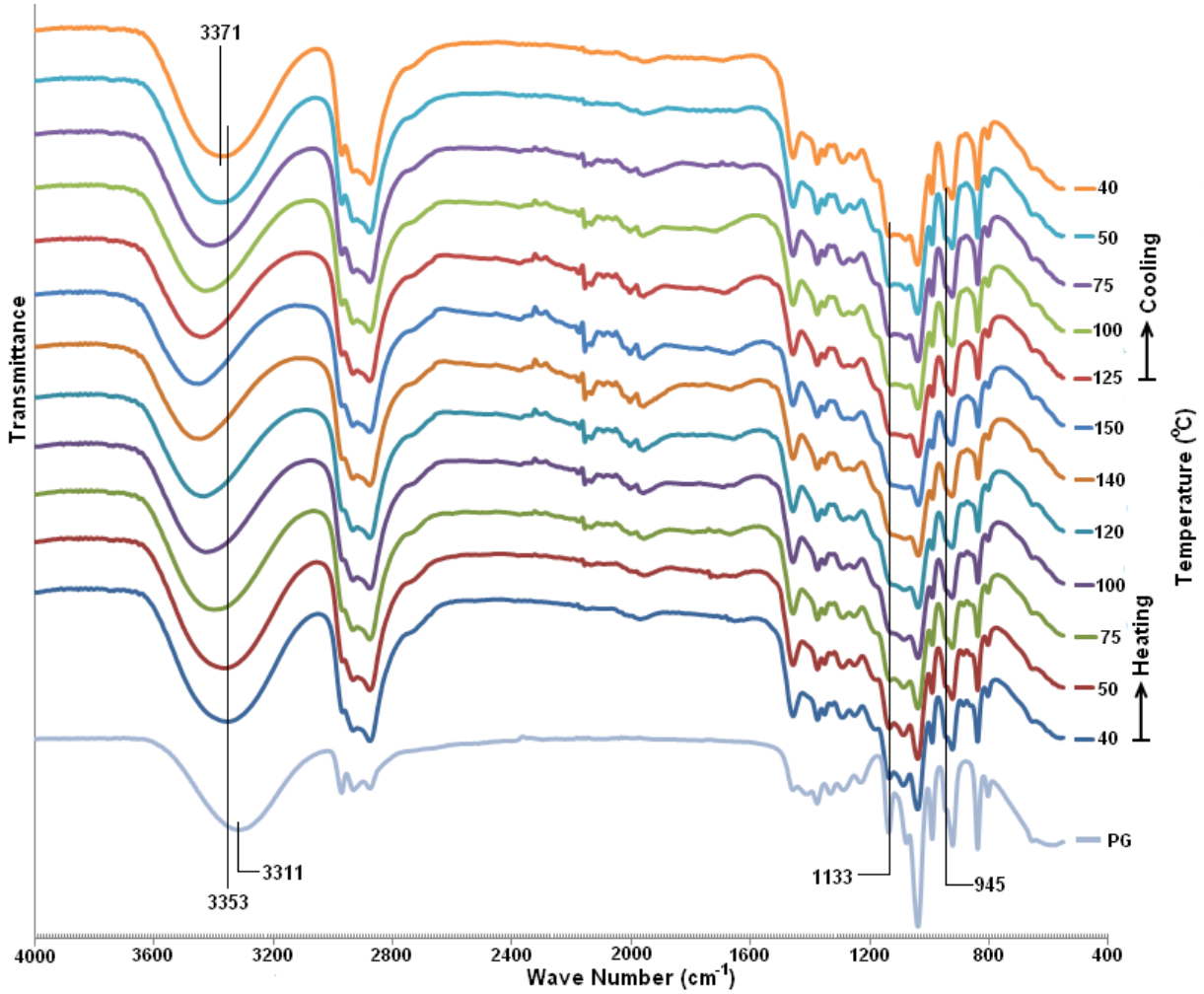

Figure 5-18. FTIR spectra of 20% MC in propylene glycol at different temperatures

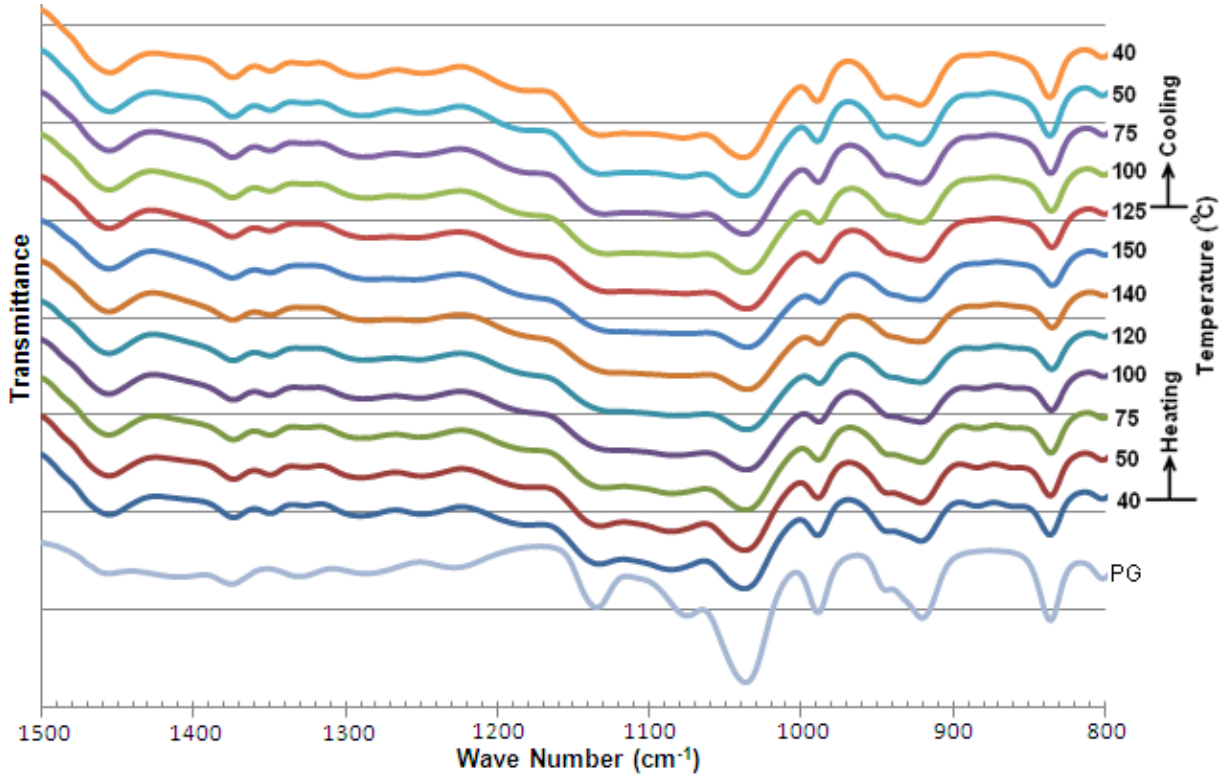

Figure 5-19. FTIR spectra of 20% MC in propylene glycol between 800 – 1500 cm^{-1}

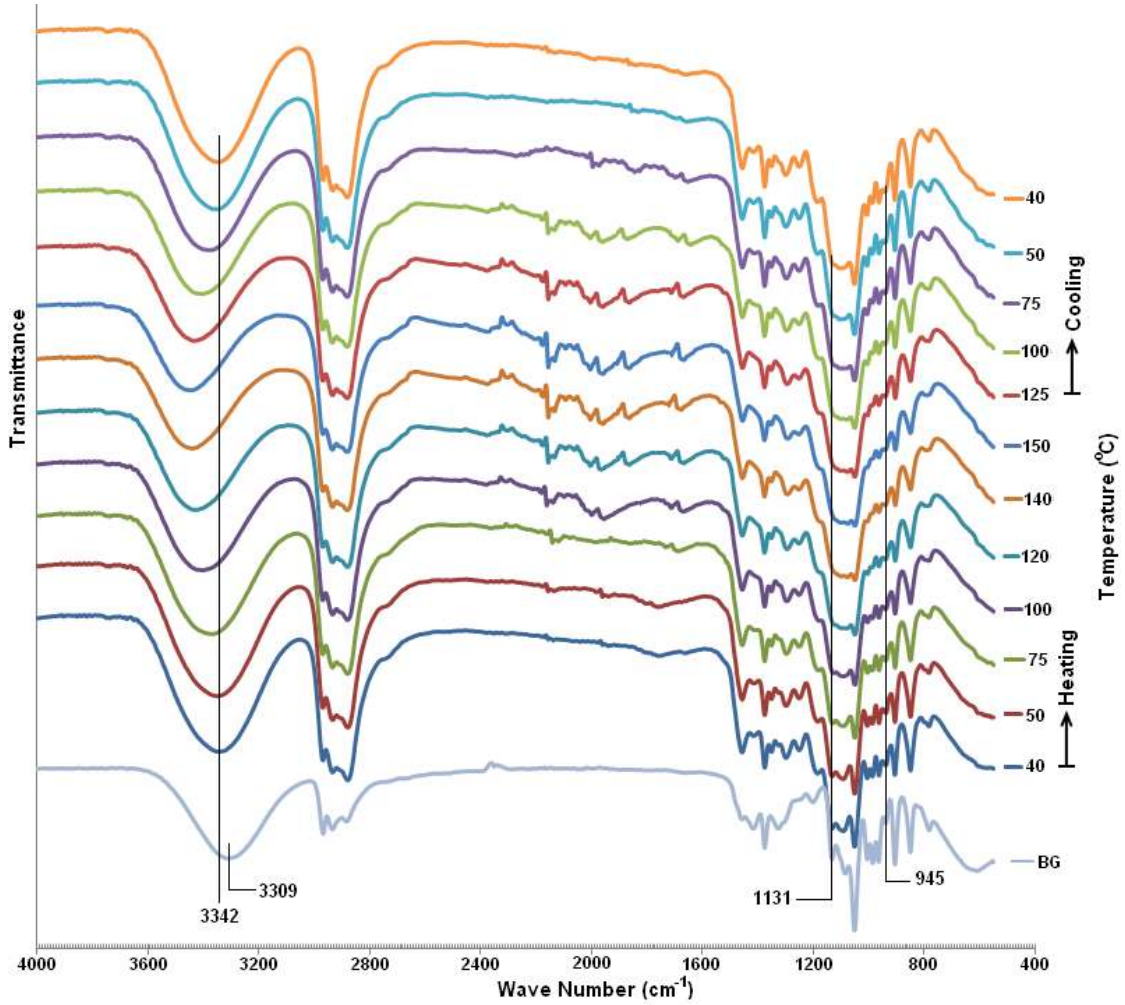

Figure 5-20. FTIR spectra of 20% MC in butylene glycol at different temperatures

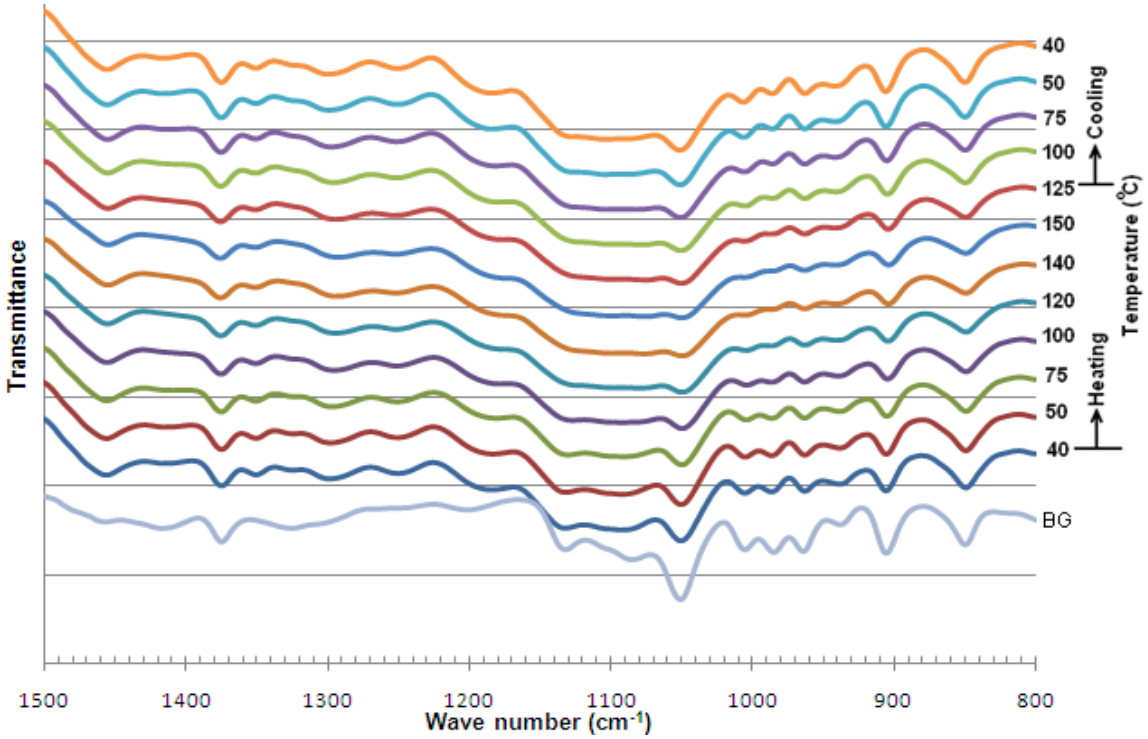

Figure 5-21. FTIR spectra of 20% MC in butylene glycol between 800 – 1500 cm^{-1}

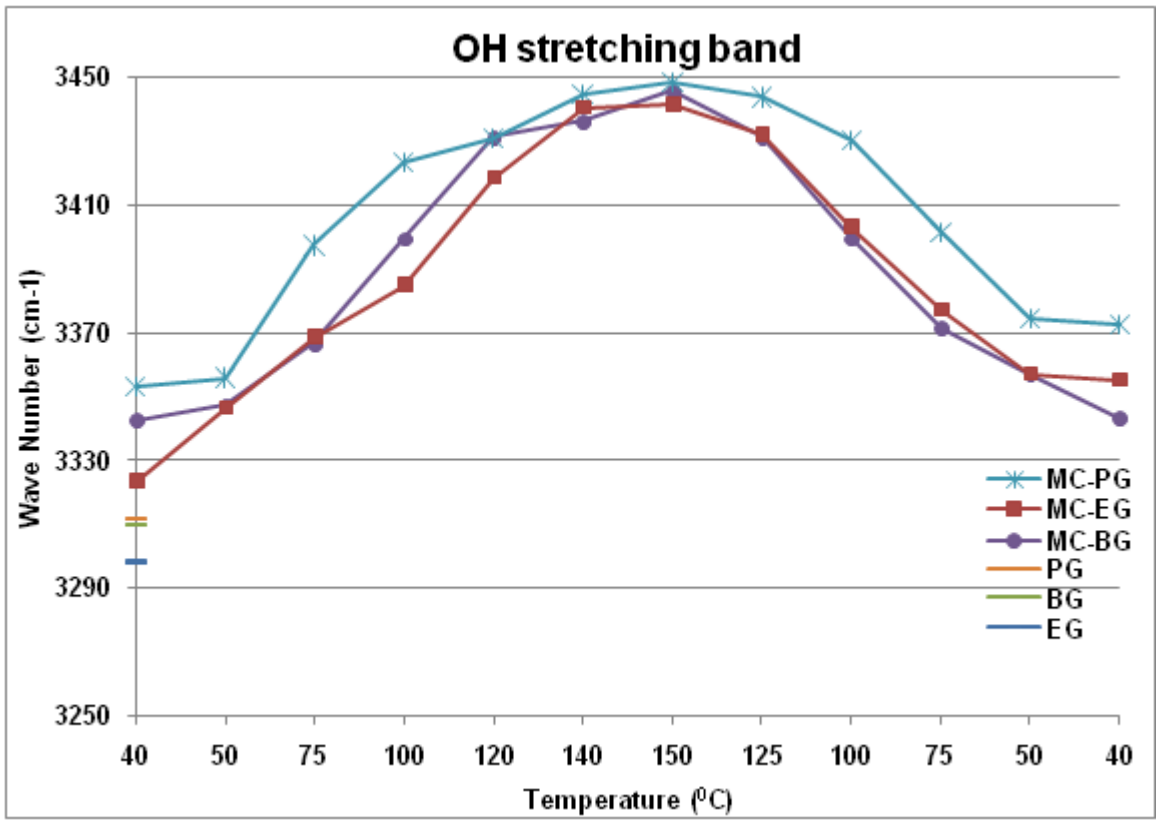

Figure 5-22. Variation in the peak position of OH stretching band with temperature for 20% MC in ethylene (EG), propylene (PG) and butylene (BG) glycol

5.4 Hot Stage Microscopy

Hot stage microscopy of MC and 20% MC in each glycol was performed to analyse the changes in the structure (i.e. crystalline/amorphous) upon heating and cooling. Micrographs of MC and MC in ethylene, propylene and butylene glycol at different temperatures are shown in the Figures 5-23, 5-24, 5-25 and 5-26 respectively.

Micrographs of MC at various temperatures (between 20 up to 268^{0}C) during heating are shown in Figure 5-23a to h. Crystalline structure was present up to 200^{0}C (Figure 5-23a to d). The crystalline structure started disappearing near 250^{0}C (Figure 5-23e) and a completely melted structure was obtained at 268^{0}C (Figure 5-23h)

Figures 5-24a and b depict the micrographs of 20% MC in ethylene glycol at 25 and 100^{0}C showing the presence of crystalline structure at these temperatures. At 120^{0}C some loss of crystallinity due to dissolution of MC was observed (Figure 5-24c). The micrograph at 150^{0}C (Figure 5-24d) shows no crystalline structure

indicating nearly complete dissolution of MC in ethylene glycol. The intensity of the microscope lamp was increased from 4 volts to 6 volts during cooling so that it was easier to observe any changes in the state of the sample. During cooling, as the sample formed a white (turbid) solid, a surface texture gradually developed (Figures 5-24e to h) and a few crystals could also be seen at 100^0C (Figure 5-24g) and 30^0C (Figure 5-24h).

Micrographs for 20% MC in propylene glycol at different temperatures are shown in Figure 5-25. The crystalline structure present due to MC at 30^0C (Figure 5-25a) mostly disappeared by 100^0C (Figure 5-25b) and at 120 and 150^0C crystallinity completely disappeared due to dissolution of MC (Figures 5-25c and d). During cooling, other than the appearance of very few crystals, which did not dissolve during heating, no change was observed and the structure remained disordered (Figures 5-25.e to h).

Figure 5-26 shows the micrographs for 20% MC in butylene glycol at different temperatures. Crystalline structure present at 30 and 100^0C (Figure 5-26a and b) disappeared almost completely at 120^0C (Figure 5-26c) and as for MC in both ethylene and propylene glycols, a disordered structure with complete dissolution of MC was observed at 150^0C (Figure 5-26d). During cooling, turbidity appeared but no texture (as seen in ethylene glycol) was observed. The disordered structure was maintained along with a very few undissolved MC crystals (Figures 5-26e to h).

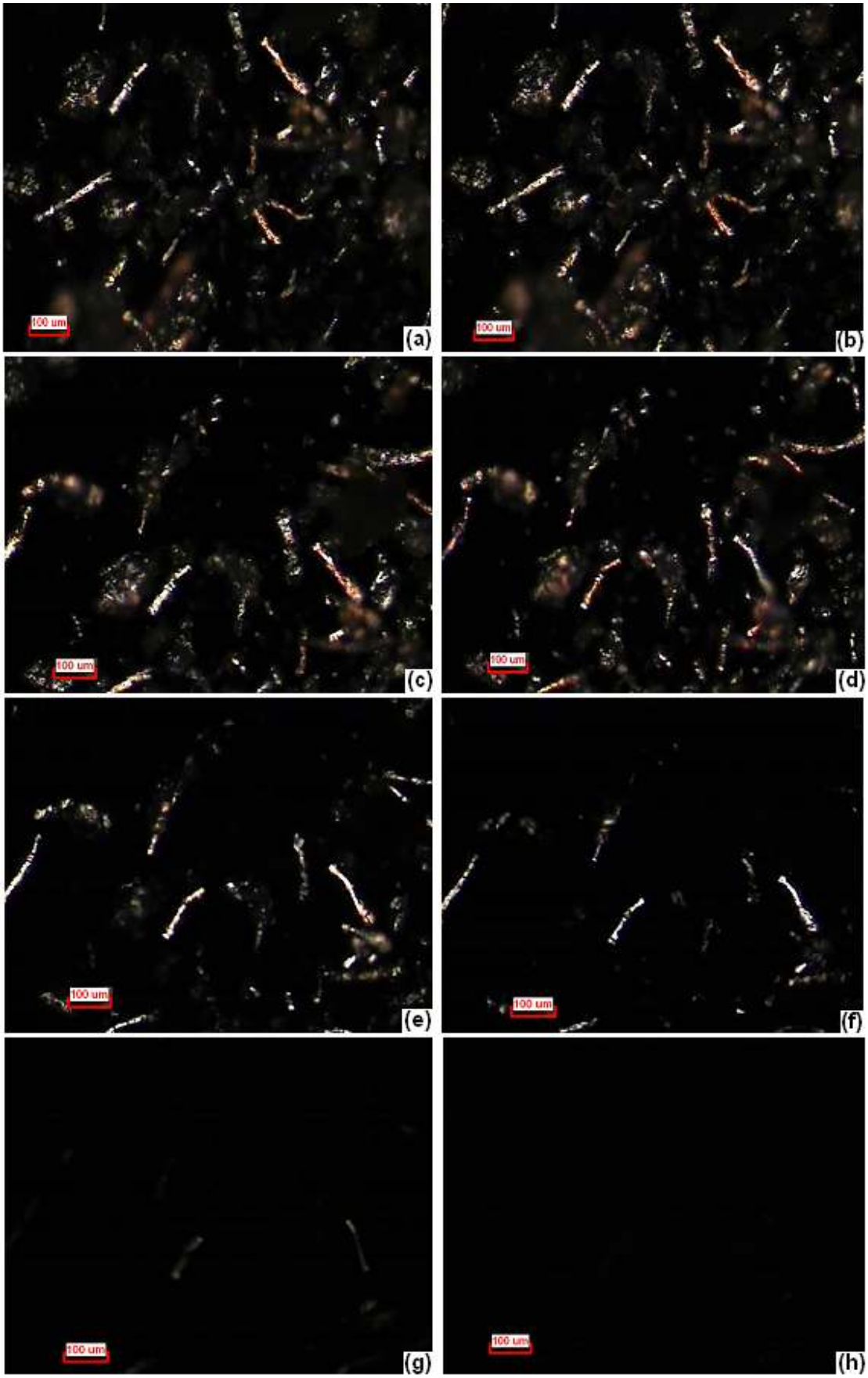

Figure 5-23. Micrographs of MC at (a) 25^{0}C (b) 100^{0}C (c) 150^{0}C (d) 200^{0}C (e) 250^{0}C (f) 260^{0}C (g) 263^{0}C (h) 268^{0}C

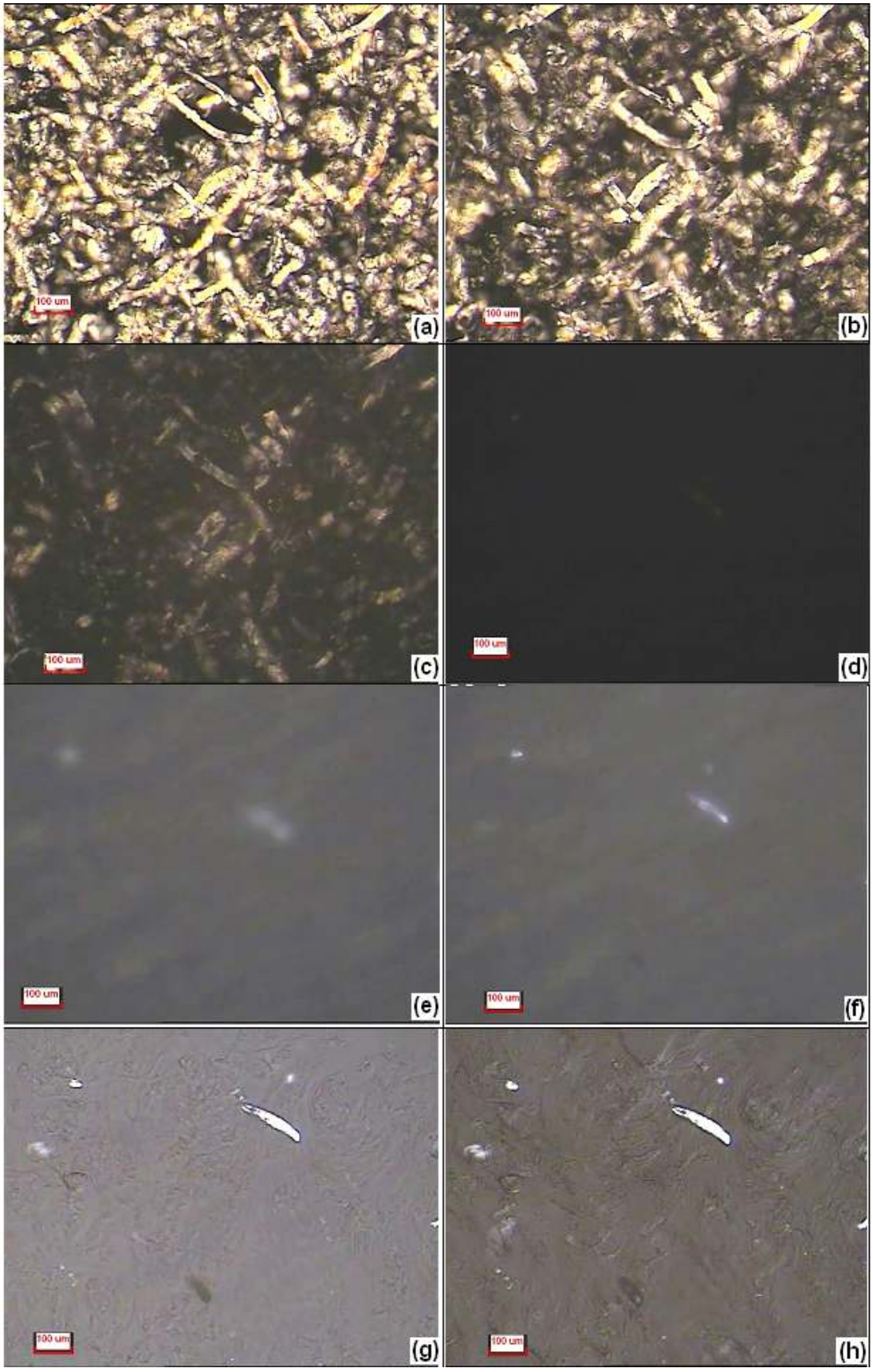

Figure 5-24. 20% MC in ethylene glycol during heating at (a) 30^{0}C (b) 100^{0}C (c) 120^{0}C (d) 150^{0}C, and during cooling at (e) 140^{0}C (f) 120^{0}C (g) 100^{0}C (h) 30^{0}C

Figure 5-25. 20% MC in propylene glycol during heating at (a) 30^{0}C (b) 100^{0}C (c) 120^{0}C (d) 150^{0}C, and during cooling at (e) 140^{0}C (f) 120^{0}C (g) 100^{0}C (h) 30^{0}C

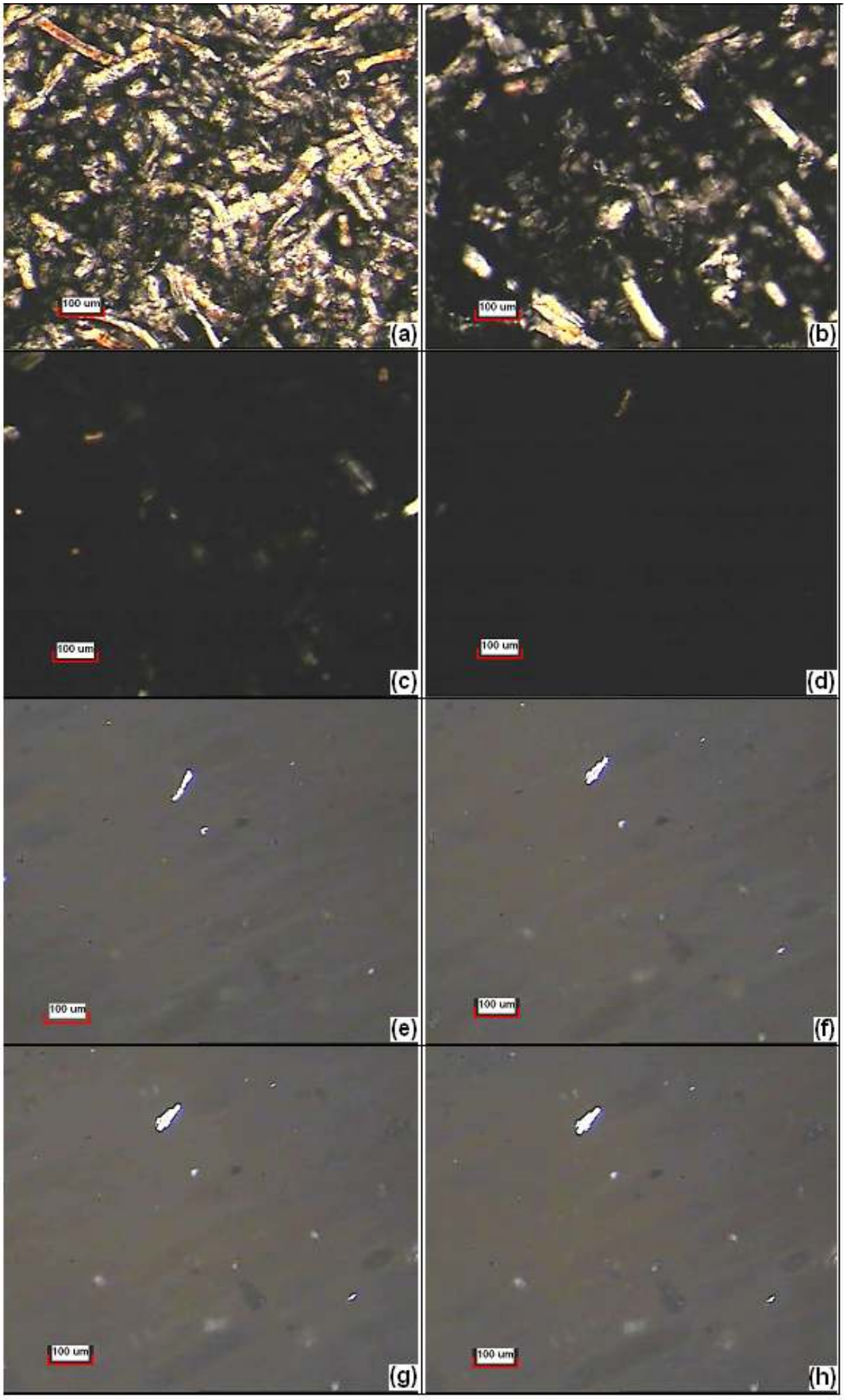

Figure 5-26. 20% MC in butylene glycol during heating at (a) 30^{0}C (b) 100^{0}C (c) 120^{0}C (d) 150^{0}C, and during cooling at (e) 140^{0}C (f) 120^{0}C (g) 100^{0}C (h) 30^{0}C

5.5 Differential Scanning Calorimetry

Microscopy provided the evidence of crystallinity in the samples before heating. However, during cooling when all the samples turned into a gel and solid respectively, apart from a few crystals, no evidence of a crystalline structure was observed. Therefore, to investigate the changes in the crystallinity of the samples upon heating and cooling, DSC of MC in each glycol was performed.

DSC curves for 20% MC in ethylene glycol liquid and solid are shown in the Figure 5-27. For the liquid sample, a broad endothermic peak near 125^0C was observed. For the solid sample, the endotherm broadened further and a heat flow maxima was observed near 132^0C. During cooling, no peaks were observed for either liquid and solid suggesting that the gel formation and subsequent solidification of MC in ethylene glycol resulted in a disordered/less perfect structure.

DSC curves for 20% MC in propylene glycol liquid and solid (Figure 5-28) show very broad endotherms with no identifiable maxima. No transitions were observed during cooling suggesting that the gel/solid formed by MC in propylene glycol had a dissolved/disordered structure.

Figure 5-29 shows the DSC curves for 20% MC in butylene glycol. For the liquid, a broad endotherm with a peak at 105^0C and for the solid, a broader endotherm with peak at 104^0C was observed. Cooling curves for these samples were similar to those for MC in ethylene glycol suggesting a disordered structure. Enthalpy values, calculated from DSC endotherms for the samples are presented in Table 5-1.

Sample		Enthalpy (J/g)
20% MC – EG	**Liquid**	322
	Solid	61
20% MC – PG	**Liquid**	21
	Solid	13
20% MC – BG	**Liquid**	22
	Solid	22

Table 5-1. Enthalpy change during heating (DSC) of samples

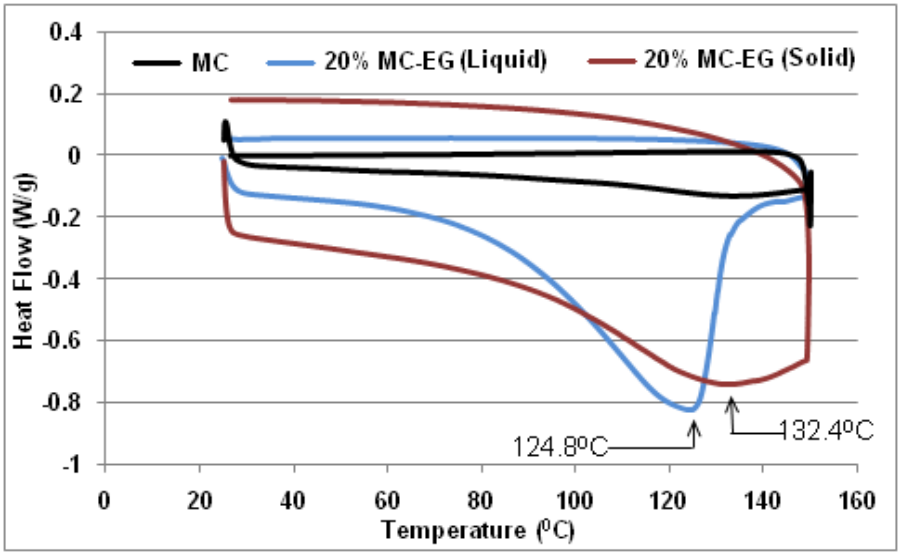

Figure 5-27. DSC curves for 20% MC in ethylene glycol

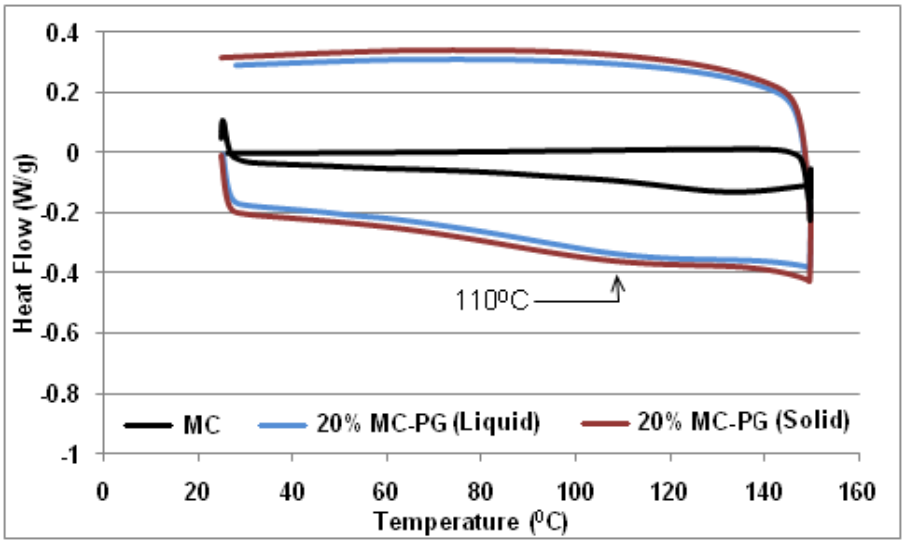

Figure 5-28. DSC curves for 20% MC in propylene glycol

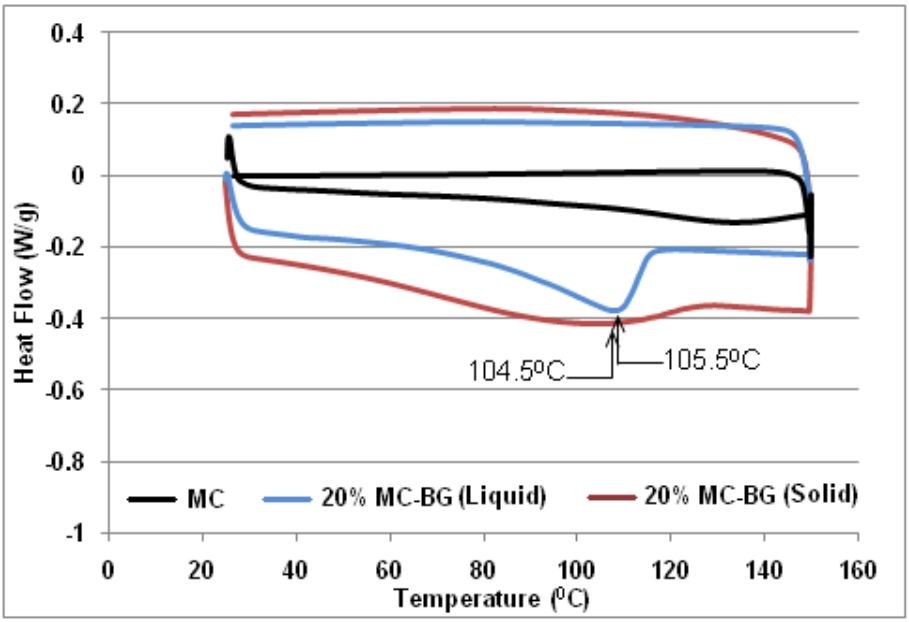

Figure 5-29. DSC curves for 20% MC in butylene glycol

5.6 X-Ray Diffraction

DSC curves for MC in each glycol showed different results for solid and liquid samples and broad endotherms were observed for solids. Therefore, X-ray diffraction (XRD) was performed to further explain the differences in the structure of the liquid and solid samples. Table 5-2 lists the diffraction peaks and corresponding interplanar (d) spacing values for different samples. X-ray diffraction patterns for 20% MC in ethylene, propylene and butylene glycol are presented in Figures 5-29, 5-30 and 5-31 respectively. Each figure shows the diffraction patterns for liquid (i.e. before heating) and solid (i.e. after heating) along with the diffractogram for MC powder.

MC powder shows evidence of some crystalline order with two broad peaks near $2\theta \sim 9^{o}$ and $2\theta \sim 19^{o}$ (Figure 5-30). In ethylene glycol, the peak near $2\theta \sim 8^{o}$ disappeared and the peak near $2\theta \sim 19^{o}$ shifted to a higher value (i.e. $2\theta \sim 22^{o}$). The diffraction pattern for the same sample after it was heated and cooled (i.e. solid) showed a sharp, low intensity peak near $2\theta \sim 8^{o}$ and the intensity of the peak near $2\theta \sim 22^{o}$ was reduced (Figure 5-30).

For MC in propylene glycol (Figure 5-31), the intensity of the peak near $2\theta \sim 9^{o}$ reduced and shifted to $2\theta \sim 10^{o}$. A second peak appeared at $2\theta \sim 21^{o}$ and was more sharp and intense than the MC peak near $2\theta \sim 19^{o}$. For solid MC in propylene glycol, the peak near $2\theta \sim 10^{o}$ almost vanished and the intensity of the peak at $2\theta \sim 21^{o}$ significantly reduced.

In butylene glycol, the MC peak near $2\theta \sim 9^{o}$ disappeared and the second peak appeared near $2\theta \sim 19.5^{o}$ (Figure 5-32). For solid MC in butylene glycol, the intensity of the peak near 19.5^{o} reduced and a shoulder near 7^{o} appeared. These results will be further explained in the following section.

Sample		2θ (degrees)	d (Å)
Methylcellulose		9.36	9.5
		19.2	4.6
20% MC-EG	Liquid	-	-
		21.92	4.1
	Solid	7.82	11.3
		21.02	4.2
20% MC-PG	Liquid	10.0	8.8
		20.0	4.4
	Solid	7.8	11.3
		20.0	4.4
20% MC-BG	Liquid	-	-
		19.56	4.5
	Solid	7.6	11.6
		19.46	4.6

Table 5-2. XRD peaks and corresponding interplanar (d) spacings

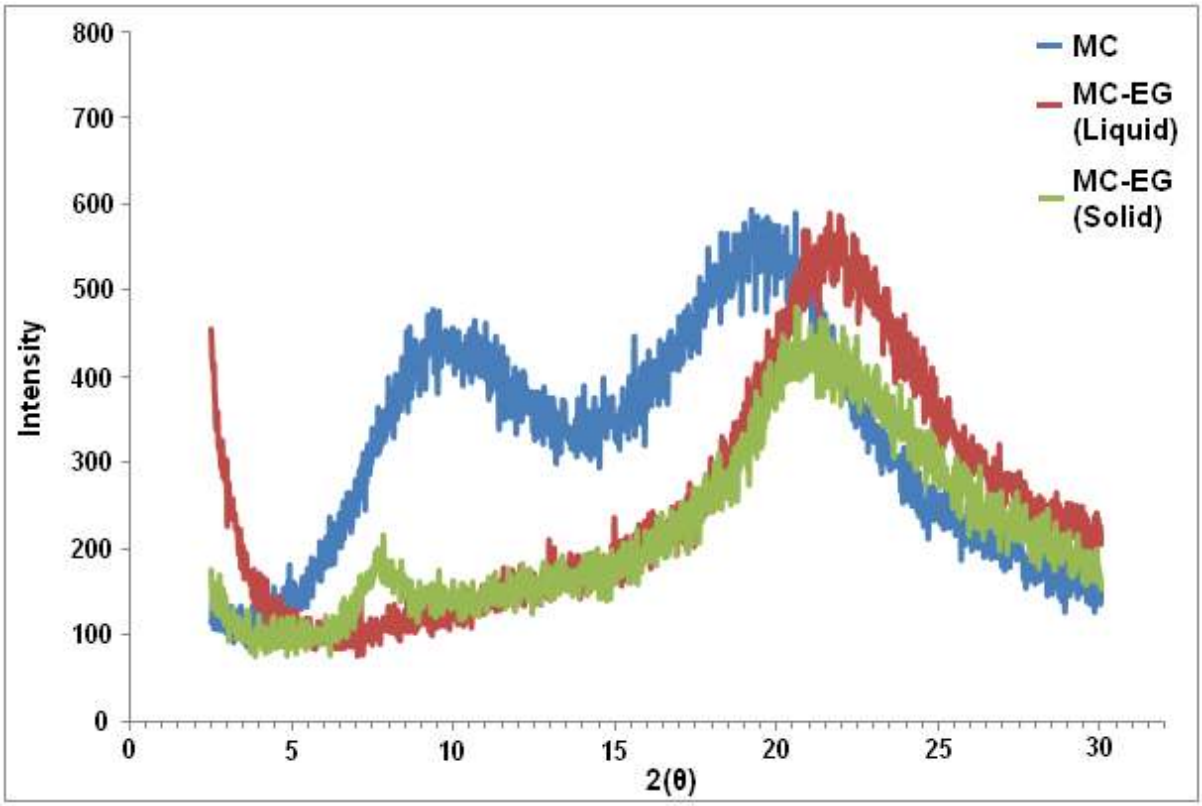

Figure 5-30. X-ray diffraction patterns for 20% MC in ethylene glycol

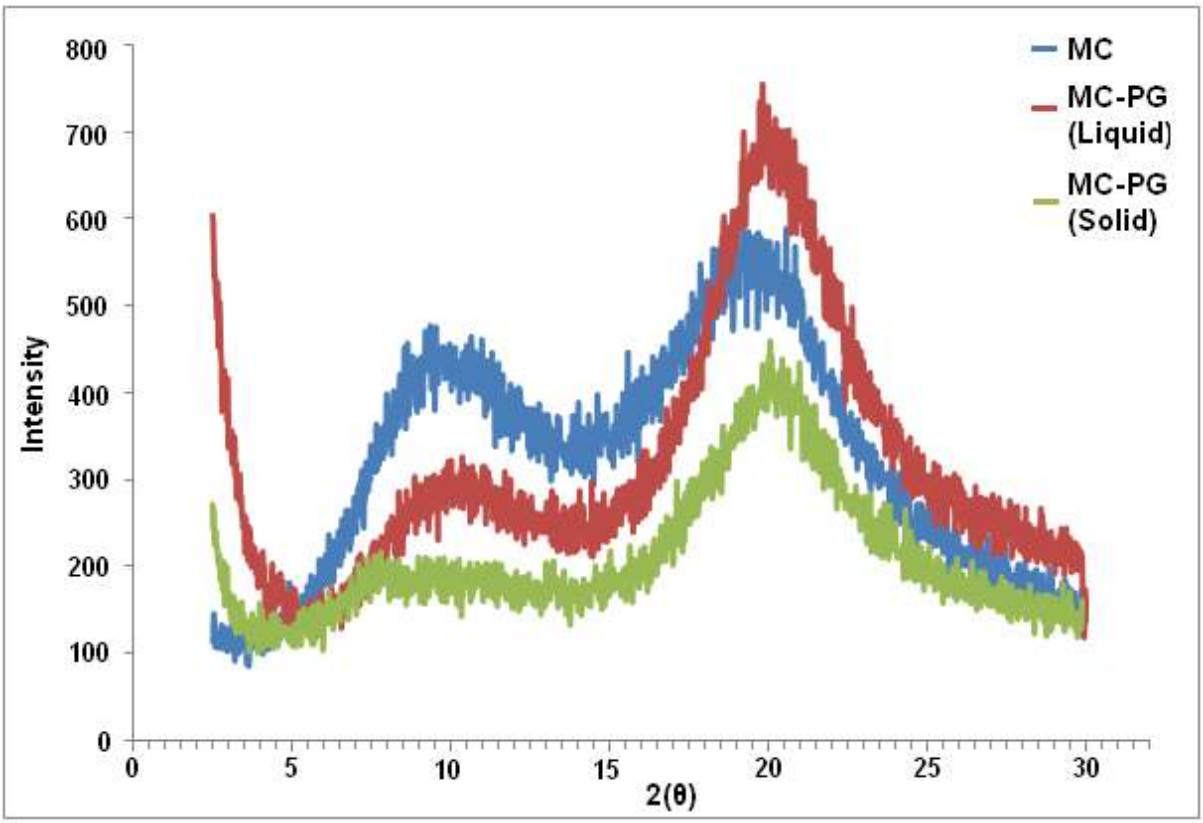

Figure 5-31. X-ray diffraction patterns for 20% MC in propylene glycol

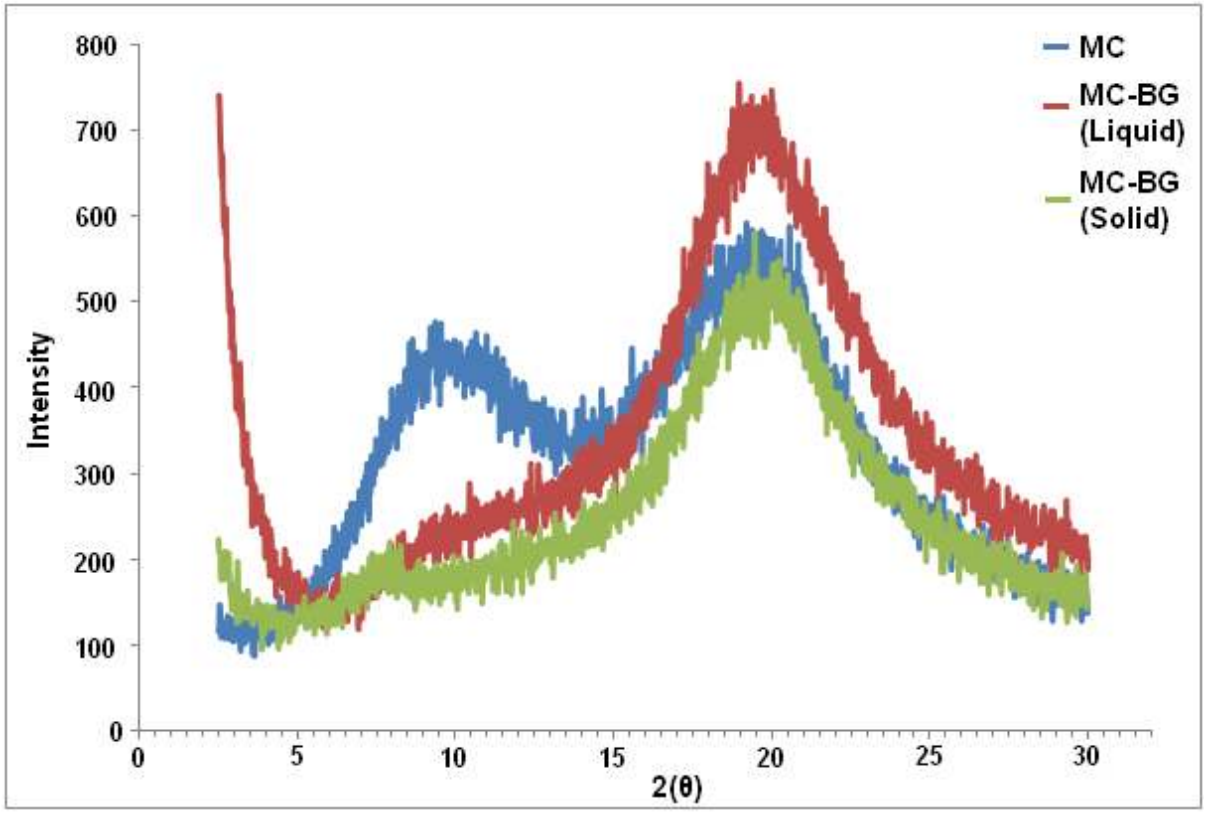

Figure 5-32. X-ray diffraction patterns for 20% MC in butylene glycol

5.7 Discussion

5.7.1 Water Based Samples

The results obtained for both aqueous solutions of MC and HPMC confirm the findings of Sarkar [109,173,174], Haque [171], Kobayashi [178], Nishanari [176], Hussain [192], Li [183] and Funami [188]. As discussed in the literature review chapter, the gel formation upon heating of both MC and HPMC is attributed to the hydrophobic associations caused by breaking of the hydrogen bonds between water and the hydrophobic groups (i.e. modified cellulose chains) in methylcellulose. As the hydrogen bonds between water and MC chains are broken, the CH_3 substituted cellulose units become dehydrated. The units containing hydrophilic groups (i.e. OH) remain hydrated (i.e. dissolved). This difference in hydration/dehydration causes interaction between the chains with CH_3 (i.e. hydrophobic association) Due to these interactions, the solution turns turbid and a gel phase is formed. Onset of turbidity and gel formation for higher concentration (i.e. 6-10%) MC samples at lower temperatures could be due to the relatively increased amount of hydrophobic groups resulting in lowering of the temperature at which the hydrophobic association takes place [109,176,183]. Aqueous MC solutions did not form gels at lower concentrations (i.e. 2-4%). This could be due to the low amount of hydrophobic moieties resulting in hydrophobic associations that are not sufficient enough to cause gel formation. However, for the same concentration of HPMC (i.e. 2-4%), gel formation was observed. This could be due to the higher molecular weight of HPMC (M_n = 86,000) resulting in sufficient hydrophobic associations to cause gel formation even at concentrations as low as 2%.

5.7.2 Ethylene Glycol Based Samples

Both MC and HPMC in ethylene glycol formed a gel upon heating but the behaviour during cooling was not the same as with the aqueous samples as they did not return to the initial state (i.e. liquid). Since both MC and HPMC showed similar behaviour in aqueous solutions as well as during heating in the ethylene glycol based samples, it could be assumed that the phenomenon of association between MC/HPMC and ethylene glycol upon heating is similar and could be due

to the breaking of intra and intermolecular hydrogen bonds present within the MC chains and subsequent formation of intermolecular hydrogen bonds between MC/HPMC chains and ethylene glycol molecules. Both FTIR and XRD results (Figures 5-16, 5-17 and 5-30) provide evidence of hydrogen bonding between MC and ethylene glycol. IR spectra of MC in ethylene glycol show changes in the position of the OH stretching band (i.e. near 3300 cm^{-1}) and the ether (C–O–C) stretching band (i.e. near 1150 cm^{-1}). The OH stretching band for MC was observed at 3475 cm^{-1} and for ethylene glycol at 3298 cm^{-1} (Figure 5-15). For MC, the band is at a higher wave number due to the presence of intramolecular hydrogen bonds between OH groups within anhydroglucopyranose units (AGU) along with intermolecular hydrogen bonds between OH of different molecules. For MC in ethylene glycol, this band is shifted to 3323 cm^{-1} for the liquid samples and upon heating, this peak shifted to higher wave numbers (Figure 5-22). For the sample cooled to 40^0C (i.e. solid), this band was observed at a higher wave number (i.e. at 3353 cm^{-1}) than that for the liquid sample. This increase in the wave number indicates the formation of hydrogen bonds between MC and ethylene glycol. Also, it has been shown previously that during gel formation in water, the ether bridge stretching band shows an increase in intensity [182,230-234] related to the breaking of hydrogen bonds between water and MC. However, for MC in ethylene glycol, the ether band (i.e. near 1150 cm^{-1}) intensity decreased during heating and the peak nearly disappeared after cooling to 40^0C (Figure 5-17). This suggests an increase in hydrogen bonding between methylcellulose and ethylene glycol. The XRD results also confirm the presence of hydrogen bonding between MC and ethylene glycol. MC powder has broad diffraction peaks at $2\theta \sim 9^o$ and $2\theta \sim 19^o$ (Figure 5-30). Similar diffraction patterns for MC have been reported previously [170,179,234-239] and it has been suggested that the diffraction peak near $2\theta \sim 19^o$ corresponds to the crystallinity in the unmodified cellulose chains (i.e. with no substitution) and the peak near $2\theta \sim 8^o$ is due to the regions with modified cellulose chains (i.e. with methoxy substitution) [179,196,234,235,238]. Micrographs of MC (Figure 5-23) also confirm the presence of crystalline structure and this crystalline structure melts at high temperature (i.e. near 260^0C) in the absence of any solvent. The XRD pattern (Figure 5-30) shows that for liquid MC in ethylene glycol, the peak near $2\theta \sim 9^o$ disappeared and the peak near $2\theta \sim 19^o$ shifted to a higher value. This could be

due to hydrogen bonding between the modified cellulose chains. In modified cellulose chains, the substitution of OH groups with methoxy groups breaks the intramolecular hydrogen bonds and these chains have OH groups available as possible hydrogen bonding sites. Therefore, hydrogen bonds were formed between modified cellulose chains and ethylene glycol breaking the ordering present in this region so that the diffraction peak near $2\theta \sim 9^{o}$ disappears. Also, this hydrogen bonding causes the unmodified chains to come closer and the inter-planar distance was reduced (i.e. $2\theta \sim 19^{o}$ increased to $2\theta \sim 22^{o}$, Figure 5-30). A crystalline structure is therefore visible in micrographs for liquid MC in ethylene glycol due to the relatively increased ordering of unmodified cellulose chains (Figures 5-24a to c). For the solid MC in ethylene glycol, a low intensity, sharp peak near $2\theta \sim 8^{o}$ is obtained and the intensity of the peak near $2\theta \sim 22^{o}$ was reduced. This shows that when MC in ethylene glycol is heated, intramolecular hydrogen bonds present within unmodified cellulose molecules (i.e. within AGUs) are broken and hydrogen bonds between ethylene glycol and both the OH groups and the ether oxygen present within the anhydrogluco-pyranose unit (AGU) are formed. The micrograph at 150^{0}C (Figure 5-24d) also shows a dissolved/disordered structure. DSC endotherms (Figure 5-27) for MC and MC in ethylene glycol (liquid) show heat absorbance due to breaking of intramolecular hydrogen bonds. Compared to solid MC in ethylene glycol, a higher value of enthalpy for liquid MC in ethylene glycol (Table 5-1) could be due to the additional heat required to break the hydrogen bonds present between ethylene glycol molecules. During cooling some of the hydrogen bonds formed between OH groups of ethylene glycol and MC chains containing high methoxy substitution are broken. This is indicated by a decrease in the OH stretching band during cooling (Figure 5-16 and 5-22). Therefore, during cooling, due to interaction of highly substituted cellulose units with each other, a turbid structure is formed. Since the ether band near 1150 cm^{-1} did not show a reversed trend (Figure 5-16), it suggests that the hydrogen bonds between ether oxygen of MC and ethylene glycol are intact. Also, some hydrogen bonds between OH groups of MC and ethylene glycol are still present (OH stretching band at 3353 cm^{-1} in Figure 5-22), a disordered/imperfect crystalline order is also present in the solid. The XRD pattern for the solid shows reduced intensity for the $2\theta \sim 22^{o}$ peak due to the presence of a less ordered/imperfect crystalline structure (Figure 5-29). Similarly,

the appearance of a low intensity, sharp peak near $2\theta \sim 8^{o}$ represents the regions with ordering in chains caused by interactions between MC chains containing bulky methoxy groups. The micrographs for MC in ethylene glycol during cooling also show some opacity (turbidity) similar to aqueous MC gels, due to the presence of very small, imperfect crystalline regions. Similarly, DSC curves (Figure 5-27) show that when the solid is reheated, the endotherm broadened due to the melting of a relatively less ordered/imperfect crystalline structure. The presence of some undissolved particles could be either due to the high concentration of MC or due to the presence of high molecular weight fractions of unmodified cellulose which have very strong intramolecular hydrogen bonded structure and therefore, do not form hydrogen bonds with ethylene glycol and remain undissolved even at high temperatures.

The gels/solids formed by MC, when subjected to a reheating cycle melted to a liquid state whereas this melting did not occur for HPMC samples in the temperature range studied (i.e. 25-150^{0}C). This could be due to the higher molecular weight and relatively complex structure (due to hydroxypropyl branches) of HPMC. Due to its longer molecular chains and presence of hydroxypropyl groups within the molecules, the interaction between HPMC and ethylene glycol is stronger than between MC and ethylene glycol. Also, the complex structure (i.e. a mixture of liquid and gel) formed by 5% HPMC in ethylene glycol is due to the low concentration of polymer chains which are not sufficient to cause gelation of the whole sample and thus only part of the sample formed a gel.

5.7.3 Propylene Glycol Based Samples

MC in propylene glycol also formed gel upon heating. However, these gels melted at higher temperatures (i.e. higher than 120^{0}C) and formed clear liquids at 150^{0}C. The liquids formed gels upon cooling in the same way as MC in ethylene glycol. This gel formation by MC in propylene glycol therefore, could be due to the hydrogen bonding between MC and propylene glycol. FTIR spectra for MC in propylene glycol (Figure 5-18 and 19) show changes similar to MC in ethylene glycol. The OH stretching band for propylene glycol was observed at 3311 cm^{-1} and it shifted to a higher wave number for liquid MC in propylene glycol (i.e. near 3350 cm^{-1}) representing enhanced hydrogen bonding in the liquid sample. This

peak shifted to higher wave numbers and the intensity of the ether stretching band (near 1133 cm^{-1}) reduced gradually upon heating. For the solid MC in propylene glycol (i.e. cooled to 40^0C), the OH stretching peak appeared at 3372 cm^{-1} and the ether stretching peak (i.e. near 1133 cm^{-1}) almost disappeared. These changes show that as for ethylene glycol, a hydrogen bonding association between MC chains and propylene glycol takes place upon heating. The XRD pattern for MC in propylene glycol (Figure 5-31) shows that the intensity of the diffraction peak near $2\theta \sim 9^o$ was slightly shifted towards $2\theta \sim 10^o$ and its intensity reduced. The peak near $2\theta \sim 19^o$ also moved to $2\theta \sim 20^o$ but showed an increase in the intensity. These results suggest that when MC was mixed with propylene glycol, hydrogen bonds between propylene glycol and MC chains containing methoxy groups were formed. However, due to the presence of CH_3 groups within the propylene glycol molecules, unlike ethylene glycol, the peak near $2\theta \sim 9^o$ did not disappear completely. The hydrogen bonds between modified cellulose chains of MC and propylene glycol cause the MC chains with unmodified cellulose structure to come closer and a reduction in interplanar distance (2θ increased from 19^o to 20^o) takes place. It should be noted that the shift in peak position for MC in propylene glycol is less than that for MC in ethylene glycol which could be due to the presence of an additional carbon atom within the propylene glycol molecule causing a slight increase in the chain length and thus the interplanar distance is higher in propylene glycol than in ethylene glycol (Table 5-2). The micrograph in Figure 5-25 confirms the presence of crystalline order in the liquid sample. For the solid MC in propylene glycol sample, the intensity of the peak near $2\theta \sim 21^o$ reduced significantly and the peak near $2\theta \sim 10^o$ turned into a shoulder near $2\theta \sim 7^o$ (Figure 5-31). This indicates that during heating, intermolecular hydrogen bonds between propylene glycol and unmodified cellulose chains/ether oxygen are formed due to the breaking of intramolecular hydrogen bonds within AGUs. The formation of these hydrogen bonds results in the breaking of order present within MC chains and the intensity of diffraction bands is reduced. Micrographs of MC in propylene glycol at 150^0C and during cooling (Figures 5-25d to h) also confirm the loss of crystallinity after heating. The DSC curve for liquid MC in propylene glycol (Figure 5-28) showed a very broad, gradual curve upon heating which indicates the breaking of intramolecular hydrogen bonds within AGUs. Compared with ethylene glycol, the DSC curves for MC in propylene glycol did not show an

identifiable peak and the curves for liquid and solid were similar with much lower enthalpy values (Table 5-1). This could be due to better solvency of propylene glycol for MC. Hansen solubility parameters for MC and the three glycols are presented in Table 5-3. These values clearly indicate that among the three glycols, propylene glycol has the nearest total solubility parameter (δ_T) value to that of MC. Therefore, the dissolution of MC upon heating is more favourable in propylene glycol and accompanies a relatively low heat flow compared with ethylene glycol. Due to its greatest compatibility with MC, the intensity of the XRD peak near 2θ ~ 21^o for solid MC in propylene glycol was much reduced owing to a more disrupted structure than in EG. Also, solid MC in ethylene glycol showed a sharp, low intensity peak near 2θ ~ 8^o whereas for solid MC in propylene glycol this peak was very broad, showing a relatively less ordering between methoxy groups due to their greater solubility. Micrographs for MC in propylene glycol during cooling (Figures 5-25e to h) also confirm a disordered structure in the solid.

Component	**Hansen Solubility Parameter ([MPa]$^{1/2}$)**				**Difference in δ_T between glycol and MC**
	δ_D	**δ_P**	**δ_H**	**δ_T**	
MC[**]	18.0	15.3	19.4	30.6	
Ethylene Glycol	17.0	11.0	26.0	32.9	2.3
Propylene Glycol	16.8	9.4	23.3	30.2	0.4
Butylene Glycol	16.6	10.0	21.5	28.9	1.7

Table 5-3. Solubility parameters for MC and the three glycols [240,241]

5.7.4 Butylene Glycol Based Samples

Similar to both ethylene and propylene glycol based samples, butylene glycol based samples showed gel formation after heating. FTIR spectra for MC in butylene glycol (Figures 5-20 and 5-21) show evidence of hydrogen bond formation upon heating as the OH stretching band (near 3300 cm^{-1}) gradually shifts to a higher wave number and the intensity of ether stretching vibration (near 1131 cm^{-1}) is reduced. The XRD pattern (Figure 5-32) is also similar to the ethylene glycol as in liquid MC in butylene glycol, the peak near 2θ ~ 9^o turned to

[**] Values for A4M (Dow Chemical) which has a same degree of substitution value (i.e. DS ~ 1.8) as the MC used in this research

a shoulder like peak (i.e. very low intensity) and an increase in the peak near 2θ ~ 19^{o} was observed. This indicates hydrogen bonds between modified cellulose units of MC and butylene glycol which disturb the ordering present in modified cellulose units while the peak near 2θ ~ 9^{o} almost disappeared. In the same way as propylene glycol, butylene glycol also has CH_3 groups in its molecules together with an additional carbon atom in each molecule which renders it less polar than propylene glycol. Also, the difference in solubility parameters between MC and butylene glycol is higher than between MC and propylene glycol and lower than the difference between MC and ethylene glycol (Table 5-3). Therefore, the peak near 2θ ~ 9^{o} showed a behaviour in between propylene glycol and ethylene glycol. The hydrogen bonds formed between modified cellulose units caused the unmodified cellulose units to come closer and the intensity of the peak near 2θ ~ 19^{o} was increased. Due to an additional carbon atom in the butylene glycol molecule, the interplanar distance was higher than that of both propylene and ethylene glycol (Table 5-2). Micrographs in Figure 5-26a and b also provide evidence of crystalline order in the liquid MC in butylene glycol. At higher temperatures, breaking of intramolecular hydrogen bonds and formation of intermolecular hydrogen bonds between MC and butylene glycol molecules disrupts the structure and a less ordered/imperfect structure is formed. The XRD pattern for solid MC in butylene glycol (Figure 5-32) shows a reduction in the intensity of the band near 2θ ~ 19^{o} due to a disordered structure. In the same way as in ethylene glycol, a low intensity diffraction peak near 2θ ~ 8^{o} appeared. This peak shows that during cooling, when some of the hydrogen bonds between MC and butylene glycol are broken, the methoxy groups are exposed and interact with each other forming a turbid gel structure. Since MC and butylene glycol are more compatible than ethylene glycol and less compatible than propylene glycol, this peak is less sharp than in ethylene glycol but sharper than in propylene glycol. For the same reason, turbidity in solid MC in butylene glycol was observed but it did not show a textured surface as with ethylene glycol (Figures 5-24.h and 5-26.h). DSC curves (Figure 5-29) also suggest that when the liquid MC in butylene glycol was heated, the structure due to strong intramolecular bonds was broken resulting in a relatively sharp endotherm. When solid MC in butylene glycol was heated, it showed a broad endotherm due to the melting of a less ordered/imperfect crystalline structure.

A major difference between butylene and propylene glycol was the dissolution of MC in butylene glycol at a temperature higher than for propylene glycol. This is evident from the micrographs at 100 and 120^{0}C for MC in propylene glycol (Figure 5-25b and c) and butylene glycol (Figure 5-26b and c) which show the presence of relatively higher crystallinity (due to undissolved MC) in butylene glycol at the same temperatures. This difference in dissolution temperature could be due to the difference in solubility parameters (Table 5-3). As mentioned earlier, the solubility parameter for butylene glycol is lower than both MC and propylene glycol. Therefore, due to its better compatibility, MC in propylene glycol dissolves earlier (i.e. at lower temperature) than in butylene glycol and the dissolution/breaking of the structure in butylene glycol is accompanied by a relatively higher value of enthalpy (Table 5-1).

Based on the results and the discussion above, a generalised gelation diagram for gel formation of MC in glycols is shown in Figure 5-33. Similar diagrams for MC gel formation in water have also been reported earlier [171,199]. The difference between MC gel formation in water and in glycols is that upon heating, MC in water forms a network structure (i.e. gel) but in glycols, MC dissolves and forms solutions. On the other hand, during cooling, MC in water returns to a dissolved state and forms a clear solution whereas in glycols, a gel network structure of MC is formed.

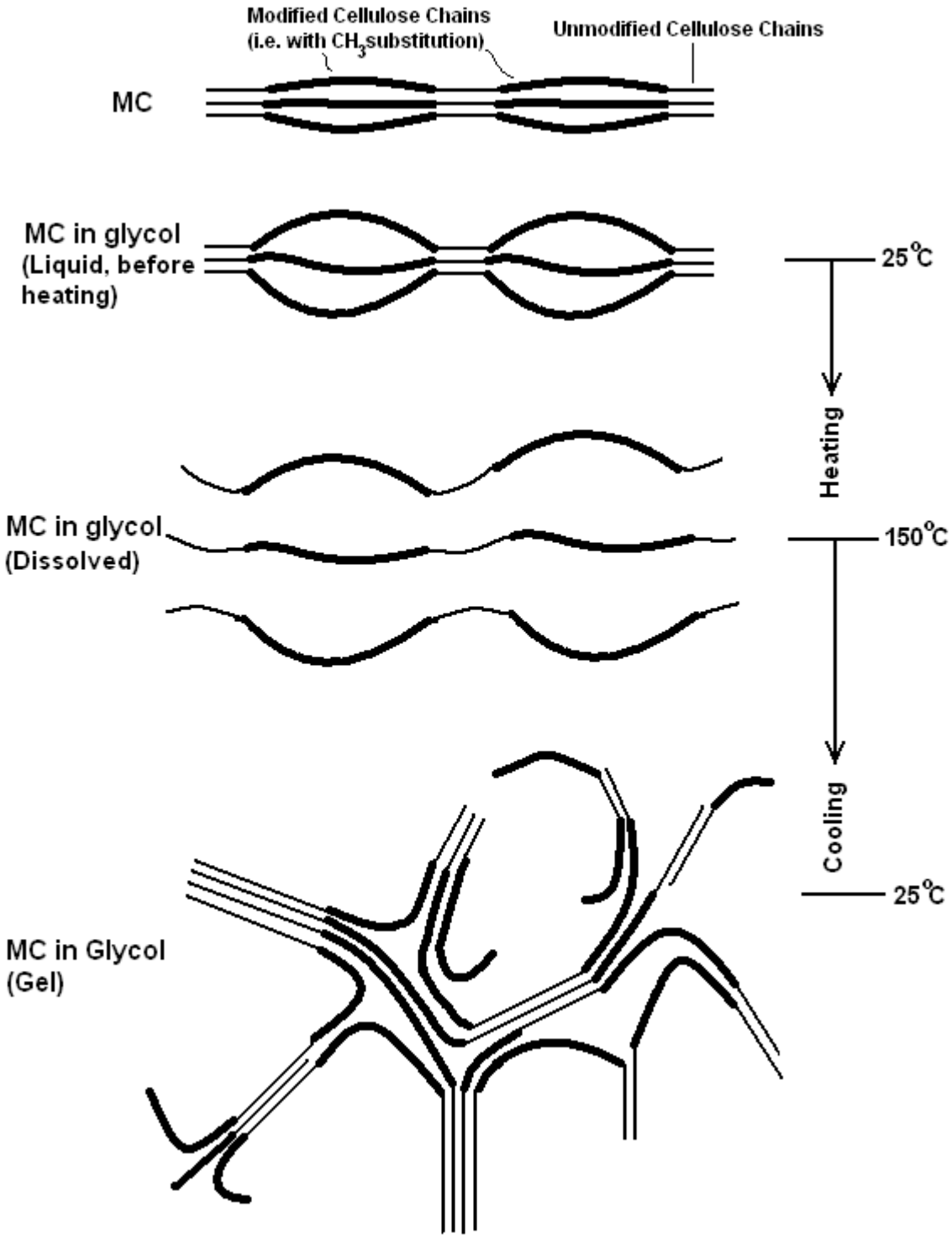

Figure 5-33. Gel (network strcuture) formation of MC in glycols

6 Ternary Compositions and Compositions Suitable for Jetting

6.1 Introduction

Methylcellulose in propylene and butylene glycol showed interesting behaviour and formed gels at concentrations as low as 1%. However, the gels melted upon heating. Therefore, to observe the gel formation upon heating (i.e. similar to aqueous MC solutions), low quantities of water were added to the compositions (i.e. ternary compositions). Since MC in ethylene glycol did not form a gel for lower concentrations (i.e. 1 and 2%) and the dissolution of MC in ethylene glycol took place at a temperature higher than 120^0C, it was decided to investigate the ternary compositions using only propylene glycol and butylene glycol. The results of heating experiments performed on ternary compositions comprising of MC, water and each of the two glycols (i.e. propylene and butylene glycol) are presented in this chapter. Viscosities of selected compositions (binary and ternary) at high temperatures and shear rates were measured to investigate their suitability for jetting at high temperatures. The surface tension of the samples that showed viscosities suitable for jetting were also measured. To quantify the strength of compositions suitable for jetting, texture analysis was performed and the results are presented in this chapter.

6.2 Sample Heating

Table 6-1 lists the ternary compositions and the percentage of each component. For the presentation of results, each ternary composition was identified using its number as it appears in the first column of Table 6-1. Also, for comparison, these compositions were grouped based on the concentration of MC. Samples 1, 5 and 8 have 2% MC. Similarly, samples 2, 4, 6 and 9 have 6% and samples 3, 7 and 10 have 10% MC. For the ternary compositions, the liquids, gels and solids were either clear or turbid depending upon the dissolution of MC. Therefore, each horizontal grid line represents the state (i.e. liquid, gel or solid etc) of the sample when it is clear whereas the small grid mark on the vertical axis between each grid line represents a similar state but with the presence of turbidity. For example, in

Figure 6-1, sample 1, 5 and 8 start as turbid liquids before heating. Therefore, on the vertical axis they all start near the small grid mark instead of the grid line just below which represents a clear liquid. Similarly, when cooled after heating, sample 8 formed a clear viscous liquid and samples 1 and 5 formed soft gels. Because sample 1 was a turbid gel and the sample 5 was a clear gel, sample 1 was marked higher than the gridline for soft gel and the sample 8 was marked at the grid line for viscous liquid (i.e. clear viscous liquid).

Sample Number	MC (%)	Water (%)	Glycol (%)
1	2	2	96
2	6	2	92
3	10	2	88
4	6	6.5	87.5
5	2	11	87
6	6	11	83
7	10	11	79
8	2	20	78
9	6	20	74
10	10	20	70

Table 6-1. Ternary compositions

6.2.1 Propylene Glycol based Ternary Compositions

Figures 6-1 to 6-3 show the behaviour of propylene glycol based ternary compositions during heating and reheating cycles. Figures 6-1, 6-2 and 6-3 represent the behaviour of samples with fixed MC concentrations of 2, 6 and 10% respectively.

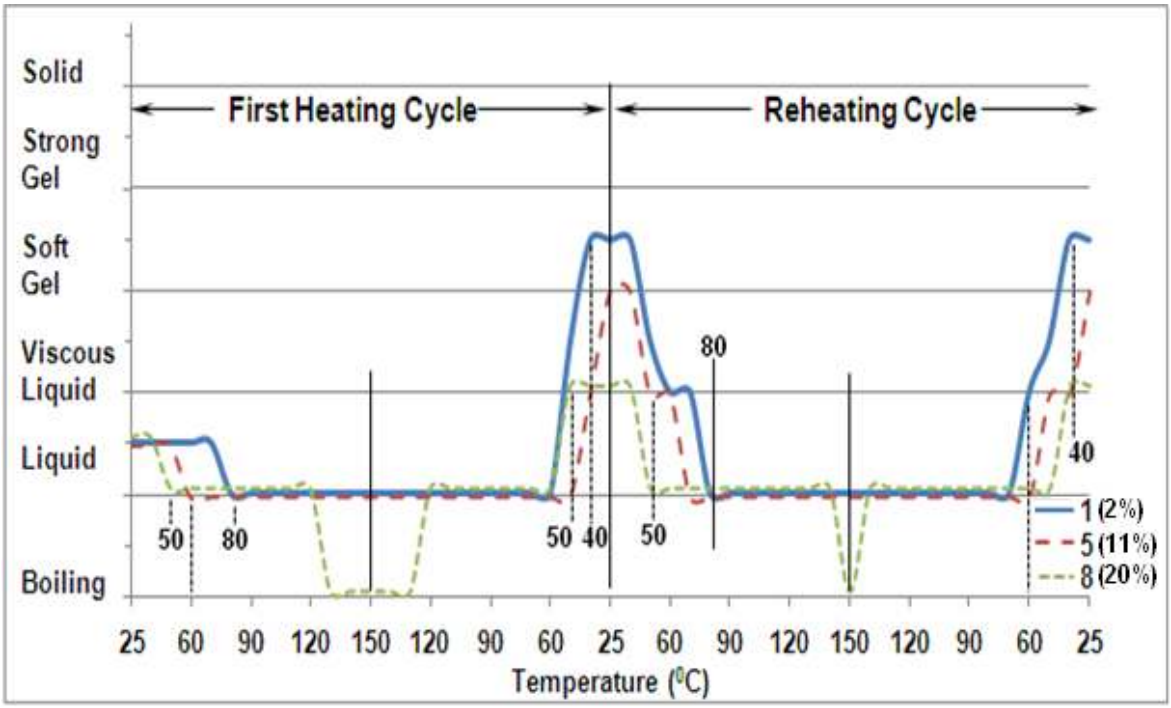

Figure 6-1. Behaviour of propylene glycol based ternary compositions (2% MC concentration, water concentration shown in brackets)

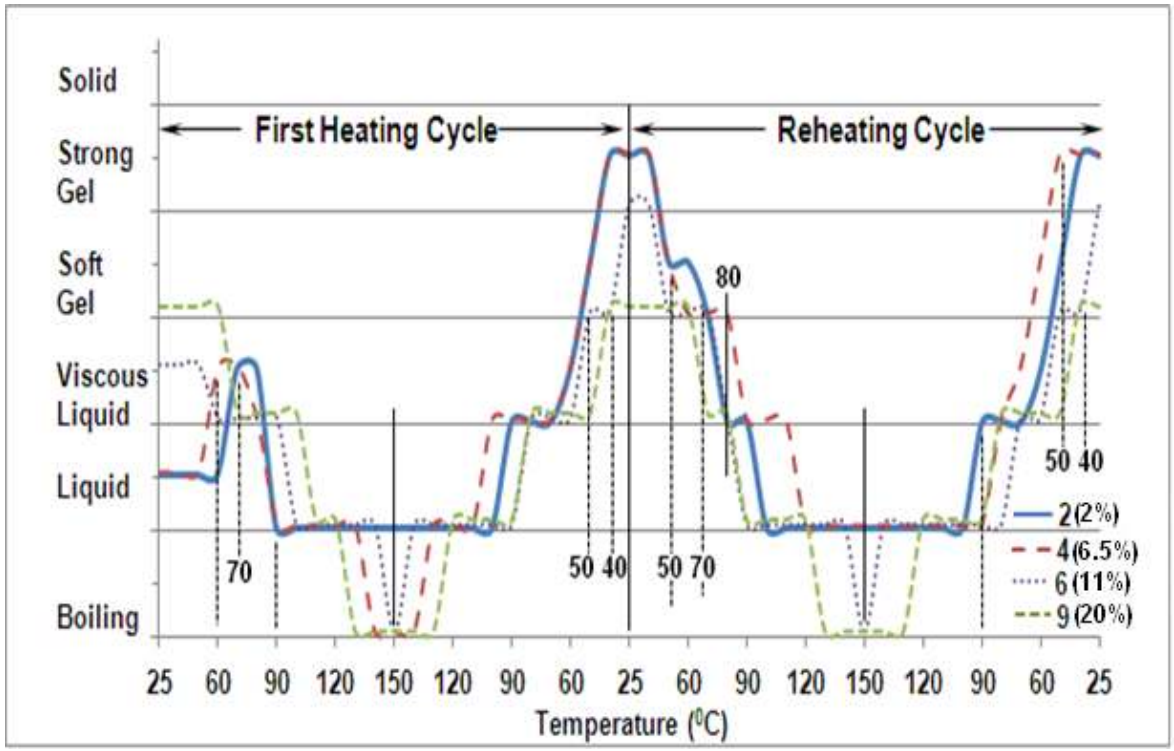

Figure 6-2. Behaviour of propylene glycol based ternary compositions (6% MC concentration, water concentration shown in brackets)

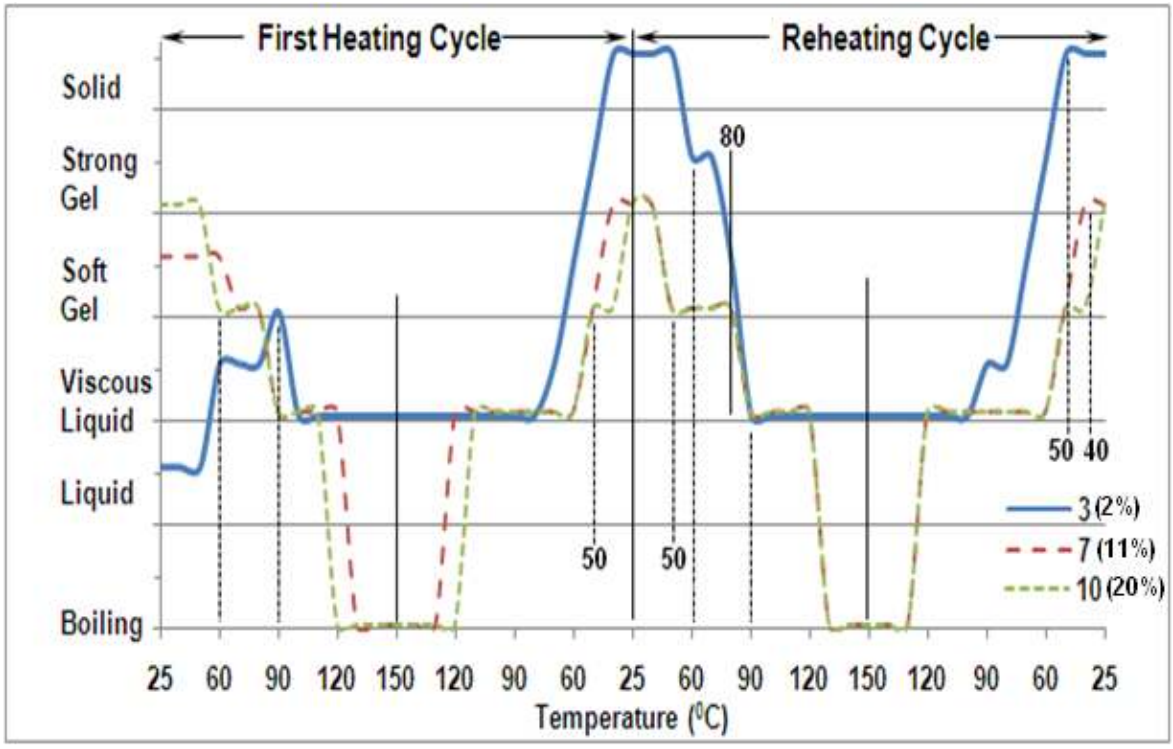

Figure 6-3. Behaviour of propylene glycol based ternary compositions (10% MC concentration, water concentration shown in brackets)

Samples with 2% MC

Sample 1, 5 and 8 contained MC at a concentration of 2% but the concentration of water increased from 2 to 20% (Table 6-1). Before heating, all these samples were turbid liquids (Figure 6-4a). Upon heating, sample 8 and 5 turned into clear liquids due to MC dissolution near 50 and 60^{0}C respectively. Sample 1 turned to a clear liquid near 80^{0}C. Near 130^{0}C, sample 8 started boiling but samples 5 and 1 remained clear liquids up to 150^{0}C. Since some of these ternary samples started boiling before 150^{0}C, images of the samples at 150^{0}C were not available. Upon cooling, sample 1 turned into a turbid viscous liquid and sample 8 turned to a clear viscous liquid near 50^{0}C. Sample 5 turned to a clear viscous liquid at 40^{0}C. A turbid gel was formed by sample 1 at 40^{0}C and the sample 5 formed a clear gel at 30^{0}C. After the samples were cooled to 25^{0}C, samples 1 and 5 were turbid and clear soft gels respectively and the sample 8 was a clear viscous liquid (Figure 6-4b).

Upon reheating, at 50^{0}C sample 1 melted to produce a turbid viscous liquid, sample 5 became a clear viscous liquid and sample 8 turned into a clear liquid. Sample 1 changed to a clear viscous liquid at 60^{0}C. The viscosity of samples 5

and 1 decreased further near 70 and 80^{0}C respectively and then converted to liquids. Sample 8 boiled above 130^{0}C whereas samples 1 and 5 remained clear liquids at 150^{0}C. Upon cooling, samples 1 and 5 changed to turbid and clear viscous liquids respectively at 50^{0}C. At 40^{0}C, sample 8 showed an increase in viscosity and sample 1 formed a turbid soft gel. A clear soft gel was formed by sample 5 at 30^{0}C and all these samples returned to the same states as in the start of the reheating cycle.

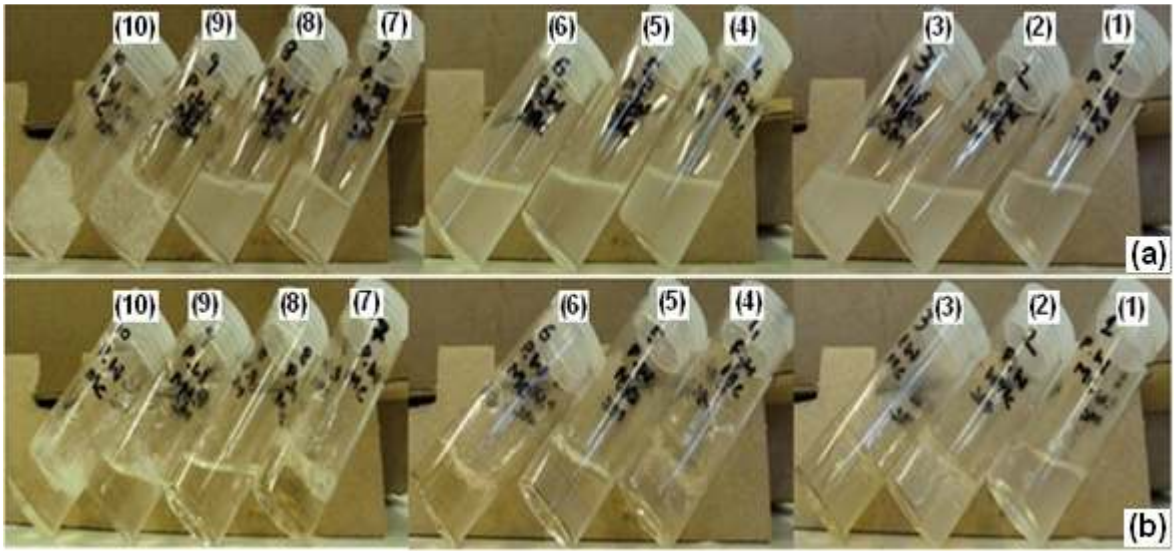

Figure 6-4. Propylene glycol based ternary samples at 25^{0}C (a) before heating (b) after heating

Samples with 6% MC

Samples 2, 4, 6 and 9 contained 6% MC. Before heating, samples 2 and 4 were turbid liquids, sample 6 was a turbid viscous liquid and sample 9 was a clear gel (Figure 6-4a). Heating the samples resulted in an increase in viscosity for samples 4 and 2 at 60 and 70^{0}C respectively. Sample 6 showed MC dissolution and converted to a clear viscous liquid at 60^{0}C. Sample 9 melted to produce a clear viscous liquid at 70^{0}C. Samples 4 changed to a clear viscous liquid at 80^{0}C and sample 2 changed to a clear liquid at 90^{0}C. All the samples showed a decrease in the viscosity and converted to clear liquids between 100-110^{0}C. Further heating resulted in the boiling of samples 9 and 6 near 130 and 150^{0}C respectively and samples 2 and 4 remained clear liquids up to 150^{0}C. During cooling, all the samples showed a gradual increase in the viscosity. At 50^{0}C, samples 2 and 4 formed a turbid soft gel and sample 6 formed a clear soft gel. At 40^{0}C, sample 9 changed to a clear soft gel and samples 2 and 4 converted to strong gels (turbid).

Sample 6 formed a strong gel (clear) near 30^0C. At 25^0C, samples 2 and 4 were strong gels (turbid), sample 6 was a clear strong gel and sample 9 was a clear soft gel (Figure 6-4b).

During reheating, the strong gels formed by samples 2, 4 and 6 softened to from soft gels (turbid) at 50^0C. Samples 4 and 2 converted to clear soft gels at 60 and 70^0C respectively. Sample 9 melted to become a clear viscous liquid at 70^0C and the samples 2 and 6 melted to produce viscous liquids at 80^0C. At 90^0C, sample 4 changed to a viscous liquid. Samples 9 and 6 started boiling near 130 and 150^0C respectively and the other two samples were clear liquids at this temperature. During cooling, samples 4 and 2 formed turbid soft gels respectively at 60 and 50^0C and clear soft gels were formed by samples 6 and 9 at 50 and 40^0C respectively. Samples 4 and 2 converted to strong gels (turbid) at 50 and 40^0C respectively and a clear strong gel was formed by sample 6 at 30^0C. At 25^0C, samples 2, 4 and 6 were strong gels and sample 9 was a soft gel.

Samples with 10% MC

Samples 3, 7 and 10 had the highest concentration of MC (i.e. 10%) and before heating, these samples were a turbid viscous liquid, a turbid soft gel and a clear strong gel respectively (Figure 6-4a). At 60^0C, sample 3 melted to produce a turbid viscous liquid and sample 10 softened to form a clear soft gel. Sample 7 formed a clear soft gel at 70^0C. At 90^0C, samples 7 and 10 melted into clear viscous liquids and sample 3 melted at 100^0C. Samples 10 and 7 started boiling near 120 and 130^0C respectively and sample 3 was a clear viscous liquid at 150^0C. Cooling the samples resulted in the formation of a turbid soft gel for sample 3 at 60^0C and clear soft gels for samples 7 and 10 at 50^0C. At 50^0C, sample 3 changed to a strong gel and formed a solid at 40^0C. Samples 7 and 10 formed strong gels near 40 and 30^0C respectively. After cooling to 25^0C, samples 10 and 7 were clear strong gels and the sample 3 was a solid (Figure 6-4b).

Upon reheating, the gels formed by these three samples softened gradually. Samples 10 and 7 softened to form soft gels at 50 and 60^0C respectively and the sample 3 formed a soft gel at 100^0C. Samples 10 and 7 melted to form viscous liquids respectively at 80 and 100^0C and sample 3 melted at 130^0C. Between 120-130^0C, samples 7 and 10 started boiling whereas sample 3 was a clear liquid at

150^{0}C. Cooling resulted in the formation of a soft gel (turbid) by sample 3 near 70^{0}C and samples 7 and 10 formed soft gels (clear) at 50^{0}C. Sample 3 changed to a strong gel and solid at 60 and 50^{0}C respectively and samples 7 and 10 formed strong gels respectively at 40 and 30^{0}C. At the end of reheating cycle, all samples returned to their initial states (i.e. before reheating).

6.2.2 Butylene Glycol based Ternary Compositions

The behaviour during heating and reheating cycles of butylene glycol based ternary compositions containing 2, 6 and 10% MC are shown in Figures 6-5, 6-6 and 6-7 respectively.

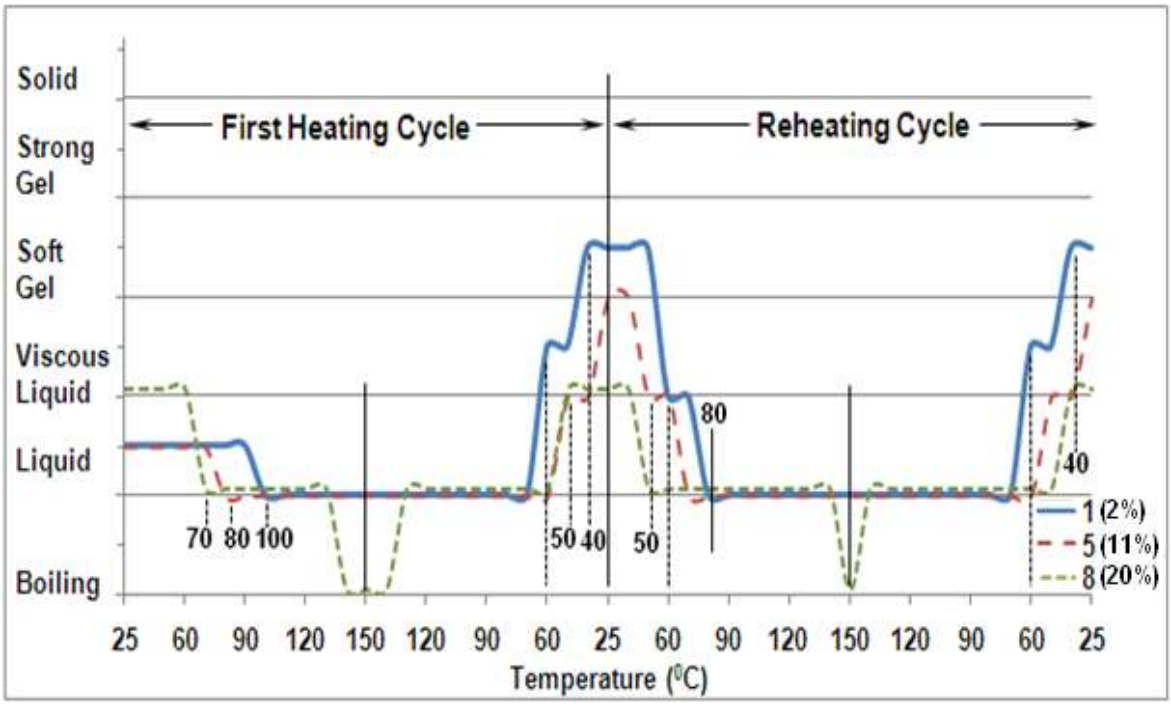

Figure 6-5. Behaviour of butylene glycol based ternary compositions (2% MC concentration, water concentration shown in brackets)

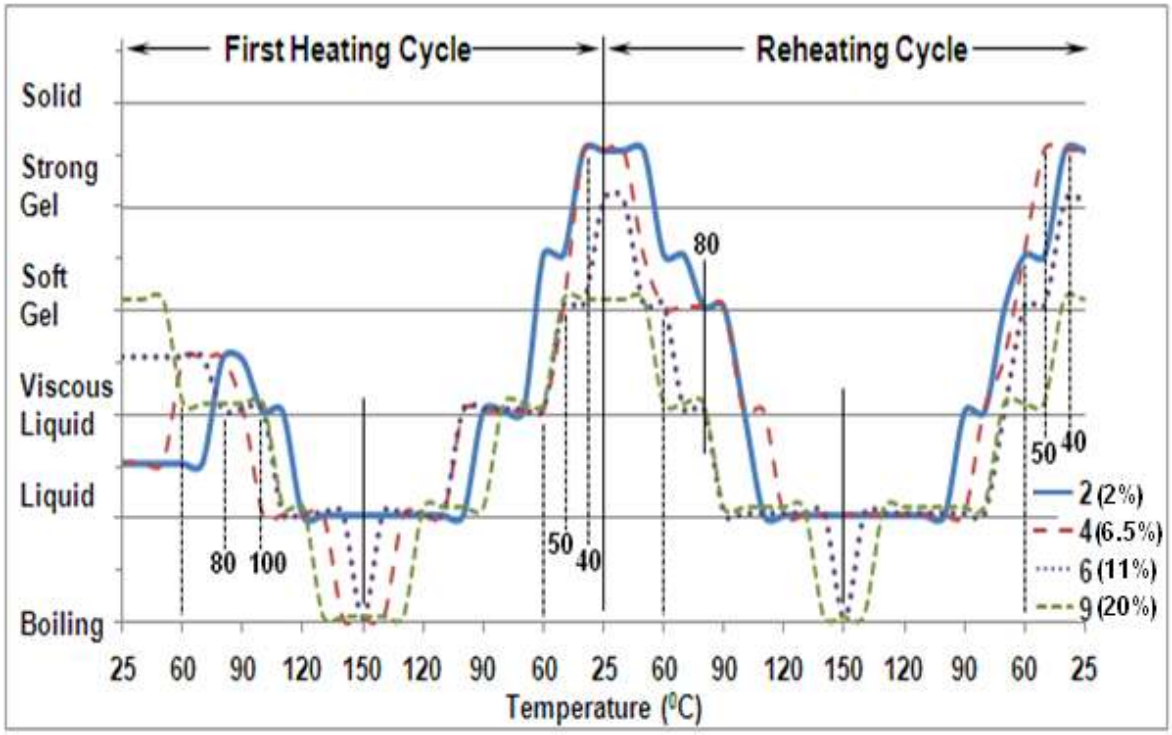

Figure 6-6. Behaviour of butylene glycol based ternary compositions (6% MC concentration, water concentration shown in brackets)

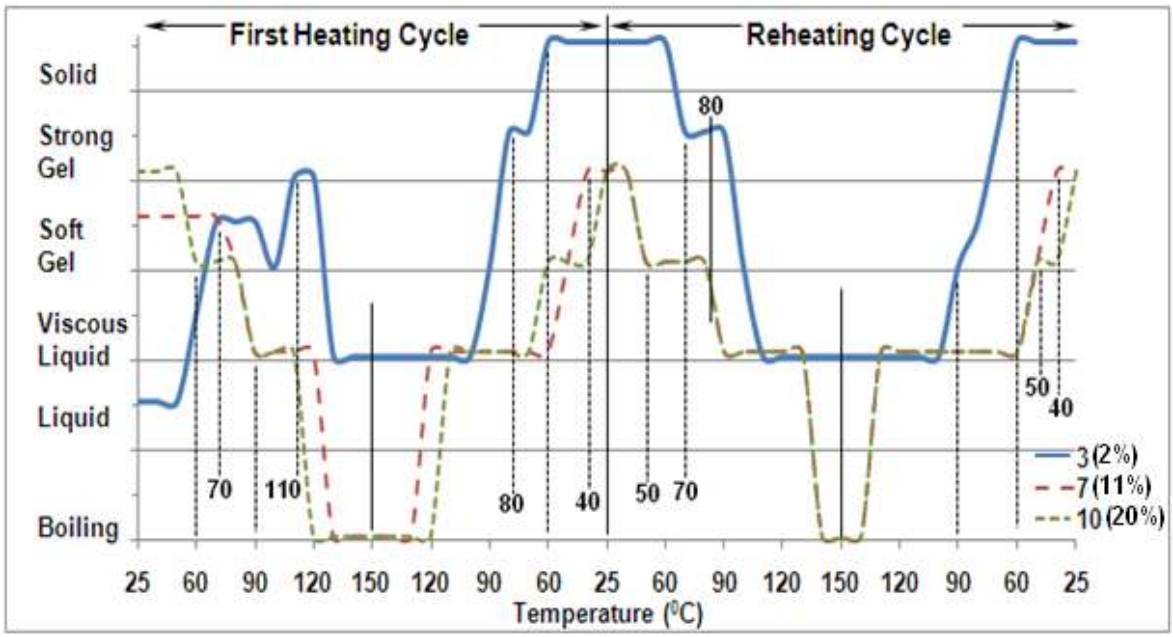

Figure 6-7. Behaviour of butylene glycol based ternary compositions (10% MC concentration, water concentration shown in brackets)

Samples with 2% MC

Samples 1, 5 and 8 contained 2% MC. Before heating, samples 1 and 5 were turbid liquids and sample 8 was a clear viscous liquid (Figure 6-8a). At 60^0C, sample 8 showed a reduction in viscosity and changed to a clear liquid. Samples 5 and 1 formed clear liquids (due to MC dissolution) near 80 and 100^0C respectively.

Sample 8 started boiling before 140^{0}C and the other two samples remained clear liquids up to 150^{0}C. Upon cooling, sample 1 converted to a turbid viscous liquid at 60^{0}C and sample 5 and 8 changed to clear viscous liquids near 50^{0}C. A turbid soft gel was formed by sample 1 at 40^{0}C and sample 5 formed a clear gel at 30^{0}C. After the samples were cooled to 25^{0}C, samples 1 and 5 were turbid and clear soft gels respectively and sample 8 was a clear viscous liquid (Figure 6-8b).

Upon reheating, sample 5 and 1 melted to produce a clear viscous liquid at 50 and 60^{0}C respectively and sample 8 converted to a clear liquid at 50^{0}C. Samples 5 and 1 changed to clear liquids (reduced viscosity) at 70 and 80^{0}C respectively. Sample 8 started boiling above 140^{0}C but samples 1 and 5 remained clear liquids at 150^{0}C. Cooling resulted in a gradual increase in the viscosity and samples 1, 5 and 8 converted to viscous liquids respectively at 70, 50 and 40^{0}C. At 40^{0}C, sample 1 formed a turbid soft gel and a clear soft gel was formed by sample 5 at 30^{0}C. At 25^{0}C, samples 1 and 5 were soft gels and sample 8 was a viscous liquid.

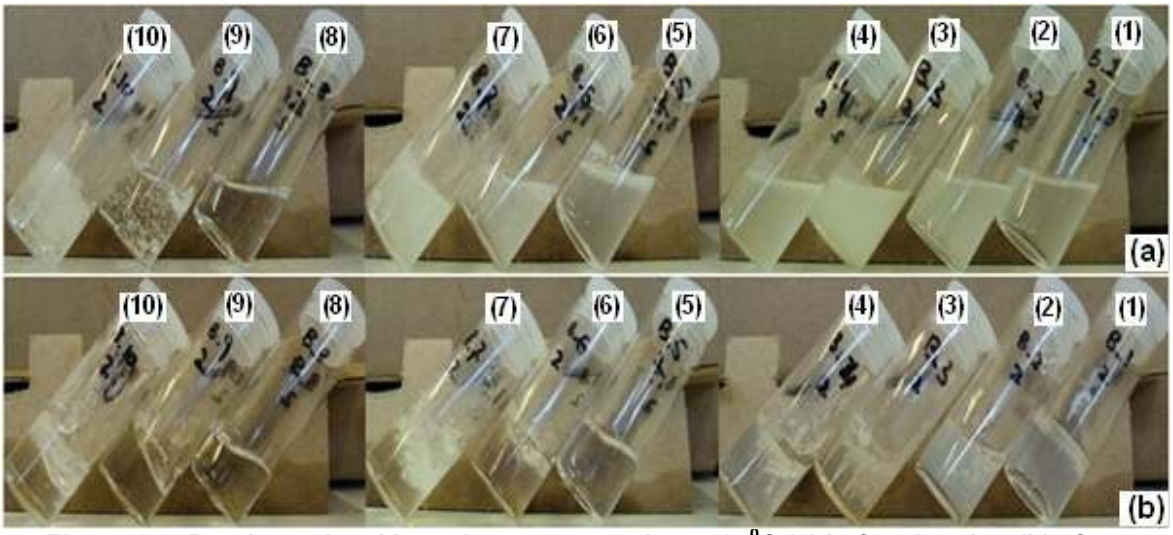

Figure 6-8. Butylene glycol based ternary samples at 25^{0}C (a) before heating (b) after heating

Samples with 6% MC

Samples 2, 4, 6 and 9 had an MC concentration of 6%. Before heating, samples 2 and 4 were turbid liquids, sample 6 was a turbid viscous liquid and sample 9 was a clear gel (Figure 6-8a). Heating increased the viscosity of samples 4 and 2 at 60 and 80^{0}C respectively. Samples 9 and 6 changed to clear viscous liquids respectively at 60 and 80^{0}C. Samples 4 and 2 showed MC dissolution (clear viscous liquids) at 90 and 100^{0}C respectively. Sample 9 and 6 started boiling near 130 and 150^{0}C respectively and samples 2 and 4 remained clear liquids up to

150^{0}C. During cooling, the viscosity of all samples increased gradually. At 60^{0}C, sample 2 formed a turbid soft gel and the other three samples (i.e. 4, 6 and 9) formed a clear soft gel at 50^{0}C. Samples 2 and 4 changed to turbid strong gels at 40^{0}C and a clear strong gel was formed by the sample 6 at 30^{0}C. After cooling to 25^{0}C, samples 2 and 4 were turbid strong gels, sample 6 was a clear strong gel and sample 9 was a clear soft gel (Figure 6-8b).

During reheating, samples 4 and 6 softened to form soft gels at 50^{0}C. At 60^{0}C, sample 2 converted into soft gel and sample 9 melted to produce a viscous liquid. Sample 6 melted to form a viscous liquid at 70^{0}C and samples 2 and 4 melted to form viscous liquids at 100^{0}C. Samples 9 and 6 started boiling near 140 and 150^{0}C respectively. The other two samples (i.e. 2 and 4) were clear liquids at 150^{0}C. During cooling, a clear soft gel was formed by sample 2 at 70^{0}C. At 60^{0}C, samples 4 and 6 formed turbid and clear soft gels respectively and sample 2 converted to a turbid soft gel. Samples 4 and 2 changed to strong gels at 50 and 40^{0}C respectively. Sample 9 formed a clear soft gel and sample 6 changed to a strong gel at 40^{0}C. At 25^{0}C, samples 2, 4 and 6 were strong gels and sample 9 was a soft gel.

Samples with 10% MC

Samples 3, 7 and 10 had the highest concentration of MC (i.e. 10%) and before heating, these samples were turbid liquid, turbid soft gel and clear strong gel respectively (Figure 6-8a). At 60^{0}C, sample 10 softened to form a clear soft gel and sample 3 formed a turbid soft gel at 70^{0}C. Samples 7 and 3 changed to clear soft gels at 80 and 100^{0}C. At 90^{0}C, samples 7 and 10 melted to form clear viscous liquids. Sample 3 formed a strong gel at 110^{0}C which melted at 130^{0}C into a viscous liquid. Samples 10 and 7 started boiling near 120 and 130^{0}C respectively and sample 3 was a clear viscous liquid at 150^{0}C. Cooling the samples resulted in the formation of a clear soft gel for sample 3 at 90^{0}C. Sample 3 showed a gradual increase in gel strength and formed a turbid strong gel and solid respectively at 80 and 60^{0}C. Clear soft gels were formed by samples 10 and 7 at 60 and 50^{0}C respectively. At 40^{0}C, sample 7 converted to a clear strong gel and at 30^{0}C, sample 10 changed to a clear strong gel. After cooling to 25^{0}C, samples 10 and 7 were clear strong gels and sample 3 was a solid (Figure 6-8b).

Reheating resulted in a gradual softening of the gels formed by these three samples. Samples 10 and 7 softened to form soft gels at 50^0C and sample 3 formed a soft gel at 80^0C. Samples 7 and 10 melted to produce viscous liquids at 90^0C and sample 3 melted at 110^0C. Between 130-140^0C, samples 7 and 10 started boiling whereas sample 3 was a clear viscous liquid at 150^0C. Upon cooling, sample 3 formed a clear soft gel near 90^0C. This soft gel changed to a turbid strong gel at 70^0C and further, to a solid at 60^0C. Samples 7 and 10 formed clear soft gels at 50^0C and turned into strong gels respectively at 40 and 30^0C. At the end of reheating cycle samples 10 and 7 were clear strong gels and sample 3 was a solid.

6.3 Viscosity Measurements

Viscosity of a liquid, along with its surface tension, plays an important role in deciding the jettability of the liquid. Since all the compositions investigated in this research showed gel formation upon cooling and these melted upon heating, some of these compositions in liquid form can possibly be jetted. Since, these gels would be heated to form liquids, therefore, a jetting head which can operate at elevated temperatures would be required for their jetting. Although industrial drop on demand inkjet print heads with maximum operating temperature as high as 240^0C are available (MicroFab Technologies Inc.), print heads with a maximum operating temperature at 80^0C are more common (Xaar, Trident, Ricoh, Diamatix). The typical viscosity required for jetting through a printhead is usually below 40 mPa.s [18], however the data sheets available from print head manufacturers (Xaar, Trident, Ricoh, Diamatix) provide an upper limit of viscosity at 20 mPa.s. To investigate the suitability of compositions for jetting, the viscosities of selected compositions were measured at high temperatures (i.e. between 50 – 90^0C). Compositions were selected based on their behaviour during heating and cooling. The compositions which formed a gel after heating and melted to form liquid upon reheating at or below 80^0C were selected. The samples with higher MC concentration (i.e. MC ≥ 5%) were viscous liquids/gels at higher temperatures and were not selected for viscosity measurements. The samples subjected to viscosity measurements are listed in Table 6-2. Although, 5% MC in both propylene and butylene glycol produced viscous liquids during heating, their viscosities were

measured in order to perform comparison with two lower concentrations (i.e. 1 and 2%) and to quantify their viscosities at high temperatures.

Binary Compositions	Ternary Compositions
1, 2 and 5% MC in glycol	Samples 1, 5, 6 and 9

Table 6-2. Compositions selected for viscosity measurements

6.3.1 Propylene Glycol Based Samples

Viscosity curves for propylene glycol and binary compositions of MC in propylene glycol at different temperatures (50-90^{0}C) and varying shear rate (100-1500 s^{-1}) are shown on log – log graphs in Figure 6-9. Viscosity curves for ternary compositions consisting of MC, propylene glycol and water are shown in the Figure 6-10. For ternary compositions, to differentiate between propylene glycol and butylene glycol based samples, letter P for propylene glycol and B for butylene glycol were used to show the respective glycol.

Increased MC concentration resulted in increased viscosity and increasing the temperature/shear rate resulted in a reduction in the viscosity. Table 6-3 lists the values at maximum shear rate (i.e. 1500 s^{-1}) and 70, 80 and 90^{0}C respectively for these samples. The viscosity values in the Table 6-3 also shows that for ternary compositions, apart from P1, which had the lowest concentration of water (i.e. 2%), addition of water (for a constant MC concentration) resulted in increased viscosity at a constant temperature.

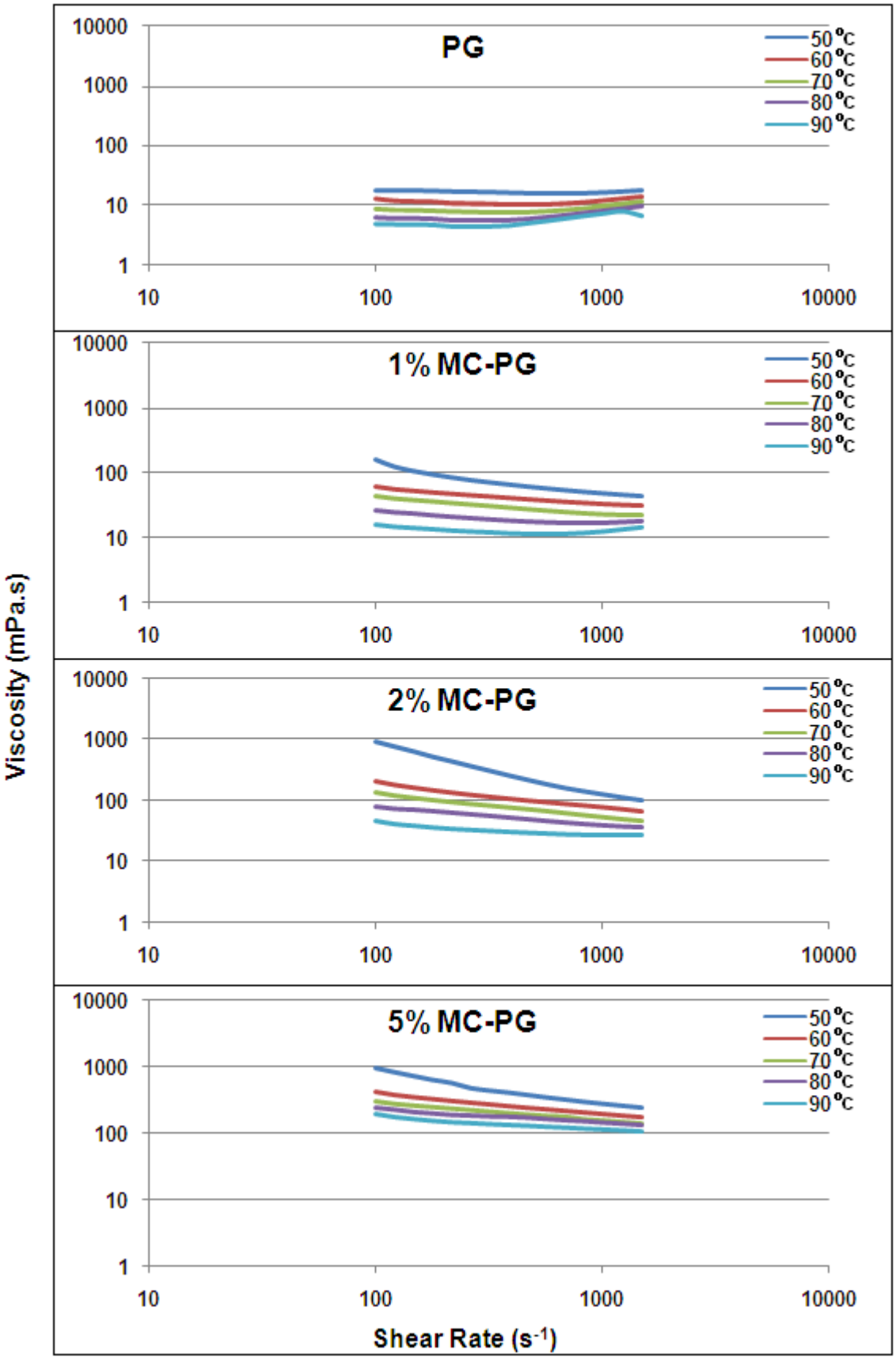

Figure 6-9. Viscosity of MC-propylene glycol compositions

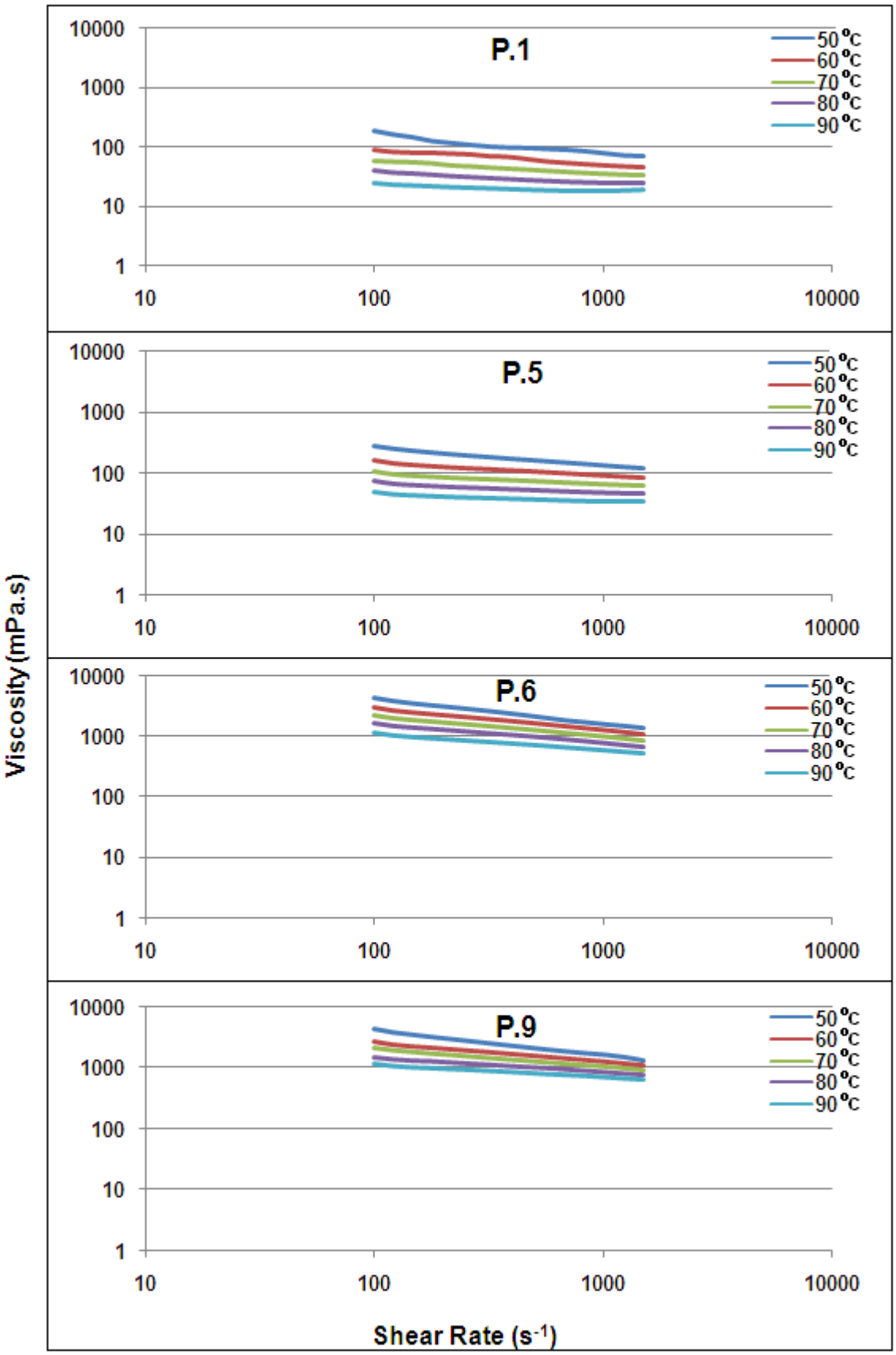

Figure 6-10. Viscosity of MC in propylene glycol and water (ternary compositions)

T (^{0}C)	Viscosity (mPa.s) at 1500 s^{-1}							
	PG	Binary Compositions			Ternary Compositions			
		1% MC	2% MC	5% MC	P1	P5	P6	P9
70	11.4	22.7	47.2	137	33.1	63.4	855.7	913
80	9.8	17.7	36.1	135.7	24.9	46.9	680.6	770.5
90	6.5	14.7	26.6	104.5	19.0	34.9	537.2	658.7

Table 6-3. Viscosity of MC in propylene glycol (binary and ternary compositions)

6.3.2 Butylene Glycol Based Samples

The viscosities at 70, 80 and 90^{0}C (at 1500 s^{-1}) of butylene glycol and MC in butylene glycol (binary and ternary compositions) are presented in the Table 6-4. Figure 6-11 and 6-12 show the viscosity curves for butylene glycol based binary and ternary compositions respectively.

As in propylene glycol, MC in butylene glycol showed increased viscosities upon increasing MC concentration. Also, the viscosity of each composition (i.e. constant MC concentration) reduced upon increasing the temperature and/or shear rate. For ternary compositions, water addition (constant MC concentration) increased the viscosity at a constant temperature. Compared with binary compositions of MC in propylene glycol, MC in butylene glycol showed lower viscosities. On the other hand, ternary compositions of MC in butylene glycol showed higher viscosity values than the same compositions in propylene glycol. These results will be explained later in the discussion section (i.e. section 6.6)

T (^{0}C)	Viscosity (mPa.s) at 1500 s^{-1}							
	BG	Binary Compositions			Ternary Compositions			
		1% MC	2% MC	5% MC	B1	B5	B6	B9
70	15.1	20.7	24.1	78.3	49.6	89.1	871.9	1373
80	12.1	16.4	18.6	63.4	35.8	68.2	699.1	1091
90	10.3	13.5	15.2	54.6	26.0	52.5	581.8	860.5

Table 6-4. Viscosity of MC in butylene glycol (binary and ternary compositions)

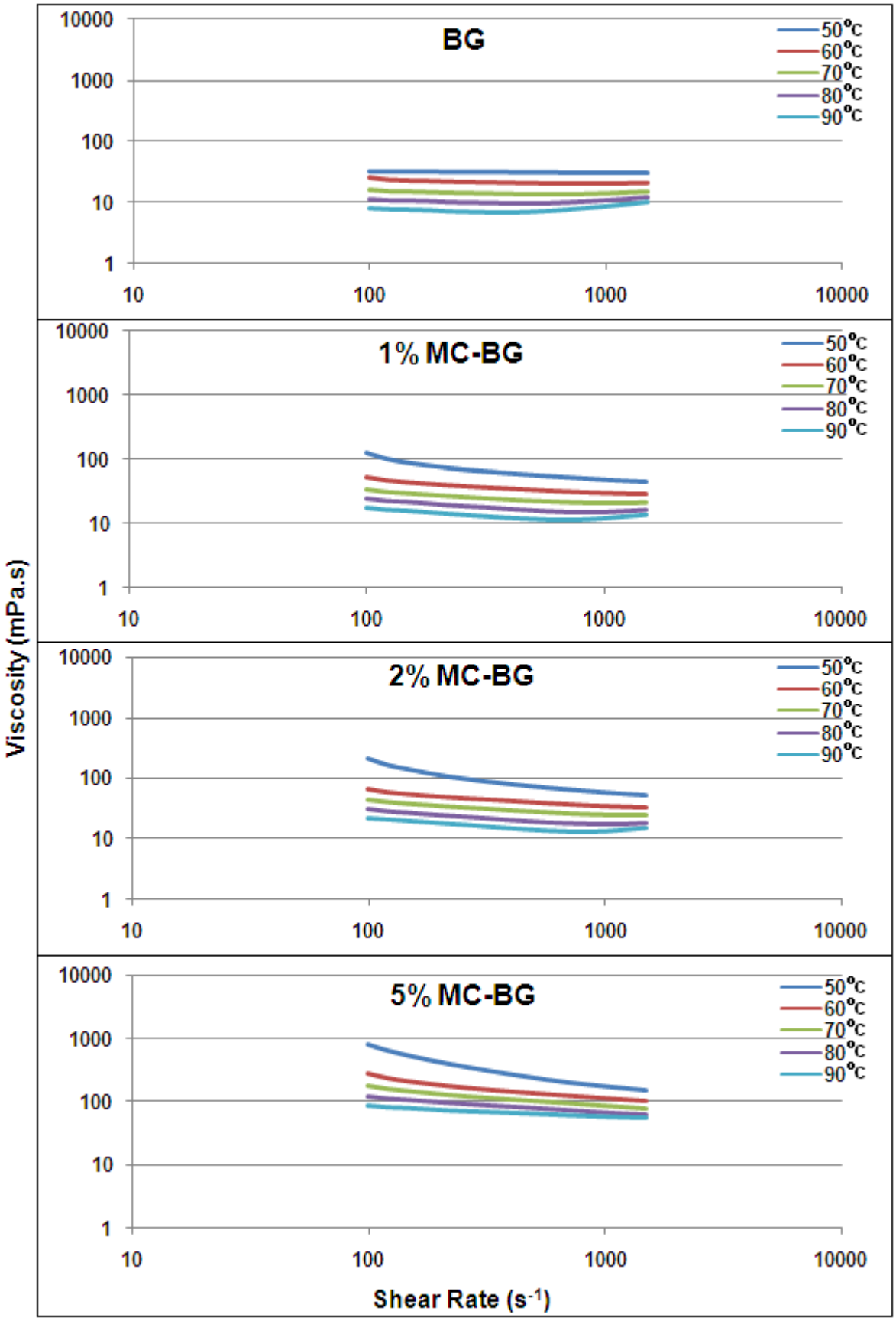

Figure 6-11. Viscosity of MC-butylene glycol compositions

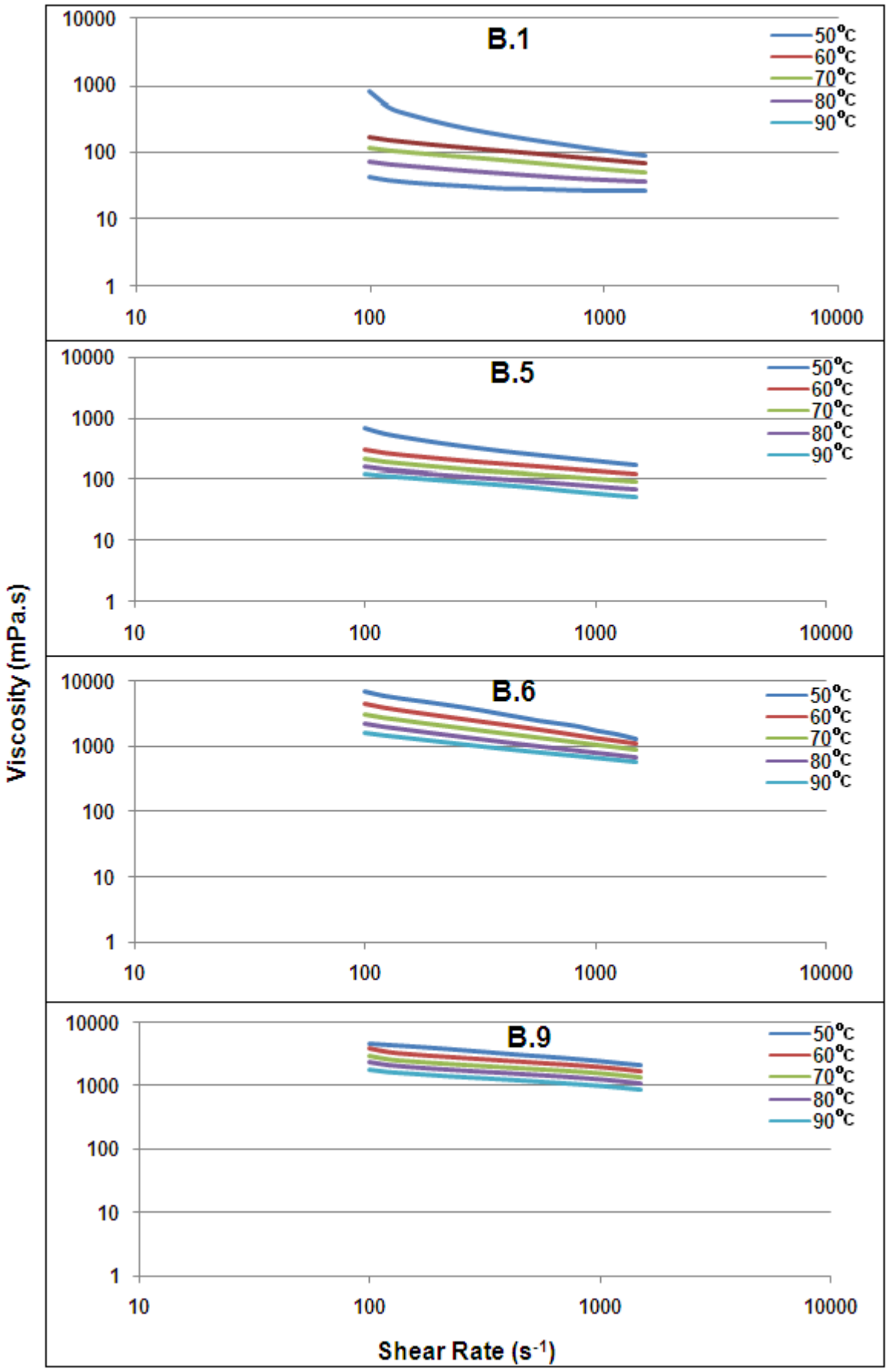

Figure 6-12. Viscosity of MC in butylene glycol and water (ternary compositions)

6.4 Surface Tension Measurements

As mentioned earlier, industrial print head manufacturers typically use 20 mPa.s as the maximum viscosity for a material to be jetted, therefore, compositions which showed 20 mPa.s or lower viscosity at 80^0C were selected for surface tension measurements. For a material to be jetted through a demand mode inkjet print head, the surface tension values should be between 20-70 mN/m [18]. Only 1 and 2% MC in both propylene and butylene glycol (binary compositions) showed viscosities lower than 20 mPa.s at 80^0C (Table 6-3 and 6-4). Therefore, it was decided to perform surface tension measurements to evaluate their jettability. Surface tensions of propylene and butylene glycols and 1 and 2% MC in both propylene and butylene glycol at different temperatures are shown in the Figures 6-13 and 6-14 respectively.

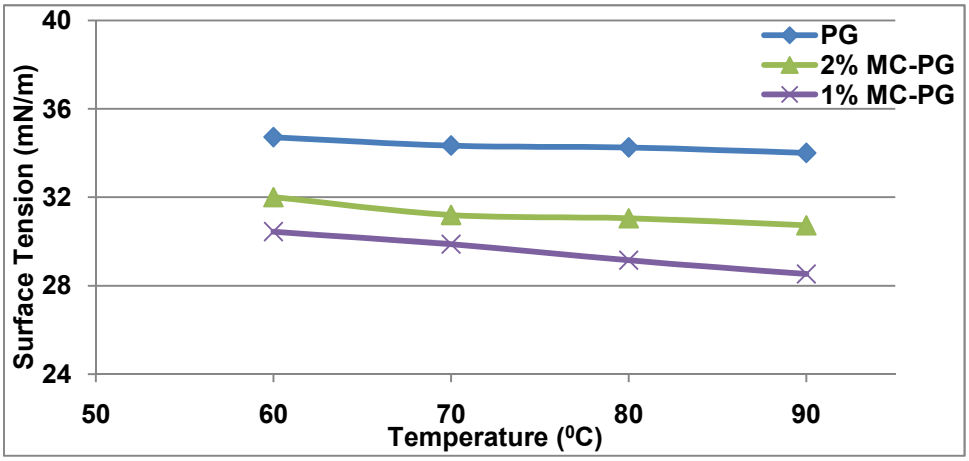

Figure 6-13. Surface tension of propylene glycol and MC (1 and 2%) in propylene glycol (binary compositions)

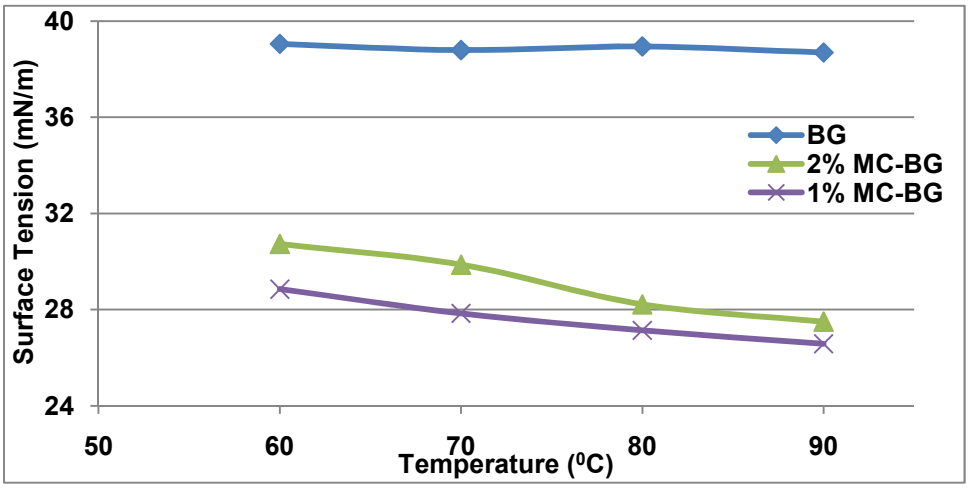

Figure 6-14. Surface tension of butylene glycol and MC (1 and 2%) in butylene glycol (binary compositions)

6.5 Texture Analysis

Both 1 and 2% MC in propylene and butylene glycol (binary) compositions showed viscosities and surface tension values within the jettable limits. Therefore, to characterise their compressive strengths, texture analysis was performed on these compositions. For comparison, texture analysis of 5% MC in both propylene and butylene glycol was also performed. Figure 6-15 shows the force – displacement curves for 1, 2 and 5% MC in propylene and butylene glycol. Figure 6-16 shows the curves for 1 and 2% compositions on a magnified scale (vertical axis).

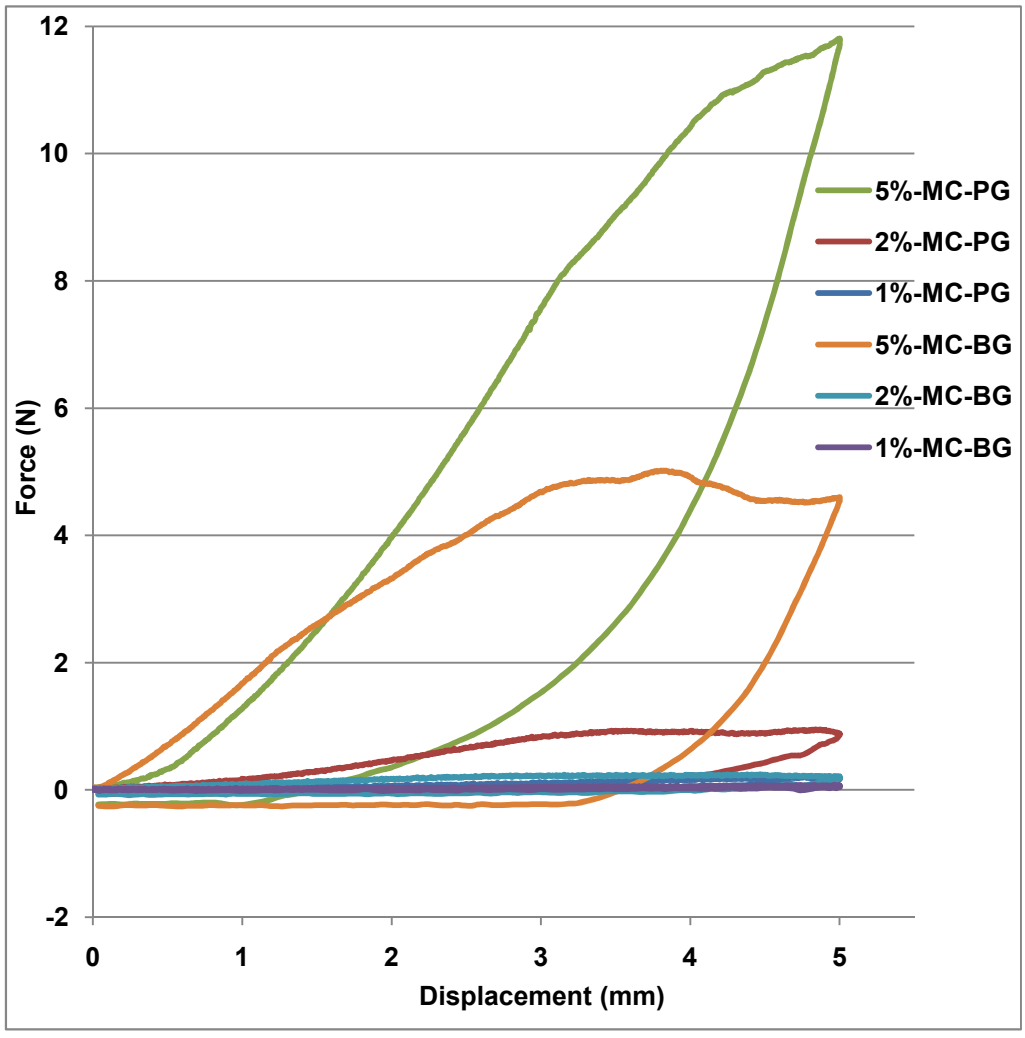

Figure 6-15. Force – displacement curves for MC in propylene/butylene glycol gels

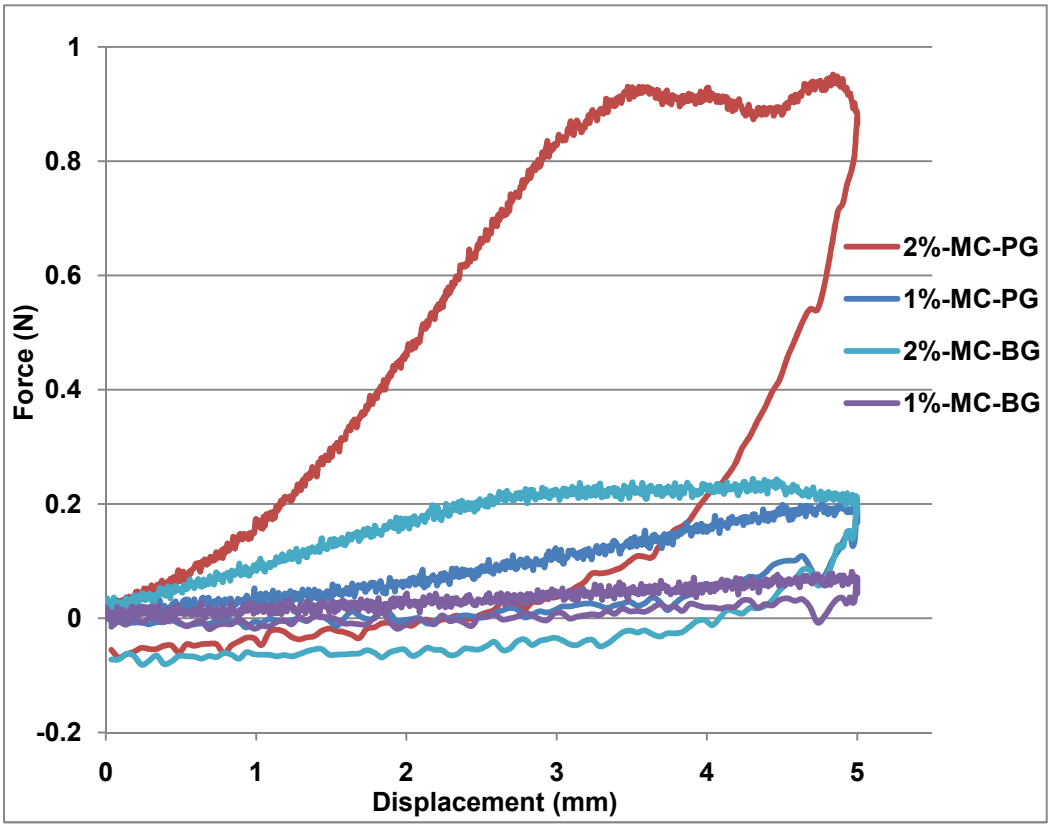

Figure 6-16. Force – displacement curves for MC in propylene/butylene glycol gels (magnified vertical axis)

6.6 Discussion

Ternary compositions showed that addition of water enhanced the dissolution of MC in both propylene and butylene glycol. From the heating/cooling graphs shown in Figures 6-1 to 6-3 and 6-5 to 6-7, it is clear that the gels which have the same concentration of MC but increasing water concentration are relatively softer and these gels form/melt at lower temperatures. For example, Figures 6-1 and 6-5 show that in both propylene and butylene glycol, 2% MC concentration forms a turbid gel for 2% water concentration (i.e. sample 1) but for 11% water (i.e. sample 5), the gel was clear and formed at lower temperatures. Similarly, further increasing water concentration to 20% (i.e. sample 8) resulted in no gel formation. Similar trends can be seen for each fixed MC concentration sample. This effect of water shows that the combination of glycol and water provides better solvency for MC which is mainly due to the strong interactions between MC and water. When water and glycol are mixed, hydrogen bonds between glycol and water are formed and when MC is added to these mixed solvents, it is not dissolved and therefore, these compositions were turbid before heating. During heating, hydrogen bonds

between solvents and MC are formed and so MC dissolves. This dissolution is evident from changing of turbid samples to clear liquids/gels upon heating. Similarly, when these samples were cooled and formed gels, modified cellulose chains remain surrounded by a network (due to hydrogen bonding) of water molecules and thus increased water resulted in clear gels. This effect is evident from Figures 6-4 and 6-8 as samples 1, 2 and 3 had increasing concentrations of MC but only 2% water. Therefore, these compositions formed turbid gels upon cooling because the concentration of water was not sufficient to form hydrogen bonds with all the MC chains and some of the MC chains which contained methoxy groups (i.e. modified cellulose units), interacted with each other during cooling to form turbid gels in the same way as binary composition gels. Samples 8, 9 and 10 which had the same MC concentration as samples 1, 2 and 3 respectively but the highest water concentration (i.e. 20%) showed clear liquids/gels during cooling due to hydrogen bonding between water and MC chains with methoxy substitution.

Viscosity measurements showed that MC in propylene glycol had higher viscosities than for the same concentration in butylene glycol (binary compositions in Table 6-3 and 6-4). These higher viscosities for MC in propylene glycol could be due to better solvency of MC in propylene glycol. As discussed in the previous chapter, propylene glycol has the nearest solubility parameter to MC. Therefore, strong hydrogen bonding association between MC and propylene glycol exists. These strong hydrogen bonding interactions result in relatively high viscosities than for the same concentration of MC in butylene glycol at the same temperature and/or shear rate. The texture analysis results also support the evidence for a stronger structure between MC in propylene glycol than between MC in butylene glycol. Figures 6-15 and 6-16 show that the force required for the same amount of displacement (i.e. deformation) was higher for MC in propylene glycol than for the same concentration of MC in butylene glycol. These higher values of force show that the network structure of MC/propylene glycol gels is stronger than the structure of MC/butylene glycol gels.

Viscosity values of ternary compositions (Table 6-3 and 6-4) show that the addition of water increased the viscosity at a fixed MC concentration, temperature and shear rate. Sample 5 had a higher concentration of water (i.e. 11%) than

sample 1 (2% water) but both contained 2% MC. Similarly, samples 6 and 9 contained MC at a concentration of 6% but water concentration was increased from 11% to 20%. The viscosities of sample 5 (i.e. P.5 and B.5) and sample 9 (i.e. P.9 and B.9) were higher than samples 1 (P.1 and B.1) and 6 (P.6 and B.6) respectively. This could be due to enhanced hydrophobic association upon heating by the addition of water. It has been reported that in aqueous MC solutions, heating results in increased hydrophobic association between MC chains and the viscosity of solutions increases [109,171,173,174,176,178]. Therefore, the development of MC interactions with water upon heating could be a reason for the increased viscosity upon water addition. However, ternary compositions of butylene glycol showed relatively higher viscosities than the same compositions in propylene glycol. This could be because propylene glycol molecules are smaller than butylene glycol. Propylene glycol is less hydrophobic than butylene glycol [132] and it has been reported that short chain alcohols act as a water structure breaker (i.e. strong interactions with water) whereas the longer chain (i.e. 4 or more carbon atoms) alcohols act as a water structure maker (i.e. relatively less interaction with water) [129]. When water is mixed with propylene glycol, it interacts more with the glycol molecules and less with MC so the hydrophobic effect is lower than in butylene glycol. On the other hand, in butylene glycol, water interacts less with butylene glycol and more with MC and enhances hydrophobic association between MC chains. This causes relatively higher viscosities for the ternary compositions with butylene glycol than with propylene glycol. Due to its lower concentration compared to the glycols, the effect of hydrophobic association caused by water only results in increased viscosity and not in the formation of gels.

The viscosity results (Table 6-3) also showed that for ternary composition of MC in propylene glycol with 2% water content (i.e. P1), the viscosity was slightly lower than the same concentration (i.e. 2%) of MC in propylene glycol in the absence of water. This lower viscosity for P1 could be due to the interaction between water and propylene glycol. Since P1 has only 2% water, this low concentration of water interacts only with propylene glycol due to the strong affinity between the two and does not contribute in the hydrophobic association which take place upon heating in the presence of relatively higher water concentration (i.e. in samples P5, P6 and

P9). Therefore, the absence of hydrophobic association in P1 at higher temperatures could be the reason for its relatively lower viscosity than the same concentration of MC in propylene glycol but with no water.

Surface tension results (Figures 6-13 and 6-14) show that adding MC results in a lowering of surface tension for both propylene and butylene glycol. However, as the concentration was increased from 1% to 2%, a slight increase in surface tension for both propylene and butylene glycol was observed. This shows that for low concentrations such as 1% or lower, MC acts as a surfactant in both the glycols. When MC concentration was increased beyond 1%, increased interactions between MC and glycol molecules resulted in increased surface tension. However, surface tension values for 1 and 2% MC in both propylene and butylene glycol were within the limits suitable for jetting.

7 Conclusions and Recommendations for Future work

7.1 Conclusions

7.1.1 Pluronic F-127

On the basis of results obtained for Pluronic F-127 in a variety of non-aqueous solvents, the following conclusions can be drawn:

- F-127 formed gel in formamide and these gels persisted up to 150^0C.
- These gels were similar to aqueous Pluronic gels and reverted back to a liquid state upon cooling.
- Due to its toxicity and possible decomposition into harmful products at higher temperatures, formamide was discarded as a solvent for this research.
- 25% F-127 in octanol, propylene glycol and butylene glycol did not show gel formation at any temperature.
- F-127 partially dissolved in ethylene glycol at low temperatures (i.e. 25^0C) resulting in turbid solutions.
- Upon increasing the temperature, the solubility of both PEO and PPO increased, resulting in clear solutions between 40 – 45^0C.
- Concentrations of up to 25% Pluronic F-127 in ethylene glycol did not form gels at any temperature up to 150^0C.
- The 25% F-127 in ethylene glycol formed a gel upon cooling near 50^0C.
- This gel formation (i.e. in ethylene glycol) was different from aqueous Pluronic gels as in ethylene glycol, hydrogen bonding between ethylene glycol and Pluronic chains and changed conformation of PEO result in an amorphous gel whereas aqueous Pluronic solutions form gels due to formation and subsequent arrangement of micelles into crystalline order.
- Upon cooling, all the samples formed white soft, wax like solids at 25^0C due to crystallisation of PEO. DSC suggested that an imperfect crystal structure was produced.

Since a gels produced from F-127 in ethylene glycol melted near 50^0C, they could not be used as a support material for jetting of caprolactam. Also, due to its high viscosity (i.e. higher than 20 mPa.s at 80^0C) the gel formed by 25% F-127 in

ethylene glycol upon cooling was not suitable for jetting. However, if used with a print head which could operate at higher temperatures (such as from MicroFab), this composition could possibly be jetted and could form a reusable, low melting point (near 50^0C), jettable support material.

7.1.2 Methylcellulose

Due to their gel formation properties, methylcellulose (MC) and hydroxypropyl methylcellulose (HPMC) were studied in ethylene glycol. MC in ethylene glycol formed gels upon cooling but these gels melted at higher temperatures (i.e. higher than 80^0C). Due to its higher molecular weight and more complex structure than MC, HPMC produced gels which did not re-melt upon heating. Therefore, MC was selected for further investigations using propylene and butylene glycol. Based on hot stage FTIR, hot stage microscopy, DSC, XRD, viscosity and surface tension measurements, the following conclusions were drawn:

- MC dissolved upon heating and formed gels during cooling in both propylene and butylene glycols.
- These gels melted during heating and the melting temperature of gels was dependent upon the MC concentration.
- The gels formed were different from aqueous MC gels. In water, association between methoxy containing MC chains take place upon heating whereas in glycols, association takes place upon cooling.
- Higher concentrations (i.e. 5% MC or more) showed gel melting at higher temperatures (i.e. higher than 80^0C) but lower concentrations (i.e. 1 and 2%) melted into liquids below 80^0C.
- Addition of water in small quantities resulted in formation of clear gels due to enhanced solvency of MC but resulted in increased viscosities at higher temperature due to increased hydrophobic association.
- Only lower concentrations of MC (i.e. 1 and 2%) in propylene and butylene glycol (binary compositions) showed viscosities within a jettable range at 80^0C.
- The surface tension values for these compositions were also within a jettable range.

The results showed that low concentrations of MC (i.e. 1 and 2%) in both propylene and butylene glycol have viscosity and surface tension values (at 80^0C) within the jettable range for commercially available print heads such as by Xaar, Diamatix, Tridant and Ricoh. The gels formed by these compositions can therefore be used as possible support materials for commercially available inkjet based AM processes such as solidscape, polyjet and multijet modelling. The fact that both components of these compositions (i.e. glycol and MC) are highly soluble in water makes these compositions easily removable by water dissolution. Also, relatively low melting points (below 50^0C) would allow these gels to be removed by melting. Removal by melting allows reuse of the material and could result in reduced cost and improved sustainability.

In conclusion, novel combinations of polymers and solvents where prepared and investigated which showed interesting behaviour upon heating/cooling. Selected compositions showed properties suitable for jetting and could be used as support materials for jetting based inkjet processes.

7.2 Recommendations for Future Work

The research carried out in this report was based on novel combinations of polymers and solvents. Since no similar combinations for applications such as three dimensional inkjet printing were previously researched, this project was a first step towards this direction and therefore, carries a vast potential for further research. Following are some of the directions in which the research can be continued in the future:

- Although the selected compositions have shown viscosity and surface tension values well within jettable limits, jetting them through commercially available jetting based AM machines and/or inkjet heads would provide useful results.
- Once jetted, formation of layers and evaluation of dimensional and/or surface characteristics would be important as this will dictate the final accuracy of the built part.
- Interaction between support material and build material (e.g. caprolactam) is also important to determine the right combination of support and build material and thus a successful build.

- If reheated, the behaviour of these gels was reversible (i.e. melt upon heating and form gel upon cooling) and therefore, they can be used for more than one build. However, it is yet to be determined after how many heating cycles they show significant change in their properties such as melting point, viscosity and surface tension.
- Effect of molecular weight (M_w) and/or degree of substitution (DS) was not investigated and this could help in developing better support materials in terms of their jettability, ease of removal and reusability by providing a better insight into the interaction between solvents and MC with different DS and M_w. Also, in the context of jetting of caprolactam, where a gel at high temperatures is required, MC with high DS values (i.e. DS ≥ 2), due to their better solvency in non-aqueous solvents could provide suitable results. Similarly, other cellulose ethers such as ethylcellulose, propylcellulose and their derivates could be investigated with solvents used in this study.
- Since higher boiling point solvents (b.p. > 175^0C) were investigated and these solvents have relatively higher viscosities, other solvents with lower boiling points and lower viscosities could provide alternatives for gel formation using either Pluronics and/or cellulose ethers (i.e. MC and HPMC). Apart from preparation of other novel combinations involving a different solvent/polymer combination, mixture of solvents (i.e. varying fractions of different solvents) can also be investigated to obtain tailored gel formation characteristics.
- Although, the effect of adding small concentrations of water was investigated for MC in propylene and butylene glycol, these ternary compositions can be further investigated using experimental techniques such as FTIR, DSC and microscopy to interpret the results further.

8 References

[1] Hopkinson N., Hague R.J.M. and Dickens P., "Rapid manufacturing: an industrial revolution for the digital age", Sussex (UK), John Wiley and Sons, 2005.

[2] Gibson I., Rosen D.W. and Stucker B., "Additive Manufacturing Technologies - Rapid Prototyping to Direct Digital Manufacturing", London (UK), Springer, 2010.

[3] Levy G.N., Schindel R. and Kruth J.P., "Rapid Manufacturing and Rapid Tooling with Layer Manufacturing (LM) Technologies State of The Art and Future Perspectives", CIRP Annals - Manufacturing Technology, 2003, Volume 52, Number 2, 589-609.

[4] Fathi S., Dickens P. Hague R., Khodabakhshi K. and Gilbert M., "Jetting of Reactive Materials for Additive Manufacturing of Nylon Parts", NIP25: International Conference on Digital Printing Technologies and Digital Fabrication, Louisville, Kentucky (USA), September 2009, 784-787.

[5] Khodabakhshi K., Gilbert M., Dickens P., Hague R. and Fathi S., "New polymerization-mixture formulation for jetting: An approach to production of polyamide 6 parts", Proceedings of Solid Freeform Fabrication Symposium, The University of Texas at Austin, Texas (USA), August 2009.

[6] Jürgens M.C., "Preservation of Ink Jet Hardcopies", Capstone Project Research Report, Cross-Disciplinary Studies, Rochester Institute of Technology, New York (USA), 1999.

[7] Le H.P., "Progress and Trends in Ink-jet Printing Technology", Journal of Imaging Science and Technology, 1998, Volume 42, Number 1, 49-62.

[8] Margolin, L., "Ultrasonic Droplet Generation Jetting Technology for Additive Manufacturing: An Initial Investigation". Georgia (USA): School of Mechanical Engineering, Georgia Institute of Technology, 2006.

[9] Keeling M.R., "Ink Jet Printing", Physics Technology, 1981, Volume 12, 196-203.

[10] Wu H.C., Shan T.R., Hwang W.S. and Lin H.J., "Study of Micro-Droplet Behaviour for a Piezoelectric Inkjet Printing Device using a Single Pulse Voltage Pattern", Materials Transactions, 2004, Volume 45, Number 5, 1794-1801.

[11] Ryosuke,U., S. Junichi, S. Kazuo, M. Hitoshi and H. Yoshihiro. ,"Electrostatic Ink-jet Recording Head", European Patent, EP0764529, 1997.

[12] Elrod,S.A., B.T. Khuri-Yakub and C.F. Quate., "Stabilization of the Free Surface of a Liquid", United States Patent, US5629724, 1997.

[13] Scott,G.,"Inkjet Print Head", United States Patent, US0227515, 2003.

[14] Kipphan H., "Handbook of Print Media", New York (USA), Springer-Verlag, 2001.

[15] J. Brünahl. "Physics of Piezoelectric Shear Mode Inkjet Actuators". Stockholm (Sweden): Royal Institute of Technology, 2003.

[16] M.B.G. Wassink. "Inkjet Printhead Performance enhancement by feedforward input design based on two-port modelling". Delft (The Netherlands): Dutch Institute of Systems and Control, Delft University of Technology, 2007.

[17] Calvert P., "Inkjet Printing for Materials and Devices", Chemistry of Materials, 2001, Volume 13, Number 10, 3299 -3305.

[18] MicroFab Technote 99-02. , "Fluid Properties Effects on Ink-Jet Device Performance", Available at: http://www.microfab.com/equipment/technotes.html (Accessed on 06/12/10).

[19] Fox R.W., McDonald A.T. and Pritchard P.J., "Introduction to Fluid Mechanics", New York (USA), John Wiley and Sons, 2004.

[20] Jan de Gans B., Kazancioglu E., Meyer W. and Schubert U.S., "Ink-jet Printing Polymers and Polymer Libraries Using Micropipettes", Macromolecular Rapid Communications, 2004, Volume 25, Number 1, 292 – 296.

[21] Jan de Gans B., Duineveld P.C. and Schubert U.S., "Inkjet Printing of Polymers: State of the Art and Future Developments", Advanced Materials, 2004, Volume 16, Number 16, 203-213.

[22] Christanti Y. and Walker L.M., "Surface tension driven jet break up of strain-hardening polymer solutions", Journal of Non-Newtonian Fluid Mechanics, 2001, Volume 100, Number 1-3, 9-26.

[23] Hyväluoma J., Raiskinmäki P., Koponen A., Kataja M. and Timonen J., "Strain hardening in liquid-particle suspensions", Physical Review E, 2005, Volume 72.

[24] Tirtaatmadja V., McKinley G.H. and Cooper-White J.J., "Drop formation and breakup of low viscosity elastic fluids: Effects of molecular weight and concentration", Physics of Fluids, 2006, Volume 18, Number 4.

[25] Piqué A. and Chrisey D.B. , "Direct-Write Technologies for Rapid Prototyping Applications: Sensors, Electronics, and Integrated Power Sources", Florida (USA), Academic Press, 2002.

[26] Martin G.D., Hoath S.D. and Hutchings I.M., "Inkjet printing – the physics of manipulating liquid jets and drops", Journal of Physics: Conference series, 2008, Volume 105.

[27] Magdassi S., Vinetsky Y., Chakshur E., Ben-Moshe M. and Rehorek D., "Glass Ink-Jet Ink for Digital Printing on Automotive Glass", 2007, DPI Inkjet Workshop 2007, Eindhoven (The Netherlands).

[28] Atkinson A., Doorbar J., Hudd A., Segal D.L. and White P.J., "Continuous ink-jet printing using sol-gel “Ceramic” inks", Journal of Sol-Gel Science and Technology, 1997, Volume 8, Numbers 1-3, 1093-1097.

[29] Biehl S., Danzebrink R., Oliveira P. and Aegerter M.A., "Refractive Microlens Fabrication by Ink-Jet Process", Journal of Sol-Gel Science and Technology, 1998, Volume 13, Numbers 1-3, 177-182.

[30] Danzebrink R. and Aegerter M.A., "Deposition of micropatterned coating using an ink-jet technique", Thin Solid Films, 1999, Volume 351, Numbers 1-2, 115-118.

[31] Paul K.E., Wong W.S., Ready S.E. and Street R.A., "Additive jet printing of polymer thin-film transistors", Applied Physics Letters, 2003, Volume 83, Number 10, 2070-2072.

[32] Yoshioka Y. and Jabbour G.E., "Desktop inkjet printer as a tool to print conducting polymers", Synthetic Metals, 2006, Volume 156, Numbers 11-13, 779-783.

[33] Yang Y., "Polymer Light Emitting Diodes, Inkjet Printing of", Encyclopedia of Materials: Science and Technology, 2001, 7381-7383.

[34] Sekitani T., Noguchi Y., Zschieschang U., Klauk H. and Someya T., "Organic transistors manufactured using inkjet technology with subfemtoliter accuracy", Proceedings of the National Academy of Sciences of the United States of America, 2008, Volume 105, Number 13, 4976-4980.

[35] Kordás K., Mustonen T., Tóth G., Jantunen H., Lajunen M., Soldano C., Talapatra S., Swastik K., Robert V. and Pulickel M.A., "Inkjet Printing of Electrically Conductive Patterns of Carbon Nanotubes", Small, 2006, Volume 2, Numbers 8-9, 1021-1025.

[36] Small W.R. and Panhuis M., "Inkjet Printing of Transparent, Electrically Conducting Single-Walled Carbon-Nanotube Composites", Small, 2007, Volume 3, Number 9, 1500-1503.

[37] Taylor A.D., Kim E.Y., Humes V.P., Kizuka J. and Thompson L.T., "Inkjet printing of carbon supported platinum 3-D catalyst layers for use in fuel cells", Journal of Power Sources, 2007, Volume 171, Number 1, 101-106.

[38] Towne S., Viswanathan V., Holbery J. and Rieke P., "Fabrication of polymer electrolyte membrane fuel cell MEAs utilizing inkjet print technology", Journal of Power Sources, 2007, Volume 171, Number 2, 575-584.

[39] Pourdeyhimi B., "ITMA 2007 Review: Implications for the “Nonwovens Industry", Journal of Engineered Fibers and Fabrics, 2008, Volume 3, Number 1, 38-46.

[40] Provost J., "Inkjet Printing on Textiles", Surface Coatings International, 1994, Volume 77, Number 1, 36-41.

[41] Baccay,R.A., W.L. Anton and M.W. Raymond., "Inkjet Printed Textiles with Improved Durability", World Patent 03/069054, 2003.

[42] Kiatkamjornwong S., Putthimai P. and Noguchi H., "Comparison of textile print quality between inkjet and screen printings", Surface Coatings International Part B: Coatings Transactions, 2005, Volume88, Number 1, 25-34.

[43] Cooley P., Wallace D. and Antohe B., "Applicatons of Ink-Jet Printing Technology to BioMEMS and Microfluidic Systems", Journal of the Association for Laboratory Automation, 2002, Volume 7, Number 5, 33-39.

[44] Wallace, D. B. and Hayes, D. J., “Solder Jet™-Optics Jet™-Aroma Jet™-Reagent Jet-Tooth Jet and other Applications of Ink-JetPrinting Technology”, Proceedings of IS&Ts NIP 18: 2002, 228-235.

[45] Sumerel J., Lewis J., Doraiswamy A., Deravi L.F., Sewell S.L., Gerdon A.E., Wright, D.W. and Narayan R.J., "Piezoelectric inkjet processing of materials for medical and biological applications", Biotechnology Journal, 2006, Volume 1, Issue 9, 976-987.

[46] Roth E.A., Xu T., Das M., Gregory C., Hickman J.J. and Boland T., "Inkjet printing for high-throughput cell patterning", Biomaterials, 2004, Volume 25, Number 17, 3707-3715.

[47] Radulescu D., Dhar S., Young C.M., Taylor D.W., Trost H.J., Hayes, D. J. and Evans, G. R., "Tissue engineering scaffolds for nerve regeneration manufactured by

ink-jet technology", Materials Science and Engineering: C, 2007, Volume 27, Number 3, 534-539.

[48] Henmi, C., Nakamura, M., Nishiyama, Y., Yamaguchi, K., Mochizuki, S., Takiura, K. and Nakagawa, H., “Development of an effective three dimensional fabrication technique using inkjet technology for tissue model samples”, Proceedings of 6th World Congress on Alternatives & Animal Use in the Life Sciences, Japan, 2007, 689-692.

[49] Lin L. and Bai X., "Ink-jet technology: status quo and future – relevance to surface coatings", Pigment & Resin Technology, 2004, Volume 33, Number 4, 238–244.

[50] Lemmo A.V., Rose D.J. and Tisone T.C., "Inkjet dispensing technology: applications in drug discovery", Current Opinion in Biotechnology, 1998, Volume 9, Number 6, 615-617.

[51] Rose D., "Microdispensing technologies in drug discovery", Drug Discovery Today, 1999, Volume 4, Number 9, 411-419.

[52] Rowe C.W., Katstra W.E., Palazzolo R.D., Giritlioglu B., Teung P. and Cima M.J., "Multimechanism oral dosage forms fabricated by three dimensional printing™", Journal of Controlled Release, 2000, Volume 66, Number 1, 11-17.

[53] Dickens P.M., "Rapid Prototyping – The Ultimate in Automation?", Assembly Automation, 1994, Volume 14, Number 2, 10-13.

[54] Burns M., "Automated Fabrication – Improving Productivity in Manufacturing", New Jersey (USA), Prentice Hall, 1993.

[55] Ibrahim M., Otsubo T., Narahara H., Koresawa H. and Suzuki H., "Inkjet Printing Resolution Study for Multi-Material Rapid Prototyping", JSME International Journal Series C, 2006, Volume 49, Number 2, 353-360.

[56] Carrión A., "Technology forecast on ink-jet head technology applications in rapid prototyping", Rapid Prototyping Journal, 1997, Volume 3, Number 3, 99–115.

[57] Blazdell P.F. and Evans J.R.G., "Application of a continuous ink jet printer to solid freeforming of ceramics", Journal of Materials Processing Technology, 2000, Volume 99, Number1-3, 94-102.

[58] Q F Xiang, Q. F., Evans J.R.G., Edirisinghe M.J. and Blazdell P.F., "Solid freeforming of ceramics using a drop-on-demand jet printer", Proceedings of the Institution of Mechanical Engineers, Part B: Journal of Engineering Manufacture, 1997, Volume 211, Number 3, 211-214.

[59] Bhatti A.R., Mott M., Evans J.R.G. and Edirisinghe M.J., "PZT pillars for 1-3 composites prepared by ink-jet printing", Journal of Materials Science Letters, 2001, Volume 20, Number 13, 1245-1248.

[60] Zhao X., Evans J.R.G. and Edirisinghe M.J., "Direct Ink-Jet Printing of Vertical Walls", Journal of the American Ceramic Society, 2002, Volume 85, Issue 8, 2113-2115.

[61] Mohebi M.M. and Evans J.R.G., "A Drop-on-Demand Ink-Jet Printer for Combinatorial Libraries and Functionally Graded Ceramics", Journal of Combinatorial Chemistry, 2002, Volume 4, Number 4, 267-274.

[62] Noguera R., Lejeune M. and Chartier T., "3D fine scale ceramic components formed by ink-jet prototyping process", Journal of the European Ceramic Society, 2005, Volume 25, Number 12,:2055-2059.

[63] Jan de Gans B. and Schubert U.S., "Inkjet printing of well defined polymer dots and arrays", Langmuir, 2004, Volume 20, Number 18, 7789-7793.

[64] Tekin E., Smith P.J. and Schubert U.S., "Inkjet printing as a deposition and patterning tool for polymers and inorganic particles", Soft Matter, 2008, Volume 4, 703 - 713.

[65] Van den Berg, A. M., Smith P.J., Perelaer J., Schrof W., Koltzenburg S. and Schubert U.S., "Inkjet printing of polyurethane colloidal suspensions", Soft Matter, 2007, Volume 3, 238 - 243.

[66] Jan de Gans B. and Schubert U.S., "Inkjet Printing of Polymer Micro-Arrays and Libraries: Instrumentation, Requirements, and Perspectives", Macromolecular Rapid Communications, 2003, Volume 24, Number 11, 659 – 666.

[67] Napadensky, E., “Ink-Jet 3D Printing of Photopolymers Materials: An Emerging Rapid Prototyping Technology”, RadTech Europe 2005 Conference & Exhibition, Barcelona, Spain.

[68] Seerden K.A.M., Reis N., Evans J.R.G., Grant P.S., Halloran J.W. and Derby B., "Ink-Jet Printing of Wax-Based Alumina Suspensions", Journal of the American Ceramic Society, 2004, Volume 84, Number 11, 2514-2520.

[69] Gao F. and Sonin A.A., "Precise Deposition of Molten Microdrops: The Physics of Digital Microfabrication", Proceedings of the Royal Society: Mathematical and Physical Sciences, 1994, Volume 444, Number 1922, 533-554.

[70] Hayes, D. J. and Cox, W. R., “Micro-Jet Printing of Polymers for Electronics Manufacturing”, Proceedings of 3rd International Conference on Adhesive Joining and Coating Technology in Electronics Manufacturing, Newyork (USA), 1998, 168-173.

[71] Pham-Van-Diep,G., E.P. Muntz, H. Watts, Johnson W., Main M., Smith R.F. and Orme-marmarelis M.E., "High Speed Jet Soldering System", United States Patent 6224180, 2001.

[72] Tseng A.A., Lee M.H. and Zhao B., "Design and Operation of a Droplet Deposition System for Freeform Fabrication of Metal Parts", Journal of Engineering Materials and Technology, 2001, Volume 123, Number 1, 74-84.

[73] Liu Q. and Orme M., "High precision solder droplet printing technology and the state-of-the-art", Journal of Materials Processing Technology, 2001, Volume 115, Number 3, 271-283.

[74] Feng C., Yan Y. and Zhang R., "Comparison and analysis of continuously jetting and discretely jetting method used in rapid ice prototype forming", Materials & Design, 2002, Volume 23, Number 1, 77-8.

[75] Liu Q., Leu M.C., Richards V.L. and Schmitt S.M., "Dimensional accuracy and surface roughness of rapid freeze prototyping ice patterns and investment casting metal parts", The International Journal of Advanced Manufacturing Technology, 2004, Volume 24, Numbers 7-8, 485-495.

[76] Gebhardt A., "Rapid Prototyping", Munich (Germany), Carl Hanser Verlag, 2003.

[77] Chua C.K., Leong K.F. and Lim C.S., "Rapid Prototyping – Principles and Applications", Second Edition ed., Singapore, World Scientific, 2003.

[78] Grimm T., "User's Guide to Rapid Prototyping", Michigan (USA), Society of Manufacturing Engineers, 2004.

[79] Upcraft S. and Fletcher R., "Rapid prototyping technologies", Assembly Automation, 2003, Volume 23, Number 4, 318–330.

[80] Cooper K.G., "Rapid Prototyping Technology - Selection and Application", New York (USA), Marcel Dekker, 2001.

[81] Hague R.J.M. and Reeves P.E., "Rapid Prototyping, Tooling and Manufacturing", Rapra Review Reports, Report 117, 2000, Volume 10, Number 9.

[82] Dimitrov D., Schreve K. and de bear N., "Advances in three dimensional printing – state of the art and future perspectives", Rapid Prototyping Journal, 2006, Volume 12, Number 3, 136-147.

[83] Pham D.T. and Dimov S.S., "Rapid prototyping and rapid tooling—the key enablers for rapid manufacturing", Proceedings of the Institution of Mechanical Engineers, Part C: Journal of Mechanical Engineering Science, 2003, Volume 217, Issue 1, 1-23.

[84] Pérez C.J.L. and Calvet J.V., "Uncertainty analysis of multijet modelling processes for rapid prototyping of parts", Proceedings of Institute of Mechanical Engineers, Part B: Journal of Engineering Manufacture, 2002, Volume 216, Number 5, 743-752.

[85] Kamrani A.K. and Sferro P.R., "Direct Engineering: Toward Intelligent Manufacturing", Massachusetts (USA), Kluwer Academic Publishers, 1999.

[86] Wieneke-Toutaoui, B. M. and Gerber, H. W., "Rapid Prototyping Technologies – New Potentials for Offshore and Abyssal Engineering", Proceedings of The Thirteenth (13th) International Offshore and Polar Engineering Conference, Honolulu, Hawaii (USA), May 25-23, 2003.

[87] Sagi O., "PolyJet Matrix™ Technology A New Direction in 3-D Printing", Objet Geometries Ltd., White Paper, 2007.

[88] Vaupotič, B., Labovič, A., Pahole, I., Drstvenšek, I., Brezočnik, M. and Balič, J., "Design Concept and Manufacture of Aids for Testing of Toy Conformity by PolyJet Process", Proceedings of the 5th International Conference of DAAAM Baltic, Tallinn (Estonia), April 20-22, 2006.

[89] "http://www.solid-scape.com/products.html" (Accessed on 14/03/11).

[90] Kucklick T.R., "The Medical Device R&D Handbook", Florida (USA), Taylor and Francis, 2006.

[91] "http://www.flickr.com/photos/organ_printer/878475970" (Accessed on 14/03/11).

[92] Collins,D.C., J.A. Nielsen, I. Faar and C. OriaKhi.,"Use of Support Material in Solid Freeform Fabrication Systems", United States Patent, US 0072113, 2005.

[93] Priedeman Jr.,W.R. and A.L. Brosch. ,"Soluble Material and Process for Three-Dimensional Modeling", United States Patent, US 6790403, 2004.

[94] Newell,K.J., S.A. Ruatta and J.S. Stockwell., "Post Processing Three-Dimensional Objects Formed by Selective Deposition Modeling", United States Patent, US 6752948, 2004.

[95] Kritchman,E.M., H. Gothait and G. Miller., "System and Method for Printing and Supporting Three-Dimensional Objects", United States Patent, US 0171177, 2002.

[96] Kritchman,E.M., H. Gothait and G. Miller., "System and Method for Printing and Supporting Three-Dimensional Objects", United States Patent, US 0207124, 2004.

[97] Nielsen,J.A., V. Kasperchick and L. Kramer., "Materials and Methods for Freeform Fabrication of Three-Dimensional Using Fusible, Water Containing Support Materials", United States Patent, US 7255825, 2007.

[98] Xu,P., S. Ruatta A., K.A. Schmidt and V.A. Doan., "Phase Change Support Material Composition", United States Patent, US 0242728, 2004.

[99] Xu,P., S. Ruatta A., K.A. Schmidt and V.A. Doan., "Phase Change Support Material Composition", United States Patent, US 7176253, 2007.

[100] Xu,P., S.A. Ruatta, K.A. Schmidt and V.A. Doan., "Phase Support Material Composition", Unites States Patent, US 73997696, 2008.

[101] Napadensky,E., "Compositions and Methods for Use in Three Dimensional Model Printing", United States Patent, US 6569373, 2003.

[102] Napadensky,E., "Compositions and Methods for Use in Three Dimensional Model Printing", United States Patent, US 7183335, 2007.

[103] Napadensky,E., E.M. Kritchman and A. Cohen., "Compositions and Methods for Use in Three Dimensional Model Printing", United States Patent, US 7300619, 2007.

[104] Levy,A., "Reverse Thermal Gels and the Use Thereof for Rapid Prototyping", United States Patent, US 6863859, 2005.

[105] Levy,A., "Reverse Thermal Gels as Support for Rapid Prototyping", United States Patent, US 7368484, 2008.

[106] Jeong B., Kim S.W. and Bae Y.H., "Thermosensitive sol–gel reversible hydrogels", Adv.Drug Deliv.Rev., 2002, Volume 54, Number 1, 37-51.

[107] Hamley I.W., "Developments in Block Copolymer Science and Technology", Chichester (UK), John Wiley, 2004.

[108] Hoare T.R. and Kohane D.S., "Hydrogels in drug delivery: Progress and challenges", Polymer, 2008, Volume 49, Number 8, 1993-2007.

[109] Sarkar N., "Thermal Gelation Properties of Methyl and Hydroxypropyl Methylcellulose", Journal of Applied Polymer Science, 1979, Volume 24, Number 4, 1073-1087.

[110] Escobar-Chávez J. J., López-Cervantes M., Naïk A., Kalia Y.N., Quintanar-Guerrero D. and Ganem-Quintanar A., "Applications of Thermo-reversible Pluronic F-127 Gels in Pharmaceutical Formulations", Journal of Pharmacy and Pharmaceutical Sciences, 2006, Volume 9, Number 3, 339-358.

[111] Liang X., Guo C., Ma J., Wang J., Chen S. and Liu H., "Temperature-Dependent Aggregation and Disaggregation of Poly(ethylene oxide)-Poly(propylene oxide)-Poly(ethylene oxide) Block Copolymer in Aqueous Solution", The Journal of Physical Chemistry B, 2007, Volume 111, Number 46, 13217-13220.

[112] Ruel-Gariépy Eve and Leroux Jean-Christophe., "In situ-forming hydrogels—review of temperature-sensitive systems", European Journal of Pharmaceutics and Biopharmaceutics, 2004, Volume 58, Number 2, 409-426.

[113] Pandit N., Trygstad T., Croy S., Bohorquez M. and Koch C., "Effect of Salts on the Micellization, Clouding, and Solubilization Behavior of Pluronic F127 Solutions", J.Colloid Interface Sci.,2000, Volume 222, Number 2, 213-220.

[114] Michels B., Waton G. and Zana R., "Dynamics of Micelles of Poly(ethylene oxide)−Poly(propylene oxide)−Poly(ethylene oxide) Block Copolymers in Aqueous Solutions", Langmuir, 1997, Volume 13, Number 12, 3111-3118.

[115] Wanka G., Hoffmann H. and Ulbricht W., "Phase Diagrams and Aggregation Behavior of Poly(oxyethylene)-Poly(oxypropylene)-Poly(oxyethylene) Triblock Copolymers in Aqueous Solutions", Macromolecules, 1994, Volume 27, Number 15, 4145-4159.

[116] Bromberg L., "Novel Family of Thermogelling Materials via C−C Bonding between Poly(acrylic acid) and Poly(ethylene oxide)-b-poly(propylene oxide)-b-poly(ethylene oxide)", The Journal of Physical Chemistry B, 1998, Volume 102, Number 11, 1956-1963.

[117] Alexandridis P. and Alan Hatton T., "Poly(ethylene oxide) ▪ poly(propylene oxide) ▪ poly(ethylene oxide) block copolymer surfactants in aqueous solutions and at interfaces: thermodynamics, structure, dynamics, and modeling", Colloids Surf.Physicochem.Eng.Aspects, 1995, Volume 96, Number 1-2, 1-46.

[118] "Pluronic Grid", Available at: http://www2.basf.us/performancechemical/bcperfpluronic_grid.html (Accessed on 14/03/11).

[119] Linse P. and Malmsten M., "Temperature-dependent micellization in aqueous block copolymer solutions", Macromolecules, 1992, Volume 25, Number 20, 5434-5439.

[120] Lindman B., Carlsson A., Karlstrom G. and Malmsten M., "Nonionic Polymers and Surfactants - Some Anomalies in Temperature Dependence and in Interactions with Ionic Surfactants", Advances in Colloid and interface Science, 1990, Volume 32, Number 2-3, 183-203.

[121] Malmsten M., Linse P. and Zhang K.W., "Phase Behaviour of Aqueous Poly(ethylene oxide)/Poly(propylene oxide) Solutions", Macromolecules, 1993, Volume 26, Number 11, 2905-2910.

[122] Linse P., "Phase behavior of poly(ethylene oxide)-poly(propylene oxide) block copolymers in aqueous solution", J.Phys.Chem., 1993, Volume 97, Number 51, 13896-13902.

[123] Alexandridis P., Holzwarth J.F. and Hatton T.A., "Micellization of Poly(ethylene oxide)-Poly(propylene oxide)-Poly(ethylene oxide) Triblock Copolymers in Aqueous Solutions: Thermodynamics of Copolymer Association", Macromolecules, 1994, Volume 27, Number 9, 2414-2425.

[124] Mortensen K., "Structural studies of aqueous solutions of PEO - PPO - PEO triblock copolymers, their micellar aggregates and mesophases; a small-angle neutron scattering study", Journal of Physics: Condensed Matter, 1996, Volume8, Number 25A, A103-A124.

[125] Cabana A., Aït-Kadi A. and Juhász J., "Study of the Gelation Process of Polyethylene Oxidea–Polypropylene Oxideb–Polyethylene OxideaCopolymer (Poloxamer 407) Aqueous Solutions", J.Colloid Interface Sci., 1997, 6/15, Volume 190, Number 2, 307-312.

[126] Newby G.E., Hamley I.W., King S.M., Martin C.M. and Terrill N.J., "Structure, rheology and shear alignment of Pluronic block copolymer mixtures", J.Colloid Interface Sci., 2009, Volume 329, Number 1, 54-61.

[127] Guzáman M., Aberturas M.R., Garcia F. and Molpeceres J., "Gelatine Gels and Polyoxyethylene-Polyoxypropylene Gels: Comparative Study of Their Properties", Drug Develeopment and Industrial Pharmacy, 1994, Volume 20, Number 12, 2041-2048.

[128] Pandit N.K. and McGowan R., "Gelation of Pluronic F127-Polyethylene Glycol Mixtures: Relationship to PEG Molecular Weight", Drug Develeopment and Industrial Pharmacy, 1998, Volume 24, Number 2, 183-186.

[129] Kwon K.W., Park M.J., Hwang J. and Char K., "Effects of Alcohol Addition on Gelation in Aqueous Solution of Poly(ethylene oxide)-Poly(propylene oxide)-Poly(ethylene oxide) Triblock Copolymer", Polymer Journal, 2001, Volume 33, Number 5, 404-410.

[130] Ivanova R., Lindman B. and Alexandridis P., "Evolution in Structural Polymorphism of Pluronic F127 Poly(ethylene oxide)−Poly(propylene oxide) Block Copolymer in Ternary Systems with Water and Pharmaceutically Acceptable Organic Solvents: From “Glycols” to “Oils”†", Langmuir, 2000, Volume 16, Number 23, 9058-9069.

[131] Alexandridis P. and Spontak R.J., "Solvent-regulated ordering in block copolymers", Current Opinion in Colloid & Interface Science, 1999, Volume 4, Number 2, 130-139.

[132] Ivanova R., Lindman B. and Alexandridis P., "Effect of Glycols on the Self-Assembly of Amphiphilic Block Copolymers in Water. 1. Phase Diagrams and Structure Identification", Langmuir, 2000, Volume 16, Number 8, 3660-3675.

[133] Alexandridis P., Ivanova R. and Lindman B., "Effect of Glycols on the Self-Assembly of Amphiphilic Block Copolymers in Water. 2. Glycol Location in the Microstructure", Langmuir, 2000, Volume 16, Number 8, 3676-3689.

[134] Schmolka I.R., "Artificial Skin 1. Preparation and Properties of Pluronic F-127 Gels for Treatment of Burns", Journal of Biomedical Materials Research, 1972, Volume 6, Number 6, 571-582.

[135] Mortensen K. and Brown W., "Poly(ethylene oxide)-poly(propylene oxide)-poly(ethylene oxide) triblock copolymers in aqueous solution. The influence of relative block size", Macromolecules, 1993, Volume 26, Number 16, 4128-4135.

[136] Bahadur P. and Pandya K., "Aggregation Behaviour of Pluronic P-94 in Water", Langmuir, 1992, Volume 8, Number 11, 2666-2670.

[137] Malmsten M. and Lindman B., "Self-Assembly in Aqueous Block Copolymers Solutions", Macromolecules, 1992, Volume 25, Number 20, 5440-5445.

[138] Hecht E., Mortensen K., Gradzielski M. and Hoffmann H., "Interactions of ABA Block Copolymers with Ionic Surfactants: Influence on Micellization and Gelation", Journal of Physical Chemistry, 1995, Volume 99, Number 13, 4866-4874.

[139] Pandit N.K. and Kisaka J., "Loss of gelation ability of Pluronic F-127 in the presence of some salts", International Journal of Pharmaceutics, 1996, Volume 145, Number 1, 129-136.

[140] Alexandridis P. and Yang L., "SANS Investigation of Polyether Block Copolymer Micelle Structure in Mixed Solvents of Water and Formamide, Ethanol, or Glycerol", Macromolecules, 2000, Volume 33, Number 15, 5574-5587.

[141] Bharatiya B., Guo C., Ma J.H., Hassan P.A. and Bahadur P., "Aggregation and clouding behavior of aqueous solution of EO–PO block copolymer in presence of n-alkanols", European Polymer Journal, 2007, Volume 43,Number 5, 1883-1891.

[142] Bharatiya B., Aswal V.K., Hassan P.A. and Bahadur P., "Influence of a hydrophobic diol on the micellar transitions of Pluronic P85 in aqueous solution", J.Colloid Interface Sci., 2008, Volume 320, Number 2, 452-459.

[143] Ivanova R., Alexandridis P. and Lindman B., "Interaction of poloxamer block copolymers with cosolvents and surfactants", Colloids and Surfaces A: Physicochemical and Engineering Aspects, 2001, Volume 183-185, 41-53.

[144] Chaibundit C., Ricardo N.M.P.S., Ricardo N.M.P.S., Costa F.d.M.L.L., Wong M.G.P., Hermida-Merino D., Rodriguez-Perez J., Hamley I.W, Yeates S.G., and Booth C., "Effect of Ethanol on the Micellization and Gelation of Pluronic P123", Langmuir, 2008, Volume 24, Number 21, 12260-12266.

[145] Yang L. and Alexandridis P., "Polyoxyalkylene Block Copolymers in Formamide−Water Mixed Solvents: Micelle Formation and Structure Studied by Small-Angle Neutron Scattering", Langmuir, 2000, Volume 16, Number 11, 4819-4829.

[146] Alexandridis P. and Yang L., "Micellization of Polyoxyalkylene Block Copolymers in Formamide", Macromolecules, 2000, Volume 33, Number 9, 3382-3391.

[147] Alexandridis P., "Structural Polymorphism of Poly(ethylene oxide)−Poly(propylene oxide) Block Copolymers in Nonaqueous Polar Solvents", Macromolecules, 1998, Volume 31, Number 20, 6935-6942.

[148] Soni S.S., Brotons G., Bellour M., Narayanan T. and Gibaud A., "Quantitative SAXS Analysis of the P123/Water/Ethanol Ternary Phase Diagram", The Journal of Physical Chemistry B, 2006, Volume 110, Number 31, 15157-15165.

[149] Chaibundit C., Ricardo N.M.P.S., Ricardo N.M.P.S., Muryn C.A., Madec M., Yeates S.G. and Booth C., "Effect of ethanol on the gelation of aqueous solutions of Pluronic F127", Journal of colloid and interface science, 2010, Volume 351, Number 1, 190-196.

[150] "BASF Technical Bulletin, Preparation of Pluronic® Surfactant Gels", 2005.

[151] Klemm D., Philipp B., Heinze T., Heinze U. and Wagenknecht W., "Comprehensive Cellulose Chemistry", Weinheim (Germany), Wiley-VCH, 1998.

[152] Ott E., Spurlin H.M. and Grafflin M.W. editors., "Cellulose and Cellulose Drivatives", Pennsylvania (USA), Interscience Publishing, 1954.

[153] Ye, D., "Preparation of Methylcellulose from Annual Plants", Chemical Engineering Department, Rovira i Virgili University, Tarragona, Spain; 2005.

[154] Brydson J.A., "Plastic Materials", Oxford (UK), Butterworth-Heinemann, 1995.

[155] Williams P.A., "Gelling Agents", Williams PA (editor), Handbook of Industrial Water Soluble Polymers, Oxford (UK), Blacwell Publishing Ltd., 2007.

[156] Nussinovitch A., "Hydrocolloid Applications - Gum technology in the food and other industries", 1997.

[157] Majewicz T.G. and Podlas T.J., "Cellulose Ethers", Kroschwitz J.I. (editor), Kirk-Othmer concise encyclopedia of chemical technology, Wiley-Interscience, 2005.

[158] Nud'ga L.A., Petrova V.A., Ben'kovich A.D. and Petropavlovskii G.A., "Comparative Study of Reactivity of Cellulose, Chitosan, and Chitin-Glucan Complex in Sulfoethylation", Russian Journal of Applied Chemistry, 2000, Volume 74, Number 1, 145-148.

[159] Dijk,B.J. and J.G. Batelaan., "Anionic cellulose ethers having temperature-dependent associative properties", US 6669863, 2003.

[160] Kondo T., "Preparation of 6-O-alkylcelluloses", Carbohydrate research, 1993, Volume 238, 231-240.

[161] Harkness B.R. and Gray D.G., "Preparation and chiroptical properties of tritylated cellulose derivatives", Macromolecules, 1990, Volume 23, Number 5, 1452-1457.

[162] Kondo T. and Gray D.G., "The preparation of O-methyl- and O-ethyl-celluloses having controlled distribution of substituents", Carbohydrate research, 1991, Volume 220, 173-183.

[163] Mann G., Kunze J., Loth F. and Fink H., "Cellulose ethers with a block-like distribution of the substituents by structure-selective derivatization of cellulose", Polymer, 1998, Volume 39, Number 14, 3155-3165.

[164] Kern H., Choi S., Wenz G., Heinrich J., Ehrhardt L., Mischnick P., Garidel P. and Blume A., "Synthesis, control of substitution pattern and phase transitions of 2,3-di-O-methylcellulose", Carbohydrate research, 2000, Volume 326, Number 1, 67-79.

[165] Koschella A., Fenn D., Illy N. and Heinze T., "Regioselectively Functionalized Cellulose Derivatives: A Mini Review", Macromolecular Symposia, Volume 244, Number 1, 59-73.

[166] Clasen C. and Kulicke W.M., "Determination of viscoelastic and rheo-optical material functions of water-soluble cellulose derivatives", Progress in Polymer Science, 2001, Volume 26, Number 9, 1839-1919.

[167] Kuang Q., Cheng G., Zhao J. and Li Y., "Thermogelation Hydrogels of Methylcellulose and Glycerol-Methylcellulose Systems", Journal of Applied Polymer Science, 2006, Volume 100, Number 5, 4120-4126.

[168] Heymann E., "Studies on Sol-Gel Transformations.I. THe Inverse Sol-Gel Transformation of Methylcellulose in Water", Transactions of Faraday Society, 1935, Volume 31, 846-864.

[169] Savage A.B., "Temperature-Viscosity Relationships for Water-Soluble Cellulose Ethers", Industrial and Engineering Chemistry, 1957, Volume 49, Number 1, 99-103.

[170] Kato T., Yokoyama M. and Takahashi A., "Melting temperatures of thermally reversible gels IV. Methyl cellulose-water gels", Colloid and Polymer Science, 1978, Volume 256, Number 1, 15-21.

[171] Haque A. and Morris H.R., "Thermogelation of methylcellulose. Part I: molecular structures and processes", Carbohydrate Polymers, 1993, Volume 22, Number 3, 161-173.

[172] Joshi,A., Ding S. and Himmelstein K. J., "Reversible Gelation Compositions and Methods of Use", US 5252318, 1993.

[173] Sarkar N., "Kinetics of thermal gelation of methylcellulose and hydroxypropylmethylcellulose in aqueous solutions", Carbohydrate Polymers, 1995, Volume 26, Number 3, 195-203.

[174] Sarkar N. and Walker L.C., "Hydration—dehydration properties of methylcellulose and hydroxypropylmethylcellulose", Carbohydrate Polymers, 1995, Volume 27, Number 3, 177-185.

[175] Itagaki H., Tokai M. and Kondo T., "Physical gelation process for cellulose whose hydroxyl groups are regioselectively substituted by fluorescent groups", Polymer, 1997, Volume 38, Number 16, 4201-4205.

[176] Nishinari K., Hofmann K.E., Moritaka H., Kohyama K. and Nishinari N., "Gel-sol transition of methylcellulose", Macromolecular Chemistry and Physics, 1997, Volume 198, Number 4, 1217-1226.

[177] Desbrières J., Hirrien M. and Rinaudo M., "A Calorimetric Study of Methylcellulose Gelation", Carbohydrate Polymers, 1998, Volume 37, Number 2, 145-152.

[178] Kobayashi K., Huang C. and Lodge T.P., "Thermoreversible Gelation of Aqueous Methylcellulose Solutions", Macromolecules, 1999, Volume 32, Number 21, 7070-7077.

[179] Bochek A.M., Zabivalova N.M., Lavrent'ev V.K., Lebedeva M.F., Sukhanova T.E. and Petropavlovskii G.A., "Formation of Physical Thermally Reversible Gels in Solutions of Methyl Cellulose in Water and Dimethylacetamide and Properties of Films Thereof", Russian Journal of Applied Chemistry, 2001, Volume 74, Number 8, 1358-1363.

[180] Li L., Thangamathesvaran P.M., Yue C.Y., Tam K.C., Hu X. and Lam Y.C., "Gel Network Structure of Methylcellulose in Water", Langmuir, 2001, Volume 17, Number 26, 8062-8068.

[181] Yin Y., Nishinari K., Zhang H. and Funami T., "A Novel Liquid-Crystalline Phase in Dilute Aqueous Solutions of Methylcellulose", Macromolecular Rapid Communications, 2006, Volume 27, Number 12, 971-975.

[182] Buslov D.K., Sushko N.I. and Tretinnikov O.N., "Study of Thermal Gelation of Methylcellulose in Water Using FTIR-ATR Sepctroscopy", Journal of Applied Spectroscopy, 2008, Volume 75, Number 4, 514-518.

[183] Li L., Shan H., Yue Y., Lam Y.C., Tam K.C. and Hu X., "Thermally Induced Association and Dissociation of Methylcellulose in Aqueous Solutions", Langmuir, 2002, Volume 18, Number 20, 7291-7298.

[184] Viridn A., Wittgren B., Andersson T., Abrahmsn-Alami S. and Larsson A., "Influence of Substitution Pattern on Solution Behavior of Hydroxypropyl Methylcellulose", Biomacromolecules, 2009, Volume 10, Number 3, 522-529.

[185] Kundu P.P., Kundub M., Sinhaa M., Choec S. and Chattopadhayayd D., "Effect of alcoholic, glycolic, and polyester resin additives on the gelation of dilute solution (1%) of methylcellulose", Carbohydrate Polymers, 2003, Volume 51, Number 1, 57-61.

[186] Guillot S., Lairez D. and Axelos M.A.V., "Non-self-similar aggregation of methylcellulose", Journal of Applied Crystallography, 2000, Volume 33, Number 3-1, 669-672.

[187] Wang Q. and Li L., "Effects of molecular weight on thermoreversible gelation and gel elasticity of methylcellulose in aqueous solution", Carbohydrate Polymers, 2005, Volume 62, Number 3, 232-238.

[188] Funami T., Kataoka Y., Hiroe M., Asai I., Takahashi R. and Nishinari K., "Thermal aggregation of methylcellulose with different molecular weights", Food Hydrocolloids, 2007, Volume 21, Number 1, 46-58.

[189] Kundu P.P. and Kundu M., "Effect of salts and surfactant and their doses on the gelation of extremely dilute solutions of methyl cellulose", Polymer, 2001, Volume 42, Number 5, 2015-2020.

[190] Hatakeyama H., Onishi T., Endo T. and Hatakeyama T., "Gelation of chemically cross-linked methylcellulose studied by DSC and AFM", Carbohydr.Polym., 2007, Volume 69, Number 4, 792-798.

[191] Joshi S.C., Su J.C., Liang C.M. and Lam Y.C., "Gelation of Methylcellulose Hydrogels Under Isothermal Conditions", Journal of Applied Polymer Science, 2008, Volume 107, Number 4, 2101-2108.

[192] Hussain S., Keary C. and Craig D.Q.M., "A thermorheological investigation into the gelation and phase separation of hydroxypropyl methylcellulose aqueous systems", Polymer, 2002, Volume 43, Number 21, 5623-5628.

[193] Hirrien M., Desbrières J. and Rinaudo M., "Physical properties of methylcelluloses in relation with the conditions for cellulose modification", Carbohydrate Polymers, 1996, Volume 31, Number 4, 243-252.

[194] Liu H.Q., Zhang L.N., Takaragi A. and Miyamoto T., "Effect of substituent distribution on water solubility of O-methylcellulose", Cellulose, 1997, Volume 4, Number 4, 321-327.

[195] Takahashi S., Fujimoto T., Miyamoto T. and Inagaki H., "Relationship between distribution of substituents and water solubility of O-methyl cellulose", Journal of Polymer Science Part A: Polymer Chemistry, 1987, Volume 25, Number 4, 987-994.

[196] Schagerlöf H., Johansson M., Richardson S., Brinkmalm G., Wittgren B. and Tjerneld F., "Substituent Distribution and Clouding Behaviour of Hydroxypropyl Methylcellulose Analyzed Using Enzymatic Degradation", Biomacromolecules, 2006, Volume 7, Number 12, 3474-3481.

[197] Carlsson, A., Karlström, G. and Lindman, B., "Thermal Gelation of Nonionic Cellulose Ethers and Ionic Surfactants in Water", Colloids and Surfaces, 1990, Volume 47, 147-165.

[198] Levy G. and Schwarz T.W., "The effect of certain additives on the gel point of methylcellulose", Journal of the American Pharmaceutical Association, 1958, Volume 47, Number 1, 44-46.

[199] Haque, A., Jones, A. K., Richardson, R. K. and Morris, E. R, "Thermal gelation of methylcellulose: mechanisms and structures", Proceedings of the 7th International Conference on Gums and Stabilisers for the Food Industry, Wrexham, Clywd, Wales (UK), July 1993.

[200] Takeuchi M., Kageyama S., Suzuki H., Wada T., Notsu Y. and Ishii F., "Rheological properties of reversible thermo-setting in situ gelling solutions with the methylcellulose-polyethylene glycol-citric acid ternary system", Colloid and Polymer Science, 2003, Volume 281, Number 12, 1178-1183.

[201] Alfonso J.E.M., Valencia R.Y.C., Franco J.M. and Dı´az M.J., "Optimization of the Methylation Conditions of Kraft Cellulose Pulp for Its Use As a Thickener Agent in Biodegradable Lubricating Greases", Industrial & Engineering Chemistry Research, 2009, Volume 48, Number 14, 6765-6771.

[202] Koeing J.L., "Spectroscopy of Polymers", 2nd Edition, New York (USA), Elsevier Science, 1999.

[203] Davis S.P., Abrams M.C. and Brault J.W., "Fourier Transform Spectrometry", California (USA), Academic Press, 2001.

[204] Chalmers J.M. and Everall N.J., "Vibrational Spectroscopy", Hunt BJ and James MI, editors. , 1st ed. London (UK), Blackie Academic and Professional, 1993,.

[205] Hsu C.P.S., "Infrared Spectroscopy", Settle F. A (editor), Handbook of Instrumental Techniques for Analytical Chemistry, New Jersey (USA), Prentice Hall, 1997.

[206] Hohne G.W.H., Hemminger W.F. and Flammersheim H.-J., "Differential Scanning Calorimetry", 2nd Edition, London (UK), Springer, 2003.

[207] Campbell D., Pethrick R. A. and White J. R., "Polymer Characterization: Physical Techniques", 2nd Edition, Cheltenham (UK), Stanley Thorns, 2000.

[208] Sutter T., "An Overview of Digital Printing for Advanced Interconnect Applications", Circuit World, 2005, Volume 31, Number 3, 4-9.

[209] Tunick M.H., "Food Texture Analysis in the 21st Century", Journal of Agricultural and Food Chemistry, 2010 (online version).

[210] Ivanova R., Lindman B. and Alexandridis P., "Modification of the lyotropic liquid crystalline microstructure of amphiphilic block copolymers in the presence of cosolvents", Advances in Colloid and Interface Science, 2001, Volume 89-90, 351-382.

[211] Höhn A.,"Formamide", Kirk-Othmer Encyclopedia of Chemical Technology, John Wiley & Sons, 2000.

[212] Bohorquez M., Koch C., Trygstad T. and Pandit N., "A Study of the Temperature-Dependent Micellization of Pluronic F127", Journal of Colloid and Interface Science, 1999, Volume 216, Number 1, 34-40.

[213] Dissanayake, M. A. K. L. and Frech R., "Infrared Spectroscopic Study of the Phases and Phase Transitions in Poly(ethylene oxide) and Poly(ethylene oxide)-Lithium Trifluoromethanesulfonate Complexes", Macromolecules, 1995, Volume 28, Number 15, 5312-5319.

[214] Guo C., Liu H., Wang J. and Chen J., "Conformational Structure of Triblock Copolymers by FT-Raman and FTIR Spectroscopy", Journal of Colloid Interface Science, 1999, Volume 209, Number 2, 368-373.

[215] Marsh L.H., Coke M., Dettmar P.W., Ewen R.J., Havler M., Nevell T.G., Smart J.D., Smith J.R., Timmins, B., Tsibouklis J. and Alexander, C., "Adsorbed poly(ethyleneoxide)-poly(propyleneoxide) copolymers on synthetic surfaces: Spectroscopy and microscopy of polymer structures and effects on adhesion of skin-borne bacteria", Journal of Biomedical Materials Research, 2002, Volume 61, Number 4, 641-652.

[216] Su Y., Wang J. and Liu H., "FTIR Spectroscopic Study on Effects of Temperature and Polymer Composition on the Structural Properties of PEO−PPO−PEO Block Copolymer Micelles", Langmuir, 2002, Volume 18, Number 14, 5370-5374.

[217] Su Y., Wang J. and Liu H., "Melt, Hydration, and Micellization of the PEO–PPO–PEO Block Copolymer Studied by FTIR Spectroscopy", Journal of Colloid Interface Science, 2002, Volume 251, Number 2, 417-423.

[218] Bellamy L.J., "The Infra-red Spectra of Complex Molecules", 3rd Edition, 1975, London (UK), Chapman and Hall

[219] Bellamy L.J., "Advances in Infrared Group Frequencies", 1st Edition, 1968, London (UK), Methuen and Co. Ltd.

[220] Koeing, J. L. and Angood, A, C., “Raman Spectra of Poly(ethylene Glycols) in Solution”, Journal of Polymer Science: Part A-2, 1970, Volume 8,Number 10, 1787-1796.

[221] Guo C., Liu H.-Z. and Chen J.-Y., "A Fourier transform infrared study of the phase transition in aqueous solutions of Ethylene oxide–propylene oxide triblock copolymer", Colloid & Polymer Science, 1999, Volume 277, Number 4, 376-381.

[222] Sperling, L. H., "Introduction to Physical Polymer Science", 4th edition, 2006, New Jersey (USA), Wiley-Interscience

[223] Brinson, H. F. and Brinson, L. C., "Polymer Engineering Science and Viscoelasticity: An Introduction", 1st edition, 2008, New York (USA), Springer

[224] Gaides, G. E. and McHugh, A. J., “Gelation in an amorphous polymer: a discussion of its relation to membrane formation”, Polymer, 1989, Volume 30, Number 11, 2118-2123.

[225] Kawanishi, K., Komatsu, M. and Inoue, T., “Thermodynamic consideration of the sol – gel transition in polymer solutions”, Polymer, 1987, Volume 28, Number 6, 980-984.

[226] Maxfield J. and Shepherd I.W., "Conformation of poly(ethylene oxide) in the solid state, melt and solution measured by Raman scattering", Polymer, 1975, Volume 16, Number 7, 505-509.

[227] Chen S., Guo C., Liu H.-Z., Wang J., Liang X.-F., Zheng L. and MA J.-H., "Thermodynamic analysis of micellization in PEO–PPO–PEO block copolymer solutions from the hydrogen bonding point of view", Molecular Simulation, 2006, Volume 32, Number 5, 409-418.

[228] Sheng S., BingJie S., Zhang G., Wei Z., QiangGuo D. and PeiYi W., "Two-dimensional correlation ATR-FTIR studies on PEO–PPO–PEO tri-block copolymer and its phosphorylcholine derivate as thermal sensitive hydrogel systems", Polymer, 2008, Volume 49, Number 11, 2738-2744.

[229] Tan, H. M., Chang, B. H., Baer, E. and Hiltner, A., “Relationship between Crystallinity and Thermoreversible Gelation”, European Polymer Journal, 1983, Volume 19, Number 10/11, 1021-1025.

[230] Rimdusit S., Jingjid S., Damrongsakkul S., Tiptipakorn S. and Takeichi T., "Biodegradability and property characterizations of Methyl Cellulose: Effect of nanocompositing and chemical crosslinking", Carbohydrate Polymers, 2008, Volume 72, Number 3, 444-455.

[231] Sammon C., Bajwa G., Timmins P. and Melia C.D., "The application of attenuated total reflectance Fourier transform infrared spectroscopy to monitor the concentration and state of water in solutions of a thermally responsive cellulose ether during gelation", Polymer, 2006, Volume 47, Number 2, 577-584.

[232] Viera R.G.P., Filho G.R., de Assunção R.M.N., S. Meireles C.d., Vieira J.G. and de Oliveira G.S., "Synthesis and characterization of methylcellulose from sugar cane bagasse cellulose", Carbohydrate Polymers, 2007, Volume 7, Number 2, 182-189

[233] Kondo T. and Sawatari C., "A Fourier transform infra-red spectroscopic analysis of the character of hydrogen bonds in amorphous cellulose", Polymer, 1996, Volume 37, Number 3, 393-399.

[234] Yin J., Luo K., Chen X. and Khutoryanskiy V.V., "Miscibility studies of the blends of chitosan with some cellulose ethers", Carbohydrate Polymers, 2006, Volume 63, Number 2, 238-244.

[235] Khomutov L.I., Ryskina I.I., Panina N.I., Dubina L.G. and Timofeeva G.N., "Structural changes during gelation of aqueous solutions of methylcellulose", Polymer Science, 1993, Volume 35, Number 3,:276-279.

[236] Pinotti A., García M.A., Martino M.N. and Zaritzky N.E., "Study on microstructure and physical properties of composite films based on chitosan and methylcellulose", Food Hydrocolloids, 2007, Volume 21, Number 1,:66-72.

[237] Kondo T., Koschella A., Heublein B., Klemm D. and Heinze T., "Hydrogen bond formation in regioselectively functionalized 3-mono-O-methyl cellulose", Carbohydrate research, 2008, Volume 343, Number 15, 2600-2604.

[238] Aziz N.A.N., Idris N.K. and Isa M.I.N., "Solid Polymer Electrolytes Based on Methylcellulose: FT-IR and Ionic Conductivity Studies", International Journal of Polymer Analysis and Characterization, 2010, Volume 15, Number 5, 319-327.

[239] Filho G.R., de Assunção, R. M. N., Vieira J.G., Meireles C.d.S., Cerqueira D.A., da Silva Barud H., Ribeiro S.J.L., and Messaddeq Y., "Characterization of methylcellulose produced from sugar cane bagasse cellulose: Crystallinity and thermal properties", Polymer Degradation and Stability, 2007, Volume 92, Number 2, 205-210.

[240] Hansen C.M., "Hansen solubility parameters : a user's handbook", 2nd Edition, Florida (USA), CRC Press, 2007.

[241] Archer W.A., "Determination of Hansen Solubility Parameters for Selected Cellulose Ether Derivatives", Industrial and Engineering Chemistry Research, 1991, Volume 30, Number 10, 2292-2298.